Validation of shellfish isolates (glycosaminoglycans, GAGs) for development as a novel anti-tumour therapy for children: GAG action on lymphocytes/ T-regulatory cells

Chloe Francesca Jones

School of Environment and Life Sciences

University of Salford

Supervisor: Dr Lucy Smyth

Collaborator: Dr David Pye

Submitted in partial fulfilment of the requirements of the Degree of Doctor of Philosophy

March 2019

Contents Page

List of Figures

List of tables

List of abbreviations

AICD- activation induced cell death

ALL- acute lymphoblastic leukaemia

CML- chronic myeloid leukaemia

CPC- cetylpyrimidinechloride

CS- chondroitin sulphate

DAMP- damage associated molecular pattern

DISC- death inducing signalling complex

DS- dermatan sulphate

EGFR- epidermal growth factor receptor

FGF- fibroblast growth factor

FPLC- fast protein liquid chromatography

GAG- glycosaminoglycan

GlcA- glucuronic acid

HS- Heparan sulphate

IC50- the dose of treatment required to reduce cell viability by 50%

IdoA- iduronic acid

iT_{reg}- peripherally induced regulatory T-cell

LL- lymphoblastic lymphoma

MHC- major histocompatibility complex

NHL- non-hodgkins lymphoma

NK- natural killer

nT_{reg}- natural regulatory T-cell

PBMC- peripheral blood mononuclear cell

PG- proteoglycan

PHA- phytohaemagglutinin

PI- propridium iodide

PMA- phorbol 12-myristate 13-acetate

PS- phosphatidyl serine

RBC- red blood cell

SAC- spindle assembly checkpoint

TCA- trichloroacetic acid

TGF- transforming growth factor

TNF- tumour necrosis factor

T_{reg} – regulatory T-cell

VEGF- vascular endothelial growth factor

WBC - white blood cell

Acknowledgments

I would like to dedicate this PhD thesis to the important people in my life, my brother, mother and father and to my partner. Thank you for all the help, support and understanding you have given me over the course of my research career.

I extend my sincerest gratitude to my supervisor Dr Lucy Smyth for giving me the opportunity to carry out this research and for all the help, support and guidance she has provided me over the last four years. I would also like to thank the research collaborator Dr David Pye for his guidance throughout the course of the research and KidsCan for providing the funding for the PhD. I would also like to thank placement students David Scannali and Parham Manouchehri for their help within the lab and Ethan Palomba for his efforts in taking my proposed new fraction doses and identifying their action. I would also like to acknowledge the NHS blood bank for providing the blood for the peripheral blood mononuclear cells (PBMCs) isolation and Dr Jeremy Allen and Manisha Patel for collecting the blood which we isolated the PBMCs from. I would also like to thank Rumana Rafiq for all her help within the lab and for her help and support during the transitioning period in between lab moves. I would also like to thank all of my colleagues for their support throughout the last four years.

Abstract

Introduction: Leukaemia is cancer of white blood cells (WBCs) mainly affecting children. Defective WBCs are prominent in blood and cannot provide immune protection. Although chemotherapy treatments are effective, they have many adverse effects which are magnified in children, with treatment proving fatal for around 10-20% of children undergoing treatment. T-regulatory cells regulate inflammatory responses; in cancer raised levels of T-regulatory cells have been linked with immune evasion of cancer cells. Understanding chemotherapy effects on T_{reg} populations is key to predicting therapy effectiveness. Ongoing research at KidsCan has identified the anti-tumour properties of novel glycosaminoglycan (GAG) compounds isolated from shellfish. However the effect of GAGs on normal lymphocyte populations is still unknown, identifying this action is essential in order to evaluate any potential use of GAGs as a cancer chemotherapy treatment in children.

Aim: In order to further understand the potential use of GAGs for clinical applications the aim of this research is to evaluate T-cell and B-cell responses (in healthy lymphocytes) to GAG treatment and to compare them to control cancer cell lines (MOLT-4, K562 and U698).

Methods: Phase 1 of the research isolated GAGs from cockles and whelks. Peripheral blood mononuclear cells (PBMCs) were extracted in bulk from whole blood from the NHS donor service. GAG isolates were tested for activity on cell growth using MTT assay on PBMCs (naïve and activated) and three cancer cell lines (MOLT-4, K562, U698). Phase 2 tested the GAG isolates for their potency via a flow cytometric annexin V/ PI apoptosis assay on the cell lines and PBMCs both activated using either PHA or PMA/ionomycin and naïve. Phase 3 studies evaluated individual FPLC separated GAG fractions to establish potentially potent domains of the compounds. This work also focussed on T-regulatory cell (T_{reg}) responses to the GAGs to provide an insight to their potential modulation of a population of cells associated with cancer progression.

Results: The MTT assays identified that both GAG extracts had a profound effect on cancer cell growth, with cell viability inhibitions of up to 90% and IC50 values ranging between 0.7 µg/ml and 12 µg/ml. This study also indicated that GAG extracts have little effect on the viability of healthy lymphocytes (PBMCs) identifying the potential of GAGs as a therapeutic treatment for cancer. MTT assays aided with the design of the apoptosis assays. Apoptosis assays indicated that cancer cells responded to GAG extract treatment via the induction of apoptosis and identified which cell types were most at risk of being targeted in healthy lymphocyte populations (stimulated and unstimulated), they also identified the whelk extract as being the more effective GAG treatment. The T_{reg} assays indicate that decreases in the cell population may be an additional benefit of the GAG compounds through reducing the risk of tumour progression. However further work with T_{reg} populations in healthy lymphocytes would help to prove this principle and future studies would be useful to further optimise the fraction assays.

CHAPTER 1- INTRODUCTION

1.0 Introduction

Cancer is the result of several malfunctions in normal cellular systems which promote cellular proliferation and systems which aid the prevention of uncontrolled cellular proliferation (Sompayrac, 2015). This study seeks to undertake the preclinical evaluation of novel shellfish isolates on healthy lymphocytes, to advance the development of more effective and tolerable therapies, especially in children.

1.1 Normal cell cycle

The cell cycle is the mechanism which cells use to divide and grow, with the eventual outcome the production of two identical daughter cells (Schafer, 1998: Yang, 2012). Thus understanding the regulation of the cell cycle is essential in cancer therapy. In healthy cells two main events occur, firstly cellular DNA is replicated and secondly division occurs which results in two identical daughter cells (Yang, 2012).

The cell cycle is made up of several phases each of which must be completed and progressed through in order, i.e. one phase cannot begin without the successful completion of the stage before it (Yang, 2012). The cycle has four phases, as shown in figure 1.1, the first three being G_1, S phase and G_2. In the G_1 phase the cell enlarges and prepares for DNA synthesis to occur, at this stage the cell can be referred to as diploid meaning it contains two copies of each chromosome (Cooper, 2000: Yang, 2012). S phase is the point where DNA is synthesised, and DNA content can vary between 2 copies and 4 copies of chromosomes depending on at which stage of replication the cell is at. G_2 is the second gap phase where cells get ready to divide, cells can be referred to as tetraploid (4 copies of chromosomes) at this stage. M phase is where actual cell division occurs and is made up of two sections. The first section is mitosis where the chromosomes are equally divided between the two daughter cells (Yang, 2012). The second stage is known as cytokinesis and is where the cytoplasm divides and forms the two distinct daughter cells. Typically, it takes 24 hours for cell division to occur, with mitosis and cytokinesis typically making up 1 hour of this time (Cooper, 2000). As well as the four stages of the cell cycle mentioned above there is a fifth stage which is known as G_0 resting phase, this stage lies outside the cell cycle

(Cooper, 2000). Cells in this stage are said to be resting and have typically come out of the G_1 stage (Cooper, 2000: Yang, 2012). G_0 phase is a resting phase where the cell can perform all its normal functions, but it does not divide. Usually a cell will enter the G_0 phase if the surrounding environment is not promoting of the cell cycle, for example if there is a lack of nutrients or growth factors (Cooper, 2000). However fully differentiated cells such as neurones will also be in the G_0 phase (Yang, 2012). Additionally, to these two cases it may also be possible for a cell to enter into the G_0 phase if there has been DNA damage identified, the entering of the G_0 phase in this case is as an alternative to cell destruction through apoptosis (Yang, 2012).

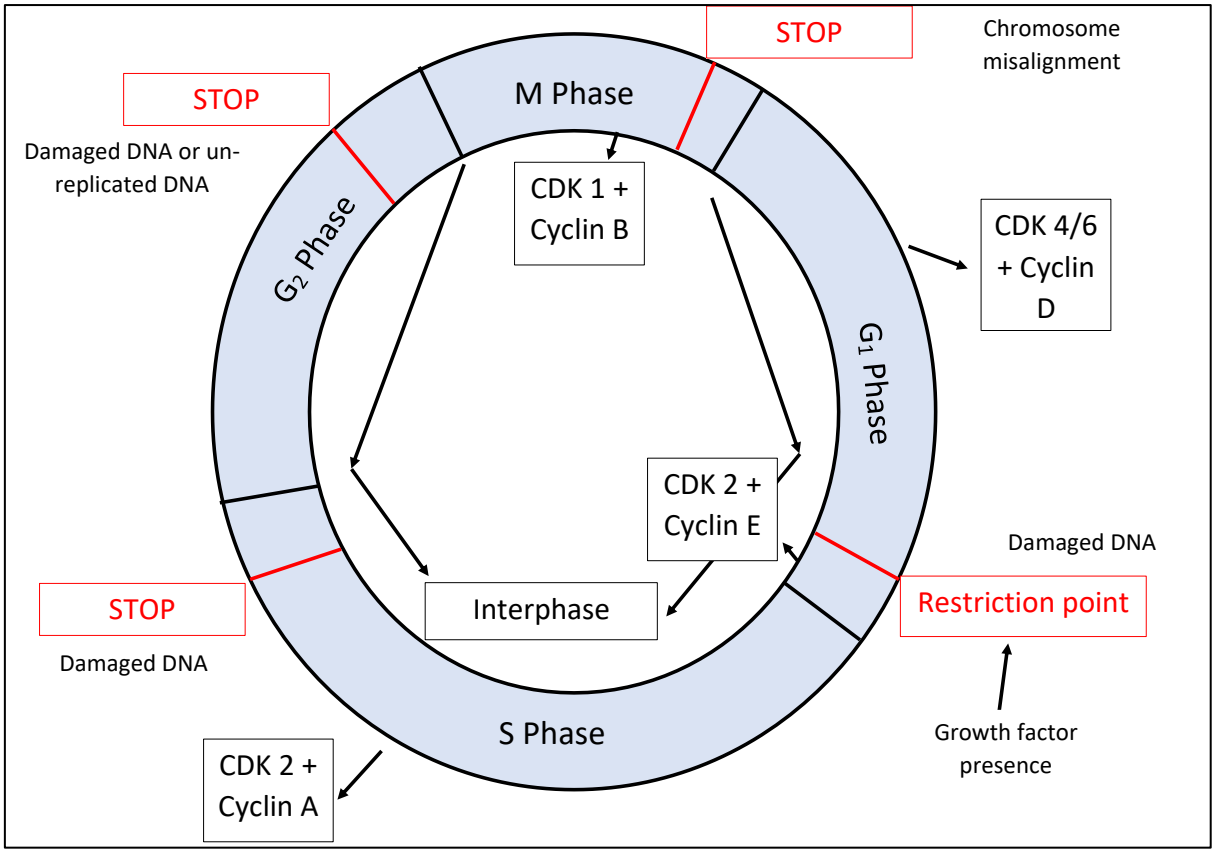

Figure 1.1 The phases of the normal cell cycle. The normal cell cycle is comprised of 4 phases, G_1, S, G_2 and M. Interphase is the stage in which the cell continuously grows this includes the G_1, S and G_2 stages. The availability of growth factors is responsible for the progression of the cell cycle at the restriction point of the G_1 phase. There are several other checkpoints within the cell cycle which are responsible for ensuring the correct and complete genome is inherited by daughter cells. The G_1, S and G_2 checkpoints cause cell cycle arrest in response to damaged DNA. The G_2 checkpoint also causes arrest due to incomplete DNA. The M phase stop point causes cell cycle arrest due to chromosome misalignment. The cell cycle is also driven by the presence of cyclin/CDK complexes, the position of these various complexes is demonstrated here. Adapted from Cooper, 2000: Schafer, 1998: Yang, 2012.

Interphase is the collective name for the initial three stages of the cell cycle. When a cell receives a signal to divide it enters into the first stage of interphase (G_1 phase). G_1 is the first growth phase in which the cell prepares for division, as it performs its normal functions it also grows in size (Cooper, 2000). The cell also begins to make copies of its organelles (Canadian Cancer Society, 2016), and begins larger productions of protein. The cell can then enter into the S phase (synthesis stage). Here the cell makes two copies of its DNA in order to gain two sets of chromosomes (one for each cell) (Cooper, 2000: Yang, 2012). The cell then progresses

onto the G_2 phase which is the second growth phase in which the cell makes more protein to get ready for cell division. The cell moves onto the final stage of the cell cycle which is the M stage which is collective name for mitosis and cytokinesis. Mitosis can also be broken down into four stages: prophase, metaphase, anaphase and telophase. In mitosis DNA condenses and allows the visibility of chromosomes. This stage is then followed by the separation of chromosomes into two clear sets. Cytokinesis is often named the final stage of mitosis as it is the point that the two daughter cells separate (Yang, 2012). The initial stage of mitosis is the prophase which is the point where the nuclear membrane breaks down and the condensation of chromosomes occurs. It is also at this point the chromosomes separate at the centrosomes (Schafer, 1998). A mitotic spindle then forms and attaches one end of the centrosome to a kinetochore, which is a protein structure located near the centromere (Yang, 2012). A delay signal may then be given in order to ensure that all the kinetochores are attached, and the chromosomes are all correctly aligned. These delay signals are also known as the spindle assembly checkpoint (SAC). Following this the chromosomes gather at the metaphase plate and this is known as metaphase. The chromosomes then separate at opposite poles of the cell which is known as anaphase (Hickson, Echard & O'Farrell, 2006). These stages are then followed by the final stage of mitosis which is telophase, in this stage new nuclear membranes are formed around the daughter nuclei and the chromosomes uncoil (Schafer, 1998). These are the stages the cell goes through to divide into two new cells. After mitosis the cells either re-enter into the G_1 phase or go into the resting G_0 phase.

Regulation of the cell cycle occurs through signalling pathways (which monitor events occurring during the cell cycle) (Schafer, 1998: Cyclacel, 2016) and through environmental cues (Cooper, 2000) (such as growth factor and mitogen availability). The cell cycle also uses a variety of checkpoints (figure 1.1) which allow the cycle to be paused in order to detect and then correct errors which may have occurred during the cell cycle. If the mistakes cannot be rectified then, in a normal cell, apoptosis (cell death) would be induced. Cell death is induced via the recognition of the damaged DNA at the various cell cycle checkpoints by kinases and P53 protein which induce the production of pro-apoptotic factors such as BAX, FAS and PUMA (Roos and Kaina, 2006). The induction of cell death due to DNA damage is complex process which involves several enzymatic reactions which will ultimately lead to the termination of the damaged cell; apoptosis is discussed further in section 1.3.7.1.

It is essential that cellular functions such as cell growth, DNA replication and mitosis are regulated during the cell cycle (Cooper, 2000), and this is accomplished through several checkpoints throughout the cycle (Schafer, 1998). The restriction point is one of the main checkpoints responsible for cell cycle regulation and occurs in the late stages of the G_1 phase (Cooper, 2000: Schafer, 1998). At this stage for the cell to progress through the cell cycle there must be adequate growth factor presence, if there are adequate amounts of growth factor then the cell progresses through the cell cycle (Cooper, 2000). However, if there is not enough growth factor presence then the cell enters into cell cycle arrest at the G_1 phase and subsequently enters into the G_0 rest phase and only re-enters the cell cycle upon the availability of the required growth factors (Schafer, 1998). If the restriction point checkpoint is passed then the cell must progress onto the S phase and continue through the cell cycle (Cooper, 2000). Damaged DNA can have progression through the S phase of the cell cycle delayed and arrested at the G_1 checkpoint, which provides time for the damage to be rectified (Cooper,2000). A G_1 Checkpoint arrest is generally mediated by the rapid elevation of the P53 protein levels (Schafer, 1998) and its action, which is discussed further in section 1.1.2. There are other checkpoints within the cell cycle which hold the responsibility of identifying damaged or incomplete DNA and ensuring that it is not replicated or inherited by daughter cells (Cooper, 2000: Schafer, 1998) (Figure 1.1). The main checkpoint of this nature is in the G_2 stage. Upon the detection of any un-replicated or damaged DNA then the G_2 checkpoint prevents the progression of the cell from the S phase into the M phase by signalling for cell cycle arrest (Cooper, 2000). This allows time for the DNA damage to be repaired or for the un-replicated DNA to be replicated correctly. Another vital checkpoint occurs towards the end of the mitosis stage and is responsible for monitoring chromosome alignment at the mitotic spindle (Schafer, 1998). This ensures that each daughter cell acquires a complete set of chromosomes. If this fails then the cell cycle arrests at metaphase until the correct alignment and acquirement of a full set of chromosomes can be achieved for each daughter cell (Schafer, 1998).

It is important that replication of the DNA of a cell only occurs once in the cell cycle, this is achieved by a family of proteins known as mcm proteins (Cooper, 2000). These proteins bind the replication origins with origin replication complex (ORC) proteins, this binding initiates replication (Schafer, 1998). As mcm proteins can only bind replication origins in the G_1 phase

the process of replication can there for begin at the start of the S phase but is regulated so it can only bind once (Schafer, 1998). Once replication has begun mcm proteins are displaced from the origin and so no further replication is able to take place until the cell re-enters the G_1 phase of the next cell cycle (Cooper, 2000).

Cell cycle progression is also dependent on the activation and deactivation of regulatory molecules known as cyclins and cyclin dependent kinases (CDKs) (figure 1.1) (Cooper, 2000: Schafer, 1998: Yang, 2012). CDKs are not active unless they are in the presence of their cyclin counterpart. Cyclins are known as such due to their cyclic nature of synthesis and degradation in each cell cycle (Yang,2012). There are four classes of cyclins in total, three of which are directly involved in the regulation of the events within the cell cycle, these are G_1/S cyclins, S cyclins and M cyclins, while G_1 cyclins are responsible for the initiation of the cell cycle (Yang, 2012). G_1 cyclins act in response to extracellular factors such as growth factors or mitogens which are essential for the initiation and maintenance of the transition to the S phase (Yang, 2012). These complexes are also regulated by proteins which include P53 and are downstream targets of cyclin-CDK complexes such as E2F and retinoblastoma protein (pRb) (Schafer, 1998). Different cyclin/CDK complexes function at different stages of the cell cycle and their target protein depends on the cyclin/CDK complex (Yang, 2012). In the G_1 phase the target protein is pRb (Schafer, 1998), hypo-phosphorylated pRb binds the E2F transcription factor which makes it inaccessible for transcription (Schafer, 1998). The G_1 cyclin/CDK complex (E-CDK2) initiates the phosphorylation of pRb which causes the pRb to release E2F, allowing it to participate in the transcription of proteins required for the progression of the cell cycle (Kato, Matsushime, Hiebert, Ewen and Sherr, 1993: Yang, 2012). This allows for the progression of the cell from the G_1 phase to the S phase, the restriction point is regulated by pRb (Schafer, 1998). Cyclin dependent kinase inhibitors (CKDI) are responsible for constraining the effects of CDKs, there are two types of CDKI (Sherr and Roberts, 1995). The first type inhibits CDK4 (INK4) proteins and bind and inhibit CDK4 and CDK6 proteins (Sherr and Roberts, 1995). The second type of CDKIs are CDK-interacting proteins cip/kip family of proteins and have a broader mechanism of action than INK4 (Sherr and Roberts, 1995). These CDKIs block the activity of CDKs by forming a trimeric complex. The cell cycle checkpoints are therefore also regulated by CDKIs as it is the checkpoints where the cell cycle is typically arrested. At the G_1 checkpoint is typically regulated by both INK4 and cip/kip inhibitors in

order to be able to arrest cells in the G_1 phase (Holland and Cleavland, 2009). This inhibition occurs via the binding of CDK4 to INK4 as opposed to D-cyclin, unbound cyclin therefore degrades and prevents the progression of the cell cycle (Diehl, Zindy and Sherr, 1997). This CDKI is activated upon the detection of DNA damage. The G_2 checkpoint is P53 protein dependent (Levine, 1997).

There are many diseases which include cancer which are the result of unregulated cell growth/ death which have occurred due to mutations within the cell cycle controlling molecules (Cooper, 2000). Therefore, understanding how a treatment interacts with the cell cycle could be key in predicting its success as an anti-cancer treatment. This research will aim to determine whether treatment with a GAG extract can induce apoptosis of cells which are going through the cell cycle in an uncontrolled manner (cancer cells).

1.1.1 Pathological outcomes of uncontrolled progression through the cell cycle

As the cell cycle is essential for cell proliferation control it is therefore understood that cancers can develop as a result of cells proliferating in an uncontrolled fashion (Sompayrac, 2015). In genomic sequencing studies there have been several somatic mutations (occur in any cell apart from germ cells) within genes identified which contribute to the initiation of cancer (Wood et al., 2007). Amongst the mutations found the most highly ranked 'cancer genes' were noted to either be directly or indirectly involved with cell cycle regulation (Sjoblom et al., 2006). One example of this is the tumour suppressor gene P53.

1.1.2 P53 tumour suppressor gene

Levine (1997) reported that over 50% of all cancers were found to have a mutated copy of the P53 tumour suppressor gene. It has been estimated that cancers which derive from over 50 human cell types and/or tissues have mutations in the P53 gene (Levine, 1997: Schafer, 1998: Somapayrac, 2015: Yang, 2012).

P53 is a protein which accumulates as a response mechanism to cellular stress caused by DNA damage, hypoxia or oncogenic activation (Helton & Chen, 2007). In a normal cell once the P53 gene has been activated and stabilised a transcriptional program is initiated and apoptosis or cell cycle arrest ensues (Yang, 2012).

The P53 protein operates at the G_1 phase of the cell cycle and causes cell cycle arrest upon recognition of DNA damage (Schafer, 1998). Upon recognition of DNA damage in the G_1 checkpoint there is an influx of P53 protein. The P53 protein then signals for the production of the P21 protein transcriptionally. The P21 family of proteins are highly important in the regulation of G_1 cell cycle arrest (Deng, Zhang, Harper, Elledge and Leder, 1995). This is because the P21 protein family can inhibit most CDKs through the binding of cyclins (cyclin E, A or B-CKD complex) (Yang,2012), this effectively blocks the phosphorylation of pRb, meaning E2F cannot be released to continue with the cell cycle (Schafer, 1998). This is one method by which the P53 protein results in cell cycle arrest. There are other P53-responsive genes other than P21, these include the BCL2-associated X protein (BAX) (Yang, 2012), when production of this protein or FAS or PUMA are induced in response to DNA damage then apoptosis is induced thus halting the cell cycle (Roos and Kaina, 2006).

Thus, a clear understanding of the mechanisms of regulating the cell cycle proliferation and differentiation of cells during cancer, along with their interactions with tumour suppressor genes such as P53 could be the key to finding an effective cure. Interestingly previous research carried out by KidsCan has identified GAG activity in a variety of cell lines including K562 which lacks the P53 gene (cells with a mutated P53 are less efficient at having apoptosis induced) (Roos and Kaina, 2006). This work aims to identify whether the extracts have activity on 'healthy' cells which go through the cell cycle in the usual manner and contain wild-type copies of the P53 gene.

1.2. Cancer

1.2.1. Cancer Pathology

Cancer is a very common condition affecting one in three people in their lifetimes (Cancer Research UK, 2019). It is recognised as cells within a certain area of the body which expand and multiply in an uncontrollable fashion, due to mutations within the proliferation control systems or safe-guarding systems that prevent against uncontrollable cell growth (Pecorino,2012). These issues can also prevent 'unhealthy' cells from entering into the controlled cell death pathway known as apoptosis. Cancer cells can be divided into two types which are either blood cell cancers or non-blood cell cancers (Sompayrac, 2015). Blood cell cancers arise when the bone marrow fills with immature cells which continuously proliferate

or when clusters of immature cells collect in the lymph nodes or secondary lymph tissues (Sompayrac, 2015). In non-blood cell cancers cancerous cells accumulate and form a body known as a tumour. Some cancerous cells also possess the ability to invade and destroy healthy tissue in surrounding areas and can spread from one part of the body to another, this process is called metastasis. The progression of cancer can be seen in figure 1.2.

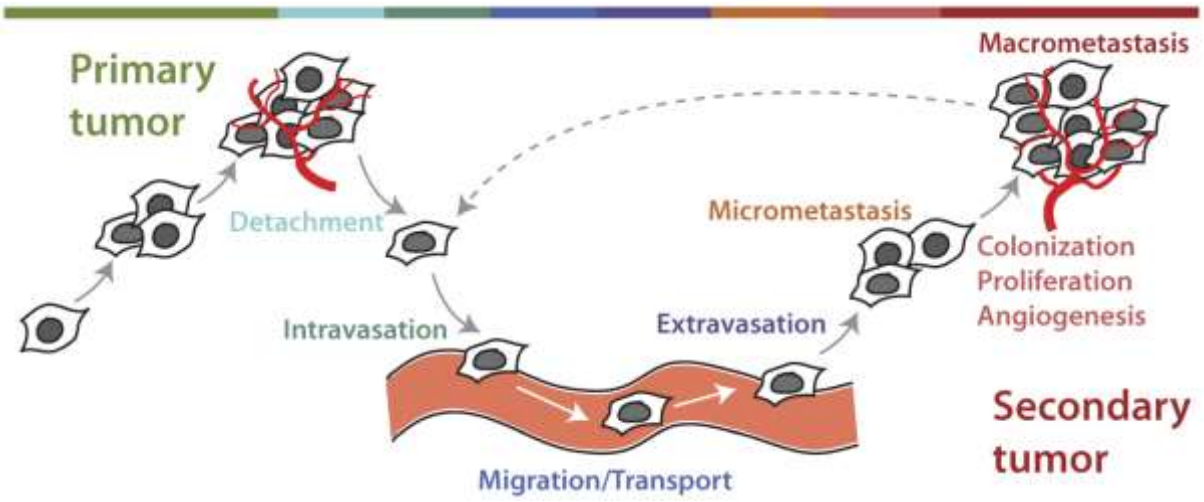

Figure 1.2 The stages of tumour progression and metastasis. (Divoli, Mendonca, Evans and Zhetsky, 2011).

1.2.1.1 Cells which can be affected by leukaemia

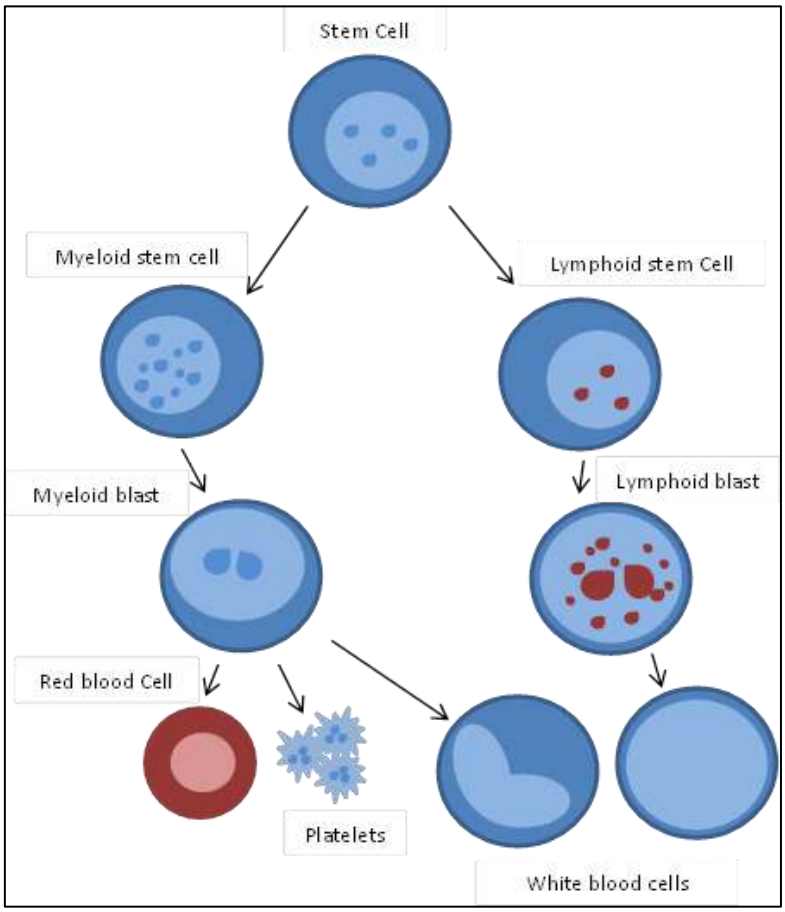

Figure 1.3 The maturation of the different type of blood cells from the stem cell progenitor cells. The maturation of blood cells from stem cell progenitors into: the lymphoid lineage and ultimate maturation into white blood cells or the myeloid lineage and maturation into red blood cells, platelets or white blood cells. (adapted from The National Institute of Cancer, 2018).

Figure 1.3 shows the progression of a stem cell into a variety of blood cells. In leukaemia the white blood cells produced from the stem cells are defective and cannot provide immune protection (Sompayrac, 2015). Defective myeloid cells produce either chronic or acute myeloid leukaemia which is determined by the speed at which the cancer progresses (Rabbitts, 1991: Journal of Leukaemia, 2018). If the leukaemia is classed as acute it means that the disease is progressing at a rapid rate (if untreated it can become fatal within months, (Appelbaum et al, 2014), the opposite can be said for chronic leukaemia. Myeloid leukaemia is more common in adults than children; however, it is possible for children to have a myeloid cell derived leukaemia (Shepard et al, 2016). Similarly, leukaemia of the lymphoid cells can also be described as acute or chronic depending on the speed of the cancer progression,

however lymphoid leukaemia is the most common amongst children (Shepard et al, 2016: Ward, Desantis, Robbins, Kohler and Jemal, 2014).

1.2.1.2 Cancer statistics

According to Siegel, Miller and Jemal (2015) there are approximately 200 different forms of cancer each with a unique set of symptoms, diagnosis method and treatment regime. With around 331,500 people in the UK diagnosed with cancer each (Cancer Research UK, 2019: Siegel, Miller and Jemal, 2015).

Ward et al., (2014) reported that approximately 1600 children are diagnosed with cancer each year, with leukaemia being the most prevalent (~500 new cases each year), and around one third of those cases prove to be fatal.

1.2.2. Leukaemia

Leukaemia mainly affects children with the most common incidence rate being before the age of 5 (Children with cancer UK, 2018: Ward et al, 2014). Survival rates for children with leukaemia have increased dramatically since the 1960s when it was deemed incurable for children, survival rates are now around 88% (Children with Cancer, UK, 2018: Ward et al, 2014) Leukaemia is a cancer of the white blood cells (WBCs) where defective WBCs are prominent in the blood and cannot provide immune protection (Sompayrac, 2015). This means that circulating levels of functioning immune cells are low and therefore leukaemia patients are prone to infection (Shepard et al, 2016: Sompayrac, 2015).

1.2.2.1 What causes leukaemia?

Bone marrow produces stem cells which have the ability to differentiate into any cell type including the three main blood cell types; white blood cells, red blood cells and platelets (Mummery, 2014: Maton et al, 1993). In a normal system stem cells fully develop into a cell type before they are released into the blood stream (Mandavilli, 2013). However, in leukaemia this system is compromised and the bone marrow releases excessive amounts of immature white blood cells, known as blast cells (Calabretta and Perrotti, 2004). As the volume of blast cells increase it causes a corresponding drop in the amount of circulating red blood cells and platelets. This decrease is generally responsible for the symptoms of

leukaemia such as fatigue, increased infection and unusual/unexplained bleeding (Shepard et al, 2016); in addition, blast cells are less effective than mature white blood cells at defending the body against bacterial and viral infections (Sompayrac, 2015). Thus, leukaemia patients are more susceptible to infection (Shepard et al, 2016: Sompayrac, 2015).

There are four main types of leukaemia (Shepard et al, 2016), which are dependent on the type of white blood cell affected, the speed of disease progression. These types are Acute lymphoblastic leukaemia (ALL), Acute myeloid leukaemia (AML), Chronic lymphoblastic leukaemia (CLL) and Chronic myeloid leukaemia (CML) (Sheppard et al, 2016). This research looked into CML and ALL responses to GAG extracts and fractions as control cancer cells.

1.2.2.2 Chronic myeloid leukaemia (CML)

Chronic leukaemia can be categorised according to which white blood cell (WBC) is affected by the cancer; lymphocytes which are responsible for fighting viral infection, myeloid cells which have many functions including aiding in fighting bacterial infection, defending against parasite infection and prevention of the spread of tissue damage (Kawamoto and Minato, 2004). It can take many years for leukaemia to advance through the different stages of the disease from the chronic stage through to the accelerated phase and finally into the blast phase meaning the concentration of blast cells in the peripheral blood has exceeded 30% (Hehlmann, 2012).

CML is a type of leukaemia which progresses slowly over a period of several years. It is a disease of haemopoietic stem cells, which results in the formation of cells which are un-functional and are in a stage of developmental immaturity (De Lavallade, 2013). These immature cells congregate within the bone marrow and are dramatically overproduced. When the blast cells are released into the blood it causes a corresponding drop in the level of circulating red blood cells (RBC) and platelets (Hehimann, Hochhaus and Baccarani, 2007).

CML is most commonly associated with a genetic mutation in which the breakpoint cluster region (BCR) gene which appears on chromosome 22 trans-locates and attaches to the ABL gene on chromosome (Kawamoto and Minato, 2004). This mutation is referred to as the Philadelphia chromosome (Goldman, 2008) and occurs in approximately 95% of CML cases (Harrison, 2001). This development leads to enhanced activity of tyrosine kinase, ultimately

leading to multiple signal cascades which involve cell growth, cell differentiation, cell adhesion and cell death (Kalidas, Kantarjian and Talpaz., 2001: Kabarowski and Whitte, 2000).

1.2.2.2.1 Symptoms of CML

CML consists of three main developmental stages. The first stage is the chronic phase where the cancer develops at a slow pace (Hehimann et al., 2007) and produces no noticeable symptoms. Patients can remain in this stage for a prolonged period of time with little or no increase in symptom severity (Shepard et al, 2016). It is within this stage that most patients are diagnosed, usually as a result of a general health check or blood test and so is considered an 'accidental' diagnosis. If symptoms are experienced at this stage they are usually considered as minor symptoms which may include weight loss and fatigue (Shepard et al, 2016). At this stage the patient will have a bone marrow blast cell level of <10% (Hochhaus et al, 2017).

The second stage of CML is referred to as the accelerated phase. At this point the cancer is progressing with a bone marrow blast cell level of around 20% (Hochhaus et al, 2017: Goldman, 2008). Further symptoms may be experienced at this stage including fever, weight loss, night sweats and bruising (Shepard et al, 2016). When CML develops into the final stage patients are said to be in the blast phase or in blast crisis. Calabretta and Perrotti (2004) described blast crisis as the terminal stage of CML, where there is a typical peripheral blood concentration of blast cells of more than 30%. This stage of the disease typically lasts only a few months and has a characteristic accelerated expansion rate of defective myeloid cells (Calabretta and Perrotti, 2004). At this point the symptom set is similar to acute leukaemia (discussed in section 1.2.2.2). The bone marrow is now full of blast cells and the circulating blood level of blast cells is also high (Goldman, 2008), the blast cells may also now be detectable in other organs.

1.2.2.2.2 Diagnosis of CML

Although diagnosis of CML is usually made via a blood test which shows elevated levels of blast cells (Hochhaus et al, 2017: Shepard et al, 2016), further tests should be carried out to confirm the diagnosis. Bone marrow aspirations allow the determination of the developmental stage the cancer is in through the measurement of the volume/ percentage

of blast cells present in the bone marrow in comparison to 'normal' cells. This can be done throughout the cancer to determine cancer progression. DNA analysis can also be carried out to detect the presence of the Philadelphia chromosome, as this is a strong indicator of CML and can determine a correct diagnosis as around 95% of CML patients have a positive result for the Philadelphia chromosome (De Lavallade, 2013).

1.2.2.2.3 How common is CML?

CML is a relatively rare form of cancer with approximately 680 people a year diagnosed in the UK (Siegel, Miller and Jemal, 2015). It mainly affects people within the 40-80 years old age bracket, but people of all ages can be affected. CML is a rare childhood leukaemia with less than 15 new cases each year (Ward et al., 2014).

This research used a CML cell line (K562) as a representative of a variety of cancers which GAGs have the potential to treat. Current treatment methods for CML aim to return blood levels back to normal levels, however leukemic cells can still be detected at some level. GAGs could potentially provide a treatment which may completely irradiate the cancer cells.

1.2.2.2.4 Treatment of CML

The current chemotherapy drug for CML patients is Imatinib tablets which are taken every day for life (Hochhaus et al., 2009). Imatinib acts via the selective inhibition of tyrosine kinase which effectively halts the cancer cell growth, (Hochhaus et al., 2009: Shah et al, 2004) causing the cell to enter into cell death (Vigneri and Wang, 2001). Imatinib does this by effectively blocking the ATP binding site of the BCR-Abl protein (Gambacorti-Passerini et al, 2003). This binding prevents tyrosine kinase being able to bind and therefore inhibits the activity (Gambacorti-Passerini et al, 2003). Imatinib however is not a cure for CML it simply aims to slow the progression of the cancer and tries to prevent the cancer entering into the next stage of the disease.

The treatment is aimed at achieving a normal blood cell count within a three month period. By 12 months post treatment it is hoped that the patient should be completely clear of bone marrow cells which contain the mutated Philadelphia chromosome (Goldman, 2008). After 18 months of treatment the patient should be at a stage where leukaemia cells can only be

detected by highly sensitive molecular testing (Goldman, 2008). At this point the patient is said to be in recovery.

1.2.2.2.4.1 Treatment of early stage CML

Imatinib is the primary treatment for early stage CML (Shah et al, 2004). Imatinib inhibits the production of abnormal WBCs through the inhibition of a tyrosine kinase and its reactions. Although between 10% and 40% of patients taking Imatinib are given alternative treatments after becoming resistant to its effects (Gambacorti-Passerini et al, 2003). An alternative would be Nilotinib, which works in a similar way to Imatinib by blocking the effects of proteins (Abl specific tyrosine kinase) responsible for cancer cell growth (Jobbour, Cortes and Kantarjian, 2009). As imatinib works by effectively closing the ATP binding site for tyrosine kinase in the BCR-Abl protein, resistance can come about when the BCR-Abl protein adjusts its equilibrium to a more active conformation or to an open position (Gambacorti-Passerini et al, 2003).

1.2.2.2.4.2 Treatment of advanced CML

Once the cancer has progressed into more advanced stages, chemotherapy is considered as the next course of action (Daiziel, Round, Stein, Garside and Price, 2004: Cancer Research UK, 2019). Oral tablets are given to begin with as side effects are considered to be milder, these tablets are generally imatinib if this was not the treatment used during the chronic phase (Daiziel, et al. 2004). If imatinib was used during the chronic phase then generally hydroxycarbamide is given orally, this drug aims to reduce the white blood cell count and control symptoms (Daiziel et al, 2004). Hydroxycarbamide does this via blocking the transfer of RNA to DNA through the inhibition of ribonucleotide reductase action effectively preventing cells from leaving the G1/ S-phase of the cell cycle (National Centre for Biotechnology Information, 2019). If symptoms persist or worsen then chemotherapy injections are required, however side effects are more severe. Chemotherapy choices would generally be a combination of cytarabine and daunorubicin, however other types may be considered (Virelizier et al., 2009: Cancer Research UK, 2019). If this treatment fails bone marrow transplants may be considered, but in most cases the risks associated outweigh the benefits (Cancer Research UK, 2019).

1.2.2.2.5 What is the outlook for a CML patient?

The outlook is dependent on treatment tolerance and response. Around 60-65% of patients treated with Imatinib tablets tolerate the treatment and go on to see an improvement in symptoms (Shah et al., 2004). More than half of patients who don't respond to Imatinib will respond to another chemotherapy drug (De Lavallade, 2013). If an improvement is not seen after the use of chemotherapy drug a bone marrow transplant may be considered. If the CML is diagnosed within the chronic stage almost 90% of patients will survive the 5-year mark post diagnosis (Goldman, 2008).

1.2.2.2.6 The K562 cell line

The K562 cell line originated from a 53year old female who was in the blast crisis phase of CML, which is Philadelphia chromosome positive (Drexler et al., 2000). In culture the cells appear rounded in shape and don't exhibit the clumping that can be noted in other suspension cells lines.

Klein et al (1976) examined the K562 cell line to look specifically into B cell and T cell properties of the cell line. They noted that the cells lacked B markers for immunoglobulins unlike B cells and drew more similarities to T cell lines. This was due to the fact the cells were lysed rapidly by C'/Fc receptor positive human blood leukocytes and also did not facilitate mixed lymphocyte culture (MLC) reactions. However, the K562 cell line doesn't have T antigens and has high radiosensitivity and is also sensitive to thyamine growth inhibition (Klein et al. 1976). This makes it difficult to determine whether the K562 cell line is of B or T cell lineage.

K562 cells also do not possess N-APase which is an enzyme that can be found in a cell line which has lymphoid lineage or in lymphoproliferative diseases (Klein et al., 1976). Klein et al. (1976) also concluded that the K562 cell line was not B cell derived and although they did contain some features of T cells. The general characteristics of the cells also suggested they were not lymphoid cells, due to the lack of or minimal differentiation making the nature of the cells difficult to determine with any degree of certainty. A cellular marker may be present for CML on the cell surface they also concluded it may be possible to describe the K562 cell line as granulocytic cells (Klein et al., 1976).

The research carried out by Klein et al. (1976) failed to determine the exact lineage of the K562 cell line due to the fact they demonstrated properties of both B and T cells.

As the K562 cell line lacks the gene for P53 (Stuppia et al., 1997), assays carried out on this cell line may provide a clearer view on how GAGs target the cells, as any activity on this cell line would suggest activity may not be through the traditionally targeted P53 pathway.

1.2.2.3 Acute Lymphoblastic Leukaemia (ALL)

Acute leukaemia refers to a cancer which progresses both rapidly and aggressively and requires immediate treatment (Inaba, Greaves and Mullighan, 2013). Acute leukaemia is classified based on the type of white blood cell which has been affected by the cancerous mutations. There are two main types of white blood cell which can be affected by acute leukaemia; lymphocytes whose main function is to fight viral infection and neutrophils which have several functions within the body, to fight bacterial infection, to defend the body against parasites and finally to prevent the spread of tissue damage (Kawamoto and Minato, 2004).

1.2.2.3.1 Symptoms of ALL

Usually the symptoms of ALL progress slowly at the early stages but swiftly increase in severity as the number of blast cells within the circulating blood increases (Shepard et al., 2016: Grigoropoulos, Petter, Van't Veer, Scott and Follows, 2013). The main symptoms of ALL are pale skin, fatigue and regular recurrent infections over short periods of time (Shepard et al, 2016). Unusual but regular bleeding can also occur during the progression of ALL (Pui and Robinson, 2008) this is generally due to the drop in platelet levels associated with the increase in blast cells (Sompayrac, 2015).

1.2.2.3.2 Diagnosing ALL

In order to diagnose ALL blood tests are carried out first to identify whether there are high amounts of white blood cells and low amounts of red blood cells and platelets. Most patients with ALL have a platelet count of less than 150,000/µl, the normal level for platelets is 150,000/µl (Jorge, Cortes, Hagop and Kantarjian, 1995). White blood cell counts can be variable in ALL patients and so the platelet count and bone marrow aspirations generally lead to the diagnosis of ALL (Jorge et al., 1995). Doctors may also use the blood tests or bone

marrow aspirations to identify the presence of blast cells which can allow a determination of the stage at which the cancer is at (Jorge et al, 1995: Shepard et al, 2016).

Bone marrow aspirations may also be carried out; this will firstly allow the identification of leukemic cells. Secondly it will allow for the classification of the cells affected by the leukaemia into size, shape and also whether the leukaemia derived from B lymphocytes or T lymphocytes. This determination will allow a correct treatment regime to be developed (Hunger et al., 2012).

X-rays, CT scans and ultrasounds may also be carried out in order to fully determine the development stage of the cancer and whether it has spread.

1.2.2.3.3 How common is ALL?

Around 654 people in the UK are diagnosed with ALL each year (Ward et al., 2014). ALL is also the most common form of childhood cancer affecting approximately 1 in 2000 children. Around 85% of children diagnosed are between the ages of 2 and 5 years old (Ward et al., 2014).

1.2.2.3.4 Treatment of ALL

The treatment regime for ALL is generally a combination therapy of chemotherapy drugs which are given in hospital until symptoms improve and then on an outpatient basis thereafter. These combinations may begin with a steroid such as dexamethasone along with chemotherapy drugs such as vincristine and asparaginase (Pui and Evans, 2006). The addition of other chemotherapy drugs such as cytarabine may be required to alleviate symptoms (Pui and Evans, 2006). Once blood levels have returned to a normal level methotrexate and mecaptopurine may be used as chemotherapy to eradicate any remaining leukemic cells (Pui and Evans, 2006). Radiotherapy may also be given if the ALL has progressed onto an advanced phase. If chemotherapy and radiotherapy fail to treat the cancer a bone marrow transplant may be offered (Kersey et al., 1987). If a cure is not possible then the absence of healthy white blood cells will ultimately mean that the patient has a higher susceptibility to a life-threatening infection. They may also be at risk of an uncontrolled serious bleed.

1.2.2.3.5 What is the outlook for an ALL patient?

Usually the outcome for a patient post ALL diagnosis is good, almost all children diagnosed and treated for ALL will enter into a remission phase and will therefore be symptom free (Inaba et al., 2013). Also, around 85% of children diagnosed with ALL will be completely cured of the cancer, (Shepard et al, 2016: Children with cancer UK, 2018). The outlook for adults sees around 40% of those patients completely cured (Pui and Evans, 2006). It is thought that the poor prognosis in adults could be linked to further chromosome mutations such as the presence of the Philadelphia chromosome which is present in 50% of adult ALL patients (Kuhnl et al., 2010: Thomas et al., 2001). The poor adult prognosis has also been linked to the inability to tolerate the intensive treatment required in ALL (Goldstone et al., 2008). Philadelphia chromosome presence is also linked to poor prognosis in childhood ALL however it only occurs in approximately 5% of cases (Koo, 2011).

1.2.2.3.6 The MOLT-4 cell line

The MOLT-4 cell line was originally obtained from a 19 year old male patient who at the time was suffering from ALL. After a multi-chemotherapy drug regime the patient entered into relapse. In culture the MOLT-4 cell line appears circular and is a suspension cell line (Minowada et al., 1972).

Klein et al., (1976) reported that the MOLT-4 cell line has T-cell characteristics as they had no surface immunoglobulins or Fc receptors. They also reported the presence of terminal deoxynucleotidyl transferase activity within the cell line. This enzyme activity is found within the thymus but not the bone marrow and so they concluded that the MOLT-4 cell line represented a leukaemia T-cell of thymocyte origin (McCaffrey, Smoler and Baltimore, 1973).

Greenberg et al., (1988) carried out a Southern blot analysis of the cell line which identified an unusual rearrangement of the gamma chain gene in the T-cell antigen receptor. This discovery led the team to carry out further immunotypic and karyotype research, in which they discovered that the MOLT-4 cell line had the immunophenotypic characteristics of thymocytes (hematopoietic progenitor cells which are present in the thymus and whose main function is the production of mature T lymphocytes) and expressed CD1 and CD5 markers which further link MOLT-4 cells to T-cell origin (Greenberg et al., 1988).

As ALL is the most common form of childhood cancer, the potential of GAGs as a treatment method would not only benefit patients through a reduction of side effects as is expected in GAG treatment but they may also have the potential to treat those patients which have not responded to current treatment methods. Also the use of an ALL cell line may also show that GAGs carry the potential to treat a variety of cancers, which may suggest a broader mechanism of action which doesn't target one particular type of cancer.

1.2.2.4 Lymphoblastic Lymphoma (LL)

Lymphoblastic lymphoma is a very aggressive form of non-Hodgkin lymphoma. It is a rare form of cancer and accounts for around 2% of non-Hodgkin lymphomas (NHL) diagnosed each year (Ward et al., 2014). LL is usually caused by a mutation in a T cells DNA but can also develop from B lymphocytes (Marcus, Sweetenham and Williams, 2013). LL is a cancer type which mainly affects children and teenagers (Wright, McKeever and Carter, 1997); the condition of lymphoblastic lymphoma is very similar to ALL as both involve mutations, abnormality and uncontrollable growth in white blood cells (Cortelazzo, Ponzoni, Ferreri and Hoelzer, 2011).

LL is an uncommon cancer which develops in the lymphatic system. In a non-Hodgkin lymphoma affected lymphocytes multiply in an abnormal manner and collect in certain areas of the lymphatic system such as the lymph nodes (Cortelazzo et al., 2011). Affected lymphocytes as in ALL lose their infection fighting abilities and so the body is more susceptible to infections.

1.2.2.4.1 Symptoms of LL

The most common symptom of LL is painless swelling of the lymph nodes usually located in the neck, arm pit or groin (Sompayrac, 2015: Evans and Hancock, 2003). LL also has a similar symptom set to ALL with associated appetite and weight losses as well as fatigue and fever (Evans and Hancock, 2003). More specific symptoms will depend on where the lymphoma is growing.

1.2.2.4.2 Diagnosing LL

A diagnosis of LL is only given once a biopsy of the lymphoma has been taken and scans have been performed. This allows for the determination of the abnormality and the spread of the cancer, this process is known as staging (Hoelzer and Gokbuget, 2003). LL diagnosis also involves using the biopsies to carryout immunophenotypic analysis in order to ensure the patient isn't suffering from a different form of lymphoid malignancy or non-lymphoid malignancy (Bassan, Maino and Cortelazzo, 2016).

1.2.2.4.3 How common is LL?

More than 12000 people are diagnosed with NHL each year but only 240 of those cases are LL (Bassan, Maino and Cortelazzo, 2016: Evans and Hancock, 2003: Wright, McKeever and Carter, 1997). The condition can develop at any stage of life however people under the age of 35 appear to be more susceptible to developing LL (Bassan, Maino and Cortelazzo, 2016: Wright, McKeever and Carter, 1997).

1.2.2.4.4 Treatment of LL

As LL is an aggressive form of cancer, treatment is required immediately upon diagnosis, the treatment regime should also consist of multiple chemotherapy drugs. Intensive chemotherapy is given in hospital with the aim of killing the cancer (Cortelazzo et al., 2011). Once this initial intensive stage of treatment is over chemotherapy is given on an outpatient basis to prevent the return of the lymphoma. Treatment of LL can take up to 2 years and is very similar to that of ALL (Hoelzer and Gokbuget, 2003).

As LL is a rare and aggressive form of cancer it would be interesting to identify whether the GAG extracts have any beneficial effect on the cell line, as efficient treatment could provide a better outlook for patients who have been diagnosed. As current treatment involves intensive chemotherapy this could prove detrimental for childhood patients. GAGs could therefore provide a milder treatment option if activity is identified.

1.2.2.4.5 The U698 cell line

The U698 cell line was originally obtained from the right tonsil of a seven year old boy who was suffering from lymphoblastic lymphoma (Nilsson and Sundstrom, 1974). Treatment had

not been administered when the biopsy was taken; the lymphoma was fairly resistant to chemotherapy and radiotherapy (Nilsson and Sundstrom, 1974: DSMZ, ACC4, 2016). The patient died around two months after the biopsy was taken. The cells are in suspension when culture and exhibit some clumping and adherence to the flask.

Nilsson and Sundstrom (1974) analysed the U698 cell line and identified that the cells appeared to be differentiated lymphoid cells which had rounded nuclei. They also concluded the majority of the cells in culture resembled lymphoblasts although a small portion of the cells had normal lymphocyte features.

The U698 cell line expresses surface IgM and resembles B cell morphology which would suggest that the cell line is of B-cell descent (Godal, 1982), as it also only produces one class of immunoglobulin it could also be assumed that the U698 cell line is a clone (Pollack et al., 1973).

GAG extracts have not yet been tested on a lymphoblastic lymphoma; any activity on this cell line could potentially suggest that GAGs may provide a milder treatment option for another type of cancer.

1.2.3 Current Chemotherapy and radiotherapy treatment

1.2.3.1 Chemotherapy

In basic terms chemotherapy (in the treatment of the three cancers previously mentioned) is given to eradicate cancerous cells in the bone marrow (Cortelazzo et al., 2011). Chemotherapy can be administered orally in the form of tablets however one or more of the treatment drugs will be given in the form of injection. This is due to the poor oral bioavailability of most chemotherapy drugs, so administering the drugs intravenously is required (Corrie, 2008). Side effects from chemotherapy can include tiredness, nausea and hair loss (Carelle et al., 2002). If at any point the side effects from chemotherapy become too severe steroidal therapy can be given to improve the side effects (Hu, Sun, Wang and Gu, 2016). Steroids such as dexamethasone are generally given to help alleviate symptoms such as nausea and loss of appetite, they may also help with pain relief (Twycross, 1994). Therapy may also be stopped entirely if the side effects become too severe to allow the patient time to recover before treatment is started again.

Chemotherapy is carried out in three stages; induction, consolidation and maintenance (Avendano and Menendez, 2015).

1.2.3.1.1 Induction

The first stage of treatment is the induction phase which is designed to kill leukemic cells in the bone marrow thus restoring the balance of the three blood cell types, white blood cells, red blood cells and platelets (Haddad et al., 2013). This stage should alleviate the symptoms of the cancer and typically last around two weeks to several months. The induction stage of treatment is usually carried out in hospital or at a specialist centre, at this point regular blood transfusions may also be necessary as it is unlikely that the patients' blood will contain sufficient levels of healthy cells (WBC counts of 4500-11000/µl and platelet levels of 150,000-450,000/µl) (Jorge et al., 1995). The chemotherapy drugs used will generally be selected based on the cancer type but may include imatinib (Daiziel et al., 2004), daunorubicin, cytarabine and vincristine (Virelizier et al., 2009: Pui and Evans, 2006). A steroid such as dexamethasone may also be administered (Pui and Evans, 2006). Chemotherapy drugs work via many mechanisms, some of which include disrupting enzymes required for DNA replication or progression through the cell cycle (Daizel et al., 2004: Goldman and Fyfe, 1974).

1.2.3.1.2 Consolidation

Stage two of chemotherapy treatment is the consolidation phase which aims to completely eradicate all remaining leukemic cells in the central nervous system, as if just one cell remains then it is entirely possible that the cancer can return (Avendano and Menendez, 2015). This stage of treatment can take several months to complete; regular chemotherapy injections are administered but this time on an outpatient basis. However hospital stays may be required if symptoms worsen or if an infection occurs.

1.2.3.1.3 Maintenance

The final stage of treatment is the maintenance phase, this stage involves regular oral chemotherapy drugs and check-ups to monitor the effectiveness of the treatment being administered (Avendano and Menendez, 2015). This stage can last up to two years and acts as an 'insurance policy' against the return of the leukaemia.

1.2.3.1.4 Side effects of chemotherapy

Side effects from chemotherapy are generally experienced as chemotherapy targets any cells which are proliferating quickly. This could be cancerous or healthy cells as there is no differentiation between the two where chemotherapy is concerned.

Side effects from early stage treatment can include bone and joint pain as well as loss of appetite and nausea (Oeffinger et al., 2006: Siegel et al., 2012). Hair loss and insomnia may also be experienced (Siegel et al., 2012). If side effects become too severe treatments may need to be halted to allow the patient to recover and have a rest period. Other complications may also require the treatment to be halted until they have been addressed; these include psychological effects and immunosuppression (Siegel et al., 2012: Holland et al., 2010).

The side effects of advanced treatment include the above with more severe forms and also include infertility and bruising. Kidney, liver and heart damage may also occur in long term chemotherapy patients (Miller et al., 2016).

1.2.3.2 Radiotherapy

Radiotherapy is the use of controlled radiation in high doses. It is mainly used when the cancer is in an advanced stage and has migrated to the nervous system or brain (Miller et al., 2016). Radiotherapy can also be used to prepare the body for a bone marrow transplant (Quast, 2006). Side effects experienced from radiotherapy treatment are similar to those of chemotherapy including hair loss, fatigue and nausea (Oeffinger et al., 2006). In young children radiotherapy can also restrict growth when puberty is reached (Miller et al., 2016). As cells within a child are proliferating at a faster rate than in adult's radiotherapy can target and alter their healthy cells as well, preventing children from growing in the correct manner (Miller et al., 2016)

A bone marrow transplant or stem cell transplant may be needed if the patient is non-responsive to chemotherapy or radiotherapy.

1.2.3.3 Why are new chemotherapy drugs needed?

Although current chemotherapy drugs are effective in the majority of patients, the side effects experienced can be detrimental to a patient (Holland et al., 2010: Siegel et al., 2012). Children in particular can prove to have fatal responses to chemotherapy treatment (Nurgali, Jagoe and Abalo, 2018). GAGs could provide new treatment methods which may potentially demonstrate the same if not better anti-cancer results while also exerting milder side effects which would provide a more beneficial treatment option for children in particular. GAGs may also potentially provide a treatment method which may prove effective for patients who have not responded to other treatment methods if their mechanism of action proves to be different to traditional treatment methods.

1.3 Glycosaminoglycans (GAGs)

GAGs are the most abundant heteropolysaccharide in the body, they are linear unbranched polysaccharides which contain a repeating disaccharide unit (Kubaski et al., 2017). The repeating units consist of an amino sugar (N-acetylglucosamine, glucosamine that is variously N-substituted and N-acteylgalactosamine) and either a uronic acid group or a galactose (Afratis et al. 2012). They are highly negatively charged and are mainly located on the extracellular matrix or on cell surface. The negative charge comes from highly sulphatated regions (Nelson and Cox, 2008) which are located at discrete positions along the GAG chains.

The properties and action of the GAGs is dependent on their structure, and they can thus be categorised into two main subgroups (Glucosaminoglycans and Galactosaminoglycans) based upon the sugar group that makes up the repeating disaccharide unit (Weyer et al. 2012). The subgroups can be further narrowed down into the molecules that make up the units, glucosaminoglycans can consist of four molecules; heparin, heparan sulphate, keratin sulphate and hyaluronan (Weyer et al., 2012). Galactosaminoglycans are made up of two types of molecules which are chondroitin sulphate and dermatan sulphate (Kim et al. 1996).

GAG actions are governed mainly by their disaccharide structures and the sulphation levels and patterns which facilitate the GAG function. These properties allow GAGs to conduct a wide range of different functions within the body, which relates to their presence on all cell surfaces (Gandhi and Mancera, 2008; Nadanaka et al, 2013). They are a major component of

the extracellular matrix (Nelson and Cox, 2008) due to their ability to bind with and interact with proteins. It is understood that GAGs play an important role in the cellular functions responsible for inflammation, cell proliferation and cell differentiation (Hori et al, 1981). This is due to their ability to interact with various signalling molecules such as growth factors, cytokines and chemokines (Sasisekharan, Shriver, Venkataraman and Narayanasami, 2002).

The biological activity of GAGs is also dependent on their side chains as it is the side chains that facilitate any interactions with protein ligands via their saccharide units (Salmivitra, Lidholt and Lindahl, 1996). Linear GAGs are mainly made up of heparan sulphate and chondroitin sulphate (Nadanaka et al, 2013). Hyaluronan is the only GAG component which contains no sulphur (Yip, Smollich and Gotte, 2006; Nakano, Beth and Pietrasik, 2009).

As GAGs can also be located on the surface of cancerous cells they could potentially be a target for cancer therapies (Sugahara and Kitagawa, 2000). Any anti-tumour effect the GAGs exhibit will be likely to depend on the individual growth factors affected, the cell type and the specific regulation for the sulphate group position.

It is not yet known which GAGs make up the cockle and whelk extracts and what concentration of each individual GAG is present however it is likely to be a mixture of HS, CS and DS. Therefore the activity of the extracts which has been noted could be due to the combination of numerous GAGs.

1.3.1 Glycosaminoglycan biosynthesis

GAGs from both glucosaminoglycans and galactosaminoglycans are synthesised at the golgi apparatus and all types of GAG apart from hyaluronan are further modified by O-sulphotransferases to add sulphate groups to the disaccharide units (Afratis et al, 2012). When GAGs are synthesised the free GAG chains are secreted to the extracellular space and distributed further to the pericellular space and the extracellular matrix (Nikitovic et al, 2004).

The side chains of GAGs are covalently bonded to a core protein via the GAG protein linkage region. The synthesis of GAGs is a step by step addition of monosaccharides (Nadanaka et al, 2013) and is completed by specific glycosyltransferases (DeAngelis, 2002). During this formation a xylose residue is also phosphorylated (Nadanaka et al., 2013).

The number of side chains is very important in GAG biosynthesis as it depicts which component of the GAG family is synthesised (Koike et al 2009). Honda et al (1982) suggested that the inhibition of sulphate and glucosamine could decrease GAG synthesis. They also deduced that abnormalities within the GAG level would also affect the synthesis of proteoglycans.

1.3.2 Proteoglycans (PG)

GAGs are commonly found to be interacting with proteins in the body; they do this through forming molecules known as proteoglycans (PG). A PG is a heavily glycosylated protein which is made up of a core protein with one or more GAGs covalently bonded to it (Meisenberg and Simmons, 2006) as can be seen in figure 1.4.

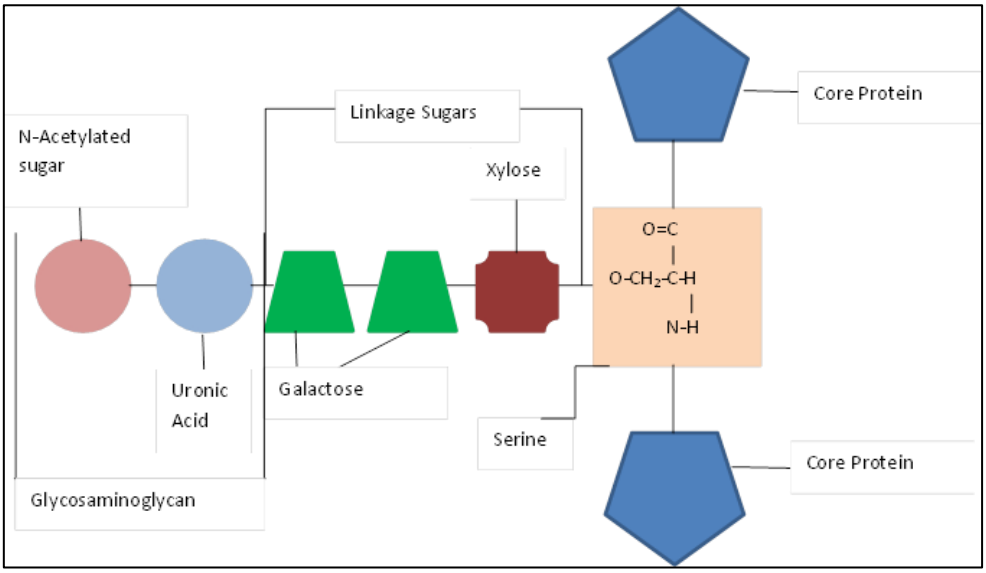

Figure 1.4 The structure of a proteoglycan. The generic structures required and the binding points to make a proteoglycan (adapted from Buzzle,2015).

In order to link a GAG to a protein core it requires a specific trisaccharide sequence that is composed of two galactose residues and a xylose residue (Gandhi and Mancera, 2008). This trisaccharide unit then covalently attaches to a serine residue via an O-glycosidic linkage (Jackson et al, 1991). When a GAG joins onto a core protein a tetrasaccharide bridge is created. Upon covalently bonding with its complementary cell surface protein the GAG creates a PG. Therefore a PG macromolecule consists of several GAG chains covalently bound to a cell surface protein (Chatzinikolaou et al, 2008). PGs are highly variable in both structure

and function; this is due to the level of variation in the composition of the protein core. The protein core differences are dependent upon the exons which are used to create the protein during the genomic sequence translation (Varki et al,. 2009).

Proteoglycans are known to function as cofactors in several biological functions (Nadanaka et al, 2013). It is the GAGs bound to the cell surface proteins which create the interactions with biological functions which include angiogenesis (discussed further in section 1.4), cell adhesion and the regulation and production of growth factors (Nadanaka et al, 2013: Yip, Smollich and Gotte, 2006).

PGs also function as fillers between cells and other complexes; these could be other PGs or fibrous proteins like collagen (Meisenberg and Simmons, 2006). Finally PGs are also heavily involved with the regulation of molecule movement and affect the stability of signals and proteins within the cellular matrix (Meisenberg and Simmons, 2006: Weyer et al, 2012).

1.3.3 Heparin and Heparan Sulphate (HS)

Both heparin and heparan sulphate (HS) are made up of repeating disaccharide units of hexuronic acid (Hex A) and glucosamine (GlcN), these units are sulphated at various positions along the disaccharide unit (Gandhi and Mancera, 2008). Heparin possesses a higher level of sulphation and is also more homogenous when compared to HS; it also lacks a domain structure (Gandhi and Mancera, 2008). There is a large amount of variation which occurs within the polysaccharide structures and high volumes of complex sulphation patterns (Skidmore et al., 2008). It is these patterns that create potential protein interaction sites. The structures of heparin and heparan sulphate can be seen in figure 1.5.

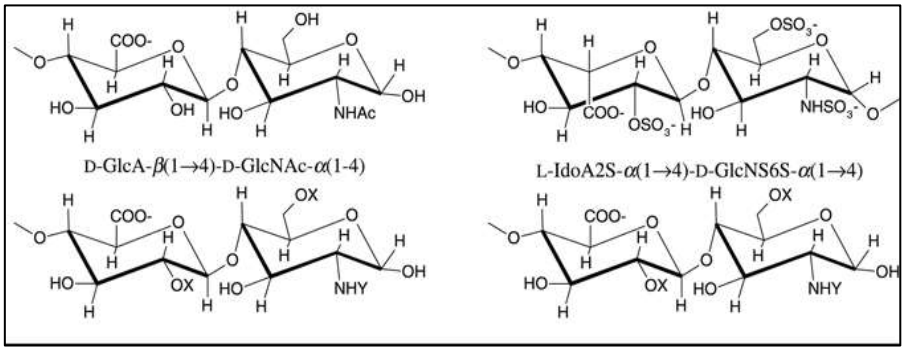

Figure 1.5 The structure Heparan Sulphate (left) and Heparin (right) respectively. (Gandhi and Mancera, 2008).

Heparin and HS are both very anionic and have linear disaccharide units. They are both also joined via 1-4 linkages (Skidmore et al, 2008). The glucosamine residues found in both can be sulphated to form an N-sulphated glycosamine (Glc NS) (Afratis et al, 2012). They can also be acetylated to form an N-acteylated glycosamine (Glc NAc).

Although heparin and HS are very similar in relation to disaccharide structure there are also several differences between the two. Firstly heparin is generally smaller measuring between 7-20 KD compared to HS which is 10-70 KD in size (Gandhi and Mancera, 2008). In comparison to HS, heparin possesses higher levels of sulphation, it also has significantly higher affinity in binding to antithrombin. Finally HS is generally synthesized in virtually all cell types whereas heparin is synthesized only in connective tissue mast cells (Varki et al, 2009).

1.3.3.1 Heparin and Heparan Sulphate biosynthesis

Heparin is exclusively produced by mast cells whereas HS is produced by virtually all cell types. Heparin also differs to HS through the amount of sugar residue modification. The modification is carried out by a series of enzymes which include sulphotransferases and epimerases (Varki et al, 2009).

The biosynthesis of HS GAGs begins in the golgi apparatus where four monosaccharides link and attach to a core protein. In HS synthesis N-acteylglucosamine (GlcNAc) is transferred to the linkage region (Nadanaka et al. 2013). The HS backbone is subsequently formed through the alternate addition of glucuronic acid (GlcUA) and GlcNAc via transferases (Nadanaka et al., 2013). The disaccharide unit additions are carried out by two different glycosyltransferases which effectively form a stable heterodimeric complex within the golgi apparatus (DeAngelis, 2002). This chain can then be modified, which can be done concurrently or independently and occurs by a series of enzymes sequentially. The main enzymes which modify the polysaccharide chain include; N-deacteylases, N-sulphotransferases and 2-O, 3-O and 6-O sulphotransferases (Nadanaka et al., 2013: DeAngelis, 2002).

The modification reactions which occur in heparan sulphate biosynthesis happen in clusters along the chain in regions which have no sulphates. The resulting HS chains are then organised into polymetric structures (larger structures made up of several repeating

monomer patterns) which have S-domains containing N-sulphated residues. It is these domains that give the GAGs their abilities to bind with growth factors and other proteins (Sugahara et al, 2000: Varki et al, 2009).

1.3.3.2 The role of heparin and heparan sulphate in health and disease

Heparin is used as an anticoagulant drug (Ludwig, 2009); it prevents and treats blood clots which may occur in the arteries, veins or lungs. It can also be given pre-surgery to reduce any risk of blood clots. Heparin is also given to patients who suffer from deep vein thrombosis or pulmonary embolisms (Ludwig, 2009).

In the inflammation process L-selectin is expressed by leukocytes and binds to HS expressed by endothelial cells (Parish, 2006). This binding initiates the attachment and rolling of leukocytes into blood vessels towards the area which has tissue damage or infection (Barthel, Gavino, Descheny and Dimitroff, 2007). This process of leukocyte extravasation has also been linked to inflammation and the metastasis of cancer cells (Barthel et al., 2007). It is thought that cancer cells achieve this through exploiting the selectin-dependent mechanism used by lymphocytes migrated to the source of tissue damage (Witz, 2006).

HS is a molecule that is present within all cell types and has numerous regulatory roles within normal and pathological conditions (Afratis, 2012). Cancer cells target HS as they need large amounts of space in order to grow past their normal limits. The cancer does this by releasing heparinises that degrade any HS located on the membranes of adjacent tissues (Sanderson, 2001). Once the HS is degraded the cancer cells can invade adjacent tissues and potentially enter into blood vessels. This gives the cancer cells the ability to metastasise and re-locate to other areas of the body (Bogenrieder and Herlyn, 2003; Jia, 2009). The invasion of blood vessels also allows angiogenesis of the cancer which allows it to grow in size. Sanderson (2001) identified that HS present on the cell membranes promoted cell adhesion, if the HS was not present then migration and invasion of malignant cells was promoted.

1.3.4 Chondroitin Sulphate and Dermatan Sulphate

Chondroitin sulphate (CS) and Dermatan sulphate (DS) GAGs are composed of alternating units of N-acetyl-D-galactosamine (GalNAc) and then either glucuronic acid (GlcA) or iduronic acid (idoA) (Afratis et al., 2012: Yamada and Sughara, 2008) shown in figure 1.6. The sugar

backbone of CS and DS can be sulphated which occurs mainly at the C2 position of the uronic acid residue. On the GalNAc residues sulphation can occur at the C4 and/or C6 positions (Yamada and Sughara, 2008). Diverse modifications of the sugar chains can also happen through C5 epimerase and O-sulphotransferases, this is responsible for the structural heterogenicity of CS and DS chains (Gandhi and Mancera, 2008: Yamada and Sugahara, 2008).

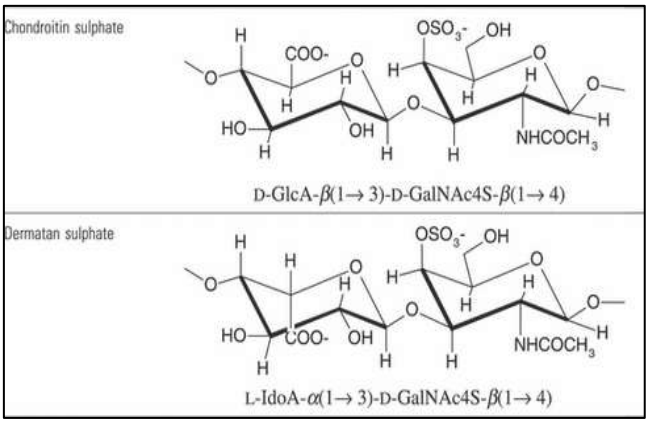

Figure 1.6 The structures of chondroitin sulphate and dermatan sulphate. (Gandhi and Mancera, 2008).

The CS and DS chains that are formed in the body have extensive sulphation modifications, there are also six different disaccharide units which come together to make up the CS and DS polysaccharide chains (Thelin et al, 2013). In order for the biosynthesis of CS and DS to begin a primary precursor polysaccharide must first be formed. This polysaccharide is made up of alternating glucuronic acid (GlcA) and N-acetyl-D-galactosamine residues (Maccarana et al, 2006). The addition of a α-GalNAc residue serves as a stop signal and prevents any further chain elongation (Koike et al, 2009).

The assembly of CS and DS chains happens in the endoplasmic reticulum but can also happen in the golgi apparatus. This process is initiated by the formation of the GAG linkage region. The linkage region is covalently bonded by serine residues which are located in different core proteins to eventually form CS and DS proteoglycans (Mikami and Kitagawa, 2013).

In previous research CS has exhibited anti-angiogenic properties by inhibiting transendothelial monocyte migration, which is the movement of monocytes through the blood vessel walls (Yip, Smollich and Gotte, 2006). CS can also be linked to cancer as it promotes an increase in the expression and activation of matrix metalloproteinases (MMPs)

and ADAMT (a disintergin and metalloproteinase with thrombospondin motif) during the extracellular matrix remodelling (Kaur and Reinhardt, 2015). Both molecules have been linked to angiogenesis, migration and roles within the degradation (MMP) or remodelling (ADAMT) of the extracellular matrix (Kelwick, Desanlis, Wheeler and Edwards, 2015: Van Lint and Libert, 2007). This expression and activation has been linked to several types of cancers (Kaur and Reinhardt, 2015).

DS adds flexibility to many normal bodily responses as well as many pathological responses which include development, growth and wound repair as well as infection and tumorgenesis (Trowbridge and Gallow, 2002). A DS proteoglycan known as decorin influences the receptors for epidermal growth factor, which plays a vital role in cell proliferation (Yip et al, 2006). As well as playing a role in many biological processes CS and DS also have interactions with key molecules within the body such as cytokines, chemokines and growth factors (Malavaki et al, 2008).

1.3.5 Keratan Sulphate

Keratan sulphate is a GAG composed of alternating 3 linked β-galactose and 4 linked N-acetyl-β-glucosamine to form a disaccharide unit (seen in figure 1.7). These units are then further linked together to form a GAG polysaccharide. The presence of β-galactose makes keratan sulphate unique as it is the only GAG which doesn't contain an acidic sugar instead it contains a pH neutral sugar in β-galactose (Pomin, 2015).

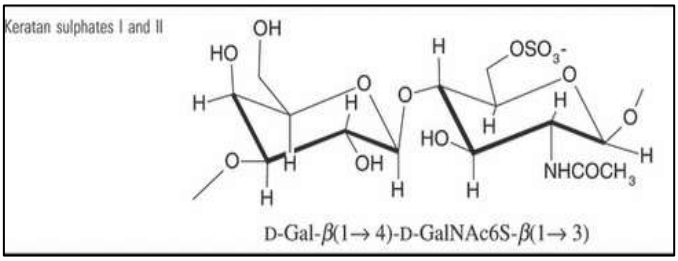

Figure 1.7 The structure Keratan sulphate. (Gandhi and Mancera, 2008).

The keratan sulphate chain is lengthened via glycosyltransferases which in an alternate fashion add β-galactose and GlcNAc to the extending polysaccharide chain until the chain is completely formed (Funderburgh, 2000). Keratan sulphate disaccharides can be unsulphated, monosulphated or disulphated. Sulphotransferase enzymes carry out the sulphation of

keratan sulphate disaccharides through the addition of sulphate groups at the carbon 6 position on both β-galactose and N-acetyl-β-glucosamine residues (Pomin, 2010).

Keratan sulphate is commonly found attached to proteins in the body. Which proteoglycan is produced is entirely dependent on what protein the GAG has bound to. Keratan sulphate is capable of forming two proteoglycans known as KS1 and KS2. KS1 is an N-linked from of keratan sulphate which is attached to asparginine. KS2 is an O-linked keratan sulphate which is linked to a serine or threonine (Pomin, 2010).

Keratan sulphate is found in the extracellular matrix of certain tissue types in the body such as bone and cartilage as well as in the cornea (Pomin, 2015). In cartilage keratan sulphate plays a major role in the maintaining of hydration levels within the tissue (Pomin, 2015). Keratan sulphate also has some involvement in cellular signalling and migration and developmental biology.

1.3.6 Hyaluronan

Hyaluronan is a linear non-sulphated GAG which has a composition of repeating units of D-glucuronic acid and N-acetylglucosaine (demonstrated in figure 1.8). These two are linked via alternating β-1, 4 and β-1,3 glycosidic bonds (Rah,2011).

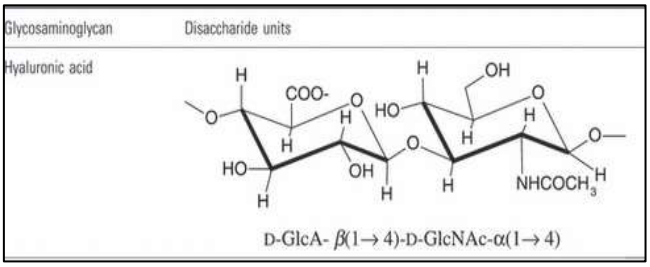

Figure 1.8 The structure of hyaluronan/ hyaluronic acid. (Gandhi and Mancera, 2008).

Hyaluronan is synthesised on the plasma membrane which is in contrast to other GAGs which are mainly synthesised in the golgi apparatus. The synthesis of hyaluronan is carried out by hyaluronan synthases which are specialised membrane proteins. In the human body there are three types of hyaluronan synthases named HAS1, HAS2 and HAS3 (Itano and Kimata, 2002). There are other enzymes which are located in the cytoplasm that play an integral role in the synthesis of hyaluronan through the creation of a UDP-sugar precursor molecule (Vigetti et al, 2014). The value of the UDP-sugar as a precursor is as a polymerisor of the

hyaluronan chain, it also extrudes it from the cell without requiring a primer or an anchor protein or lipid (Vigetti et al, 2014).

Post production, hyaluronan disaccharides are then polymerised at the interface of the plasma membrane (Dicker et al, 2014). The levels of hyaluronan synthesis and degradation are controlled during embryonic development as well as in many homeostatic processes. Hyaluronan interacts with many cell surface receptors and binding proteins in order to activate intracellular events and mediate cell functions. Hydrated hyaluronan makes the extracellular matrix an optimum environment in which cells can proliferate and move. It is this ability that allows hyaluronan to participate in tissue metabolism (Varki et al, 2009).

Increased levels of hyaluronan have been identified in correlation with elevated growth factor activity and increased cytokine levels normally associated with rapidly remodelling tissue, like those found in wound healing and embryonic development. In elevating growth factor levels hyaluronan is also known to cause several pathological conditions which include blood vessel thickening, inflammation and tumour progression (Dicker et al, 2014).

Some cancers can transform hyaluronan synthases in order to maximise the production of hyaluronan (Karbownik and Nowak, 2013). As the environment hyaluronan creates is pro proliferation and inhibits differentiation it also promotes an optimum environment for malignant cell proliferation and thus the progression of cancer.

1.3.7 Cell death pathways

Cell death is a key component in several cellular systems which include development, immune regulation and homeostasis (Duprez, Wirawan, Vanden Berghe and Vandenabeele, 2009). As with the cell cycle, if cell death is not controlled correctly pathologies can ensue this can include too little cell death which can result in conditions such as cancer, lupus or osteoporosis. Or too much cell death which can lead to Parkinson's disease rheumatoid arthritis or multiple sclerosis (Zhivotovsky and Orrenius, 2010). In some instances, cell death may also be used as a defence mechanism against pathogen infection, however pathogens have evolved, and many can now modulate host cell death.

There are several mechanisms of cell death, these being apoptosis, necrosis, autophagy and mitotic catastrophe related (Duprez et al., 2009). It is believed that caspase-dependent apoptosis is the predominant form of cell death in healthy cells (Galluzzi et al., 2007).

1.3.7.1 Apoptosis

In 1972 apoptosis was first described as a type of cell death with distinct morphological features. These include cell shrinkage, membrane blebbing and chromatin condensation (Youle and Strasser, 2008), which result in controlled and programmed cellular suicide of unrequired cells. Apoptosis results in the controlled breakdown of apoptotic bodies which can be recognised and engulfed by surrounding cells and phagocytes (Fuentes-Prior and Salvesen, 2004). In adults the amount of cell death is balanced with the level of cell division, to ensure that there are minimal changes to either tissue growth or shrinkage (Becker et al., 2003).

During the early stages of apoptosis the cell shrinks and the chromatin condenses. Cells then become smaller and the cytoplasm becomes dense, which in turn tightly packs the cell organelles (Youle and Strasser, 2008). Plasma blebbing occurs and is then followed by karyotthexis which fragments the nucleus. With the nucleus fragmented the cell is separated into apoptotic bodies and fragments through budding (Elmore, 2007). Macrophages engulf and phagocytose the apoptotic bodies. As it is phagocytes which take up the apoptotic bodies, it is thought the process occurs before the cell loses the integrity of its plasma membrane and is therefore believed to be immunologically silent (Krysko and Vandenabeele, 2008). Meaning that unlike necrosis, apoptosis does not produce inflammation and doesn't release cellular contents into circulation. Phagocytosis occurs quickly which has two main benefits: it prevents secondary necrosis from occurring and as mentioned it also prevents pro-inflammatory cytokines from being released (Elmore, 2007).

In apoptotic cells phosphatidyl serine (PS) is expressed on the outside of the cell instead of its normal inward facing position, this acts as a marker for phagocytes (Elmore, 2007). PS on the outside of a cell also allows Annexin V, a recombinant binding molecule to bind with quite a high affinity to it (Elmore, 2007). This binding can be used to detect cells undergoing apoptosis. Propidium iodide (PI) cannot cross the cell membrane in live cells, it also binds to nucleic acids and can therefore be used to detect cell death (Lecoeur, 2002). Therefore the

amount of bound Annexin V and PI can be used to predict what stage of apoptosis a cell is in, this can be seen in figure 1.9.

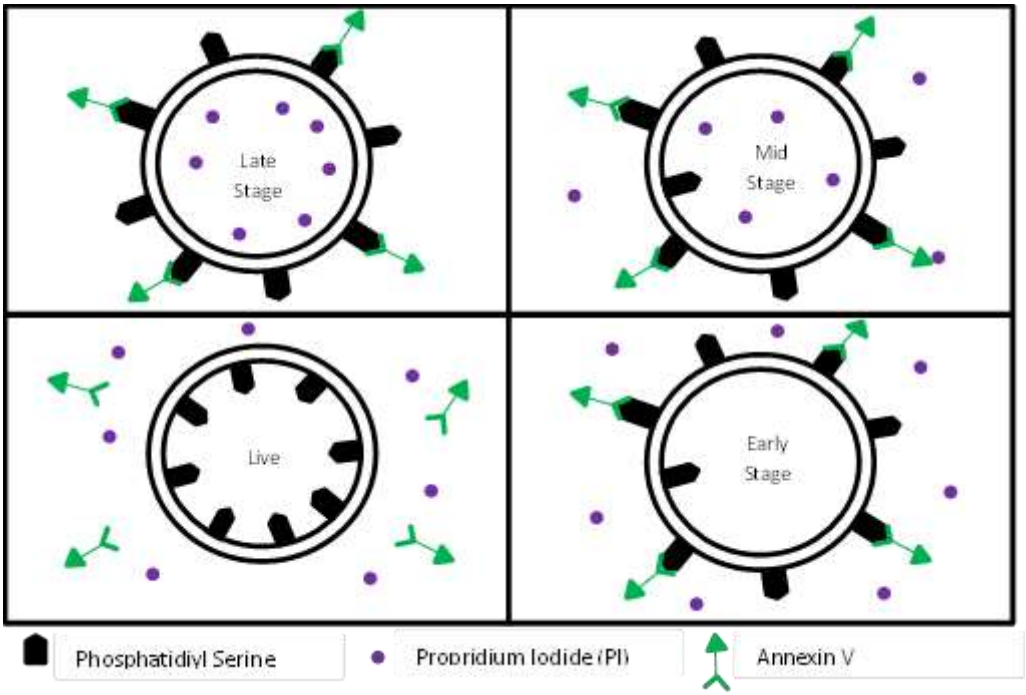

Figure 1.9 The binding of annexin V to PS and the binding of PI to nucleic acid and the stage of apoptosis at which the cell would be. Adapted from University of Dundee, Cell death and apoptosis, (2016).

Apoptosis is a naturally useful process which induces cell death in normal cells which have developed a mutation. If apoptosis doesn't balance out with cellular proliferation then diseases such as cancer or autoimmune diseases may occur (Duprez et al., 2009). Apoptosis is also a useful process which can be targeted by drugs to artificially induce apoptosis to slow cancer progression or stop progression all together.

Yue et al., (2009) identified that GAGs may play a role in the regulation of apoptosis in cells undergoing oxidative stress. They deduced this was most likely through protection from the disruption of the lysosome membrane via reducing intracellular ROS levels and cytochrome C and caspases -3 and -9 release. It has also been concluded that GAGs do not affect the extrinsic pathway of apoptosis (Yue et al., 2009).

It is not yet known whether GAGs affect the cancer cell lines through the induction of apoptosis and whether the GAG extract treatment would induce apoptosis in 'healthy' cells also. Through the use of the annexin V/ PI apoptosis assay my research aims to identify

whether and how much apoptosis is induced in both the cancer cells lines and the 'healthy' lymphocytes.

1.3.7.1.1 Intrinsic and extrinsic apoptosis

Apoptosis is a caspase dependent cell death pathway and these caspases can become activated in two ways (Danial and Korsmeyer, 2004). Intrinsic apoptosis is where the caspases have been activated via the mitochondria. Extrinsic apoptosis is when cell death has been activated through a cell death receptor (Danial and Korsmeyer, 2004).

The intrinsic apoptosis pathway is determined through mitochondria permeabilisation and subsequent cytochrome C release (Kroemer, Galluzzi and Brenner, 2007). Once cytochrome C has entered the cytoplasm a quaternary protein complex known as an apoptosome is formed. The apoptosome formation results in a caspase cascade through the activation of caspase-9 (Taylor, Cullen and Martin, 2008). Intrinsic apoptosis plays a crucial role in development and tissue homeostasis as well as being critical in immunoregulation. Intrinsic cell death also plays a role in neurodegeneration and cancer (Xiong, Mu, Wang and Jiang, 2014). The BCL-2 protein family also play a vital role in the intrinsic apoptosis pathway via the regulation of the proapoptotic proteins effluxing from the mitochondria (Ricci and Zong, 2006). BCL-2 proteins which contain four BH domains (BCL-2 homology) are antiapoptotic and include BCL-2 and BCL-W (Ricci and Zong, 2006). Proapoptotic members lack the BH4 domain and include BAX and BAK which usually exist as inactive monomers (Ricci and Zong, 2006). In many forms of cancer, the BCL-2 family of proteins have found to contain mutations and in some cases overexpression has been noted and is also linked to chemotherapy resistance (Ricci and Zong, 2006).

Extrinsic apoptosis is triggered by death receptors which are members of the tumour necrosis factor (TNF) receptor superfamily (Hirsova and Gores, 2015). Upon activation these receptors then result in the development of a death inducing signalling complex (DISC). This complex constitutes of caspase-8 and adaptor proteins (Hirsova and Gores, 2015).

1.3.7.2 Necrotic cell death

Previously necrotic cell death has been described as an accidental and uncontrolled pathway which lacks signalling events (Duprez et al., 2009). However evidence now suggests that a

caspase-independent pathway exists, whose function is to strictly regulate necrotic cell death in a developmental way, like in interdigital cell death (Chautan, Chazal, Cecconi, Gruss and Golstein, 1999). The defining necrotic factors are cytoplasm and organelle swelling, followed by the loss of cell membrane integrity and thus the cellular contents are released into the surrounding extracellular space (Elmore, 2007). It has now become apparent that necrosis is the result of highly regulated signalling events which can be initiated through a variety of stimuli (Duprez et al., 2009). For most cells the death receptor ligand will always activate the apoptotic pathway in favour of the necrotic one (Duprez et al., 2009). However, there are cases where caspase activation may be damaged or ineffective and necrotic cell death will provide a back-up route for cell death (Chautan et al., 1999). Generally, a cell will enter necrosis as opposed to apoptosis if there is a lack of intercellular energy supply or if there is direct damage to the cellular membranes such as would be found during injury or hypothermia (Elmore, 2007).

Necrosis also plays an important physiological role in signalling processes such as ovulation and cellular turnover in both the large and small intestines (Festjens, Vanden Berghe and Vandenabeele, 2006). In addition to this necrosis also plays a role in activation-induced cell death (AICD) of T-lymphocytes which is very important when T-cell numbers require reducing after an immune response (Holler et al., 2000). Another factor which supports the idea that necrotic cell death acts as a back-up mechanism for apoptosis is that necrosis occurs alongside apoptosis or in the presence of caspase inhibitors (Elmore, 2007). Necrosis rarely occurs as a sole mechanism of cell death.

In contrast to apoptosis, necrotic cell recognition and uptake via macropinocytosis is much slower and inefficient (Neumar, 2000). The plasma membrane also loses its integrity before uptake occurs, this then elicits a pro-inflammatory response (Krysko, Brouckaert, Kalai, Vandenabeele and D'Herde, 2003). This is done through the release of damage associated molecular patterns (DAMPs) and through the release inflammatory cytokines (Fadok, Bratton, Guthrie and Henson, 2001).

1.3.7.3 Autophagic cell death

Autophagy is a highly conserved catabolic pathway which gives eukaryotes the ability to degrade and recycle their cellular components. Autophagy plays an important role in many

cellular processes such as cellular stress, differentiation and development (Maiuri, Zalckvar, Kimchi and Kroemer, 2007). Although it is now accepted that autophagy does play some form of a survival role it has become a debate topic as to whether autophagy plays a causative role in cell death. As autophagic vacuoles have been identified in dying cells it has led to the introduction of autophagic cell death. However it is also accepted that autophagy accompanies cell death rather than actually causing it (Maiuri et al., 2007).

1.3.7.4 Pyroptosis/ mitotic related catastrophe

Pyroptosis is known to be a programmed cell death which has its own distinct set of morphological and biochemical features which are distinctly different to those of necrosis and apoptosis (Labbe and Salen, 2008). Generally, pyroptosis has been described after infection with a range of microbial pathogens, cells which have been noted to be affected include monocytes, macrophages and dendritic cells (Bergsbaken, Fink and Cookson, 2009). Pyroptosis has unique characteristics in that it is dependent on caspase-1, further to this although usually associated with infection, non-infectious stimuli like DMAPS can induce pyroptosis but only in non-macrophage cells (Bergsbaken et al., 2009).

Pyroptosis like apoptosis is also a cellular suicide and forms a section of a hosts defence system against pathogens. As the death of the host cell also destroys the pathogen, microbial replication is slowed and allows for other immune mechanisms to occur (Johnston, 2005). However there are also some limitations of pyroptosis as host cell death may also be beneficial to the pathogen for example if it occurs in and destroys immune cells.

It has become apparent in recent years that apoptosis is the main mechanism for cell death in mammals however it is not the sole form of destruction and removal of unwanted cells through a cell death pathway. Necrosis is also now known to be as a result of signalling events which result in the rupture of the plasma membrane however there are cases in which necrosis occurs without the underlying signalling events (Ricci and Zong, 2006).

Although it was previously thought that apoptosis was the primary form of cell death brought about by chemotherapy treatment, there is more evidence to suggest that other forms of cell death may be elicited (Ricci and Zong, 2006).

However, as apoptosis is the favoured form of cell death in regard to chemotherapy treatment, this research will evaluate the role GAG induced apoptosis plays in cancer cell death. Also, if GAG treatment results in apoptosis in 'healthy' activated and naïve PBMCs, as this is still unknown. Through the use of Annexin V and Propridium iodide using the flow cytometry assay the research identified any apoptosis induced cell death post GAG treatment in either cancer cell lines or PBMCs (naïve and activated).

1.4 Angiogenesis

Angiogenesis is known to play a role in the growth and metastasis of tumour cells, via a multi-step process which involves the extracellular matrix degrading and the activation and proliferation and finally the migration of endothelial cells (Agauayo et al., 2000: Pule et al., 2002: Trujillo, McGee and Cogle, 2012). However multiple studies have now identified that angiogenesis and angiogenic factors may also play a role in the progression of several types of leukaemia (Trujillo, McGee and Cogle, 2012: Agauayo et al., 2000: Mangi and Newland, 2008). Pathological angiogenesis can persist over a long period of time and can be noted in several diseases such as rheumatoid arthritis, diabetic retinopathy and in cancer (Folkman, 1995: Koch, 1998).

1.4.1 Angiogenesis and cancer

When a new blood vessel is created from a pre-existing vessel the process is termed as angiogenesis (Birbrair et al. 2013). Angiogenesis is a normal biological function and plays a vital role in development and growth (Birbrair et al. 2013).

Although angiogenesis is a normal process it also plays an integral part in the progression of a benign tumour into a malignant cancerous tumour (Penn, 2008). The work carried out by Agauayo et al., (2000) also suggests that angiogenesis and angiogenic factors play a significant role in the process of leukaemia as well. The nature of cancer cells is to divide uncontrollably without entering into any cell death pathways (apoptosis or necrosis). A tumour can be defined as a population of cancerous cells which are growing and dividing both uncontrollably and rapidly. While leukaemia is the saturation of the bone marrow and blood with proliferating defective WBCs (Calabretta and Perrotti, 2004). If a tumour is going to grow beyond two millimetres in size the cancer cells require a dedicated blood supply to provide

them with oxygen and nutrients (Mcdougall, Anderson and Chaplain, 1971). During their rapid growth phase tumour cells release chemical signals to trigger angiogenesis (Folkman, 2004).

Muthukkaruppan, Kubai and Auerbach (1982) proved that where angiogenesis stimulation did not occur then tumour cells did not surpass one to two millimetres in size after which growth ceased entirely. However if the tumour cells were able to secure a blood supply then they also exceeded a diameter of two millimetres.

In the same way Holmegren et al, (1995) demonstrated that if angiogenesis did not occur then tumour cells could actually enter into the uncontrolled cell death pathway of necrosis or even into the controlled cell death pathway of apoptosis. It can therefore be concluded that tumour progression is dependent on angiogenesis. As tumour cells secrete chemical signals which stimulate the production of growth factors. This can be seen in elevated levels of vascular endothelial growth factor (VEGF) and fibroblast growth factor (FGF) in the serum of cancer patients (Cross and Claesson-Welsh, 2001). The release of these growth factors in turn induces blood vessel growth, this demonstrates that angiogenesis is an important factor in cancer progression (Birbrair et al, 2013).

Perez-Atayde et al., (1997) demonstrated increased micro-vessel density (MVD) in ALL patients when compared to the control samples, Folkman, Browder and Palmblad (2001) also described increased MVD in ALL patients. This level of increased MVD has also been noted in several other bone biopsies taken from a variety of patients with different forms of leukaemia (Agauayo, 2000: Trujillo, McGee and Cogle, 2012). Increased microvessel density was also noted in CML patient bone biopsies (Kini et al., 1998: Agauayo et al., 2000). Pule et al., (2002) also noted that MVD were increased in most childhood ALL patients tested upon presentation with the disease in comparison to the controls. They also demonstrated that the levels of MVD were reduced almost back to normal levels with patients who had entered into remission. Hussong, Rodgers and Shami (2000) also noted that in a similar fashion to tumour cells that leukemic cells rely on angiogenesis in the bone marrow in acute myeloid leukaemia (AML) patients. They too linked the presence of MVD with the overall survival of the leukaemia and linked a higher level of MVD in AML patients with a poor prognosis. (Hussong, Rodgers and Shami, 2000).

Therefore, angiogenesis must also play a role in the disease process of some forms of leukaemia as well as in the progression of solid tumour cancers.

There has also been reported increases in levels of two specific potent angiogenic regulators vascular endothelial growth factor (VEGF) and fibroblast growth factor (FGF) in both leukaemia and in solid tumours (Agauayo et al., 2000).

1.4.2 Fibroblast Growth Factor (FGF) and Vascular Endothelial Growth Factor (VEGF)

1.4.2.1 FGF

In basic terms FGF is a heparin binding protein (Stegmann, 1999). FGF also has the ability to interact with heparan sulphate proteoglycans which are found on the surface of cells. In terms of signal transduction and tissue and cell differentiation the interaction of GAGs with FGF has proven to be a key component (Stegmann, 1999).

The fibroblast growth factor receptor (FGFR) is composed of several domains; which include extracellular: three immunoglobulin-like domains, a single transmembrane helix domain and an intracellular domain which has the ability to facilitate tyrosine kinase activity (Porta et al., 2017).

The main function of FGF is to initiate the organisation of cells into tubular structures, FGF also promotes the proliferation of endothelial cells (DeCicco-Skinner et al., 2014). The interaction of FGF and endothelial cells is what promotes angiogenesis (Cross and Claesson-Welsh, 2001). Stegmann (1999) discovered that in the cardiac system FGF is a far more potent angiogenic factor when compared to VEGF.

FGF does not possess the ability to migrate and so the growth factor can be released in a highly regulated fashion (Cross and Claesson-Welsh, 2001). Ultimately FGF secretion results in a pool of un-migrated growth factor (Localised).

FGFR/FGF interactions have the ability to regulate several biological processes which include cellular proliferation and differentiation (Tiong, Mah and Leong, 2013). The signalling pathways between FGF and FGFR have also been identified to play a role in the progression of several types of cancer (Porta et al., 2017: Tiong, Mah and Leong, 2013).

1.4.2.2 VEGF

VEGF and the vascular endothelial growth factor receptor (VEGFR) have major physiological roles and play a part in pathological angiogenesis such as can be found in cancer (Shibuya, 2011). VEGF is an angiogenesis stimulating protein (Nishida et al, 2006). VEGF can also promote capillary growth (Gonzalez, Ruben and Rueda, 2013) this means VEGF has a vital role in angiogenesis. VEGF can be present on both normal tissues and on neoplastic tissues. On cancerous tissue VEGF is present adjacent to the stroma (Nishida et al, 2006). In combination with growth factors and cytokines VEGF can also be a very powerful anti-angiogenic factor.

VEGF secretion from tumour cells into blood vessels and surrounding tissue can induce capillary growth and ultimately the production of new blood vessels (Gonzalez et al., 2013). VEGF production can also produce vascular leakage which when teamed with hypoxia can be regulated during tumour expansion (Cross and Claesson-Welsh, 2001).

Studies have shown that if a mutation occurs in the gene responsible for the production of VEGF then the blood vessels produced are abnormal in shape and can lead to embryonic death (Schoenfelder and Einspanier, 2003). This re-enforces the idea that VEGF is a highly potent angiogenic factor.

The VEGF/VEGFR pathway has become an important target for therapeutic treatments including anti-angiogenic treatments in cancer and pro-angiogenic treatments in neuronal degeneration and ischemic diseases (Shibuya, 2011).

1.4.3 Angiogenesis, FGF and VEGF

Cross and Claesson-Welsh (2001) determined that VEGF and FGF exhibited their angiogenic effects by binding to receptors on the cell surface which contain tyrosine kinase activities. Upon binding the kinase receptors become activated and enable a downstream signal transduction production this regulates endothelial cells. FGF and VEGF can also stimulate endothelial cells to secrete proteases responsible for membrane degradation.

Once endothelial cell membranes have been degraded the cell can then migrate into surrounding cell matrixes, there they deposit a new cell membrane. The new membrane then

begins secreting both VEGF and FGF in order to secure the new vessels stability (Cross and Claesson-Welsh, 2001).

It has been noted that elevated levels of both FGF and VEGF have been identified in several forms of leukaemia including ALL and CML (Agauayo et al., 2000: Fielder et al., 1997: Trujillo, Mcgee and Cogle, 2012: Hussong et al., 2000). Perez-Atayde et al., (1997) also noted an increase in FGF in childhood ALL patients however they also found the increase to be insignificant to the prognosis. Kini et al., (1998) also reported an increase in the levels of urinary FGF and VEGF in CML patients.

Suggesting that angiogenic factors VEGF and FGF may also play a role in the progression of several types of leukaemia which include ALL and CML.

1.4.4 Angiogenesis and GAGs

GAGs are present on the surface of cells as well as in the extracellular matrix of endothelial cells (Pardue, Ibrahim and Ramamuth, 2008). GAGs have a vital role in signalling and structural cues which are essential for many physiological processes within the body and these include angiogenesis (Schoenfelder and Einspanier, 2003).

In the serum of cancer patients, a dramatic increase in the GAG hyaluronan can be noted (Chanmee, Ontong and Itano, 2015). The increase of hyaluronan can be linked to an increase in not only the production of but also the release of growth factors (Schoenfelder and Einspanier, 2003).

GAGs can also have interactions with cell receptors in order to aid with the migration and proliferation of angiogenesis related endothelial cells (Deed, Rooney and Kumar, 1997). However in basic terms GAGs have extremely varying effects on angiogenesis. Long chain GAGs bind to the CD44 receptors which are present on the surface of all cell types. The binding of GAGs onto the receptor interrupts cell proliferation, which conclusively halts angiogenesis (Gao et al, 2008). In contrast short term oligosaccharides binding to cell surface receptors promotes the production of growth factors which in turn promotes angiogenesis.

Heparin and heparan sulphate are most likely to exert an effect on angiogenesis however chondroitin sulphate, dermatan sulphate, keratan sulphate and hyaluronan may also interact.

Further studies may be able to identify specifically which GAG interacts with angiogenesis the most.

1.4.4.1 GAG interactions with angiogenesis and growth factors

GAGs are essential in signal transduction in receptor-ligand reactions; this is due to their ability to act as co-receptors for VEGF and FGF. GAGs also play a crucial role in angiogenesis of tumours (Raman, Ninomiya and Kuberan, 2011). Angiogenesis associated with tumours can be initiated through inhibiting the formation of proteoglycans in endothelial cells (Raman, Ninomiya and Kuberan, 2011).

The sulphation patterns located in the structures of GAGs is what allows growth factors like FGF and VEGF to bind onto them (Raman, Ninomiya and Kuberan, 2011: Cross and Claesson-Welsh, 2001). For the angiogenesis process to begin it is essential for GAG units and growth factors to bind which results in the binding of endothelial cells (Cross and Claesson-Welsh, 2001). This binding series results in the initiation of angiogenesis.

GAGs which are excreted externally enter into competition with endogenous proteoglycans, the competition results in the prevention of further GAG production by the cells, this inhibits angiogenesis (Raman, Ninomiya and Kuberan, 2011). Exogenous GAGs are incapable of binding growth factors (Cross and Claesson-Welsh, 2001). Exogenous GAG does however bind to the cells and so it effectively blocks any further binding of GAGs to growth factors which further prevents angiogenesis from occurring (Cross and Claesson-Welsh, 2001). With angiogenesis effectively blocked the blood supply to the tumour is cut off and would therefore cause the cancer to shrink and it could also potentially enter the tumour into a cell death pathway.

The GAGs obtained from shellfish therefore may potentially exert their anti-cancer through the binding to cancer cells or to the growth factors, however the mechanism of action for shellfish originated GAGs is still unknown.

1.4.5 Inhibition of angiogenesis in cancer

If angiogenesis is prevented then the formation of new blood vessels is inhibited. Inhibitors can be found in two forms, endogenous inhibitors are one form of angiogenesis inhibitor and

they play a normal role in the control of bodily functions (Hayden, 2009). Another form an angiogenesis inhibitor can take is in the form of a pharmaceutical drug or from the diet, this type of inhibitor is gained via an external source (Hayden, 2009).

Tumour cells which have secured a blood supply can produce pro-angiogenic substances to stimulate further angiogenesis; these can include FGF and VEGF (Folkman, 2004). To inhibit angiogenesis, it is necessary to use anti-angiogenesis substances, these aim to minimise the effect that the pro-angiogenic factors are producing. This treatment is given to prevent and/ or block any ligand-receptor binding (Cao, 2001).

The major focus of anti-angiogenic drugs is to block or inhibit the VEGF pathway. The main reason for this target is the raised levels of VEGF which can be seen in the serum of patients who have a malignant tumour (Folkman, 2004). There are various ways in which the VEGF pathway can be inhibited. One way to block the VEGF pathway is through the use of tyrosine kinase inhibitors. The pathway can also be blocked through the use of antibodies which are specific to the VEGF ligand; this treatment prevents VEGF from being able to bind proteins on the cell surface.

The epidermal growth factor receptor (EGFR) is a transmembrane protein which is activated by specific ligands including tyrosine kinase (Zhang et al., 2007). Mutations in the EGFR have been linked to several diseases including Alzheimer's and cancer (Zhang et al., 2007). Inhibitors which target tyrosine kinase via the EGFR can result in the inhibition of angiogenesis.

Endogenous inhibitors are naturally produced by the body to aid with angiogenesis regulation. If a patient is suffering from a tumour then the regulation pathway is defective. Due to this defect the volume of pro-angiogenic factors outweighs the anti-angiogenic effects and so new blood vessels are formed in an uncontrollable fashion (Nyberg, Xie and Kalluri, 2005).

Natural anti-angiogenic agents can provide a good treatment option as a cancer therapy target as the noted side effects could have significantly milder toxicity than alternative treatment methods.

In some animal studies it has been determined that the most beneficial treatment would be using a large dose for a prolonged period. However, it has not yet been determined if this type of treatment would be safe or beneficial in humans. As the VEGF pathway is being disrupted through the use of angiogenic inhibitors side effects can include raised blood pressure and bleeding (Elice and Rodeghiero, 2012).

1.4.6 Angiogenesis inhibitors

An angiogenesis inhibitor is a substance which can prevent the growth of a new blood vessel (Hayden, 2009). Angiogenesis can be prevented through the tyrosine kinase pathway or through the blockage of growth factor binding. After the discovery of VEGF in 1989 it became expected for VEGF to be the driving force of tumour angiogenesis. It was then further predicted that pharmaceuticals which specifically targeted VEGF as a molecule or its binding receptor would be a big breakthrough in the treatment of cancer (Hayden, 2009: Arbor and Garber, 2002). However it has now come to light that that type of treatment has its limitations which put doubt into their use as a cancer therapy. In spite of the discovery of issues with this treatment method some anti-angiogenic drugs are still used in cancer therapy and can work quite effectively (Hayden, 2009).

Approximately 60% of malignant tumours have been shown to express VEGF (Cao, 2001) which is why most anti-angiogenic drugs have a mechanism of action aimed at blocking the VEGF pathway. Several methods are used to block the VEGF pathway which include antibodies against VEGF, tyrosine kinase inhibitors and using VEGF itself as a target (Folkman, 2004). Agauayo et al., (2000) suggested that the evidence to suggest angiogenesis play a role in leukaemia that angiogenic inhibitors may prove to be a useful treatment in leukaemia patients.

Tarceva is an angiogenic inhibitor which has entered into clinical trials. It inhibits angiogenesis through first inhibiting tyrosine kinase and its effects can be seen on the epidermal growth factor receptor (EGFR) (Raymond, Faiure and Armond, 2000). When tarceva has inhibited the initiation signal for angiogenesis to occur the growth of new blood vessels is halted. However tarceva has shown limitations as eight to twelve months after the start of treatment drug resistance has generally occurred. This resistance happened through a mutation in the EGFR binding pocket, which prevented the drug from being able to bind the receptor.

Another angiogenesis inhibitor is endostatin which was proposed to exert its action through blocking FGF and VEGF which would have made it a potential candidate in cancer therapy (Folkman, 2006). Trials of endostatin found it to be in-effective when used as a sole treatment method. Nexavar (sorafenib) is a treatment for kidney and liver cancers, which is another tyrosine kinase inhibitor (Zhang, 2014). Other tyrosine kinase inhibitors which are treatments for cancer include; sunitinib, a treatment for renal cell carcinoma, gastrointestinal and pancreatic tumours, (Motzer, Escudier, Gannon and Figlin, 2017). Pazopanib is also a multi-targeted tyrosine kinase receptor inhibitor which has been approved for the treatment of metastatic renal cell carcinoma (Mendez-Vidal et al., 2018).

SU5146 is an anti-angiogenic drug which is aimed at inhibiting tyrosine kinase through blocking the VEGF receptor (O'Donnell et al., 2005). It is an unlicensed drug which has entered into clinical trials and was expected to have anti-cancer activity. However patients in the trials who were treated with SU5146 experienced an unexpected level of toxicity. Two patients treated suffered from strokes while other patients experienced blood clots (Arbor and Garber, 2002). This toxicity put their future as a cancer therapy drug into doubt.

The most common angiogenesis inhibiting drug is bevacizumab which is sold under the name of Avastin (Rini, 2007). Unlike the other drugs Avastin exerts its action through directly binding with VEGF. Avastin was the first drug that binds VEGF to make it through to phase 3 clinical trials. However, Avastin failed to meet its trial targets, although it did shrink tumours it did not delay the cancer progression or improve survival rates (Arbor and Garber, 2002). After the failure of SU5146 and Avastin the use of VEGF as an anticancer therapy target was questionable. It has now been suggested that using VEGF as a sole target may not be enough to exert a permanent effect on tumour growth.

It is predicted that GAGs will target multiple pro-angiogenic factors and thus they have been suggested as a possible cancer therapy and may potentially also be effective at avoiding the drug resistance which has been seen after the use of other angiogenic inhibitors. However GAGs may also act via an unknown mechanism and so further research is required into the mechanism of GAG action in cancer.

The side effects of GAG treatment are expected to be minimal due to the fact that GAGs are naturally found in the human body therefore should not produce many adverse side effects

upon treatment. However the effect of GAGs on 'healthy' cells is not yet known, this research aims to identify what effect if any the GAG extract treatment has on both activated lymphocytes and naïve lymphocytes. These results should provide some information on what effect the GAGs may have on 'healthy' blood cells in a patient.

1.5 Physiology of white blood cells

A peripheral blood mononuclear cell (PBMC) can be described as any blood cell which contains a round nucleus such as; lymphocytes, macrophages or monocytes (Delves, Martin, Burton and Rositts, 2017: De Mello et al., 2012). PBMCs play a vital role within the immune system allowing it to adapt to foreign bodies and fight infections.

PBMCs can be extracted from whole blood using lymphosep and gradient centrifugation to separate out the different layers of blood. The bottom layer will be a mixture of lymphosep and red blood cells. The next layer is known as the buffy coat and contains the PBMCs and the top layer is plasma cells. The PBMCs can be further characterised into lymphocytes such as; T-cells, B-cells and natural killer (NK) cells, monocytes and dendritic cells also (Delves et al., 2017). For humans the volumes of these types of cells vary from individual to individual. As a general composition 70-90% of PBMCs ae made up of lymphocytes, monocytes make up around 10-30% of PBMCs and dendritic cells account for a minimal amount of PBMCs making up only around 1-2% (Kleiveland, 2015). The lymphocyte population can be further divided down. Generally, 70-85% of lymphocytes are CD3+ T-cells, 5-20% are B-cells and 5-20% are NK cells (Kleiveland, 2015). CD3+ cells can also further be divided down into CD4+ and CD8+ cells which occur in a 2:1 ratio (Kleiveland, 2015). Both CD4+ and CD8+ cells can occur in a naive or antigen-experienced memory and effector memory forms (Sanguine Biosciences, 2012). The cells which make up the lymphocyte population can be seen in figure 1.10.

1.5.1 Lymphocytes

Lymphocytes are mononuclear cells which account for 33% of all white blood cells circulating in the blood (Moore, Knight and Blann, 2010). It is lymphocytes which provide specific immunity for the body against molecules it has previously been exposed to. Upon analysis two individual populations of lymphocytes can be identified. One population is small and of similar size to red blood cells and contains a minimal amount of cytoplasm; these cells are

referred to as small lymphocytes. The other population found in blood analysis are known as large lymphocytes due to their size and large volume of cytoplasm (Pallister and Watson, 2011).

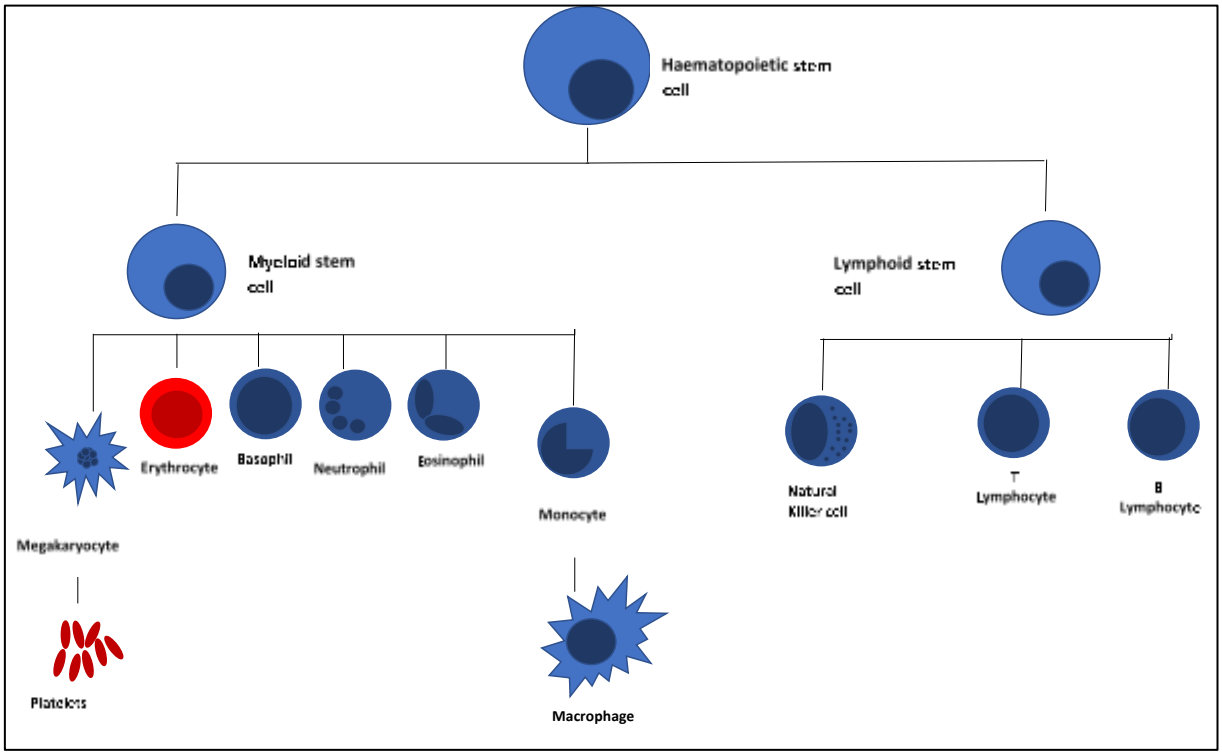

Figure 1.10 The subsets of lymphocytes which derive from haematopoietic stem cells. The lymphocyte subsets which derive from haematopoietic stem cells, and whether they are myeloid or lymphoid lineage. Adapted from, National Cancer Institute 2018: Skak, Kragh, Hausman, Smyth and Sivakumar, (2008).

There are two main types of lymphocytes which make up the adaptive immune system these are T-cells and B-cells.

1.5.1.1 T-Cells ($CD4^+$ T-helper cells, $CD8^+$ T-effector/ cytotoxic T-cells)

T-cells are formed in the bone marrow in adults and can be found in the liver of foetuses (Becker et al, 2003). T-cells are then formed from lymphoid stem cells; in order to mature T-cells must enter the thymus (Hannigan, Moore and Quinn., 2009). On the migration to the thymus from the bone marrow, immature T-cells gain surface glycoproteins which enable them to develop specific functions (Hannigan, Moore and Quinn., 2009). It is the surface glycoproteins which determine their effect and function.

The main two types of T-cell surface glycoprotein are CD4 and CD8 (Pallister and Watson, 2011). CD4+ T-cells are known as T-helper cells and are responsible for recognising major histocompatibility complex (MHC) II molecules. Another function of T-helper cells is to release cytokines which trigger naïve B cells to differentiate; the cytokines can also activate macrophages and cytotoxic T-cells (Becker et al, 2003). CD8+ T-cells are responsible for the recognition of MHC I molecules and are referred to as cytotoxic T-cells. Cytotoxic T-cells also have the ability to kill foreign cells by binding to them and releasing enzymes into the foreign cell which in turn induce apoptosis (Becker et al., 2003).

1.5.1.2 Regulatory T-cells (T_{Reg})

T-regulatory cells are a family of T cells which function to naturally regulate any inflammatory response the body has. They do this through several mechanisms which included cell-cell contact through CTLA-4 (Cederbom, Hall and Ivars, 2000) and via cytokine release, specifically IL-10 and TGFβ1 (Lui et al, 2010). There are two vital populations of CD4+ T_{reg} cells which originate from different sources: natural Tregs (nT_{reg}) which are derived from the thymus and peripherally induced T_{regs} (iT_{reg}). Natural T_{regs} have a more potent regulatory ability and also express FOXP3 which is a transcription factor (Zhang and Zhao, 2007). As CD4+ helper T-cells and CD8+ cytotoxic T-cells have immunoregulatory activity they may be useful therapeutic targets.

In cancer, immune evasion is linked to elevated levels of circulating T_{reg} cells within the microenvironment of the tumour (Facciabene, Mortz and Coukos, 2012: Elkord et al., 2010). Facciabene, Motz and Coukos (2012) described how T_{regs} are found in the microenvironment of many tumours and can be linked to poor prognosis. As T_{regs} are potent immune suppressors it is thought that tumour cells target and elicit T_{reg} functions and secretions (Facciabene et al., 2012). Through utilising T_{reg} function tumour cells can promote cancer progression through angiogenesis stimulation and through the promotion of peripheral tolerance towards the cancer cells. This effectively allows the tumour cells to evade the immune system (Facciabene et al., 2012). In the circumstance of cancer, raised T_{reg} levels actually negatively impact the outcome of immunotherapy on tumour progression (Elkord et al, 2010). Children who are suffering from ALL have been reported to have raised levels of circulating T_{reg} cells (Stasiak-

Barmuta et al, 2009). This has led to the suggestion that understanding chemotherapy effects on T_{reg} cells is key to predicting the effectiveness of a therapy.

1.5.1.3 B-cells

B-cells are also formed from lymphoid stem cells derived from adult bone marrow and in the liver of foetuses (Becker et al, 2003). B-cells mainly derive from adult bone marrow, B-cells move through numerous stages and eventually become naïve B-cells. The development to the naïve stage happens via a process known as antigen independent differentiation (Pallister and Watson, 2011). Naïve B-cells are then capable of being activated through antigens which are released by foreign cells which have entered the body. Upon binding the foreign antigens naïve B-cells then further differentiate and can become either a memory B-cell or a plasma cell (Pallister and Watson, 2011). Memory B-cells provide a long term record for the immune system against antigens to which it has been previously exposed. It is memory cells that allow the body to respond quickly to an antigen upon reinfection (Becker et al, 2003). Plasma cells secrete clones of antibodies which are specific to the antigen that originally initiated the immune response and activation of the naïve B-cell (Moore et al., 2010).

1.5.1.4 The role of T_{regs} in cancer

T_{reg} cells play a major role in autoimmune disease as they can inhibit any immune response against both non-self and self-antigens (Wang, 2008). However T_{reg} cells can promote tumour growth through the suppression of anti-tumour immunity. There is increasing evidence to suggest CD4+ T_{reg} cells supress anti-tumour immunity and are also present in several cancer types.

A host's immune system plays an important role in immunosurveillance and destruction of cancer, however immune cells such as T-cells also play a vital role in tumour growth during the early stages of cancer (Wang, 2008). CD4+ and CD8+ T_{regs} become suppressive after over stimulation and tumour interaction which promotes tumour progression and cancer development.

It has been reported that elevated levels of CD4+ T_{reg} cells have been identified in cancer (Griffiths et al., 2007). Although little is known about CD8+ T_{regs} in cancer there is increasing

evidence to suggest that CD8+ T_{regs} also accumulate in the tumour microenvironment (Wang, 2008).

High levels of $CD8^+$ and $CD4^+$ T_{regs} in cancer create a microenvironment which is immunosuppressive and therefore promotes tumour growth (Wang, 2008). Understanding how T_{regs} can be generated within the tumour microenvironment and furthermore how their suppressive activity can be blocked is required to better improve the therapeutic potential of cancer therapies (Wang, 2008).

$CD4^+$ T-cells are responsible for the control of the function, maintenance and memory of $CD8^+$ T-cells. In the absence of $CD4^+$ T-cells immunotherapy of cancer through the use of $CD8^+$ T-cells against the tumour was enhanced (Antony et al, 2005). As most cancer patients cannot produce enough of an immune response to the tumour it suggests there may be a tumour specific immune evasion strategy (Wolf et al, 2003).

Tumour metastasis has previously been linked to a drop in MHC I expression and also in the proteins responsible for recognising antigen peptides. This effectively downregulates the epitopes which activate T-cells from being presented (Wolf et al, 2003). It has also been suggested that tumours may also express immune-suppressive elements like IL-10 and TGF-β (Wolf et al, 2003).

1.6 Previous research

1.6.1 Previous preclinical research evaluating GAG actions for the development in cancer diagnosis and therapy

Vallen et al. (2012) identified that an increase in the level of CS circulating in the stroma in ovarian cancer patients could be identified using a single chain antibody. This could make it a potential biomarker which would make it ideal for diagnosing ovarian cancer.

Chatzinikolaou et al. (2008) identified that upon treatment with exogenous heparin, colon cancer cells had proliferation stimulated, this suggested that heparin may bring about behavioural changes in cells. The cells remained unaffected by endogenous GAGs. This may suggest that GAGs can exert changes in cancer cell function after treatment

Nikitovic et al. (2004) determined that the production of GAGs and PGs within the osteosarcoma (MG-63) cell line was stimulated by transforming growth factor (TGF-β2). They also noted that the growth factor exerted no effect on the osteosarcoma (SA0S2) cell line. The differences between the cell lines continued as the GAGs that were produced inhibited cell growth in the MG-63 cells while growth was actually stimulated in the SA0S2 cells. The group eventually determined that the changes within the GAG synthesis were due to the heparan sulphate produced. Their research identified TGF-β2 as a vital component in GAG and PG biosynthesis as well as regulating cell growth and cancer progression.

Pye and Kumar (1998) determined that HS chains have differing affinity for binding growth factors and activity levels which could be due to the differing levels of sulphation within the structural domain. They also concluded that the spacing of the sulphated domains proved to be important for both the binding of HS chains to growth factors and for the biological activity.

Makatsori et al., (2001) concluded that all cell lines they tested excreted HS and CS in both the cellular membrane and in the culture medium. They also determined that the volume of distinct GAGs that were secreted by the cancer cell lines was different to that of normal PBML cells and therefore GAGs could have a major role in the malignant transformation of human monocytes and lymphocytes.

Various studies have identified the involvement of GAG extracts in cancer therapy either as a biomarker for diagnosis or as targets themselves for therapy.

Ongoing research headed by Dr David Pye at Kidscan has identified the anti-tumour properties of GAG compounds which are isolated from shellfish: cockles and whelks (Aldairi, Ogundipe and Pye, 2018). Rigorous testing on a variety of cell lines including: breast cancer, colon adenocarcinoma and leukaemia cell lines have shown GAG isolates are effective at the reduction of cancer cell populations within the cell lines.

Aldairi, Ogundipe and Pye (2018) found that the anti-cancer activity noted in the cockle extract was affected by the digestion of the extract with heparinase, while digestion with chondroitinase ABC had little effect on the antiproliferative activity of the cockle extract. They therefore suggested that the heparin/ heparan sulphate component of the cockle extract was in part responsible for the level of activity noted. It was also suggested that due to a lack of

antiproliferative effect of mammalian GAGs that the GAG structures present in the cockle extract were unique and partly responsible for the antiproliferative effects (Aldairi, Ogundipe and Pye, 2018). Murphy Mclay and Pye (2008) also suggested that the conformation and sulphation patterns within HS chains could be directly linked to the biological activity of the GAG.

Both the cockle and whelk extracts have been shown to be potent against the K562 cell line (CML line). This cell line lacks the P53 gene. Various modes of action have been proposed based on GAG structures and their adhesive properties interacting with structures on tumour cell surfaces which include heparan sulphate (Murphy, Mclay and Pye, 2009). However the mechanism of action of the GAGs is still unknown. This research also interestingly identified that commercially available GAGs did not possess any anti-cancer activity against the cancer cell lines. It is likely that the alterations in the sulphation patterns within the shellfish GAGs and commercial GAGs is responsible for the differences in anti-cancer activity.

Ongoing KidsCan research is aiming to identify the most potent fraction from the FPLC separation. Their research has also confirmed that the composition of the shellfish GAGs is likely to be a mixture of HS, CS and DS.

GAGs may be the key to providing a 'kinder' alternative anti-tumour therapy for children with cancer. Further *in vitro* studies are still required to identify GAG action on healthy lymphocytes including CD4, CD8 and T-regulatory populations to truly determine the feasibility of GAGs as a cancer therapy.

Ongoing KidsCan placement studies are looking into lymphocytes and have established a source for units of blood from the clinical donor services and PBMC isolation from the whole blood via filtration methods. Identification of CD4, CD8 naive ($CD45ROA^+$) and memory T-cells ($CD45RO^+$) and T_{reg} cells ($CD4^+FOXP3^+$) by flow cytometry has been achieved in the KidsCan labs. A model for thorough interrogation for each cell family in response to GAG doses over time has now been established.

The effect of GAGs on 'healthy' lymphocyte populations is still unknown. This research aimed to identify what effect the GAGs have on both activated and naïve lymphocytes. The effect of GAGs on individual lymphocyte populations was also unknown; this could provide a clearer

view on whether the GAG extracts are a viable treatment option that will not produce severe side effects.

1.6.2 T_{reg} interactions with cancer

Beyer and Schultze (2006) found that T_{regs} block anti-tumour immune responses and in terms of T-cell function and frequency T_{reg} cells are important as elevated levels favour tumour growth and development. This can have a huge effect on the progress of the disease.

In mouse colon fibrosarcoma and adenosarcoma models un-fractioned tumour draining lymph nodes cells were isolated on day 9 post tumour challenge; this resulted in the rejection of the established tumours (Bayer and Schultze, 2006). Even removing four times the volume of cells on day 12 did not prevent lethal tumour progression. Bayer and Schultze (2006) concluded that the failure of treatment was due to the transfer of tumour induced T_{regs}. They determined that there was a short time span in which tumour development and the induction of suppressive T_{reg} populations. Bayer and Schultze (2006) concluded their findings show T_{reg} cells were vital regulators of tumour immunity. Tumour immunity could be defined as the host's ability to produce T_{regs} which would function to alert the immune system to the invasion of tumour cells, allowing the immune system to eradicate the tumour. Bayer and Schultze (2006) demonstrated tumour immunity has a finite window of opportunity before the tumour cells recruit T_{regs} which downregulate an immune response making the tumour effectively invisible to the immune system.

Woo et al, (2002) reported high percentages of T_{reg} cells in small cell carcinoma and ovarian cancer. They determined that T_{regs} excreted TGF-β which contributed to the immune dysfunction that cancer patients suffer. However, they concluded that this induction of TGF-β could have been in part through interaction with CTLA-4 molecule. The CTLA-4 interaction could have led to the production of TGF-β by T_{reg} cells, but it could also be a biomarker for T_{reg} cells (Woo et al., 2002).

Bayer and Schultze (2006) also determined in malignant melanoma patients that T_{reg} levels were linked to raised H-ferritin levels. H-ferritin lead to the activation of IL-10 which produced functional T_{reg} cells as a potential mechanism of T_{reg} production in cancer patients. Poor prognosis and decrease in survival rate have been linked to T_{reg} cell frequencies.

1.7 Aims and Objectives

Firstly this research aimed to determine if normally proliferating lymphocytes may be at risk of being targeted by these novel compounds (shellfish isolates) in a similar way that leukaemia cells are targeted. As T-regulatory (T_{reg}) cells have been linked to the progression and immune evasion of cancer as well as the eradication of cancer (Beyer and Schultze, 2006: Elkord, 2010). The second aim was to evaluate the action of these novel GAG compounds on T_{reg} cells, in order to determine if the clinical use of GAGs may be helpful in reducing the levels of T_{reg} cells in leukaemia patients or if, in fact, treatment is likely to exacerbate tumour evasion by promoting T_{reg} activation/ potency.

The primary aim of this research was to progress the pre-clinical assessment of novel GAG compounds for the treatment of leukaemia. This was achieved through the evaluation of cancer cell line responses and healthy lymphocyte responses to the GAG compounds.

Phase 1 of the research involved isolating the GAG compounds in bulk using a method similar to that set out by Kim et al., (1996). Peripheral mononuclear cells (PBMCs) were extracted from whole blood in bulk. Cell viability assays (MTT) were performed in order to assess responses of cancer cells (acute lymphoblastic leukaemia (MOLT-4), chronic myeloid leukaemia (K562) and lymphoblastic lymphoma (U698)) and activated (PHA or PMA/ Ionomycin) or naïve PBMCs to the novel GAG compounds. These assays allowed for the identification of a suitable dose and treatment incubation time point to be assessed in subsequent flow cytometry assays.

Phase 2 studies used the obtained IC50 GAG isolate dose, from the MTT assays, to test for their potency via flow cytometric analysis in the annexin V/ PI apoptosis and CFSE proliferation assays, on the cancer cell lines and PMA/ Ionomycin activated or naïve PBMCs. In order to determine GAG isolate effect on cell death and proliferation in cancer cells and healthy lymphocytes (activated or naïve). Phase 2 studies also used the FPLC technique to isolate potentially potent fractions of the crude whelk extract, in order to determine if a smaller chemotherapeutic molecule for potential clinical use was possible.

Phase 3 of the research evaluated individual FPLC fractions to establish potentially potent fragments of the compounds, through the use of the cell viability MTT assay. This work also

focussed on T-regulatory (T_{reg}) cell and cytokine responses to the crude GAG isolates, to provide insight into their potential modulation of a population of cells associated with cancer progression.

The quest for new therapies is ever pressing and this study aims to undertake preclinical evaluation of novel marine mollusc derived GAG compounds, in order to further advance the development of these compounds into more effective and tolerable therapies, especially for children.

CHAPTER 2- METHODS

2.0 Methods

2.1 Cell culture

2.1.1 Freezing/ Thawing manipulations

The thawing of cryo-frozen human cancer cell lines MOLT-4 (acute lymphoblastic leukaemia), K562 (chronic myeloid leukaemia), U698 (lymphoblastic lymphoma) and PBMCs (gained from the NHS blood bank, upon ethical approval, which were from healthy patients and screened by the donor service) occurred in 30 second intervals at 37 ^{o}C. The cellular solution was added drop wise, to ensure even distribution of cells, to 10X (*v/v*) culture RPMI-1640 medium with 1g/L glucose (Lonza group ltd., Basel, Switzerland), 10% (*v/v*) inactivated FBS (labtech international ltd., Heathfield, UK), 1% (*v/v*) L-glutamine (labtech international ltd.,) and 1% (*v/v*) penicillin streptomycin (labtech international ltd.,) supplements. The cell: medium solution was centrifuged at 200xg for 5 minutes. The cell pellet was retrieved and re-suspended in fresh medium and seeded into 25 cm^2 flasks at a dilution of 1:10 ratio of cells: medium or 2:10 ratio. All cells were maintained and humidified atmosphere of air 95% and 5% CO_2 at 37 ^{o}C.

2.1.2 Suspension cell subculture

Suspension cell subculture was carried out every 2-3 days depending on cell confluency. This was done through centrifuging cells from the flasks for 5 minutes at 400xg. The cell pellets were re-suspended into 3 mL of media made up as explained in method 2.1.1. 1 mL of cells was added to one flask and 2 mL of cells were added to another new flask, media was then added to the flasks to make the final flask volume 10 mL. Cells were frozen periodically, via re-suspension of the cell pellet into 9 parts FBS to 1-part DMSO (final concentration of 10% (*v/v*)). The solution was then stored in cryovials and frozen at -80 ^{o}C for 24 h in “Mr frosty” (a freezing container which utilises 100% isopropyl alcohol to gain a constant cooling rate of 1 ^{o}C/minute), allowing for optimum cell preservation. The cells were then transferred to liquid nitrogen and archived into the liquid nitrogen store records.

2.2 PBMC isolation

To isolate the PBMCs whole blood was diluted at a 1:1 ratio with RPMI-1640. The diluted blood was layered onto lymphosep at a 1:1 ratio in falcon tubes. The tubes were then centrifuged at 400xg for 30 minutes with brake setting zero. Upon completion of the centrifugation the blood had separated into layers. The bottom layer of lymphosep and red blood cells, a buffy coat containing the PBMCs and a top layer containing plasma. The buffy coat was carefully retrieved via pasteur pipette and further diluted at a ratio of 1:1 with RPMI-1640. The RPMI acts as a washing solution in this step. The cell solution was centrifuged at 400xg for 10 minutes and the cell pellet retrieved and re-suspended in culture medium. A cell count was then performed by mixing a 1:1 (*v/v*) ratio of cells and tryphan blue for the assessment of cell viability. The cell: tryphan blue solution was then pipetted onto a haemocytometer and the cells were counted. Once the cell count had been performed the cells could be used in an assay or frozen as previously described.

2.3 GAG extraction

Marine polysaccharides were extracted from the common cockle (*cerastoderma edule)* and whelk (*Buccinum undatum*), obtained from the Irish sea, British Isles, using a standard protocol (Kim et al., 1996). Both cockles and whelks were obtained with the shells removed (2.5 kg each). The soft bodies of the shellfish were chopped and placed into separate beakers. The cockles and whelks were then defatted over a period of 72 hours in acetone, the acetone was replaced every 24 hours. After 72 hours the acetone was decanted off and the defatted shellfish were dried in a fume hood for a further 72 hours. Once dry, the cockles and whelks were ground into a fine powder.

The powder (50 g) was incorporated into 500 mL of 0.05 M sodium carbonate buffer pH 9.2 and 25 ml of alcalase enzyme (Merk, Millipore, Watford, UK). The samples were then placed into oil baths and incubated at 60 ^{o}C and stirred constantly at 200 rpm for 48 hours. This step aims to digest protein within the shellfish powder.

After 48-hour incubation the shellfish mix was cooled to 4 ^{o}C. 5% (*w/v*) trichloroacetic acid (Sigma Aldrich, Gillingham, UK) was added. The solution was centrifuged for 20 minutes at 10400xg and 4 ^{o}C. The supernatant was stored in the fridge. Three times the sample volume

of ethanol was used to make a 5% (*w/v*) potassium acetate solution. This was combined with the sample supernatant and stored overnight at 4 ^{o}C. The mix was centrifuged at 10400xg for 30 minutes. The pellet was re-suspended in 480ml of 0.2 M NaCl buffer and centrifuged (30 minutes, 10400xg), to remove insoluble material.

A 5% cetylpyrimidinechloride (CPC) (Sigma Aldrich) was added to the supernatant and mixed. This solution was centrifuged (10400xg for 30 minutes). The pellet was re-suspended in 125 ml of 2.5 M NaCl buffer, five volumes of ethanol was then added to the mix and combined. This solution was then centrifuged (16300xg for 30 minutes) and the pellet retained and re-suspended in distilled water.

2.3.1 Desalting the GAG extracts

GAG extract samples which were obtained through the procedure described in method 2.3 were then desalted using dialysis. Dialysis tubing (Fisher scientific, UK) was treated with 100 mM EDTA. The molecular weight cut off point for the dialysis tubing was 8 kDa.

The polysaccharide: d2O mix was then dialysed against (100X the sample volume) distilled water over a 72-hour period, with the distilled water being replaced every 24 hours. The resulting sample was then frozen at -20 ^{o}C and freeze dried to obtain a crude extract powder (approximately 0.145 g retrieved from 2 kg of cockle or whelk) which could then be used in subsequent assays.

2.4 MTT/ cell viability assay

MTT assays were all performed in triplicate and repeated 3 times. The MTT assay used was an adaptation of the method set out by Mossman (1983).

Cell viability was determined through the use of the MTT assay (3-(4,5-dimethylthiazol2-yl)-2,5diphenyltetrazoliumbromide) (Sigma Aldrich). First a viable cell count was carried out using trypan blue and viable cells subsequently seeded into a 96-well plate to a final concentration of $3x10^5$ cells per well in order to ensure the cancer cell line and PBMC assays were matched.

For PBMC assays the cells were supplemented with PHA (Sigma Aldrich) (10 µg/ml) (for optimisation assays), PMA/ionomycin (Sigma Aldrich) (10 ng/ml/ 1 µg/ml) or media (1:1 ratio

(*v/v*)) dependent on whether the assays were stimulated (+PHA or +PMA/ionomycin) or unstimulated (+media) assay. Cancer cell assays were also supplemented at a 1:1 ratio (*v/v*) with media.

Cockle, whelk or cisplatin (Sigma Aldrich) doses were prepared in serial dilutions in culture medium. The final drug concentrations used in the wells is shown in table 2.1. The drug concentrations are displayed in µg/ml to allow the comparison of cockle and whelk polysaccharide treated cells to the control cisplatin (Sigma Aldrich), as a molar concentration is not yet achievable for the polysaccharide extracts as there is not currently an accurate molecular weight for the GAG samples.

Table 2.1 The final concentrations (µg/ml) of each drug (cisplatin, cockle extract and whelk extract) dose in the well of an MTT plate.

Cisplatin (wells 2-14)	Cockle extract (wells 5-7)	Whelk extract (wells 8-10)
15.00 µg/ml	25.00 µg/ml	25.00 µg/ml
7.50 µg/ml	12.50 µg/ml	12.50 µg/ml
3.75 µg/ml	6.25 µg/ml	6.25 µg/ml
1.88 µg/ml	3.13 µg/ml	3.13 µg/ml
0.94 µg/ml	1.56 µg/ml	1.56 µg/ml
0.47 µg/ml	0.78 µg/ml	0.78 µg/ml
0.23 µg/ml	0.39 µg/ml	0.39 µg/ml
0.00 µg/ml	0.00 µg/ml	0.00 µg/ml

The cells were initially incubated for a given time period between 1-5 days in a humidified atmosphere of 95% air and 5% CO_2 at 37 ^{o}C. All assays were carried out in triplicate and repeated three times. Following initial optimisation studies, a three-day incubation period was decided upon for all remaining assays.

Following drug dosing (plus activation in the PBMCs) incubation, 50 µl of MTT solution (3 mg/ml in PBS) (Fisher Scientific) was added to each well. The plate was incubated for a further 3 hours. After incubation the supernatant was carefully aspirated to leave purple formazan

crystals. 200 µl of DMSO (Fisher Scientific) was then added to each well and the plate was gently agitated in order to dissolve the crystals. The plate was then read using a plate reader at 540 nm and 690 nm to eliminate background noise (Ascent software). Cell viability and the effects of the cisplatin control and the cockle extract and whelk extract treatments were then analysed as a percentage of the untreated control cell absorbance. The average cell viability was obtained from 3 sets of triplicate data at each drug concentration and was subsequently plotted as a dose-response curve. IC50 values were obtained using non-linear regression analysis (Microsoft excel).

2.4.1 MTT assay using fractions obtained from the FPLC assay

The MTT assay protocol described in method 2.4 was used for the fraction MTT assays. Fractions were obtained as per method 2.8 and fractions were identified as shown in figure 2.2.

The final concentrations of the fractions used are shown in table 2.2, cisplatin was used in the same concentration as seen in table 2.1. The fractions used for the MTT assay were fraction 3, 4, 5, 6, 8, 9, 10, 11, 12, 13, 14 and run off.

Table 2.2 The final concentrations (mg/ml) of each fraction (3,4,5,6,8,9,10,11,12,13,14 and run off sample) dose in the well of an MTT plate.

Fraction concentration (mg/ml) (3,4,5,6,8,9,10,11,12,13)	Fraction concentration (mg/ml) (14)	Fraction concentration (mg/ml) (run off)
1	0.5	2
0.5	0.25	1
0.25	0.13	0.5
0.13	0.06	0.25
0.06	0.03	0.13
0.03	0.02	0.06
0.00	0.00	0.00

2.5 Antibody staining of cancer cell lines and PBMCs for use in flow cytometry assays

A cell count was performed, and the cell solution was adjusted to give a cell concentration of $1x10^6$ cells/ml. Cells were then seeded at a concentration of $1x10^5$ cells/well of a 24 well plate and incubated for 24 hours. All doses were carried out three times in triplicate. For PBMCs a 1:1 ratio (*v/v*) of cells and either PHA (Sigma Aldrich) solution (10 µg/ml) or PMA/ionomycin solution (Sigma Aldrich) (10 ng/ml PMA & 1 µg/ml Ionomycin) (made up as per 2.7 method protocol) were added to the wells of stimulated assays. A 1:1 ratio (*v/v*) of media was added to the cells in unstimulated assays. After appropriate incubation (24 hours for cancer cell assays and unstimulated assays mirrored to PHA stimulated assays, or 4 hours for PMA/ionomycin stimulated assays and unstimulated PBMC assays mirrored to the stimulated assays (incubated with media for 4 hours or 24 hours, as opposed to PMA/ionomycin or PHA stock respectively).

An equal volume of drug solution (made up to 2x the IC50 values established from the MTT assays) was added to the wells to achieve the IC50 value in the assay. Media was added to control wells as opposed to a drug dose. The drug and cells were gently mixed and incubated for a 3-day period.

The samples were then transferred from the plate into Eppendorf tubes, antibodies (all from BD bioscience, Oxford, UK) were added to the tubes according to the manufacturer's instructions, PBS was added instead of antibodies to one set of untreated triplicate wells as a control. Cell labelling profiles can be seen in table 2.3, plate layout can be seen in table 2.4.

Table 2.3 The antibodies and their stains and with which apoptosis assay they were used in

Antibody	Florescent Stain	Assay used in
CD3	APC	MOLT-4 & K562
CD4	APC-Cy7	PBMC (stimulated & unstimulated)
CD8	PerCp-Cy 5.5	PBMC (stimulated & unstimulated)
CD45RO	PeCy7	PBMC (stimulated & unstimulated)
CD45RA	APC	PBMC (stimulated & unstimulated)
CD19	APC-Cy7	U698

Table 2.4 The layout of a typical apoptosis assay plate dosed with media for control wells +/- Ab, dosed with the IC50 values for drug doses cisplatin (6 µg/ml), cockle and whelk extracts (12 µg/ml) +Ab.

Cells + Media control Ab^-	Cells + Media control Ab^-	Cells + Media control Ab^-
Cells + Media control Ab^+	Cells + Media control Ab^+	Cells + Media control Ab^+
Cells + cisplatin Ab^+	Cells + cisplatin Ab^+	Cells + cisplatin Ab^+
Cells + Cockle extract Ab^+	Cells + Cockle extract Ab^+	Cells + Cockle extract Ab^+
Cells + Whelk extract Ab^+	Cells + Whelk extract Ab^+	Cells + Whelk extract Ab^+

The antibody: cell solutions were then incubated at room temperature for 30 minutes in the dark. The tubes were then pulsed in a micro-centrifuge (Accuspin Micro R, Fisher Scientific UK) to maximum speed until the cells had pelleted. The supernatant was discarded, and the cell pellet was then washed twice with cold PBS. The cell pellet could then be re-suspended in the desired medium. (Annexin V binding buffer for apoptosis assays, PBS for proliferation assays).

2.5.1. Apoptosis assays

After following method 2.5 for antibody staining the pellet was then re-suspended in 1X Annexin V binding buffer (BD bioscience). Cells were then stained with Annexin V and propidium iodide (PI) (according to manufacturer's instructions) (BD bioscience) with the exception of the antibody free controls which had 10 µl of PBS added. The cells were then gently vortexed and incubated in the dark for 15 minutes.

The flow cytometer (BD FACSVerse, Franklin lakes, NJ, USA) was calibrated using CS&T beads (BD bioscience). After incubation 400 µl of 1X Annexin V binding buffer was added to each tube. The tubes were then gently vortexed. Gates were set up to capture FSC and SSC cell

basic properties and the appropriate fluorescence for the assay being used. Voltages were adjusted based on the antibody free and stained controls respectively and software automatic compensation was employed. The samples were analysed by the cytometer to identify the presence of individual cell types and to quantify cell numbers undergoing apoptosis in response to the compounds.

The use of stimulated and unstimulated PBMCs in the assays allowed for the comparison of healthy naïve and rapidly proliferating PBMCs to simulate an infection. PHA or PMA/ionomycin were used as they effectively activate the T-cell division. PHA works via forming cross-links with glycosylated proteins on the cell surface of T-cells. PMA/ionomycin stimulation is a 'cleaner' method of activation as it works via an intracellular target as opposed to a cell surface target. PMA stimulated assays followed the stimulation method as set out in method 2.7.

2.5.2. CFSE proliferation assay

A cell trace stock solution was prepared by adding 18 ul of DMSO to one vial of cell trace (5 mM stock concentration) (fisher scientific) in dark conditions and mixed well. A working concentration of 5 µM was added to cell suspension in PBS (1 ul stock/1 ml cells). Cells were incubated at room temperature for 20 minutes in the dark.

Five times the original staining volume of culture medium (v/v) was added to the cells and was then incubated at room temperature for 5 minutes. This step aimed to remove any free dye remaining in solution. Cells were pelleted via centrifugation (400xg for 5 minutes) and re-suspended in culture medium. Cells were then incubated for at least 10 minutes before proceeding to seeding or stimulation. Cancer cells and PBMCs being used in unstimulated assays proceeded to seeding as per method 2.5. PBMCs being used in stimulation assays proceeded to be stimulated as per method 2.7 and then continued onto method 2.5. The delay in using the CFSE stained cells allowed the cell trace reagent to undergo acetate hydrolysis.

2.6 Antibody staining of PBMCs (naïve and stimulated) for cytokine and T_{reg} response assays

A cell count was performed, and the cell solution was adjusted to give a cell concentration of 1x106 cells/ml. Cells were then seeded at a concentration of $1x10^5$ cells/well of a 24 well plate and incubated for 24 hours. All doses were carried out three times in triplicate. A 1:1 ratio (v/v) of cells: PMA/ionomycin solution (Sigma Aldrich) (10 ng/ml PMA & 1 µg/ml Ionomycin) (made up as per 2.7 method protocol) were added to the wells of stimulated assays. A 1:1 ratio (v/v) of media was added to the cells in unstimulated assays. After appropriate incubation (4 hours for PMA/ionomycin stimulated assays and unstimulated PBMC assays performed in tandem).

An equal amount of drug solution (made up to the IC50 values obtained from the MTT assays) was added to the wells: cisplatin: 6 µg/ml, cockle extract: 12 µg/ml and whelk extract: 12 µg/ml. Media was added to control wells as opposed to a drug dose. The drug and cells were mixed and incubated for a 3-day period at 37 ^oC and 5% CO_2. The plate layout can be seen in table 2.6.

The samples were then transferred from the plate into Eppendorf tubes, cells were pulsed in a micro-centrifuge (Accuspin Micro R, Fisher Scientific UK) to maximum speed, then washed twice with PBS. Cells were then resuspended in flow cytometry staining buffer (Fisher Scientific). 50 µl of brilliant stain buffer (BD biosciences) was then added to each sample in order to prevent non-specific binding. Extracellular stains were then added (as seen in table 2.5) (CD4, CD8, GARP) (5 µl each), the anti-body free samples had 15 µl of PBS added instead of antibody. Samples were then incubated for 30 minutes in darken conditions in the fridge (4 ^oC).

Cells were again pulsed in a micro-centrifuge (Accuspin Micro R, Fisher Scientific UK) to maximum speed. Cells were washed with flow cytometry staining buffer (Fisher Scientific UK). 1 ml of fixation and permeabilization solution (fisher scientific UK) was then added to each sample (1 ml of fixation/permeabilization concentrate + 3 ml of fixation/permeabilization diluent, and 1 ml of 10X fixation/permeabilization solution in 9 ml of distilled water). Cells were then incubated for 30 minutes in the fridge. Cells were transferred to 15 ml falcon tubes (Fisher Scientific UK) and 2 ml of flow cytometry buffer was added to each sample. Cells were centrifuged for 5 minutes at 400xG.

100 µl of flow cytometry buffer was added to each cell pellet, and 2 µl of normal rat serum (Fisher Scientific UK) was added to each sample to block the cells. Cells were then incubated in the fridge for 15 minutes. Intracellular stains: FOXP3, IL-4 and IFN-γ (5 µl, 1 µl and 5 µl respectively) were added to the appropriate samples (not Ab free or FMO samples), PBS was added to samples which did not get antibodies (11 µl). Cells were then incubated for 30 minutes in the fridge. 2 ml of flow cytometry buffer were added to each sample. Cells were then centrifuged for 5 minutes at 400xG. Cells were resuspended in 1 ml of flow cytometry buffer and transferred to Eppendorf tubes. Cells were then ready to be analysed by flow cytometry.

Table 2.5 The antibodies and their stains used in the FOXP3/ cytokine staining. And whether it is an intracellular or extracellular stain.

Antibody	**Florescence Stain**	**Intracellular or Extracellular stain**
CD4	PeCy7	extracellular
CD8	APC-Cy7	extracellular
GARP	APC-A	extracellular
IL-4	FITC	intracellular
IFN-γ	PerCpCy 5.5	intracellular
FOXP3	PE	intracellular

Table 2.6 The layout of a FOXP3/cytokine assay plate dosed with media for control wells +/- Ab, dosed with the IC50 values for drug doses cisplatin (6 µg/ml), cockle and whelk extracts (12 µg/ml) +Ab. Where FMO cells have all the extracellular stains but no intracellular stains.

Cells + Media control Ab^-	Cells + Media control Ab FMO	Cells + Media control Ab^+	
Cells + cisplatin Ab^+	Cells + cisplatin Ab^+	Cells + cisplatin Ab^+	Cells + cisplatin FMO
Cells + Cockle extract Ab^+	Cells + Cockle extract Ab^+	Cells + Cockle extract Ab^+	Cells + Cockle extract FMO
Cells + Whelk extract Ab^+	Cells + Whelk extract Ab^+	Cells + Whelk extract Ab^+	Cells + Whelk extract FMO

2.7 PMA stimulation of PBMCs

PHA is a lectin which stimulates T-cell proliferation through the formation of multiple cross-links of glycoproteins present on cell surfaces. PMA however is a small organic compound, which stimulates proliferation through the activation of protein kinase C. It does this by diffusing into the cytoplasm of the cell through the cell membrane and directly activates protein Kinase C. Ionomycin addition provides the trigger for the release of calcium.

Initial assays were carried out using the PHA stimulation in order to set up the stimulation assays; however, as PHA is a lectin it may interact with the GAGs, therefore the PMA/ionomycin stimulation method was adopted to provide a cleaner assay.

PMA powder was reconstituted in DMSO to a 0.1 mg/ml concentration. The PMA stock was then frozen at -20 ^oC in 20 µl aliquots. For use in assays the stock was diluted 1:100 (*v/v*) in sterile PBS. PMA was used at a working concentration of 10 ng/ml of cell suspension.

Ionomycin powder was reconstituted in ethanol to a 0.5 mg/ml concentration and stored in smaller aliquots at -20 ^{o}C. Stock ionomycin was diluted 1:10 (*v/v*) in sterile PBS for use in assays. Final working concentration of ionomycin was 1 µg/ml of cell suspension.

A combination of ionomycin and PMA at the working concentrations was used to dose each well of PBMCs which were to be stimulated at a 1:1 ratio (*v/v*).

2.8 The purification of crude whelk extract via fast pace liquid chromatography (FPLC)

Crude whelk extracts were fractionated using an AKTA Start FPLC system (GE life sciences, Buckinghamshire, UK) via an anion exchange protocol. Samples were applied to an ion-exchange column (X16x20cm) (Fisher Scientific UK, Loughborough, UK) packed with 10 ml of DEAE-sepharose (GE life sciences). The column was equilibrated, and samples were eluted and dissolved in a 50 mM sodium phosphate buffer (50 mM sodium dihydrogen phosphate monohydrate (Fisher Scientific) and 50 mM sodium phosphate dibasic anhydrous (Fisher Scientific), pH 7.0). Whelk samples were eluted off the column initially using a linear gradient of 0-3 M NaCl (Fisher Scientific) in 50 mM sodium phosphate buffer. This was carried out over 145 minutes using a 1 ml/minute flow rate. Elution was spectrophotometrically monitored at 232 nm.

After initial analysis of the FPLC graph it became apparent that the gradient was not sufficient to bring about any level of separation in the whelk sample.

In a subsequent attempt whelk extract was diluted using a 0-0.75 M NaCl gradient over a 60-minute period. The gradient was held for 5 minutes and then further increased to a final concentration of 2M NaCl over a 30-minute period. This gradient was still insufficient to separate the whelk extract, although a slight level of separation had occurred.

A further assay was carried out using a 0-0.5 M NaCl gradient achieved over a 60-minute period and held for 5 minutes. The gradient was then further increased over a 30-minute period to 1.5 M NaCl. Although further separation was achieved it was deemed a further change to the gradient may have brought about a higher level of separation.

Therefore, an initial gradient to be achieved over a 30-minute time frame was set to 0-0.25 M NaCl and was held for 5 minutes when the maximum concentration was reached. The

gradient was then increased to 0.5 M NaCl over 30 minutes and held for 5 minutes. The gradient was then further increased to 1 M NaCl and achieved over 60 minutes. This method obtained the highest level of separation achieved to date and so fractions were collected every 2.5 minutes. The fractions were then pooled into peak sections according to the recorded graph. The FPLC graphs obtained using this method and the fractions identified and taken can be seen in figure 2.1. Pooled samples were then de-salted via PD-10 columns (Fisher scientific) (as per manufacturer instructions) and freeze dried.

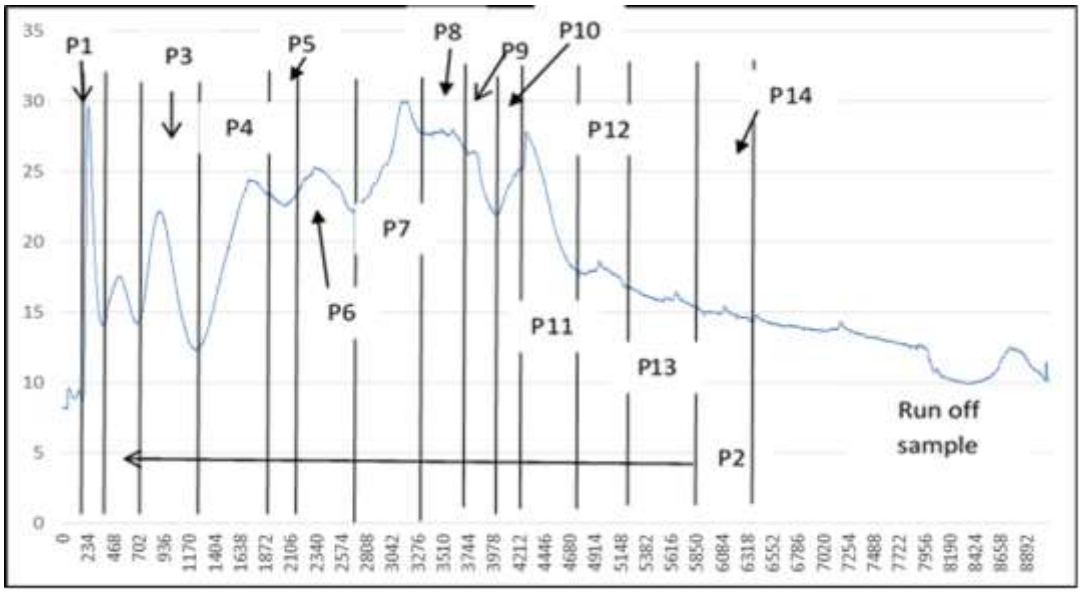

Figure 2.1 FPLC absorbance vs time graph of whelk extract sample. Whelk sample applied to a DEAE-sepharose packed X16-20cm column, eluted using a 0-0.25 M, 0.25-0.5 M and 0.5-1 M NaCl step gradient over a 130-minute time period. Elution was monitored at 232 nm.

The gradient achieved over a longer period of time appeared to help with the level of separation. As the longer time taken to achieve a gradient the more likely it is to pull the components of the whelk extract through the column at different speeds due to differing levels of negative charge, therefore achieving higher levels of separation.

The graphs which were obtained through the optimisation of the FPLC technique used on the whelk extract and the steps taken to achieve the further level of separation can be found in the appendix.

Graphs and tables displayed in the chapter 3 and 4 results were created using Microsoft excel and in chapter 5 were created using excel and Prism 8.0. Error bars shown demonstrate the

SEM. In chapters 4 and 5 the percentage differences were calculated through the subtraction of treated cell data from untreated cell data or subtraction between treatment types.

2.9 Statistical analysis

Statistical analysis was performed using GraphPad Prism 8.0 and GraphPad InStat 3.0.

In all chapters statistical analysis was performed between the treatment groups using the Two-way ANOVA test and a non-paired T-test analysis. Significance where multiple comparisons were carried out i.e. control and three treatment methods, a two way ANOVA was performed. In the case of single comparisons, a two tailed student t-test was used. Significant differences are indicated using * or equivalent depending on the level of significance, i.e: $P<0.05$ (*) and if a result was very significant $P<0.01$ (**) and extremely significant $P<0.001$ (***).

In chapter 3. The IC50 values were used to perform statistical analysis, if an IC50 value was not obtained in one of the treatments then the maximum dose of that treatment was used in order to provide a comparison to the treatment method.

In chapter 4 and 5 the percentage differences, in comparison to the untreated control, or treatment method comparison, were used to perform the statistical analysis.

CHAPTER 3- MTT/ CELL VIABILITY ASSAY

3.0 MTT/ Cell Viability Assay

3.1 Introduction

There have been numerous studies which have identified potential medicinal properties of marine GAGs, some have also identified cytotoxic activity both *in vitro* and *in vivo* models (de Jesus Raposo, 2015). The study conducted by Aldairi, Ogundipe and Pye (2018) identified for the first-time that marine polysaccharides isolated from the common cockle, which had similarities to mammalian GAGs, demonstrated anti-cancer activity on cancer cell lines *in vitro*. However the effects of GAGs on healthy cells were unknown, this research aimed to identify the effects of GAG compounds isolated from the common cockle and the common whelk on healthy lymphocytes (naïve and stimulated, PBMCs), in order to establish potential side effects of the novel compounds. The MTT assay is widely used *in vitro* in order to measure the cytotoxicity of compounds on cells lines or in primary patient cells (Van Meerloo, 2011). The use of the MTT assay allowed for the rapid identification of a suitable dose range and incubation time period for the isolated GAGs (from both the cockle and whelk sources), via testing on three cancer cell lines, to be tested on naïve and stimulated PBMCs. As the MTT was not a time-consuming assay it allowed for a wide range of doses and incubation periods to be tested on a variety of cell lines as well as the PBMCs in a short period of time.

3.1.1 Principle of the MTT assay

The MTT assay is a colorimetric assay used to measure the reduction of thiazolyl blue tetrazolium bromide (MTT dye), which is yellow in colour, by mitochondrial succinate dehydrogenase (Berridge, Herst and Tan, 2005). This occurs when the MTT dye enters the mitochondria of a cell and is reduced into a formazan salt, which is purple in colour, (Mossman, 1983). As this reduction only occurs in cells which are metabolically active the assay can be used to determine cell viability. The cells and formazan salt are solubilised using an organic solvent such as DMSO and can be measured using spectrophotometry (540 nm and 690 nm).

3.2 Method

For this research marine GAGs were isolated from both the common cockle and the common whelk via a typical extraction method using cetylpyridinium chloride (Kim et al., 1996) as set out in the methods section 2.3.

Cells were seeded for the MTT assays at a volume of 3 x 10^5 cells per well for the cancer cell assays and for the PBMC assays. In all assays cisplatin was used as a control comparison drug.

As effects of the GAG compounds on PBMCs were unknown, initially both cockle and whelk extracts were tested for anti-cancer activity against three cancer cell lines: two leukemic lines (MOLT-4 and K562) and a lymphoma cell line (U698) over a time course of 1-5 days in order to first establish an effective dose range to then carry forward onto testing in the lymphocyte assays. Once a suitable range of doses was established the healthy human lymphocyte (unstimulated PBMCs) and activated/ proliferating lymphocyte (stimulated PBMCs) assays were performed over a period of 1-5 days in order to determine a suitable incubation time point.

An initial maximum dose of 25 µg/ml was used for both the cockle extract and the whelk extract, a maximum dose of 15 µg/ml of cisplatin was used for the control. However, after the initial assay it became apparent that the cisplatin treatment was having little effect on the U698 cell line at the smaller doses and so the maximum dose of cisplatin was increased in the U698 assays to 30 µg/ml. The U698 cells demonstrated a better response to cisplatin at the new dose. The maximum dose of 25 µg/ml was effective in the MOLT-4 assays and so was used as the maximum dose for subsequent repeats. However, the maximum dose of 25 µg/ml had little effect on the K562 cell line and so the dose was increased to 100 µg/ml to try to elicit a response from the cells. In the U698 cell line the maximum dose of cockle and whelk GAGs of 25 µg/ml did appear to exert a response however the drop in cell viability was very large and so made the determination of an IC50 value difficult and so an increased maximum dose of 200 µg/ml was used to aid the capturing of an IC50 value, which proved to be effective and IC50 values were obtained. As the maximum dose of 25 µg/ml was only used for the MOLT-4 cell line, a maximum dose of 100 µg/ml was used in the PBMC assays as this represented a dose which exerted an effect on all the cell lines.

Slight batch-to-batch variability was identified by Aldairi, Ogundipe and Pye (2018). This is likely to be due to the complex nature of the mixture of polysaccharide chains present in the extracts, therefore for this research a large batch was generated in the initial stages of research in order to avoid this issue.

All MTT assays were carried out in triplicate and repeated three times, therefore data displayed in figures and tables are average values, error bars within the figure represent standard error. IC50 values were obtained using a non-linear regression analysis performed in Excel.

3.3 MTT/ cell viability results

Cell viability response assays were tested over a range of cancer cell lines to the novel GAG extracts. Cell viability response assays were also performed on naïve PBMCs and on PHA activated PBMCs in initial assay and PMA/ ionomycin activated PBMCs in subsequent assays, to identify the effects of the novel GAG compounds on healthy lymphocytes.

3.3.1 Cancer cell MTT assays

3.3.1.1 MOLT-4 cell line assays

Both cockle and whelk extracts demonstrated similar and, in some cases, exceeded the reduction of MOLT-4 cell viability exerted by the known chemotherapy drug cisplatin.

The cell viability graph (figure 3.1) identifies little effect on cell viability one and two days post incubation with cisplatin (green and light blue lines). At later time points doses from 1.8 µg/ml upwards show up to 80% reduction in MOLT-4 cell viability (dark blue, purple and red lines on figure 3.1) post cisplatin treatment. After a 3-day incubation period cisplatin appeared to have exerted its maximum effect as viability reduction was almost identical across 3-5-day incubation periods as can be seen in figure 3.1. Table 3.1 supports the cell viability data displayed in figure 3.1 as an IC50 value could not be reached after 1-day incubation with cisplatin, meaning MOLT-4 cell viability did not drop below 50%. IC50 values were then achieved in correspondence with the increase in incubation period. Although as demonstrated in table 3.1, in a similar way to the data presented in figure 3.1, there were marginal differences in IC50 values obtained between 3-5-day incubation periods post cisplatin treatment. Therefore, it can be concluded that cisplatin exerts it maximum effects at low doses post three-day incubation periods.

After 1-2-day incubation periods the cockle extract did not exert much effect (as seen in figure 3.2). In a similar way the whelk extract didn't exert much effect after 1-day incubation although an IC50 value was achieved after 2 days incubation (seen in figure 3.3 and table 3.1). The cockle and whelk extract both achieved 50% MOLT-4 cell viability reduction or more after 3-5 days incubation period with IC50 values ranging from 9.81 µg/ml- 15.56 µg/ml and 0.27 µg/ml- 10.4 µg/ml respectively (table 3.1, figures 3.2 and 3.3 respectively). The whelk extract

exerted the largest effect on the MOLT-4 cell line by reducing cell viability by up to 90% at the lowest doses (seen in figure 3.3 red and green lines).

Table 3.1 Average IC50 values obtained using the MTT assay for the MOLT-4 cell line treated with cisplatin, cockle extract and whelk extract with maximum doses 15 µg/ml, 25 µg/ml and 25 µg/ml respectively. With incubation periods between 1-5 days where N=3. IC50 values were obtained using a non-linear regression analysis (Microsoft Excel). Significance (shown via the asterisk system) - after 1 day incubation is noted by ⌂ significance in after 2 day incubation denoted by *, significance after 3 day incubation denoted by ×, significance after 4 day incubation is denoted by o and significance after 5 day incubation is denoted by Δ. Absence of significance markers indicates no significance.

Incubation time (days)	1	2	3	4	5
Treatment Maximum dose (µg/ml)					
Cisplatin (15)	Not possible	11.03 (** p= 0.0032)	4.74	5.31 (o p= 0.0134)	5.17 (Δ p= 0.03)
Cockle extract (25)	Not possible	Not possible	15.56	9.81 (o p = 0.0134)	13.15 (Δ p= 0.0103)
Whelk extract (25)	Not possible	20.33 (** p= 0.0012)	10.4	0.34 (o p= 0.0134)	0.27 (Δ p= 0.0306)

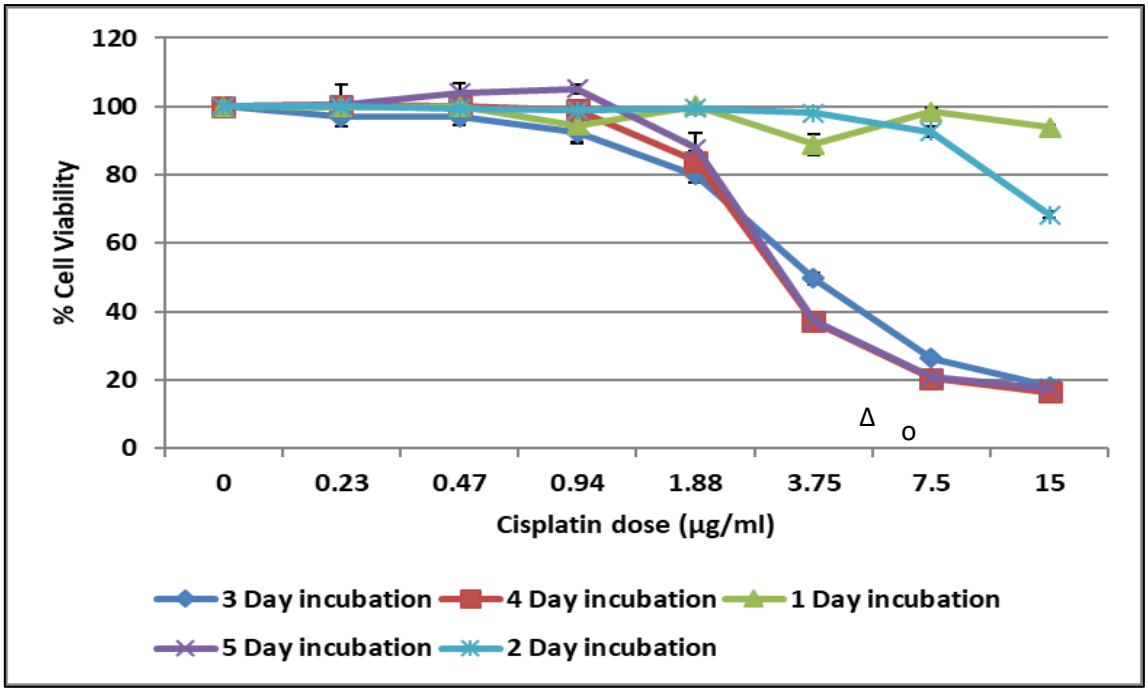

Figure 3.1 Anti-proliferative activity of cisplatin on the MOLT-4 cell line. Average cell viability for the MOLT-4 cell line treated with increasing doses cisplatin (with a maximum dose of 15 µg/ml) and incubation period ranging 1-5 days using the MTT assay. Where N=3, changes in cell viability were calculated as a percentage in comparison to untreated control cells. Error bars show SEM, significance after 1 day incubation is noted by ⌂ significance in after 2 day incubation denoted by *, significance after 3 day incubation denoted by ×, significance after 4 day incubation is denoted by o and significance after 5 day incubation is denoted by Δ.

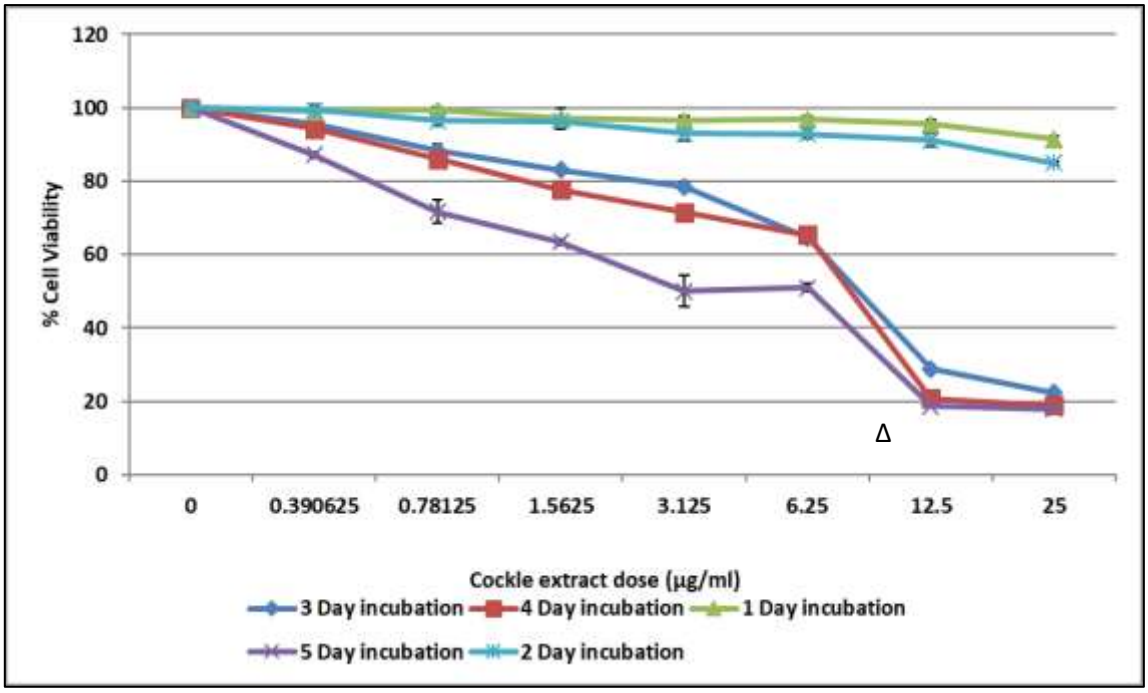

Figure 3.2 Anti-proliferative activity exerted by the cockle extract on the MOLT-4 cell line. Average cell viability for the MOLT-4 cell line treated with increasing doses of the cockle extract (with a maximum dose of 25 µg/ml) and incubation period ranging 1-5 days using the MTT assay. Where N=3, changes in cell viability were calculated as a percentage in comparison to untreated control cells. Error bars show SEM, significance after 1 day incubation is noted by ⌂ significance in after 2 day incubation denoted by *, significance after 3 day incubation denoted by ×, significance after 4 day incubation is denoted by o and significance after 5 day incubation is denoted by Δ.

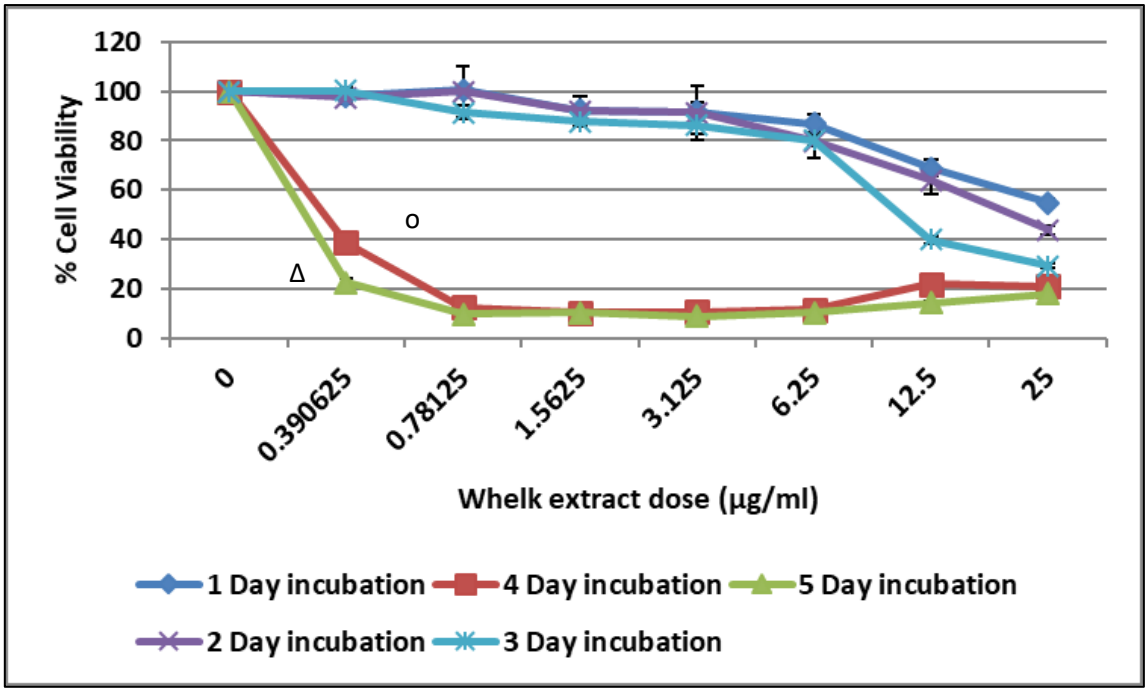

Figure 3.3 Anti-proliferative activity exerted by the whelk extract on the MOLT-4 cell line. Average cell viability for the MOLT-4 cell line treated with increasing doses of the whelk extract (with a maximum dose of 25 µg/ml) and incubation period ranging 1-5 days using the MTT assay. Where N=3, changes in cell viability were calculated as a percentage in comparison to untreated control cells. Error bars show SEM, significance after 1 day incubation is noted by ⌂ significance in after 2 day incubation denoted by *, significance after 3 day incubation denoted by ×, significance after 4 day incubation is denoted by o and significance after 5 day incubation is denoted by Δ.

3.3.1.2 K562 cell line assays

From the results obtained through the MTT assay there appeared to be little difference in the reduction of K562 cell viability between chemotherapy drug cisplatin and the cockle and whelk extract treatments. The K562 cell line did appear to be slightly more resistant to the GAG therapies than the MOLT-4 or U698 cell lines. But as the same is true for standard therapies it may be that mutations have occurred within the cell line as the passage number increased.

IC50 values demonstrated in table 3.2 show that cisplatin reduced cell viability by a minimum of 50% between 2-5 days incubation with IC50 values between 13.91 µg/ml and 10.71 µg/ml. However, the cell viability graph (figure 3.4) demonstrates that there is no real further drop in cell viability beyond 50% even with increasing doses of cisplatin.

The cockle and whelk extracts both exerted an effect on the K562 cell line from the first day of incubation which can be identified in table 3.2. The cell viability graphs (figure 3.5 and figure 3.6) show that the exerted cockle extracts effects were similar on the K562 cell line regardless of the incubation time and reduced cell viability by up to 50%. The lowest dose required to do this was 32.80 µg/ml (seen in table 3.2). The whelk extract exerted a similar effect to the cockle extract on cell viability which can be seen in table 3.2. The cell viability graphs identified that the five-day incubation period was where the whelk extract exerted the most prolific effect on the K562 cell line (light blue line in figure 3.6).

Table 3.2 Average IC50 values obtained using the MTT assay for the K562 cell line treated with cisplatin, cockle extract and whelk extract with maximum doses 15 µg/ml, 100 µg/ml and 100 µg/ml respectively. With incubation periods between 1-5 days where N=3. IC50 values were obtained using a non-linear regression analysis (Microsoft Excel), significance (shown via the asterisk system) - after 1 day incubation is noted by ⌂ significance in after 2 day incubation denoted by *, significance after 3 day incubation denoted by ×, significance after 4 day incubation is denoted by o and significance after 5 day incubation is denoted by Δ. Absence of a significance marker indicates no significance.

Incubation time (days)	1	2	3	4	5
Treatment Maximum dose (µg/ml)					
Cisplatin (15)	Not possible	13.91 (* p= 0.0312)	12.88 (×× p=0.002)	14.98	10.71 (Δ p=0.0074)
Cockle extract (100)	186.06	118.29	69.95	32.80	46.74
Whelk extract (100)	142.81	121.73	71.49 (× p=0.047)	87.31	57.97 (Δ p=0.0074)

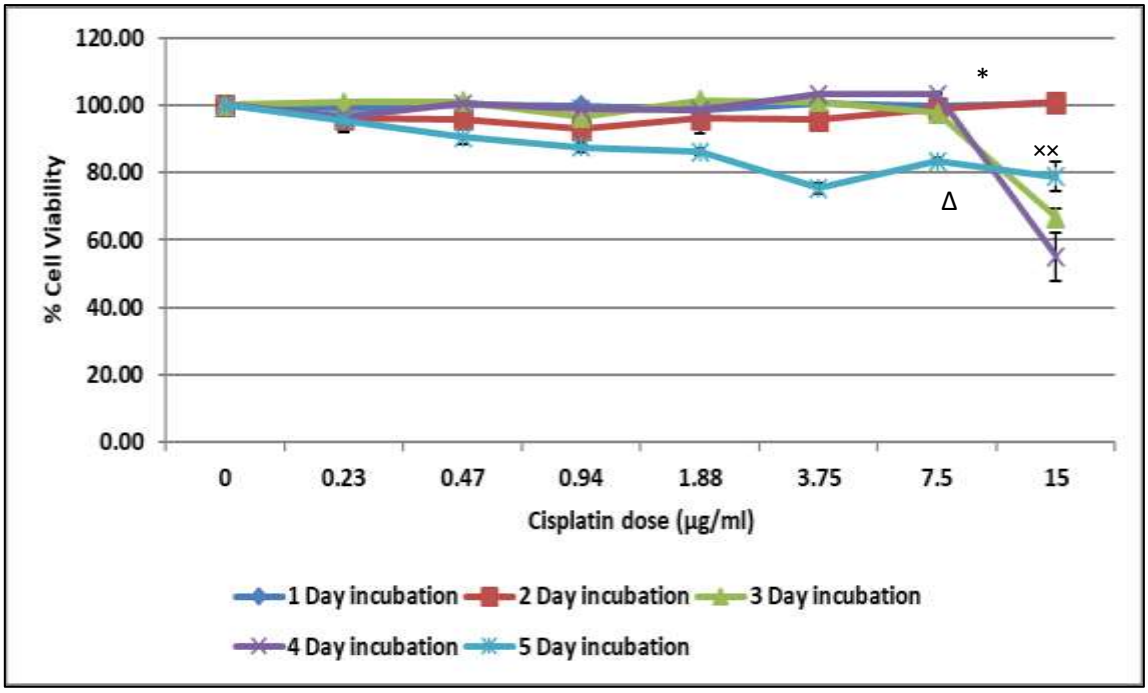

Figure 3.4 Anti-proliferative activity of cisplatin on the K562 cell line. Average cell viability for the K562 cell line treated with increasing doses cisplatin (with a maximum dose of 15 µg/ml) and incubation period ranging 1-5 days using the MTT assay. Where N=3, changes in cell viability were calculated as a percentage in comparison to untreated control cells. Error bars show SEM, significance after 1 day incubation is noted by ⌂ significance in after 2 day incubation denoted by *, significance after 3 day incubation denoted by ×, significance after 4 day incubation is denoted by o and significance after 5 day incubation is denoted by Δ.

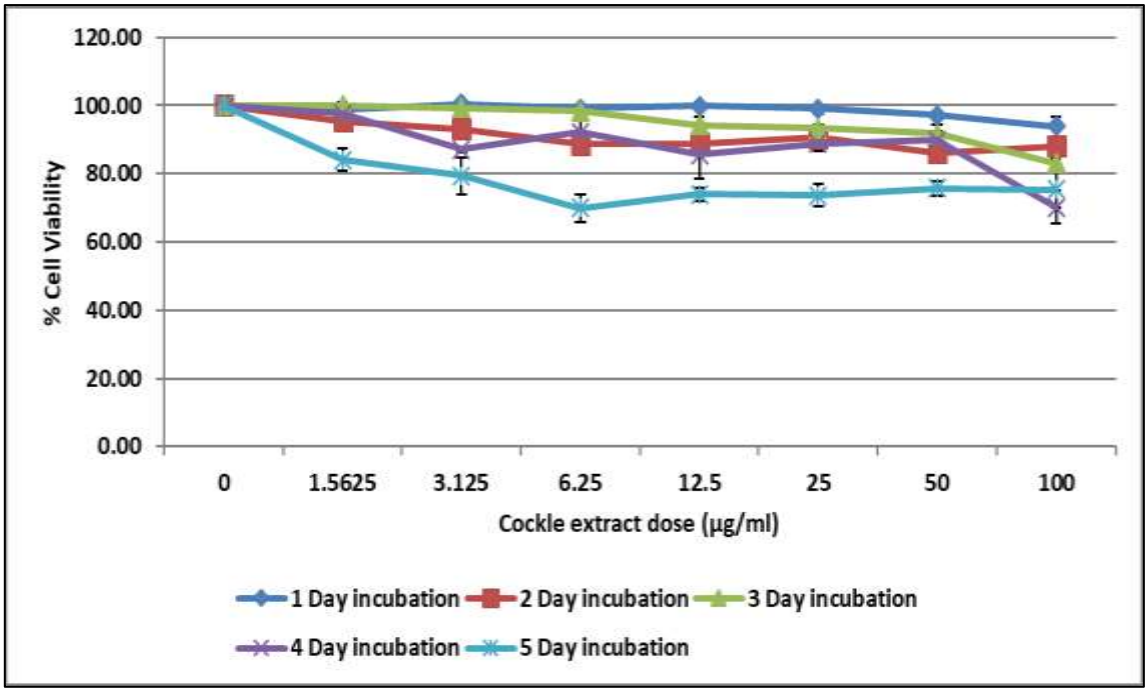

Figure 3.5 Anti-proliferative activity exerted by the cockle extract on the K562 cell line. Average cell viability for the K562 cell line treated with increasing doses of the cockle extract (with a maximum dose of 100 µg/ml) and incubation period ranging 1-5 days using the MTT assay. Where N=3, changes in cell viability were calculated as a percentage in comparison to untreated control cells. Error bars show SEM, significance after 1 day incubation is noted by ⌂ significance in after 2 day incubation denoted by *, significance after 3 day incubation denoted by ×, significance after 4 day incubation is denoted by o and significance after 5 day incubation is denoted by Δ, absence of asterisk system indicates no significance.

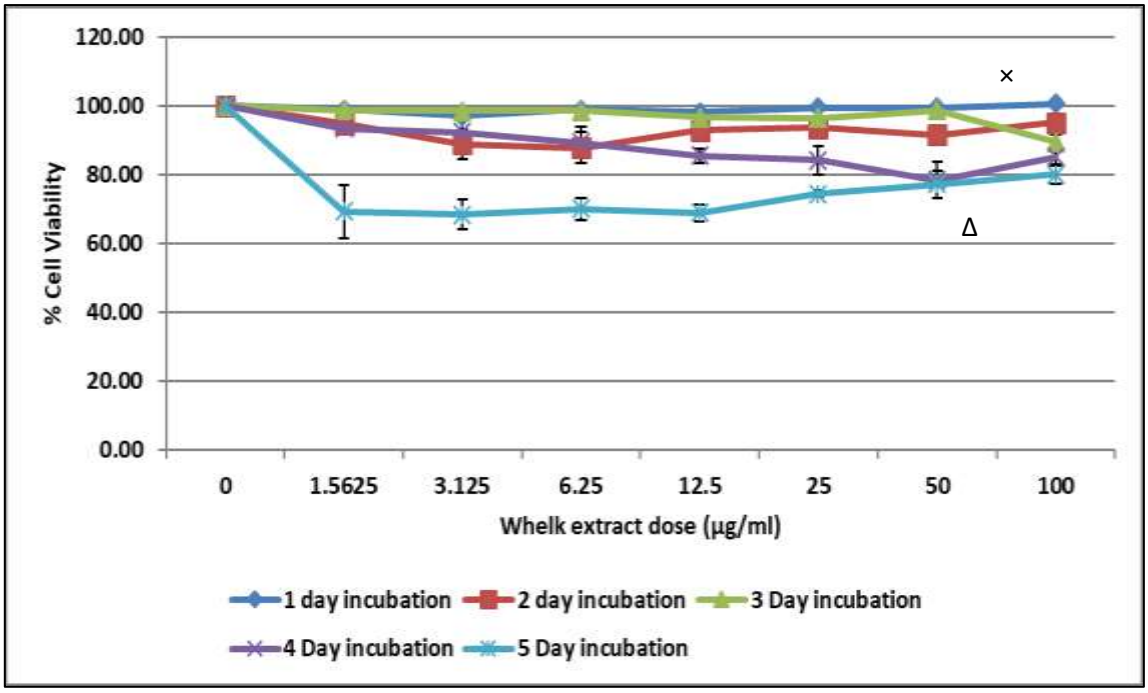

Figure 3.6 Anti-proliferative activity exerted by the whelk extract on the K562 cell line. Average cell viability for the K562 cell line treated with increasing doses of the whelk extract (with a maximum dose of 100 µg/ml) and incubation period ranging 1-5 days using the MTT assay. Where N=3, changes in cell viability were calculated as a percentage in comparison to untreated control cells. Error bars show SEM, significance after 1 day incubation is noted by ⌂ significance in after 2 day incubation denoted by *, significance after 3 day incubation denoted by ×, significance after 4 day incubation is denoted by o and significance after 5 day incubation is denoted by Δ.

3.3.1.3 U698 cell line assay

Both IC50 data (table 3.3) and cell viability data (figures 3.7, 3.8, 3.9) demonstrate that cell viability is affected in similar ways post treatment with cisplatin and cockle and whelk extract treatments.

Initial U698 responses to cisplatin were small so a higher maximum dose (30 µg/ml) was used to ensure IC50 values could be captured. This allowed for the identification of the drugs effect on U698 cell viability. A higher starting dose was also used for both GAG extracts to ensure IC50 values could be captured. The larger doses were carried out in order to identify the large drop in cell viability as this was difficult to identify in assays carried out with a maximum GAG dose of 25 µg/ml.

Cisplatin exerted an effect on cell viability which can be noted after only one day of incubation (figure 3.7). This effect can also be seen in table 3.3 as the dose of cisplatin reduced cell viability by a minimum of 50% after day one of incubation. The IC50 table 3.3 identifies low IC50 values for all cisplatin incubation periods, with values ranging between 5.63 µg/ml-0.8 µg/ml. The percentage viability graph in figure 3.7 also shows a rapid decline in U698 cell viability of up to 90%.

Both the cockle and whelk extract treatments exerted an effect on U698 cell viability. The cockle extract reduced cell viability by approximately 80-90% (seen in figure 3.8) at doses between 102.55 µg/ml and 6.31 µg/ml (as per table 3.3). This can be seen in the cell viability graphs also as even at the minimum dose of cockle extract cell viability is reduced by around 30%. The whelk extract reduced U698 cell viability by 60-90%, which is demonstrated in figure 3.9, with doses between 71.17 µg/ml and 9.54 µg/ml, seen in table 3.3.

Table 3.3 Average IC50 values obtained using the MTT assay for the U698 cell line treated with cisplatin, cockle extract and whelk extract with maximum doses 30 µg/ml, 200 µg/ml and 200 µg/ml respectively. With incubation periods between 1-5 days where N=3. IC50 values were obtained using a non-linear regression analysis (Microsoft Excel), significance (shown via the asterisk system) after 1 day incubation is noted by ⌂ significance in after 2 day incubation denoted by *, significance after 3 day incubation denoted by ×, significance after 4 day incubation is denoted by o and significance after 5 day incubation is denoted by Δ. Absence of a significance marker indicates no significance.

Incubation time (days)	1	2	3	4	5
Treatment Maximum dose (µg/ml)					
Cisplatin (30)	5.63 (⌂⌂ p= 0.0021)	1.80 (* p=0.0282)	1.27 (×× p=0.0048)	0.95 (o p=0.0211)	0.80
Cockle extract (200)	102.55 (⌂⌂ p=0.0021)	26.79 (* p=0.0282)	7.51 (× p=0.0117)	11.47 (o p=0.0218)	8.40
Whelk extract (200)	71.17 (⌂ p=0.05)	51.33 (* 0.0282)	18.00 (××× p= 0.0001)	16.15 (oo p=0.001)	13.30

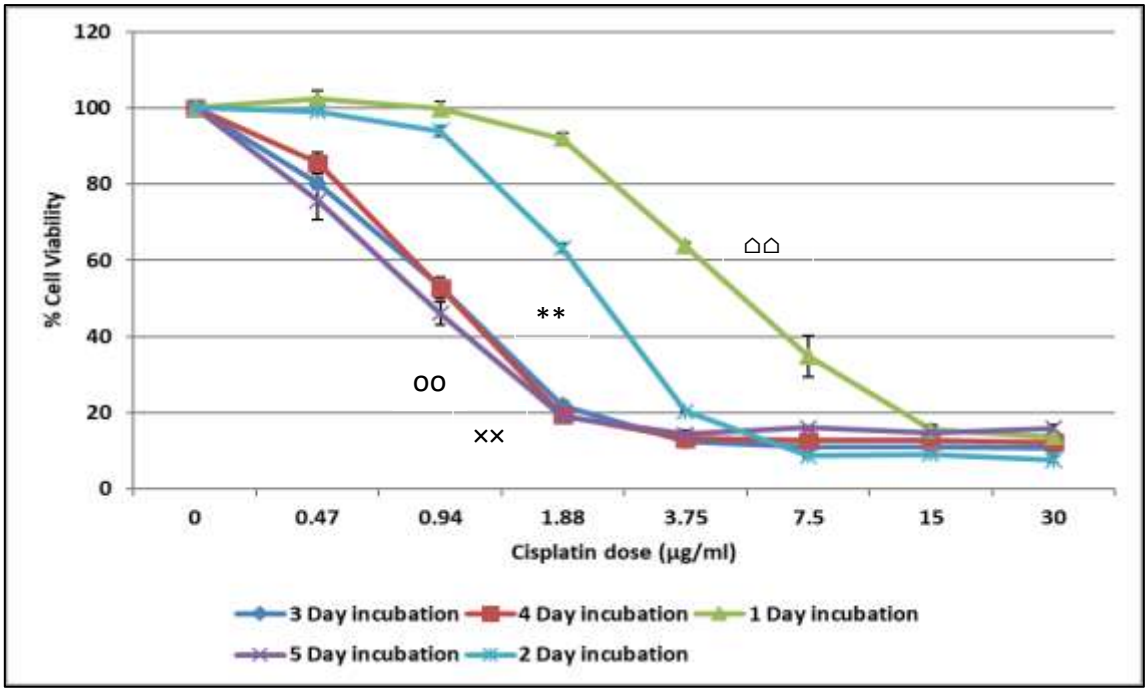

Figure 3.7 Anti-proliferative activity of cisplatin on the U698 cell line. Average cell viability for the U698 cell line treated with increasing doses cisplatin (with a maximum dose of 30 µg/ml) and incubation period ranging 1-5 days using the MTT assay. Where N=3, changes in cell viability were calculated as a percentage in comparison to untreated control cells. Error bars show SEM, significance after 1 day incubation is noted by ⌂ significance in after 2 day incubation denoted by *, significance after 3 day incubation denoted by ×, significance after 4 day incubation is denoted by o and significance after 5 day incubation is denoted by Δ.

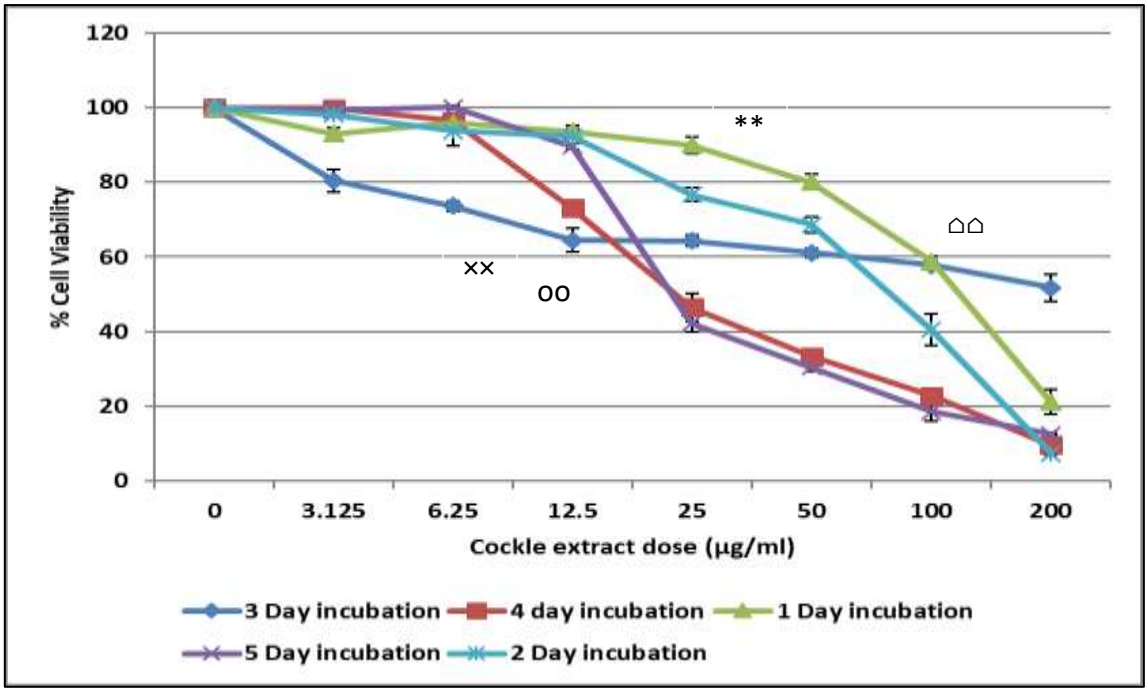

Figure 3.8 Anti-proliferative activity exerted by the cockle extract on the U698 cell line. Average cell viability for the U698 cell line treated with increasing doses of the cockle extract (with a maximum dose of 200 µg/ml) and incubation period ranging 1-5 days using the MTT assay. Where N=3, changes in cell viability were calculated as a percentage in comparison to untreated control cells. Error bars show SEM, significance after 1 day incubation is noted by ⌂ significance in after 2 day incubation denoted by *, significance after 3 day incubation denoted by ×, significance after 4 day incubation is denoted by o and significance after 5 day incubation is denoted by Δ.

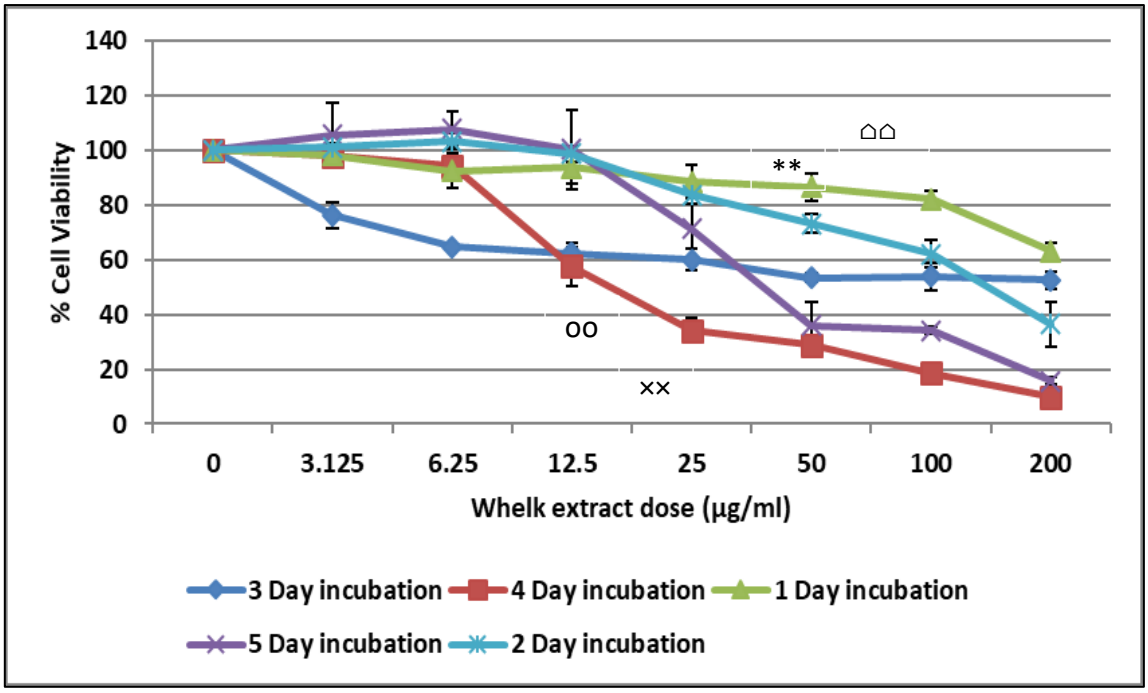

Figure 3.9 Anti-proliferative activity exerted by the whelk extract on the U698 cell line. Average cell viability for the U698 cell line treated with increasing doses of the whelk extract (with a maximum dose of 200 µg/ml) and incubation period ranging 1-5 days using the MTT assay. Where N=3, changes in cell viability were calculated as a percentage in comparison to untreated control cells. Error bars show SEM, significance after 1 day incubation is noted by ⌂ significance in after 2 day incubation denoted by *, significance after 3 day incubation denoted by ×, significance after 4 day incubation is denoted by o and significance after 5 day incubation is denoted by Δ.

3.3.2 MTT assay using isolated PBMCs

3.3.2.1 Unstimulated/ naïve PBMC MTT assays

As demonstrated in table 3.4 neither the cisplatin, cockle extract or whelk extract treatments were able to reduce the naïve PBMC population by 50%, as an IC50 value could not be achieved for any treatment method at any incubation time point.

Figure 3.10 identifies a marginal decrease in cell population at a higher dose of cisplatin, but never more than 50% therefore as demonstrated in table 3.4 an IC50 value was not obtained.

For the cockle extract treated cells as demonstrated in figure 3.11 the naïve PBMCs remained fairly unaffected and cell population was only reduced by a maximum of 10%. Whelk extract treated naïve PBMCs (seen in figure 3.12) showed the largest effects to cell population after

2 or 4-day incubation periods. The maximum doses of whelk extract almost reduced the cell population by 50% however the reduction was still lower than 50% thus an IC50 value was not obtained for any incubation period (table 3.4). This data demonstrates that at higher doses the GAGs extracts, in particular the whelk extract, exert a marginal effect on naïve lymphocytes. The apoptosis assay however would allow for a better determination of how the extract treatments were affecting the naïve lymphocytes.

Table 3.4 Average IC50 values obtained using the MTT assay for unstimulated PBMCs treated with cisplatin, cockle extract and whelk extract with maximum doses 15 µg/ml, 100 µg/ml and 100 µg/ml respectively. With incubation periods between 1-5 days where N=3. IC50 values were obtained using a non-linear regression analysis (Microsoft excel).

Incubation time (days)	1	2	3	4	5
Treatment Maximum dose (µg/ml)					
Cisplatin (15)	Not possible	Not possible	Not possible	Not possible	Not possible
Cockle extract (100)	Not possible	Not possible	Not possible	Not possible	Not possible
Whelk extract (100)	Not possible	Not possible	Not possible	Not possible	Not possible

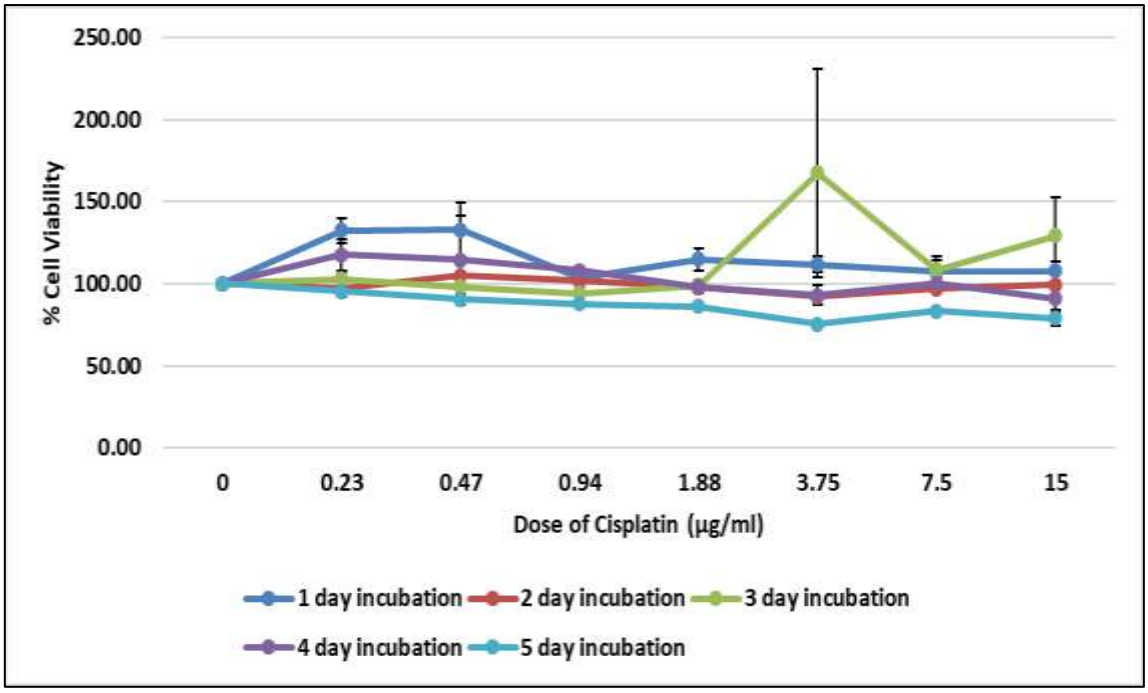

Figure 3.10 Anti-proliferative activity of cisplatin on naïve PBMCs. Average cell viability for naïve PBMCs treated with increasing doses cisplatin (with a maximum dose of 15 µg/ml) and incubation period ranging 1-5 days using the MTT assay. Where N=3, changes in cell viability were calculated as a percentage in comparison to untreated control cells. Error bars show SEM.

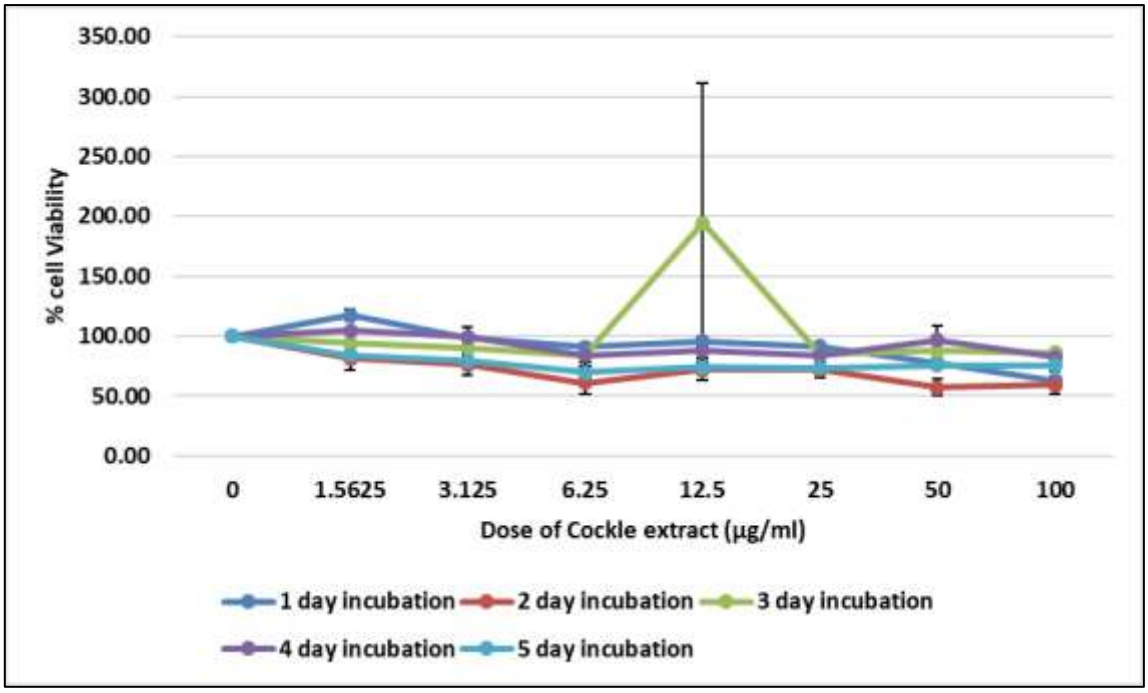

Figure 3.11 Anti-proliferative activity exerted by the cockle extract on naïve PBMCs. Average cell viability for naïve PBMCs treated with increasing doses of the cockle extract (with a maximum dose of 100 µg/ml) and incubation period ranging 1-5 days using the MTT assay. Where N=3, changes in cell viability were calculated as a percentage in comparison to untreated control cells. Error bars show SEM.

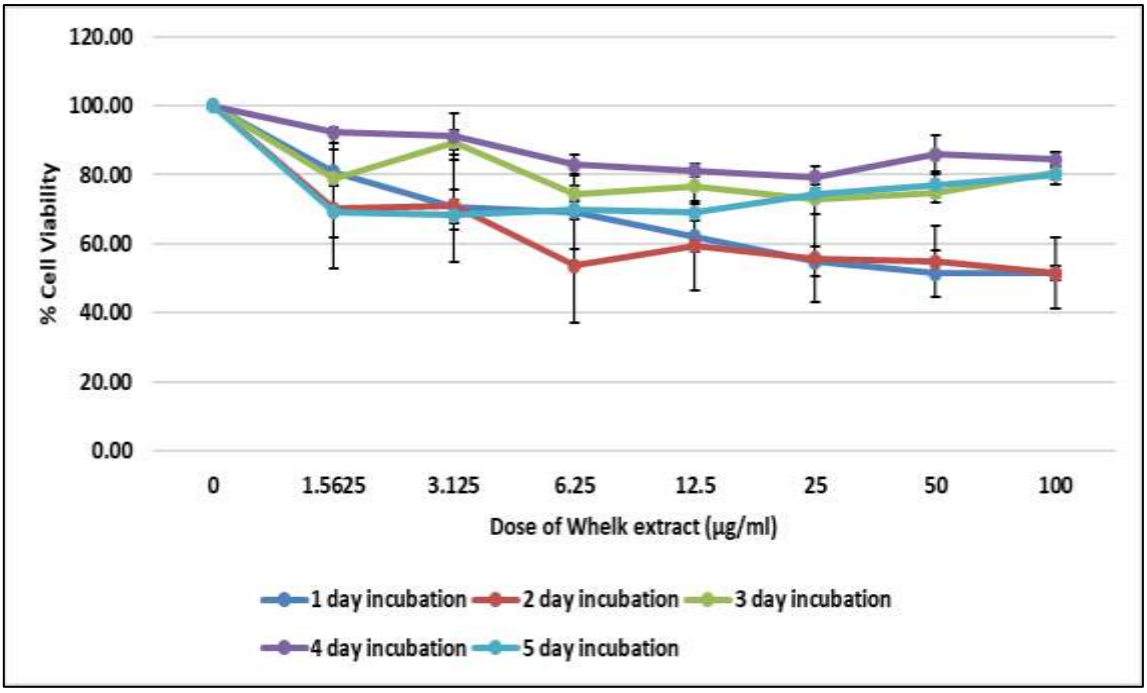

Figure 3.12 Anti-proliferative activity exerted by the whelk extract on naïve PBMCs. Average cell viability for naïve PBMCs treated with increasing doses of the whelk extract (with a maximum dose of 100 µg/ml) and incubation period ranging 1-5 days using the MTT assay. Where N=3, changes in cell viability were calculated as a percentage in comparison to untreated control cells. Error bars show SEM.

3.3.2.2 PHA activated/ stimulated PBMC MTT assays

As the PBMCs were stimulated by PHA they were expected to react/ behave like activated lymphocytes upon infection. I.e. proliferate.

For the PHA stimulated PBMCs it could be noted that all three treatment methods cisplatin, cockle and whelk extracts had very little effect on the cells during 1,4 and 5 day incubation periods. However, cisplatin appeared to exert less effect on the cell populations during the 2-day incubation period as no IC50 value could be reached (table 3.5), whereas an IC50 value was obtained for both the cockle and whelk extract treatments. All three treatment methods achieved an IC50 value post 3-day incubation with PHA activated cells thus that incubation period was decided upon for all subsequent assays.

The IC50 values seen in table 3.5 show that cisplatin reduced the stimulated PBMC population by 50%, this occurred after 3 days of incubation with cisplatin with an IC50 value of 10.69 µg/ml. This result is mirrored in the percentage growth data seen in figure 3.13. The

percentage growth graph (figure 3.13) also indicated that the simulated PBMCs were inhibited by almost 50% after 2 and 5-day incubation periods also post cisplatin treatment, although it did not quite meet a 50% decrease.

The cockle and whelk extract treatments both demonstrated the largest effect on the stimulated PBMCs after 2-3-day incubation, obtaining IC50 values ranging between 45.69 µg/ml and 29.80 µg/ml and 20.31 µg/ml and 15.49 µg/ml respectively (which can be seen in table 3.5). This is also represented in the cell viability graphs as the cockle extract reduced cell viability by around 60% both after 2 and 3-day incubation periods at maximum dose (figure 3.14). While at 1, 4 and 5-day incubation periods there appears to be minimal effect on the stimulated PBMCs. Similarly, in the whelk extract treated cells after 2 and 3-day incubation periods the stimulated PBMC population was reduced by up to 70% at maximum dose (figure 3.15). However, after 1, 4 and 5-day incubation periods even at maximum dose little effect could be seen on the population of stimulated PBMCs. Again, the apoptosis assays will provide more detail about the effect that the GAG extracts have on stimulated PBMCs.

Table 3.5 Average IC50 values obtained using the MTT assay for PHA stimulated PBMCs treated with cisplatin, cockle extract and whelk extract with maximum doses 15 µg/ml, 100 µg/ml and 100 µg/ml respectively. With incubation periods between 1-5 days where N=3. IC50 values were obtained using a non-linear regression analysis (Microsoft Excel), significance (shown via the asterisk system) - after 1 day incubation is noted by ⌂ significance in after 2 day incubation denoted by *, significance after 3 day incubation denoted by ×, significance after 4 day incubation is denoted by o and significance after 5 day incubation is denoted by Δ.

Incubation time (days)	1	2	3	4	5
Treatment Maximum dose (µg/ml)					
Cisplatin (15)	Not possible	Not possible	11.54 (×× p=0.0052)	Not possible	Not possible
Cockle extract (100)	Not possible	45.69 (** p= 0.0027)	29.80 (×× p=0.0077)	Not possible	Not possible
Whelk extract (100)	Not possible	20.31 (** p=0.0069)	15.49 (×× p=0.0052)	Not possible	Not possible

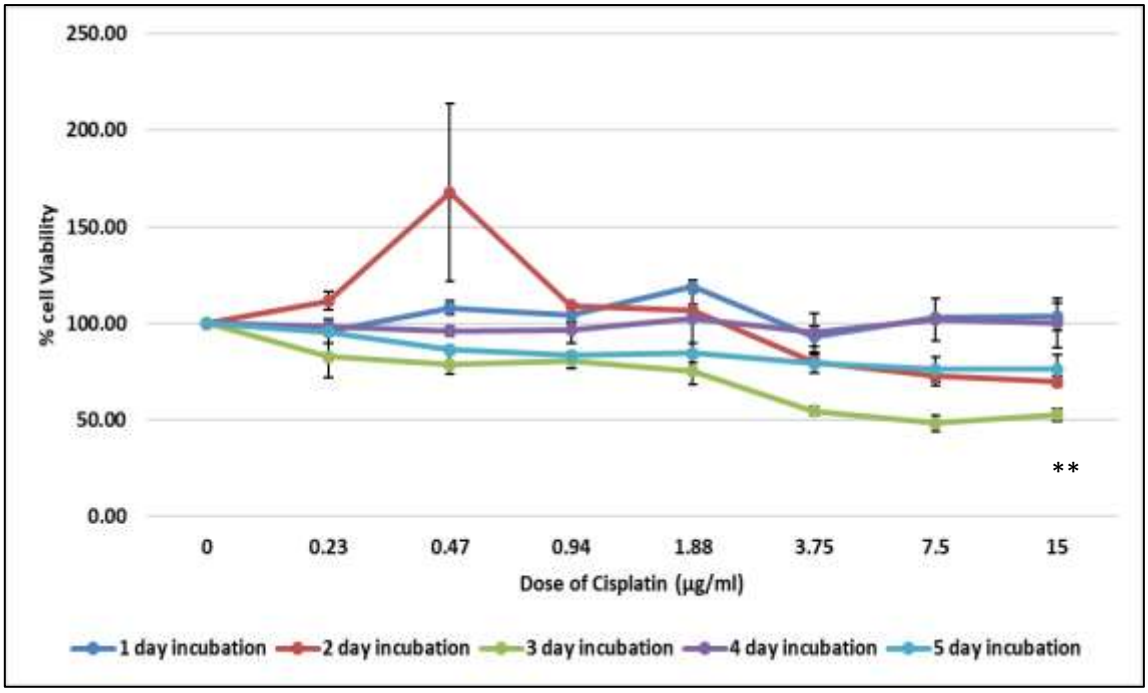

Figure 3.13 Anti-proliferative activity of cisplatin on PHA stimulated PBMCs. Average cell viability for PHA stimulated PBMCs treated with increasing doses of cisplatin (with a maximum dose of 15 µg/ml) and incubation period ranging 1-5 days using the MTT assay. Where N=3, changes in cell viability were calculated as a percentage in comparison to untreated control cells. Error bars show SEM, significance after 1 day incubation is noted by ⌂ significance in after 2 day incubation denoted by *, significance after 3 day incubation denoted by ×, significance after 4 day incubation is denoted by o and significance after 5 day incubation is denoted by Δ, absence of asterisk system indicates no significance.

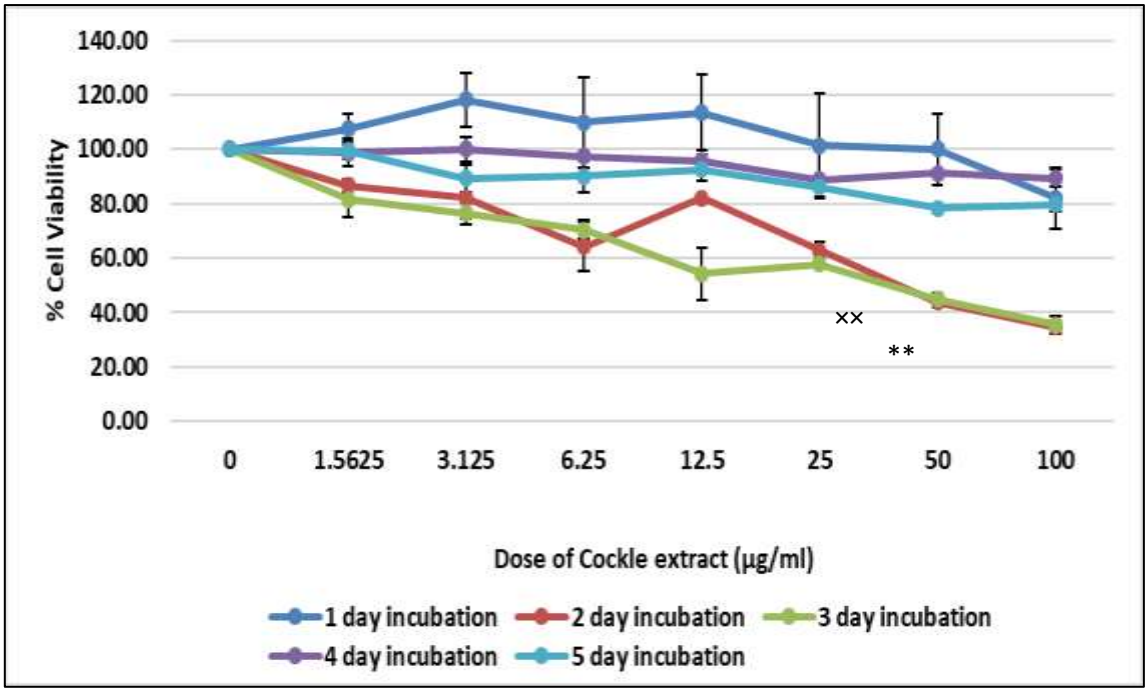

Figure 3.14 Anti-proliferative activity exerted by cockle extract on PHA stimulated PBMCs. Average cell viability for PHA stimulated PBMCs treated with increasing doses of cockle extract (with a maximum dose of 100 µg/ml) and incubation period ranging 1-5 days using the MTT assay. Where N=3, changes in cell viability were calculated as a percentage in comparison to untreated control cells. Error bars show SEM, significance after 1 day incubation is noted by ⌂ significance in after 2 day incubation denoted by *, significance after 3 day incubation denoted by ×, significance after 4 day incubation is denoted by o and significance after 5 day incubation is denoted by Δ, absence of asterisk system indicates no significance.

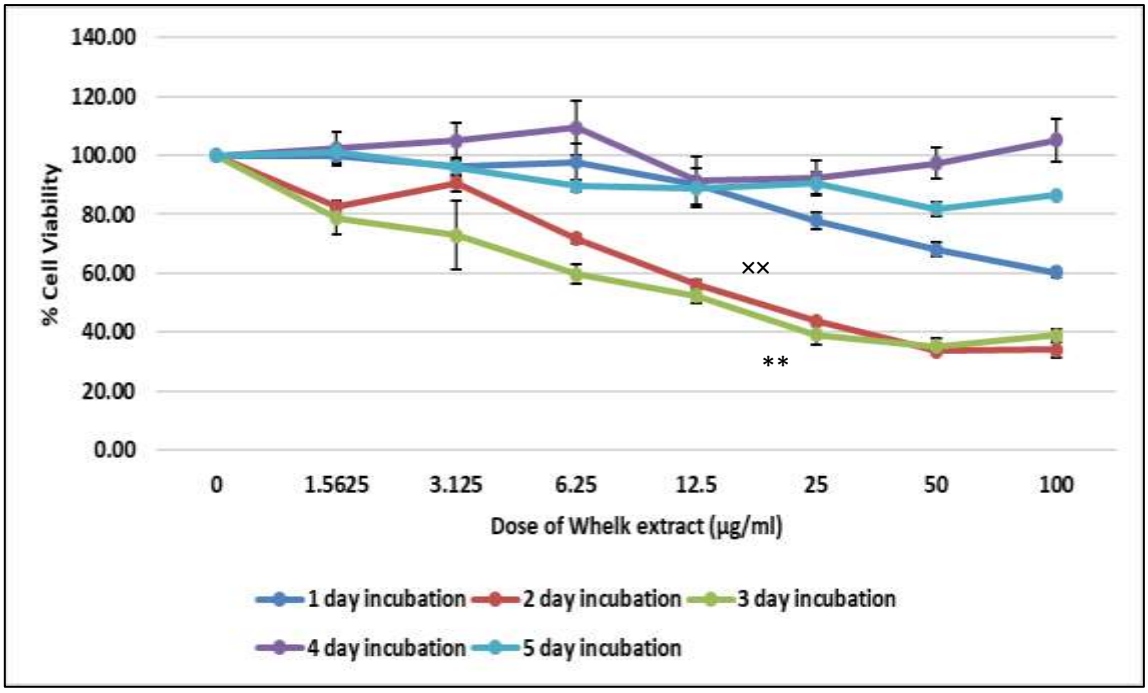

Figure 3.15 Anti-proliferative activity exerted by the whelk extract on PHA stimulated PBMCs. Average cell viability for PHA stimulated PBMCs treated with increasing doses of the whelk extract (with a maximum dose of 100 µg/ml) and incubation period ranging 1-5 days using the MTT assay. Where N=3, changes in cell viability were calculated as a percentage in comparison to untreated control cells. Error bars show SEM, significance after 1 day incubation is noted by ⌂ significance in after 2 day incubation denoted by *, significance after 3 day incubation denoted by ×, significance after 4 day incubation is denoted by o and significance after 5 day incubation is denoted by Δ, absence of asterisk system indicates no significance.

3.3.2.3 PMA/ ionomycin stimulated PBMC MTT assays

Results obtained from previous MTT assays using all three cancer cell lines and in both the PHA activated and naïve PBMC assays identified that a 3-day incubation period appeared to be the most suitable incubation period to carry forward into further assays. This was mainly due to the level of activity noted in the PBMC assays at this incubation period. Although the 4 and 5-day incubation periods also appeared effective in the assays they could be deemed to be too long an incubation time in order to evaluate apoptosis. The PBMC assay had been optimised using PHA, the PMA/ionomycin stimulation method will now be used, at the chosen incubation period for subsequent assays.

The PMA/ionomycin stimulation method was chosen as opposed to PHA due to its ability to provide a more specific stimulation to T-cells. In a comparison assay it was noted that the percentage of viable cells increased from 100% to 176.3% in PBMCs treated with PHA. However, the percentage of viable cells increased from 100% to 221.5% in PBMCs treated with PMA/ionomycin. Due to these results the PMA/ionomycin stimulation method was chosen as this replication level may provide a better insight into GAG action on rapidly proliferating cells.

For PMA/ionomycin stimulated PBMCs the cockle and whelk extracts exerted less of an effect on the cell population than the known drug cisplatin as an IC50 value could be obtained in the cisplatin treated cells (table 3.6), whereas both the cockle and whelk extract treated cells did not produce an IC50 value. Although the cockle extract cells did exert similar population reduction to cisplatin, the whelk extract exerted much less of an effect on the population ($p=0.0108$).

In table 3.6 cisplatin is identified as the only treatment method to have reduced the PMA/ionomycin treated PBMC population by 50% achieving an IC50 value of 7.35 µg/ml. This is supported by the cell growth data in figure 3.16 as cisplatin can be seen as reducing cell growth by 50%. The cockle and whelk extracts did not reduce the cell population by 50% and thus did not achieve an IC50 value as can be seen in table 3.6.

The cockle extract results seen in figure 3.17 identify that even at maximum treatment dose the cell population is not reduced by 50% therefore an IC50 value could not be calculated. Although the cell population was decreased to 51% post cockle treatment which was close to reaching an IC50 value. Figure 3.18 demonstrates that the whelk extract reduced the cell population of PMA/ionomycin stimulated PBMCs to 72%. This treatment method proved to exert the least effect on the PMA/ionomycin activated cells and had an almost 40% difference in unaffected cells compared to the cells treated by cisplatin.

Table 3.6 Average IC50 values obtained using the MTT assay for PMA/ionomycin stimulated PBMCs treated with cisplatin, cockle extract and whelk extract with maximum doses 15 µg/ml, 100 µg/ml and 100 µg/ml respectively. With an incubation period of 3 days, where N=3. IC50 values were obtained using a non-linear regression analysis (Microsoft Excel), significance after 3 day incubation denoted by ×. Significance in the cisplatin group was in comparison to the cockle and whelk extract.

Incubation time (days)	3
Treatment Maximum dose (µg/ml)	
Cisplatin (15)	7.35 (×××× p= 0.0001)
Cockle extract (100)	Not possible (× p=0.0108)
Whelk extract (100)	Not possible (× p= 0.0108)

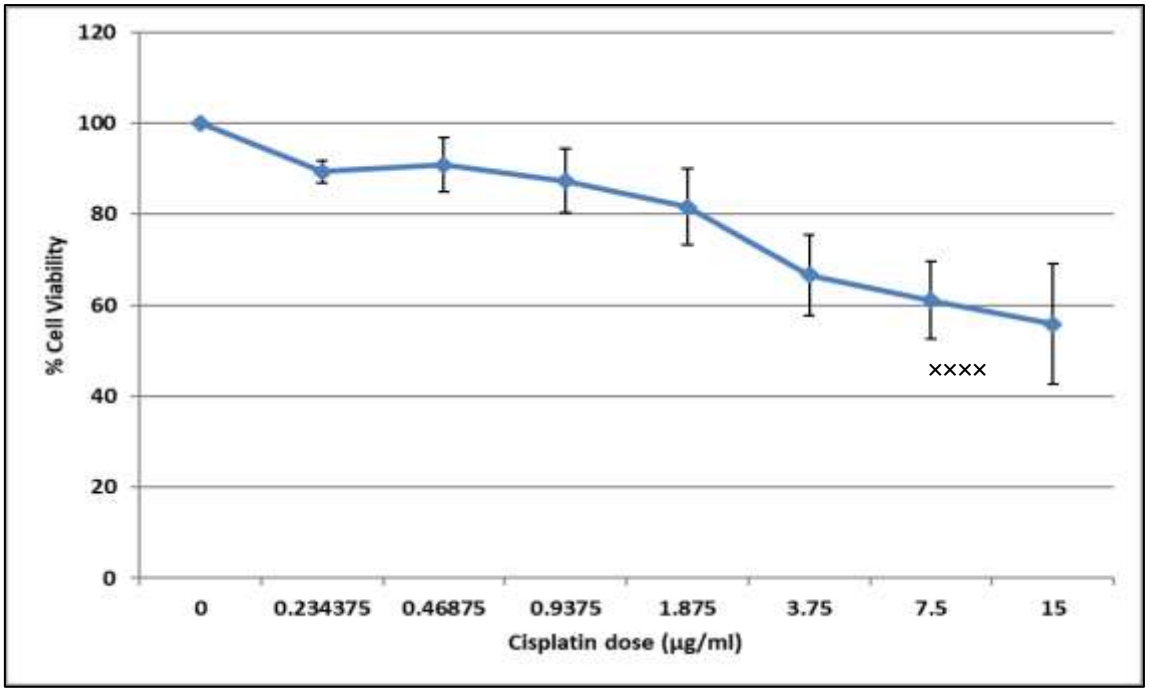

Figure 3.16 Anti-proliferative activity of cisplatin on PMA/ionomycin stimulated PBMCs. Average cell viability for PMA/ionomycin stimulated PBMCs treated with increasing doses cisplatin (with a maximum dose of 15 µg/ml) and an incubation period of 3 days using the MTT assay. Where N=3, changes in cell viability were calculated as a percentage in comparison to untreated control cells. Error bars show SEM, significance after 3 day incubation denoted by ×. Significance in the cisplatin treated cells was in comparison to the cockle and whelk extract.

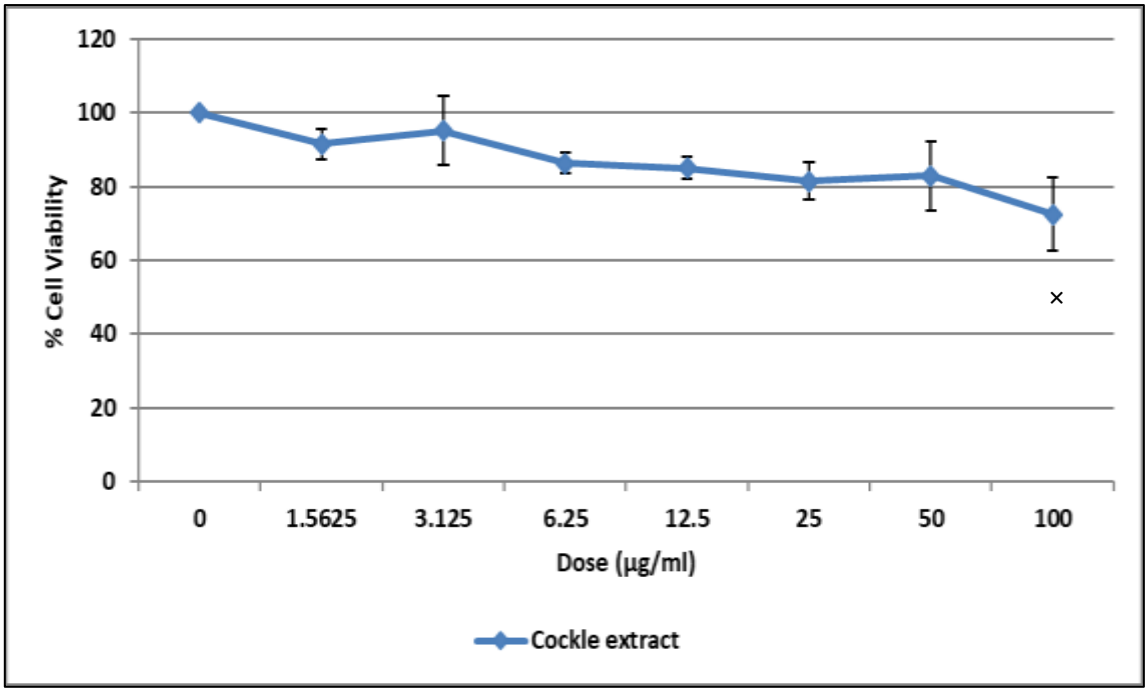

Figure 3.17 Anti-proliferative activity exerted by the cockle extract on PMA/ionomycin stimulated PBMCs. Average cell viability for PMA/ionomycin stimulated PBMCs treated with increasing doses of the cockle extract (with a maximum dose of 100 µg/ml) and an incubation period of 3 days using the MTT assay. Where N=3, changes in cell viability were calculated as a percentage in comparison to untreated control cells. Error bars show SEM, significance after 3 day incubation denoted by ×.

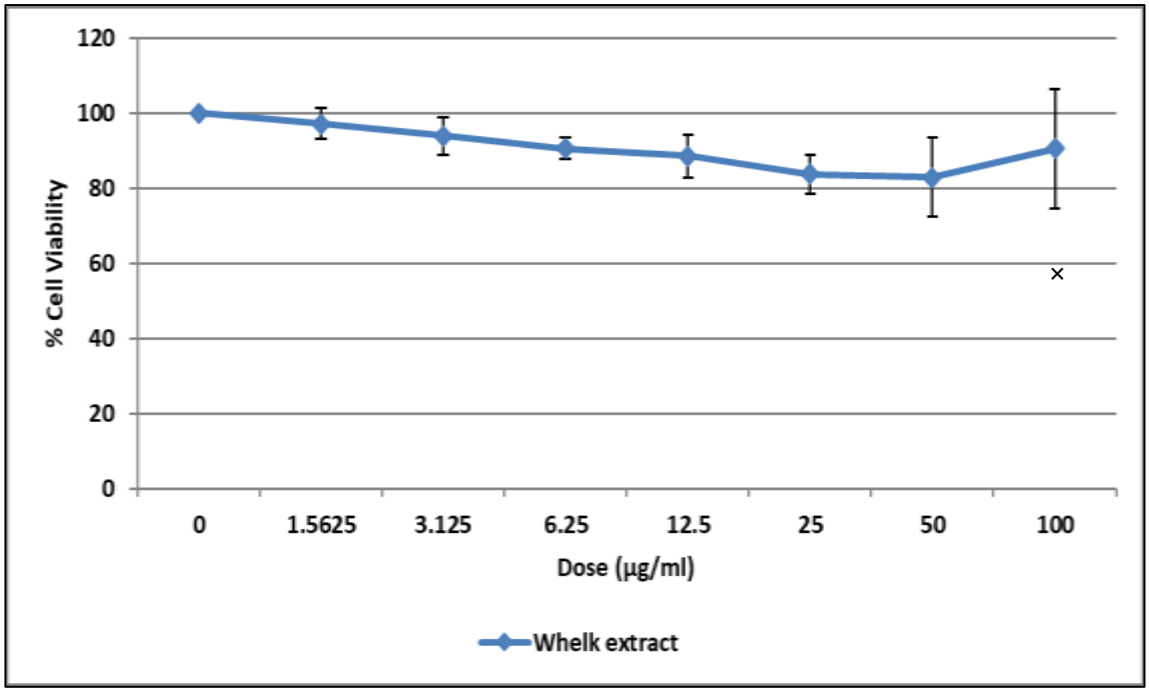

Figure 3.18 Anti-proliferative activity exerted by the whelk extract on PMA/ionomycin stimulated PBMCs. Average cell viability for PMA/ionomycin stimulated PBMCs treated with increasing doses of the whelk extract (with a maximum dose of 100 µg/ml) and an incubation period of 3 days using the MTT assay. Where N=3, changes in cell viability were calculated as a percentage in comparison to untreated control cells. Error bars show SEM, significance after 3 day incubation denoted by ×.

3.3.3 FPLC Fraction MTT/ Cell viability results

The study conducted by Aldairi, Ogundipe and Pye (2018) identified that fraction 5, of a cockle extract, obtained via FPLC had the most anti-proliferative activity of the fractions they obtained. For this research the whelk extract fractions obtained via the FPLC (method 2.8) assay were tested for any anti-proliferative activity using the MTT assay. Fractions 3, 4, 5, 6, 8, 9, 10, 11, 12, 13, 14 and the fraction run off were tested on all three cancer cell lines (MOLT-4, K562 and U698). Fractions were also tested on PBMCs both naïve and PMA/ionomycin stimulated, however formazan crystals were difficult to obtain during this set of assays in most plates across all three repeats. In all assays cisplatin was used as the control comparison drug. Cells were incubated post treatment with the drug for three days.

As there were not sufficient volumes of fraction 14 obtained during the FPLC assays, the maximum dose used for fraction 14 was half that of the other fractions. While the amount of

run off fraction obtained was higher and as it was expected to contain little quantity of GAGs the maximum dose was double that of the other fractions.

All MTT assays were carried out in triplicate and replicated three times. Therefore data displayed in the figures are average values, error bars within the figures represent standard error. IC50 values could not be obtained for any of the initial MTT results. If an IC50 was obtained this was through a linear regression analysis performed in excel.

3.3.3.1 MOLT-4 Cell line GAG fraction assays

None of the fractions tested exerted much of an effect on the MOLT-4 cells in comparison to the known drug cisplatin. This therefore led to an increase in fraction dose to be considered.

The cell viability graph in figure 3.19 identifies that cisplatin treatment reduced MOLT-4 cell growth by almost 50%. Whilst figure 3.20 demonstrates that treatment with fraction 3 (blue line), fraction 4 (orange line), fraction 5 (grey line) and fraction 6 (yellow line) exerted very little effect on the MOLT-4 cells. With a maximum reduction in cell viability of around 20%. Fraction 5 in figure 3.20 appears to be exerting the most effect on the MOLT-4 cells. In figure 3.21 it can be seen that the isolated fraction 8 (blue bar), fraction 9 (orange bar) and fraction 10 (grey bar) exert little effect on the MOLT-4 cell line with the doses that had been selected. In this instance all the fractions appear to be exerting similar effects with a maximum cell viability reductions of around 15%. Fraction 11 (blue line), fraction 12 (orange line) and fraction 13 (grey line) in figure 3.22 have little effect on the MOLT-4 cell line. Fraction 11 and fraction 13 appear to have promoted cell proliferation slightly in the MOLT-4 cells, as percentage cell viability is consistently above 100%. Fraction 12 (orange line, figure 3.22) appears to have exerted the most effect with cell viability reductions of around 20% post treatment. Figure 3.23 identifies some antiproliferative activity in fraction 14 treated MOLT-4 cells, with cell viability reductions of around 15%. The run off sample (figure 3.24) also appears to exert some effect on the MOLT-4 cells with cell viability reductions of around 15%, in a similar manner to that seen in the other fraction treated cells.

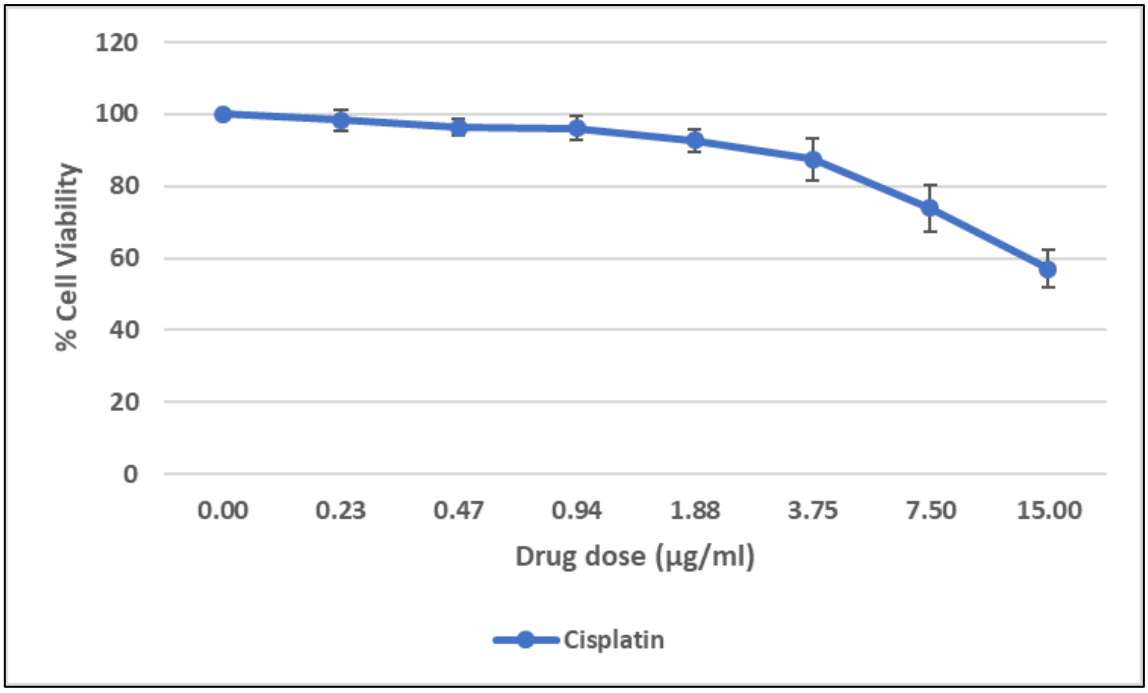

Figure 3.19 Anti-proliferative activity exerted by cisplatin treatment on the MOLT-4 cell line. Average cell growth for the MOLT-4 cell line treated with increasing doses of cisplatin (with a maximum dose of 15 µg/ml) and incubation period of 3 days using the MTT assay. Where N=6, changes in cell growth were calculated as a percentage in comparison to untreated control cells. Error bars show SEM.

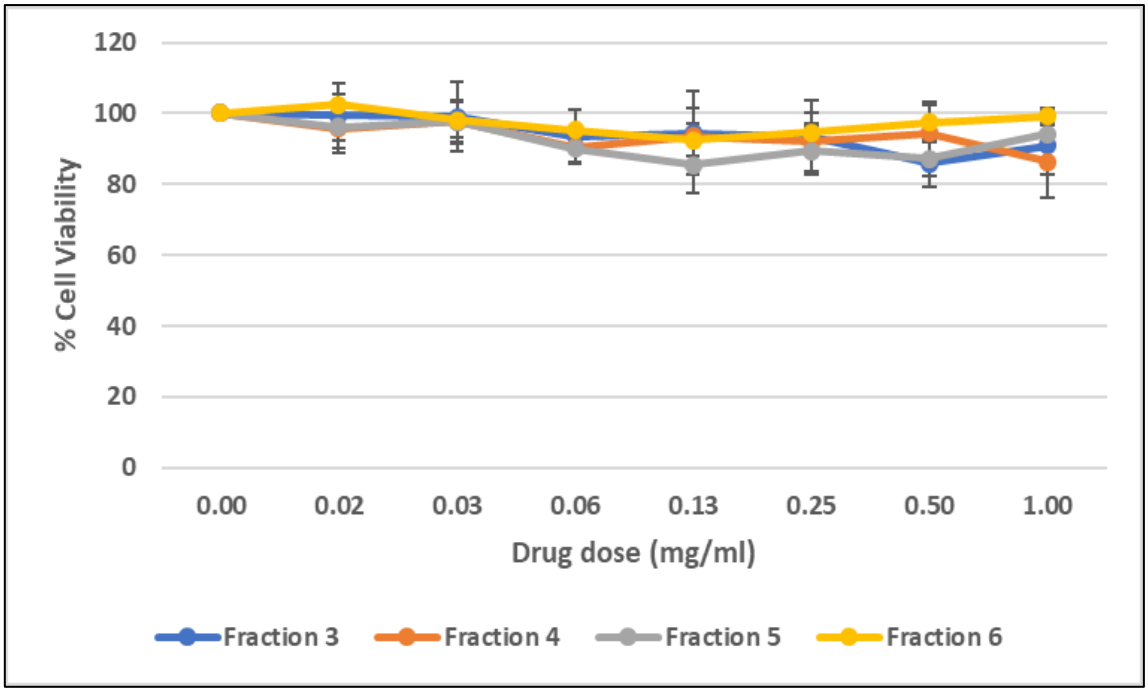

Figure 3.20 Anti-proliferative activity exerted by FPLC fractions 3,4, 5 and 6 (of the whelk extract) treatment on the MOLT-4 cell line. Average cell growth for the MOLT-4 cell line treated with increasing doses of whelk extract fractions 3 (blue line), 4 (orange line), 5 (grey line) and 6 (yellow line) (with a maximum dose of 1 mg/ml) and incubation period of 3 days using the MTT assay. Where N=3, changes in cell growth were calculated as a percentage in comparison to untreated control cells. Error bars show SEM.

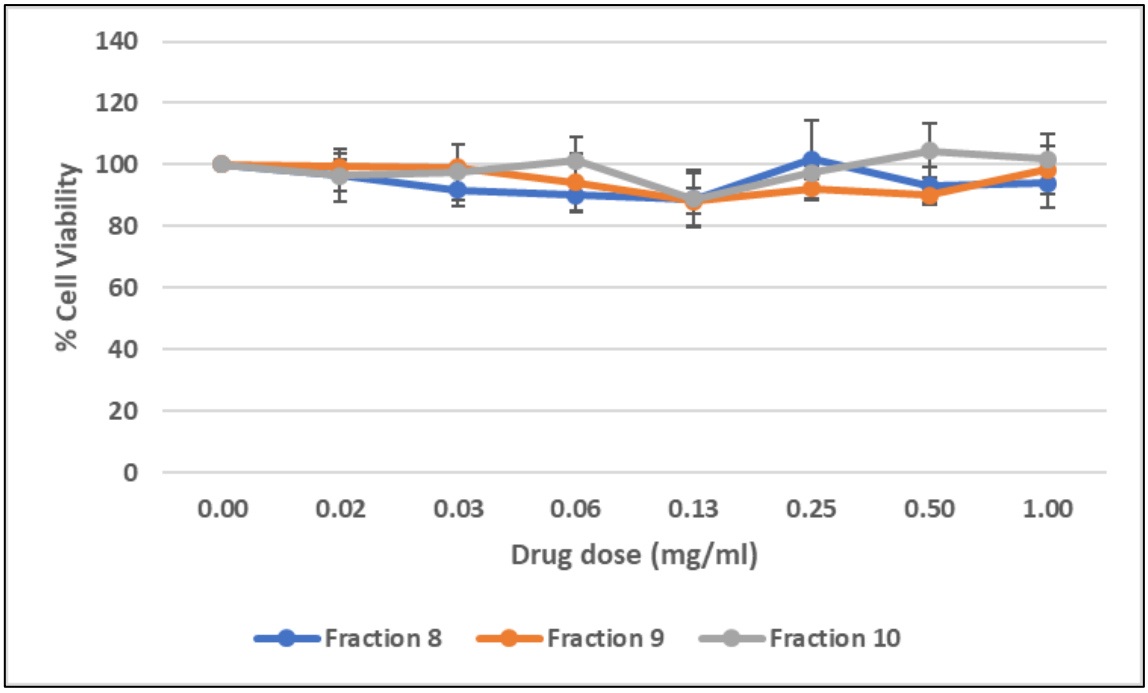

Figure 3.21 Anti-proliferative activity exerted by FPLC fractions 8, 9 and 10 (of the whelk extract) treatment on the MOLT-4 cell line. Average cell growth for the MOLT-4 cell line treated with increasing doses of whelk extract fractions 8 (blue line), 9 (orange line) and 10 (grey line) (with a maximum dose of 1 mg/ml) and incubation period of 3 days using the MTT assay. Where N=3, changes in cell growth were calculated as a percentage in comparison to untreated control cells. Error bars show SEM.

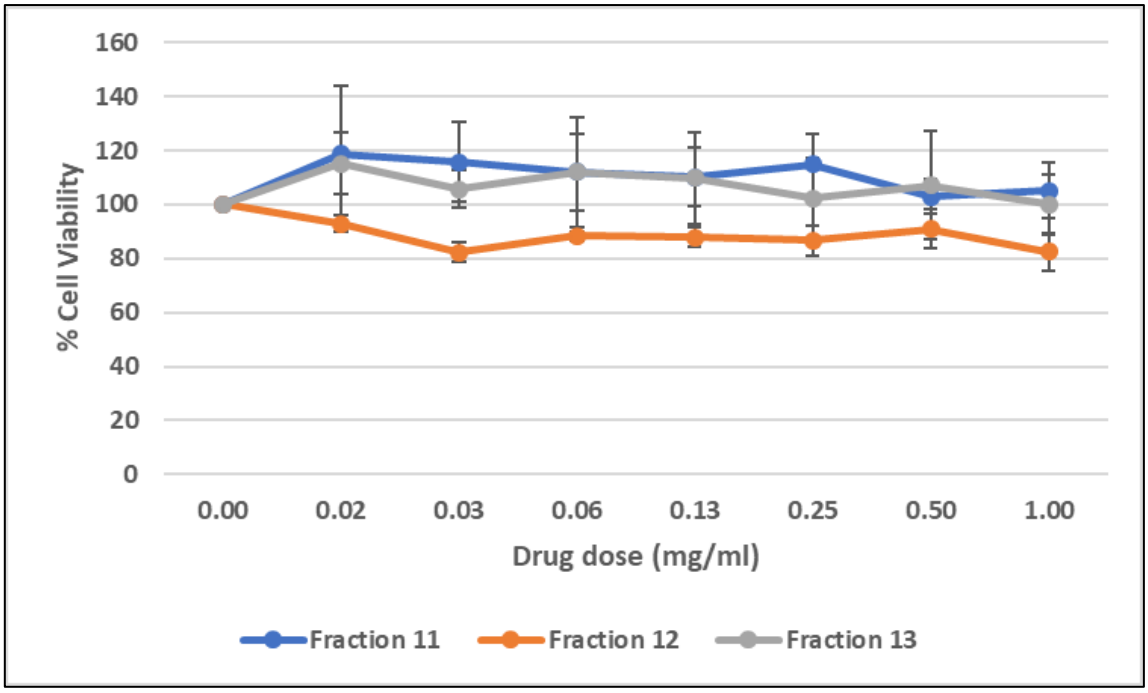

Figure 3.22 Anti-proliferative activity exerted by FPLC fractions 11, 12 and 13 (of the whelk extract) treatment on the MOLT-4 cell line. Average cell growth for the MOLT-4 cell line treated with increasing doses of whelk extract fractions 11 (blue line), 12 (orange line) and 13 (grey line) (with a maximum dose of 1 mg/ml) and incubation period of 3 days using the MTT assay. Where N=3, changes in cell growth were calculated as a percentage in comparison to untreated control cells. Error bars show SEM.

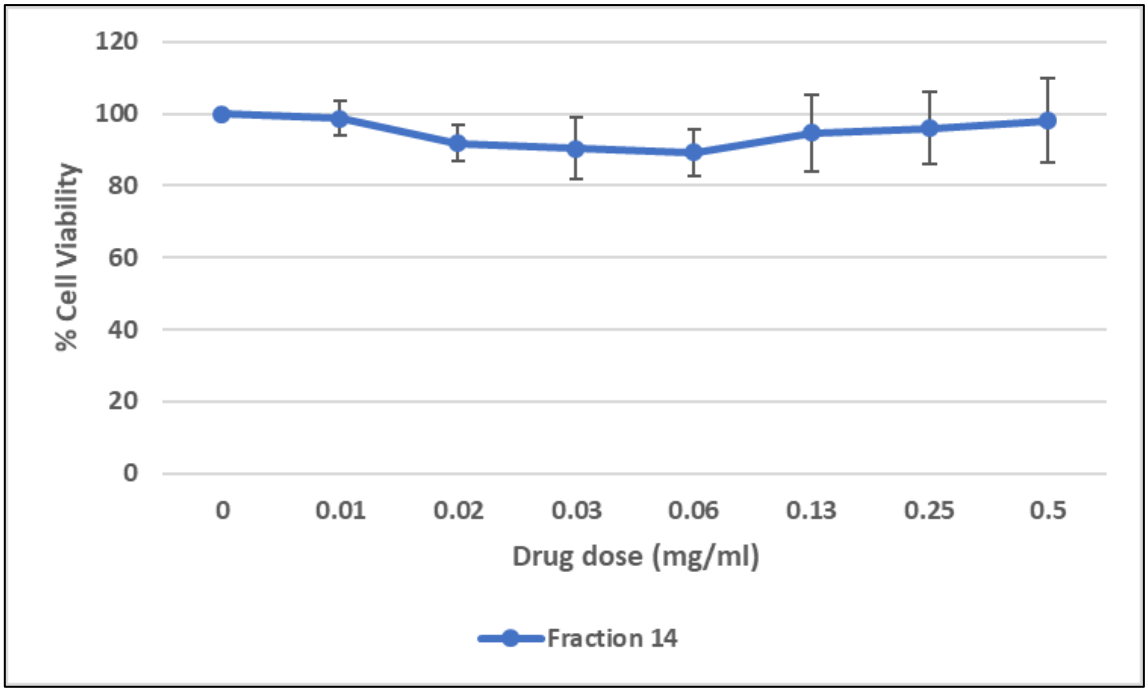

Figure 3.23 Anti-proliferative activity exerted by FPLC fraction 14 (of the whelk extract) treatment on the MOLT-4 cell line. Average cell growth for the MOLT-4 cell line treated with increasing doses of whelk extract fraction 14 (blue line) (with a maximum dose of 0.5 mg/ml) and incubation period of 3 days using the MTT assay. Where N=3, changes in cell growth were calculated as a percentage in comparison to untreated control cells. Error bars show SEM.

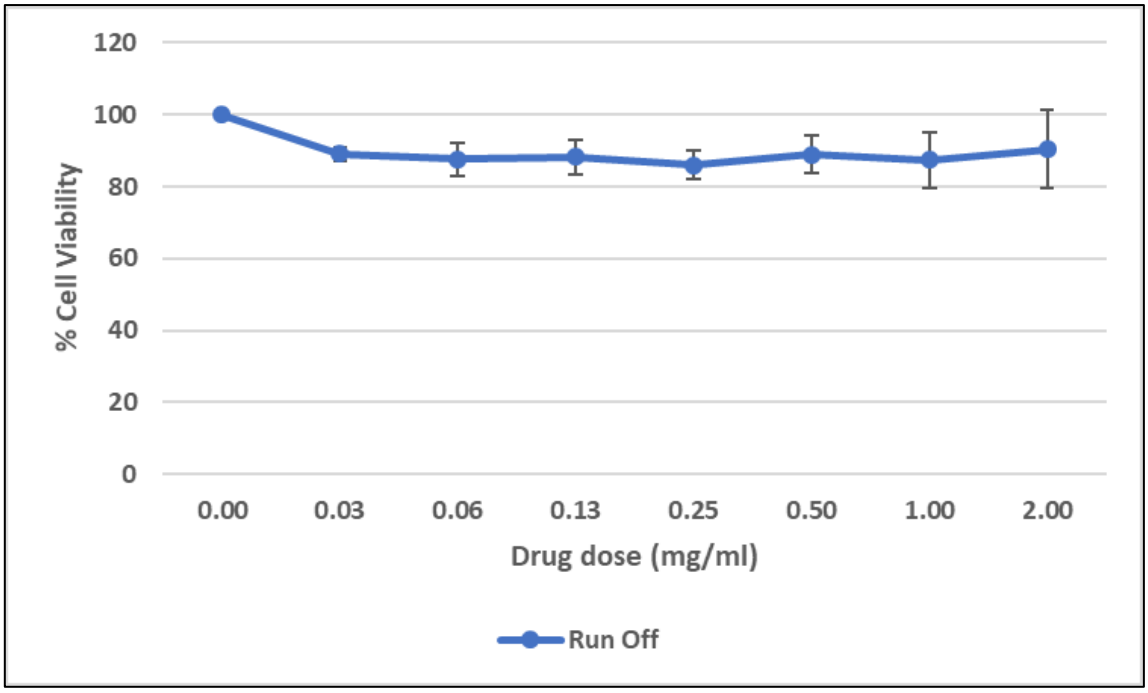

Figure 3.24 Anti-proliferative activity exerted by FPLC run off sample (of the whelk extract) treatment on the MOLT-4 cell line. Average cell growth for the MOLT-4 cell line treated with increasing doses of whelk extract run off sample (blue line) (with a maximum dose of 2 mg/ml) and incubation period of 3 days using the MTT assay. Where N=3, changes in cell growth were calculated as a percentage in comparison to untreated control cells. Error bars show SEM.

3.3.3.2 K562 cell line GAG fraction assays

The whelk extract fractions exerted little effect on the K562 cell line, however did exert more of an effect that the known drug cisplatin due to the poor response of the K562 cell line to treatment as had been noted in all previous assays. This was the reason that the K562 cell line had been discounted from previous assays.

It can be noted that cisplatin treatment in the K562 cell line brought about no more than a 4% decline in K562 cell viability (figure 3.25). Treatment with fractions 3 (blue line), fraction 4 (orange line), fraction 5 (grey line) and fraction 6 (yellow line) (figure 3.26) brought about cell viability reductions of around 5-10% in the K562 cell line. With all the fractions appearing to result in similar effects on the cell line. Figure 3.27 demonstrates that fraction 8 (blue line) exerted the best effect on the K562 cell line with a reduction of around 15% in cell viability. Fraction 9 (orange line, figure 3.27) exerted the next best effect on the K562 cell line in this figure, however didn't actually reduced the K562 cell viability by more than a few percent.

Fraction 10 (grey line, figure 3.27) appeared to promote K562 cell proliferation, as cell viability increased by around 20% at the higher doses of fraction 10. In figure 3.28 it can be seen that both fraction 11 (blue bar) and fraction 12 (orange bar) had an increase in cell viability/ proliferation in the K562 cell line with increases between 10-20%. Fraction 13 (grey line, figure 3.28) exerted little effect on the K562 cell line with cell viability failing to drop lower than 98% even at the highest treatment dose. Figure 3.29 identifies that treatment with fraction 14 reduced K562 cell viability by around 5% during the middle treatment doses (0.03mg/ml and 0.06mg/ml). However cell viability then began to rise with further increasing of fraction 14 doses (figure 3.29). The runoff treatment (figure 3.30) exerted little effect on the K562 cell line with cell viability only dropping below 98% at the treatment dose of 0.25mg/ml.

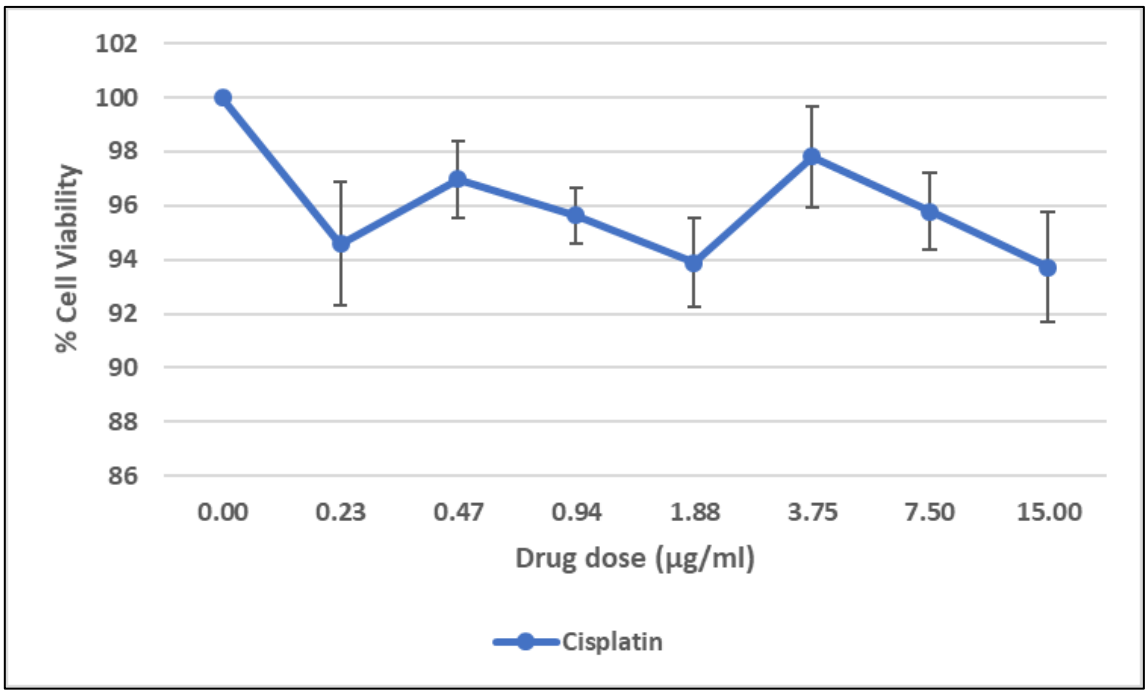

Figure 3.25 Anti-proliferative activity exerted by cisplatin treatment on the K562 cell line. Average cell growth for the K562 cell line treated with increasing doses of cisplatin (with a maximum dose of 15 µg/ml) and incubation period of 3 days using the MTT assay. Where N=6, changes in cell growth were calculated as a percentage in comparison to untreated control cells. Error bars show SEM.

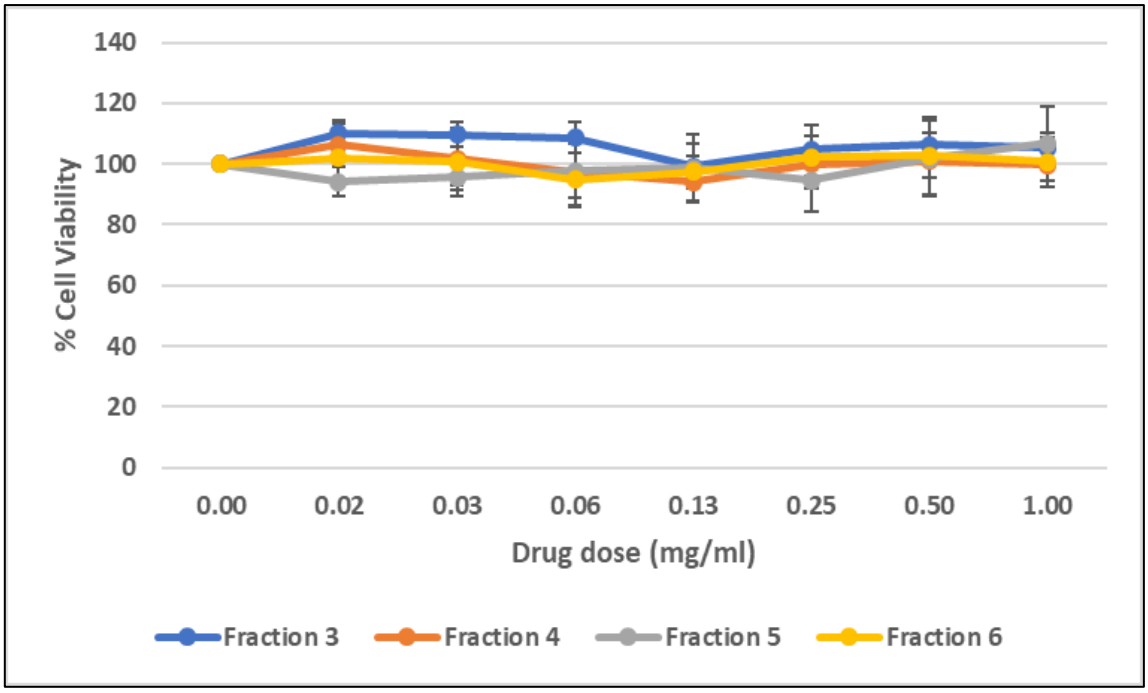

Figure 3.26 Anti-proliferative activity exerted by FPLC fractions 3,4, 5 and 6 (of the whelk extract) treatment on the K562 cell line. Average cell growth for the K562 cell line treated with increasing doses of whelk extract fractions 3 (blue line), 4 (orange line), 5 (grey line) and 6 (yellow line) (with a maximum dose of 1 mg/ml) and incubation period of 3 days using the MTT assay. Where N=3, changes in cell growth were calculated as a percentage in comparison to untreated control cells. Error bars show SEM.

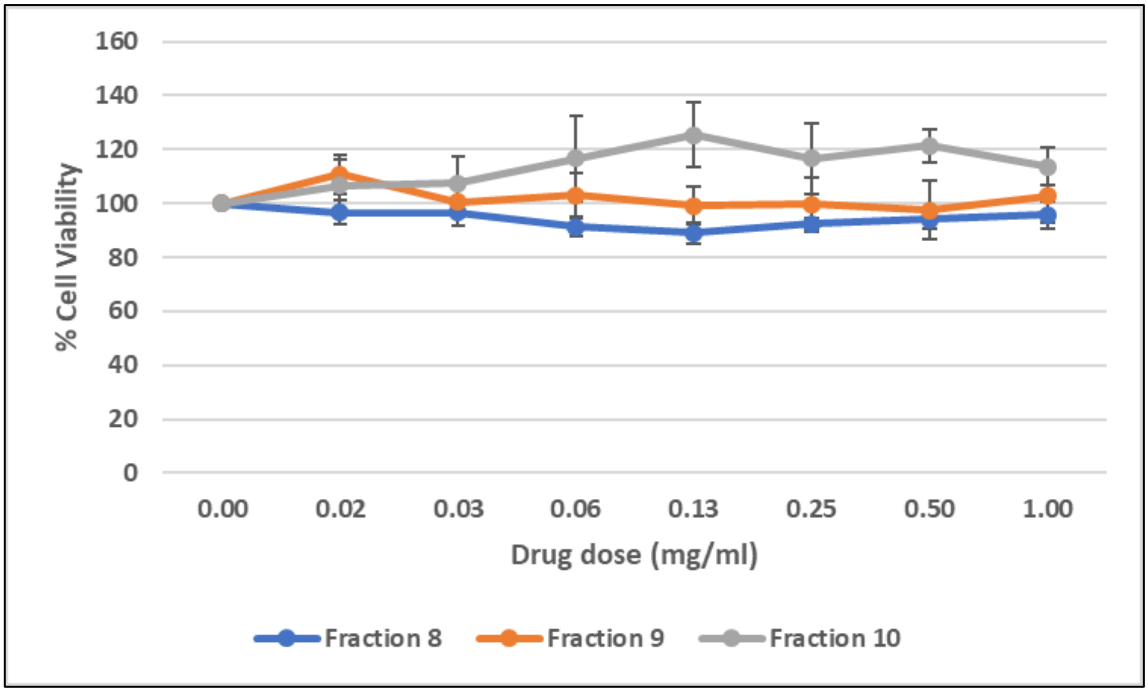

Figure 3.27 Anti-proliferative activity exerted by FPLC fractions 8, 9 and 10 (of the whelk extract) treatment on the K562 cell line. Average cell growth for the K562 cell line treated with increasing doses of whelk extract fractions 8 (blue line), 9 (orange line) and 10 (grey line) (with a maximum dose of 1 mg/ml) and incubation period of 3 days using the MTT assay. Where N=3, changes in cell growth were calculated as a percentage in comparison to untreated control cells. Error bars show SEM.

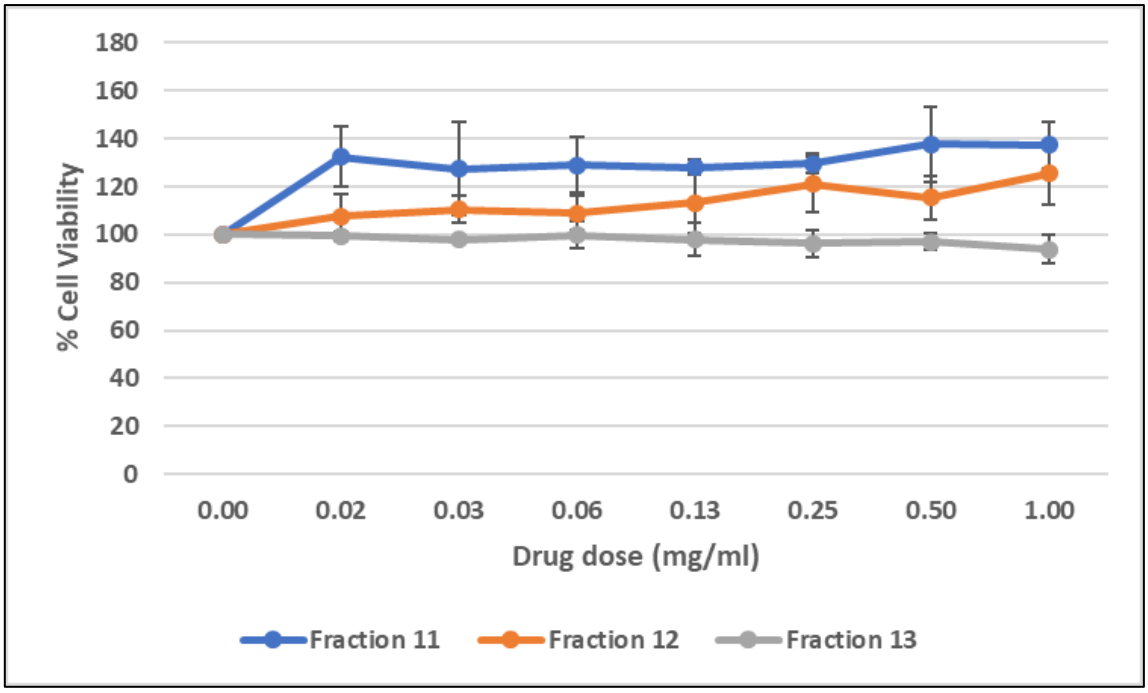

Figure 3.28 Anti-proliferative activity exerted by FPLC fractions 11, 12 and 13 (of the whelk extract) treatment on the K562 cell line. Average cell growth for the K562 cell line treated with increasing doses of whelk extract fractions 11 (blue line), 12 (orange line) and 13 (grey line) (with a maximum dose of 1 mg/ml) and incubation period of 3 days using the MTT assay. Where N=3, changes in cell growth were calculated as a percentage in comparison to untreated control cells. Error bars show SEM.

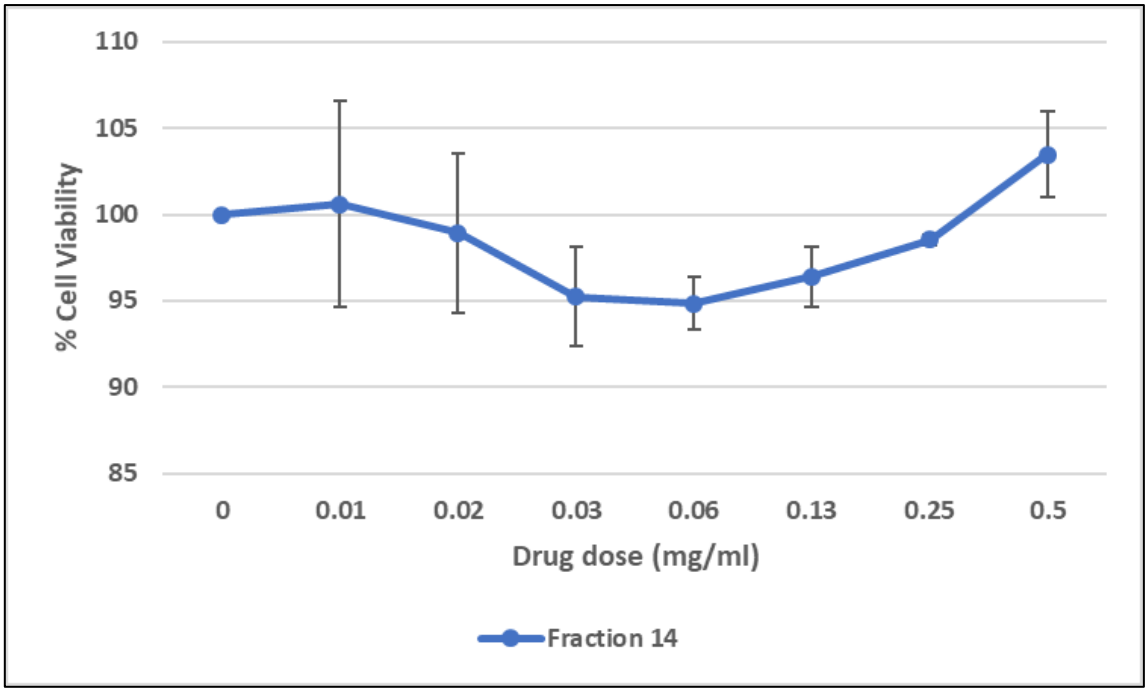

Figure 3.29 Anti-proliferative activity exerted by FPLC fraction 14 (of the whelk extract) treatment on the K562 cell line. Average cell growth for the K562 cell line treated with increasing doses of whelk extract fraction 14 (with a maximum dose of 0.5 mg/ml) and incubation period of 3 days using the MTT assay. Where N=3, changes in cell growth were calculated as a percentage in comparison to untreated control cells. Error bars show SEM.

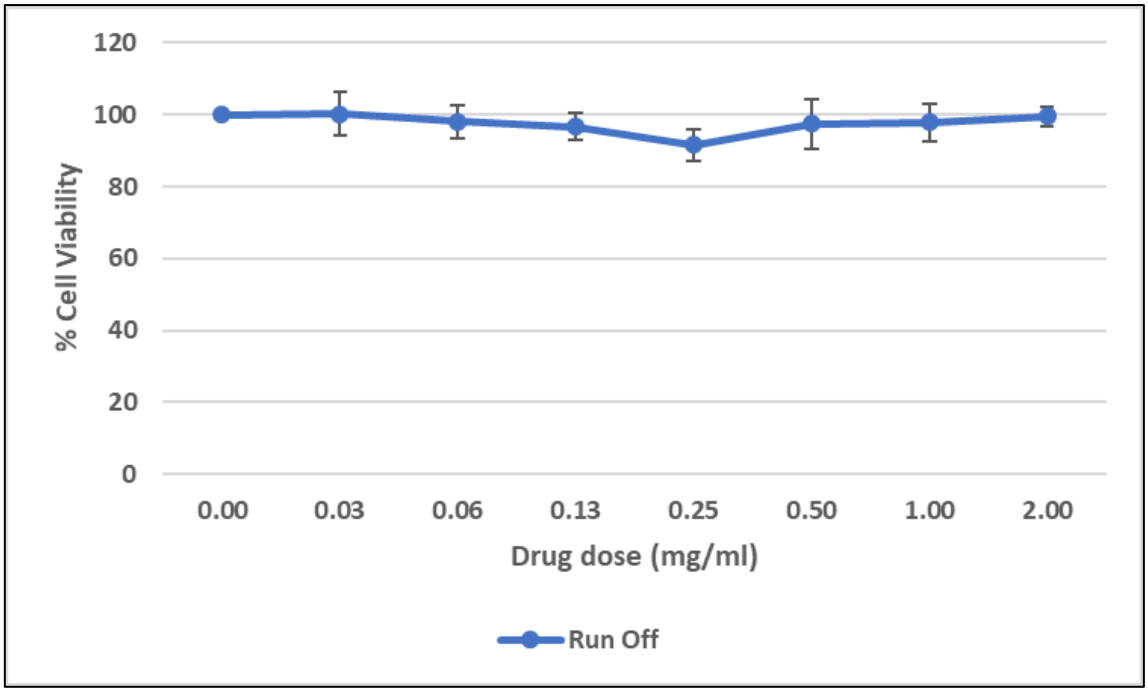

Figure 3.30 Anti-proliferative activity exerted by FPLC run off sample (of the whelk extract) treatment on the K562 cell line. Average cell growth for the K562 cell line treated with increasing doses of whelk extract run off sample (with a maximum dose of 2 mg/ml) and incubation period of 3 days using the MTT assay. Where N=3, changes in cell growth were calculated as a percentage in comparison to untreated control cells. Error bars show SEM.

3.3.3.3 U698 cell line assays

As seen in the other cell lines the fraction treatments exerted little to no effect on the U698 cell line in comparison to the control treatment cisplatin.

Cisplatin treatment brought about a steep decline in U698 cell viability towards the last three doses used (figure 3.31). Treatment with fraction 3 (blue line), fraction 4 (orange line), fraction 5 (grey line) and fraction 6 (yellow line) in figure 3.32 exerted little effect on the U698 cell line with cell viability dropping by a maximum of 10% (fraction 3, treated cells). Treatment with all 4 of these fractions as seen in figure 3.32 mainly led to no change in cell viability which remained around 100% in all the fraction treated samples in figure 3.32. In figure 3.33 it can be noted that cell viability was reduced by around 10% in the U698 cells at the maximum dose of fraction 10 (grey line). While fraction 8 (blue line, figure 3.33) exerted little effect on the U698 cells with cell viability around 100%, even at the maximum dose. Fraction 9 treatment (orange line, figure 3.33) appeared to promote cell proliferation slightly in the U698 cell line,

with viability increasing by around 15-20%. U698 cells treated with fraction 11 (blue line), fraction 12 (orange line) or fraction 13 (grey line) (all in figure 3.34) all have cell viability reduced by around 15% post treatment. Fraction 14 treated U698 cells (figure 3.35) had cell viability reduced by a maximum of 10% (dose 0.06 mg/ml). The U698 cells treated with the runoff sample (figure 3.36) have cell viability reduced by a maximum of 10% at dose 0.25 mg/ml then cell viability began to increase with the increasing dose. Cell viability returned back to 100% with the maximum dose of 2 mg/ml of the runoff sample (figure 3.36).

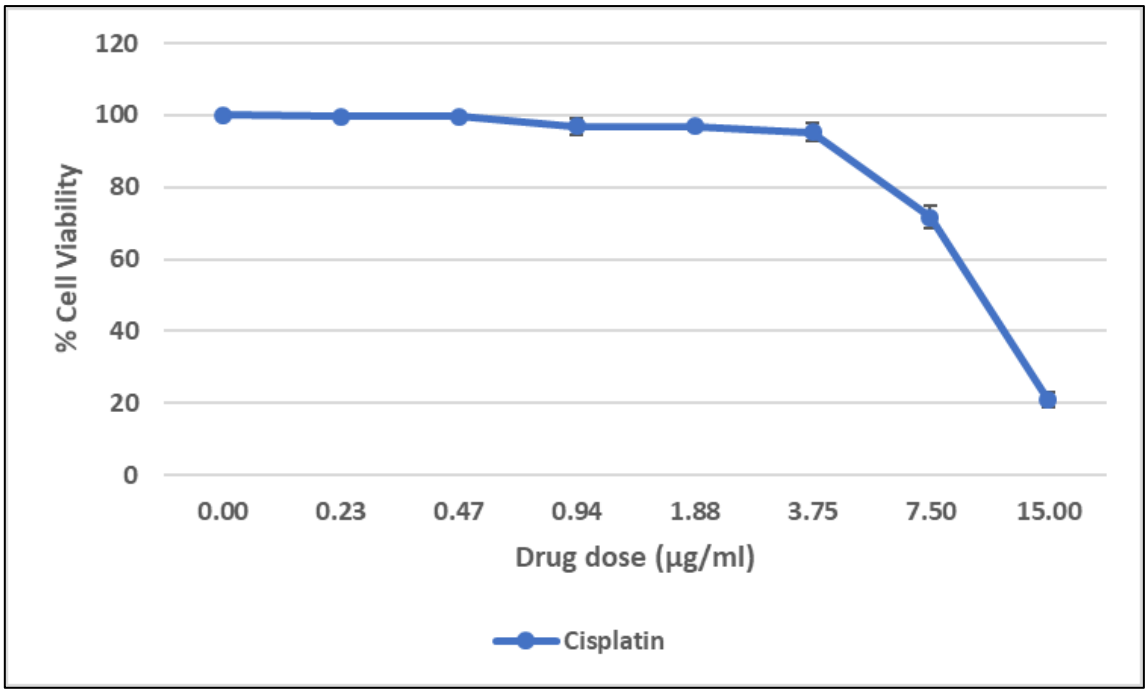

Figure 3.31 Anti-proliferative activity exerted by cisplatin treatment on the U698 cell line. Average cell growth for the U698 cell line treated with increasing doses of cisplatin (with a maximum dose of 30 µg/ml) and incubation period of 3 days using the MTT assay. Where N=6, changes in cell growth were calculated as a percentage in comparison to untreated control cells. Error bars show SEM.

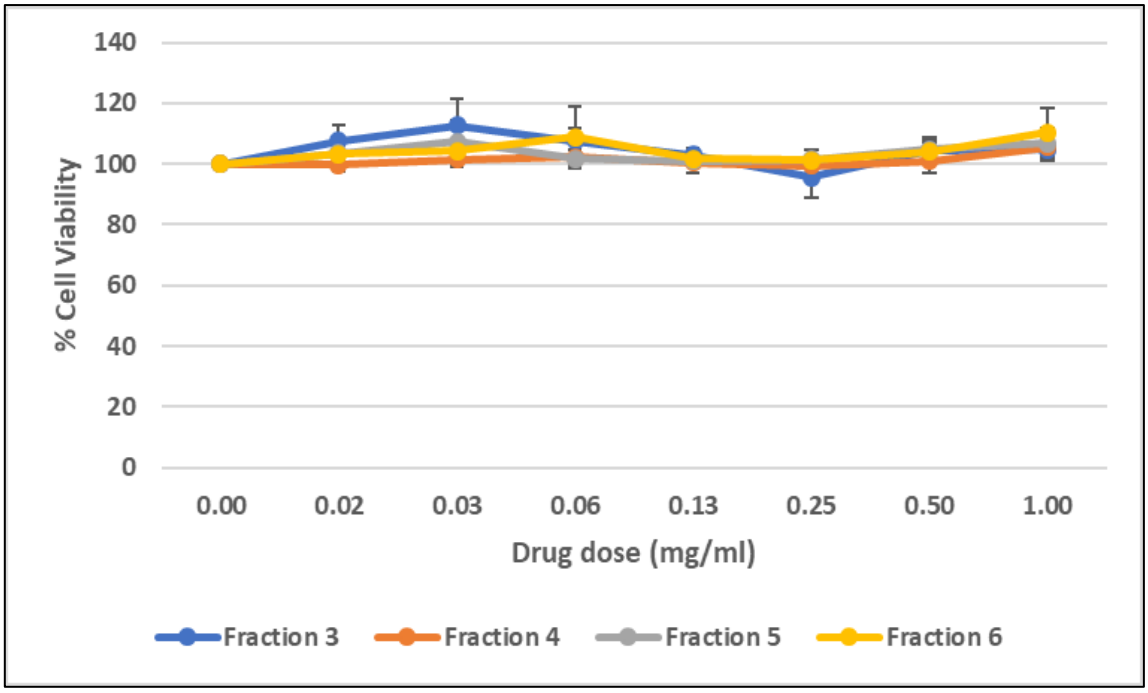

Figure 3.32 Anti-proliferative activity exerted by FPLC fractions 3,4, 5 and 6 (of the whelk extract) treatment on the U698 cell line. Average cell growth for the U698 cell line treated with increasing doses of whelk extract fractions 3 (blue line), 4 (orange line), 5 (grey line) and 6 (yellow line) (with a maximum dose of 1 mg/ml) and incubation period of 3 days using the MTT assay. Where N=3, changes in cell growth were calculated as a percentage in comparison to untreated control cells. Error bars show SEM.

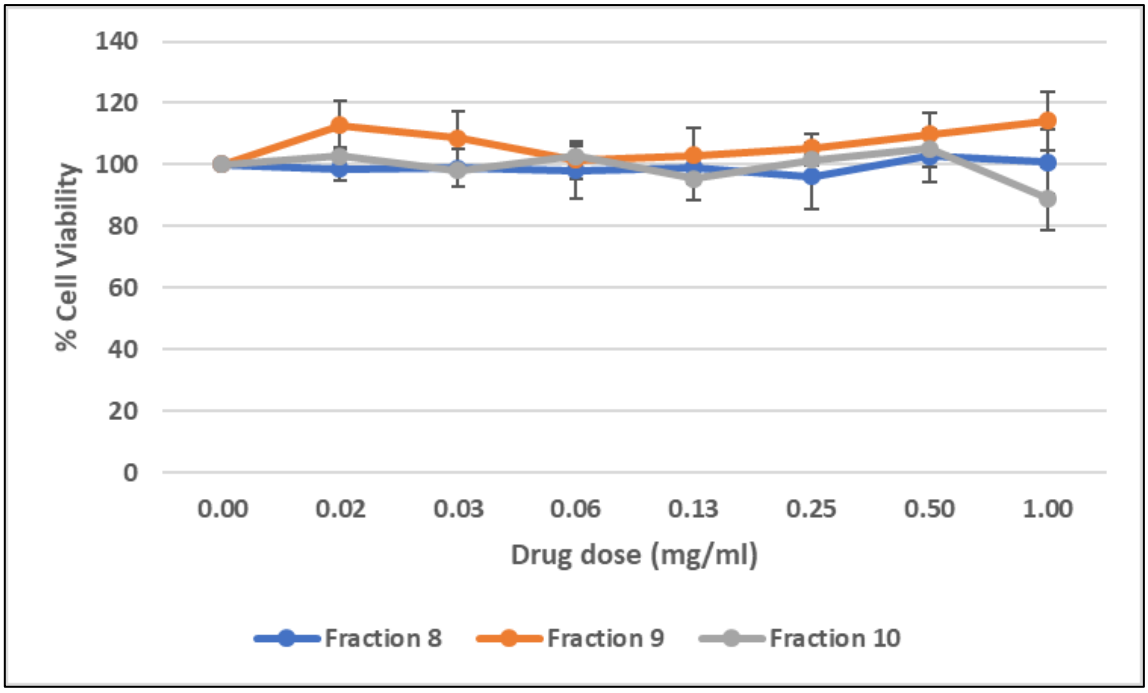

Figure 3.33 Anti-proliferative activity exerted by FPLC fractions 8, 9 and 10 (of the whelk extract) treatment on the U698 cell line. Average cell growth for the U698 cell line treated with increasing doses of whelk extract fractions 8 (blue line), 9 (orange line) and 10 (grey line) (with a maximum dose of 1 mg/ml) and incubation period of 3 days using the MTT assay. Where N=3, changes in cell growth were calculated as a percentage in comparison to untreated control cells. Error bars show SEM.

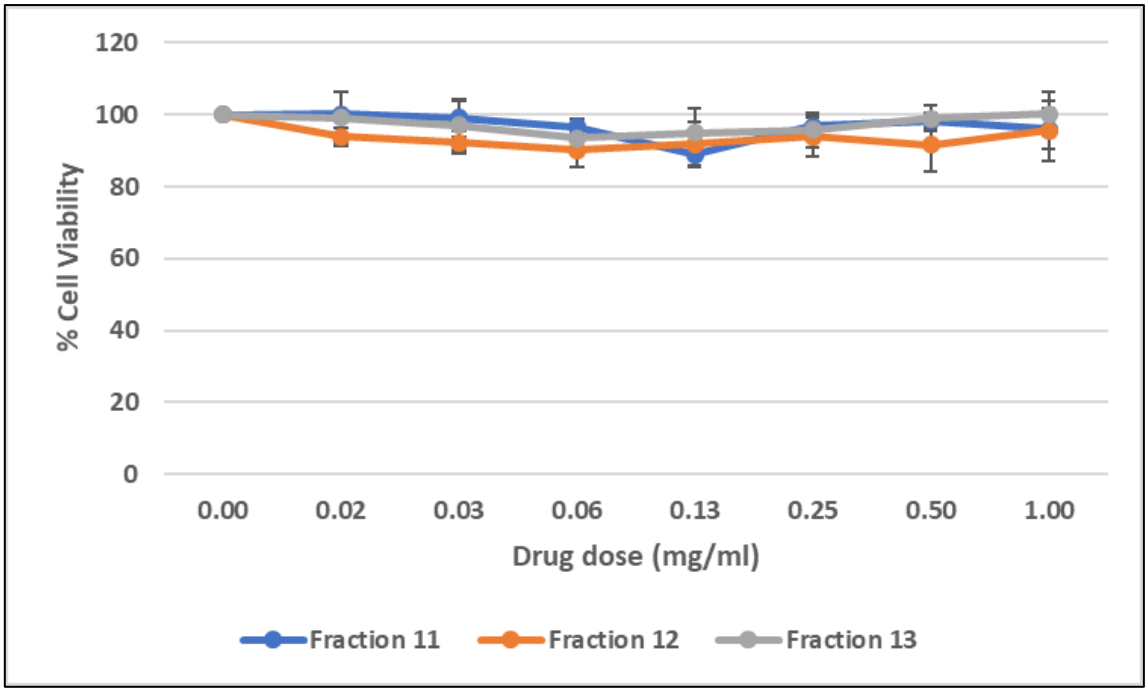

Figure 3.34 Anti-proliferative activity exerted by FPLC fractions 11, 12 and 13 (of the whelk extract) treatment on the U698 cell line. Average cell growth for the U698 cell line treated with increasing doses of whelk extract fractions 11 (blue line), 12 (orange line) and 13 (grey line) (with a maximum dose of 1 mg/ml) and incubation period of 3 days using the MTT assay. Where N=3, changes in cell growth were calculated as a percentage in comparison to untreated control cells. Error bars show SEM.

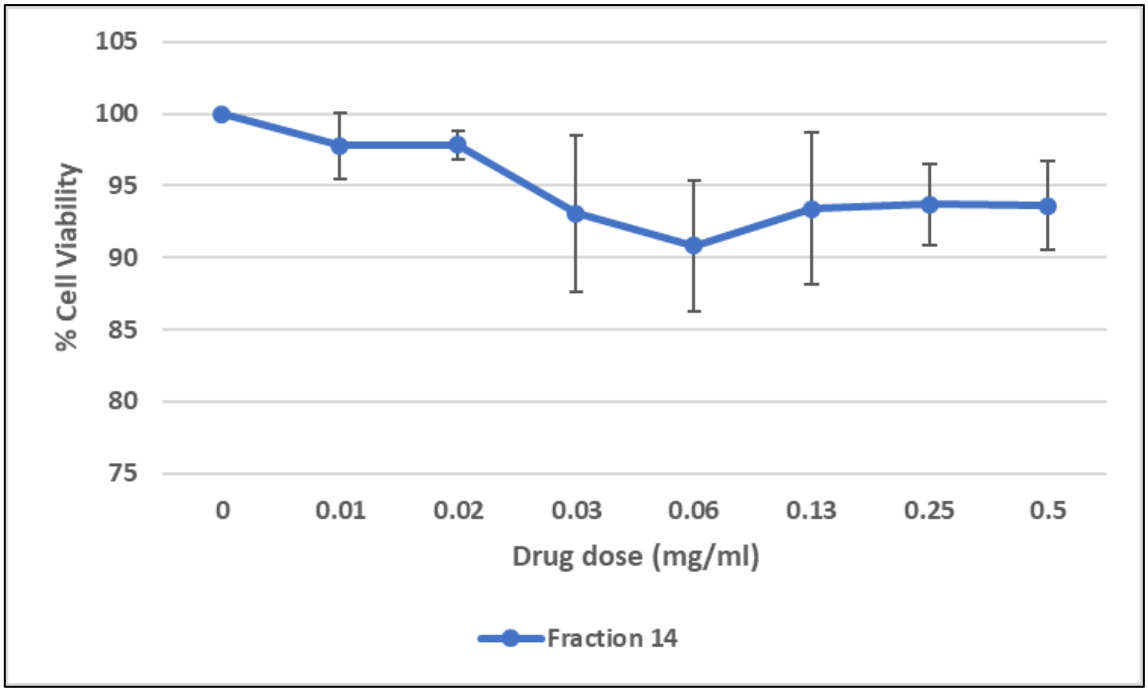

Figure 3.35 Anti-proliferative activity exerted by FPLC fraction 14 (of the whelk extract) treatment on the U698 cell line. Average cell growth for the U698 cell line treated with increasing doses of whelk extract fraction 14 (with a maximum dose of 0.5 mg/ml) and incubation period of 3 days using the MTT assay. Where N=3, changes in cell growth were calculated as a percentage in comparison to untreated control cells. Error bars show SEM.

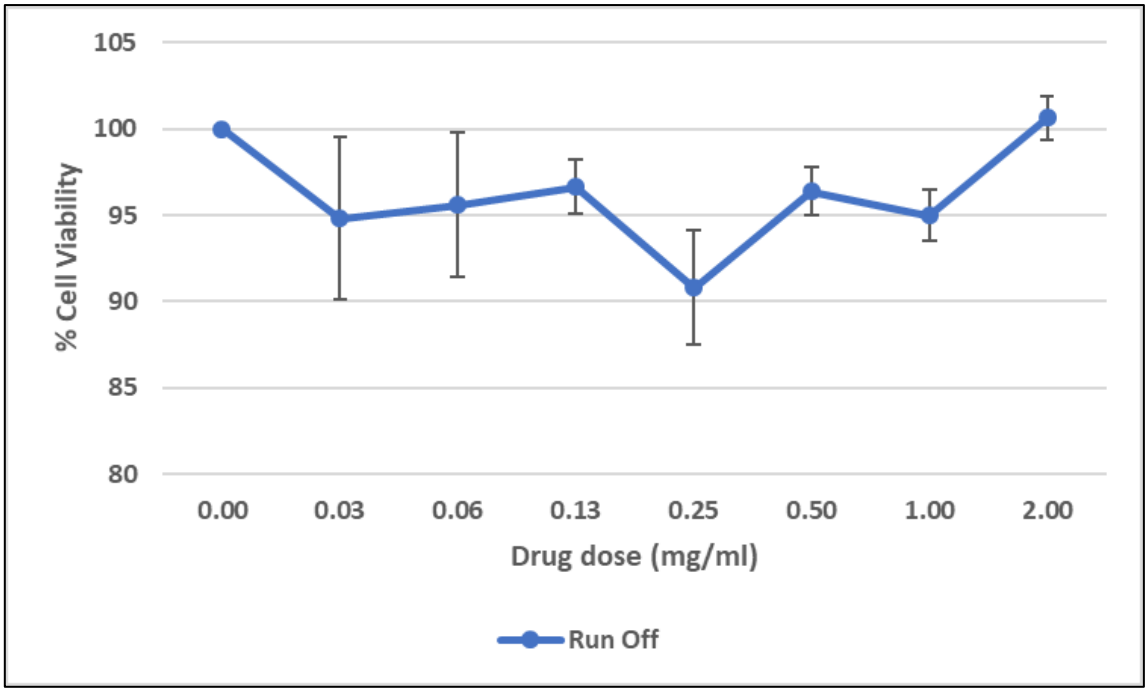

Figure 3.36 Anti-proliferative activity exerted by FPLC run off sample (of the whelk extract) treatment on the U698 cell line. Average cell growth for the U698 cell line treated with increasing doses of whelk extract run off sample (with a maximum dose of 2 mg/ml) and incubation period of 3 days using the MTT assay. Where N=3, changes in cell growth were calculated as a percentage in comparison to untreated control cells. Error bars show SEM.

3.3.3.4 Stimulated PBMC assays

Results were obtained for PBMCs stimulated with PMA/ionomycin and treated with cisplatin and fractions 8,9 14 and the run off sample.

As can be seen in figure 3.37 cisplatin reduced the stimulated PBMC cell viability by a maximum of 20%. Figure 3.38 demonstrates that post treatment with fraction 9 (orange bar) the stimulated PBMCs had cell viability reduced by around 10%. Treatment with fraction 8 (blue bar, figure 3.38) demonstrated increases in stimulated PBMC viability of around 20%. In a similar way figure 3.39 identifies an increase in cell viability of the stimulated PBMCs of between 5-20% post treatment with fraction 14. In the runoff sample treated cells demonstrated some slight increases in cell viability, however mainly cell viability remained around 100% post treatment (figure 3.40).

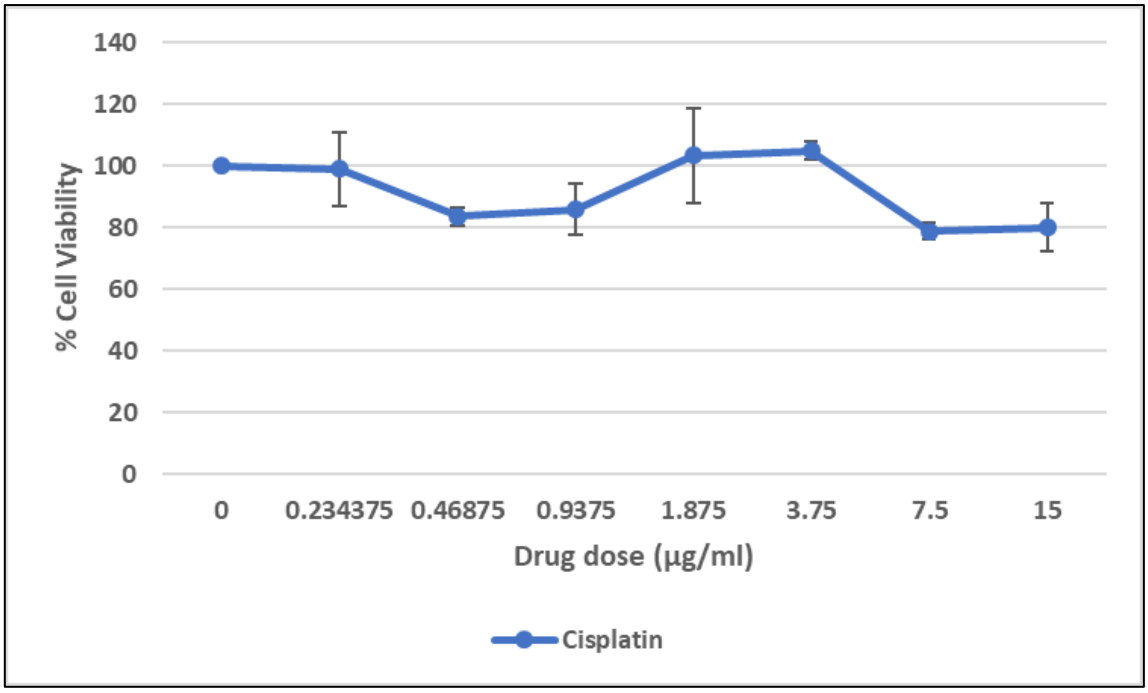

Figure 3.37 Anti-proliferative activity exerted by cisplatin treatment on PMA/ ionomycin stimulated PBMCs. Average cell growth for the stimulated PBMCs treated with increasing doses of cisplatin (with a maximum dose of 15 µg/ml) and incubation period of 3 days using the MTT assay. Where N=1, changes in cell growth were calculated as a percentage in comparison to untreated control cells. Error bars show SEM.

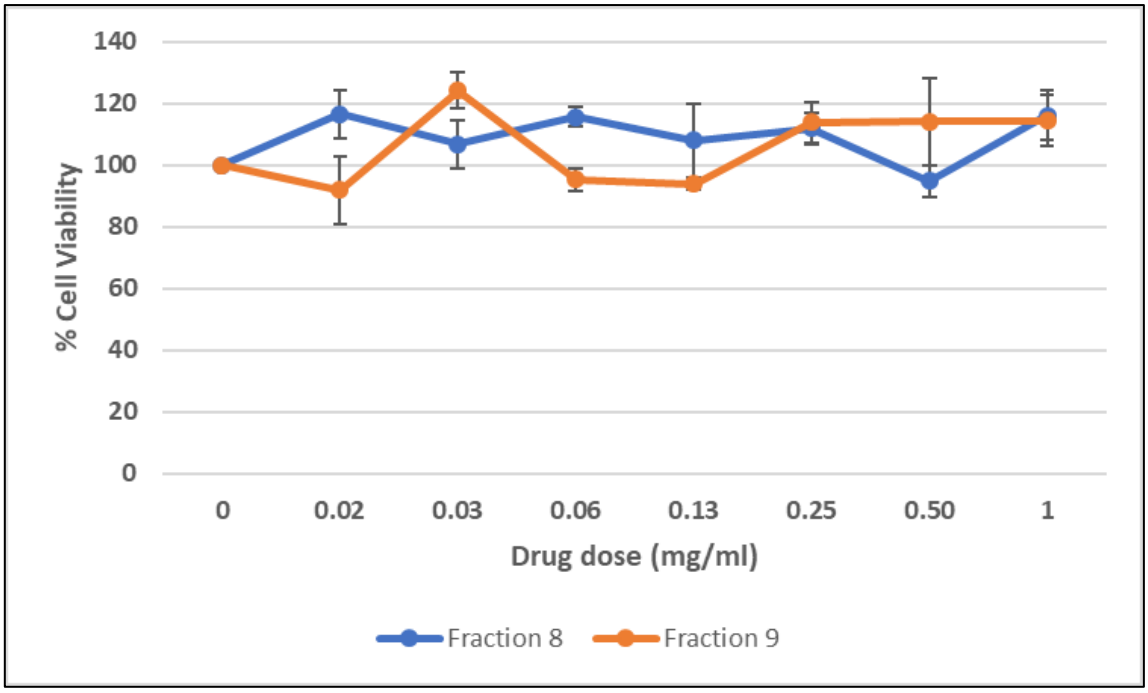

Figure 3.38 Anti-cancer activity exerted by FPLC fractions 8 and 9 (of the whelk extract) treatment on the PMA/ ionomycin stimulated PBMCs. Average cell growth for the stimulated PBMCs treated with increasing doses of whelk extract fractions 8 (blue line) and 9 (orange line) (with a maximum dose of 1 mg/ml) and incubation period of 3 days using the MTT assay. Where N=1, changes in cell growth were calculated as a percentage in comparison to untreated control cells. Error bars show SEM.

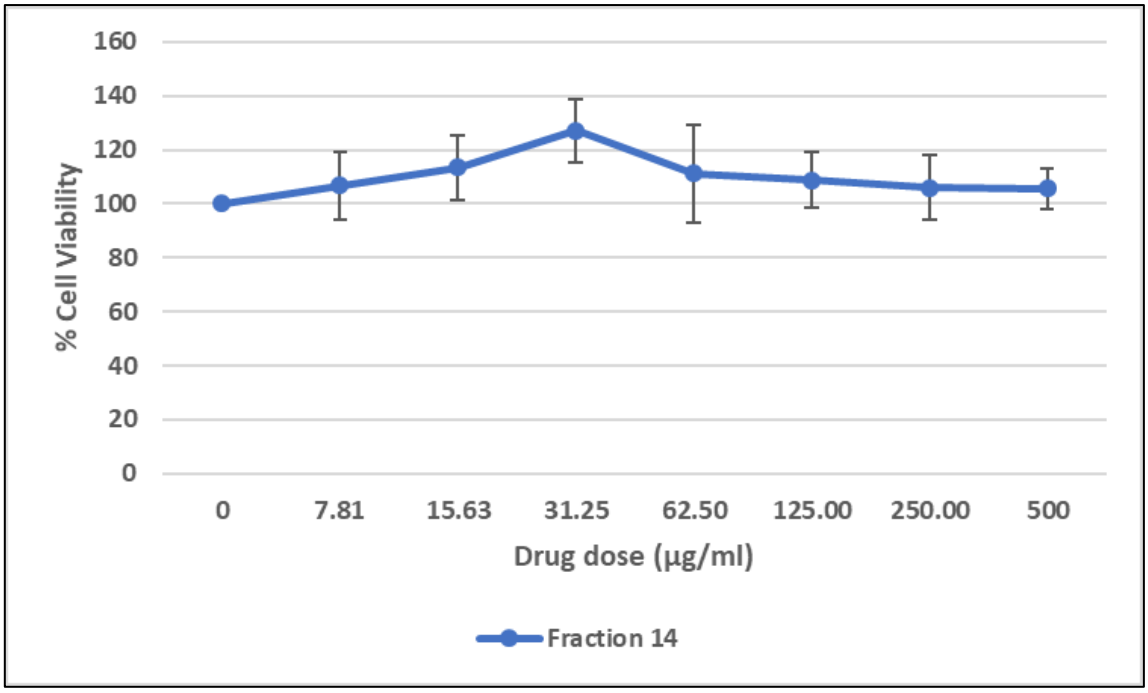

Figure 3.39 Anti-proliferative activity exerted by FPLC fraction 14 (of the whelk extract) treatment on the PMA/ ionomycin stimulated PBMCs. Average cell growth for the stimulated PBMCs treated with increasing doses of whelk extract fraction 14 (with a maximum dose of 0.5 mg/ml) and incubation period of 3 days using the MTT assay. Where N=1, changes in cell growth were calculated as a percentage in comparison to untreated control cells. Error bars show SEM.

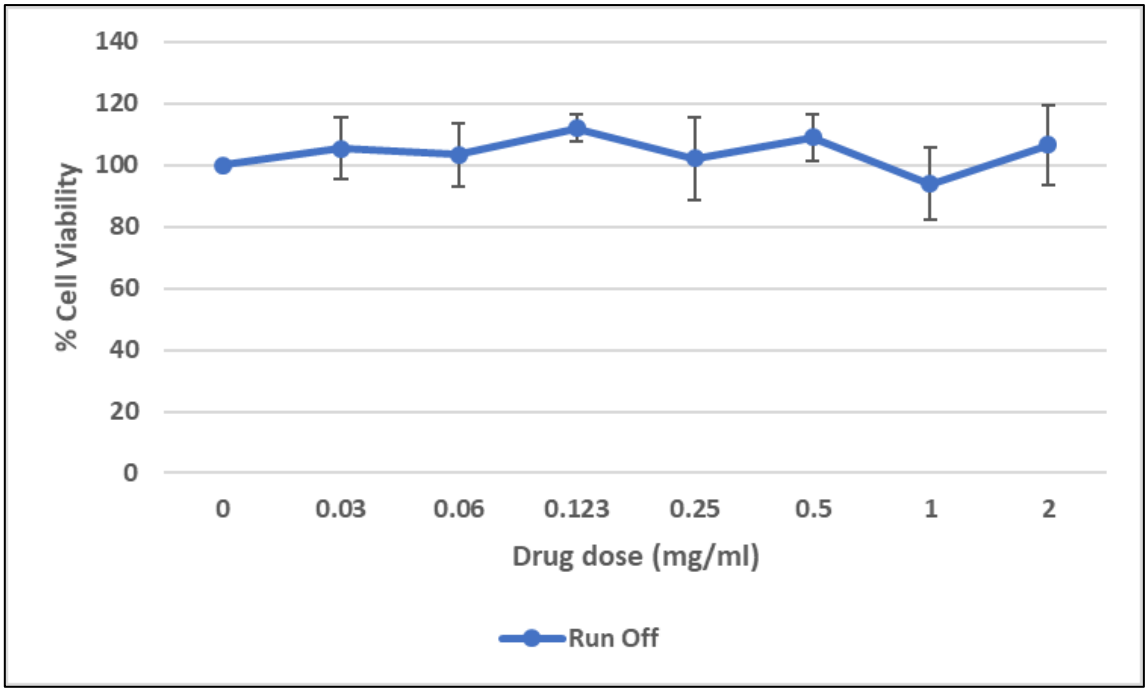

Figure 3.40 Anti-proliferative activity exerted by FPLC run off sample (of the whelk extract) treatment on the stimulated PBMCs. Average cell growth for the stimulated PBMCs treated with increasing doses of whelk extract run off sample (with a maximum dose of 2 mg/ml) and incubation period of 3 days using the MTT assay. Where N=1, changes in cell growth were calculated as a percentage in comparison to untreated control cells. Error bars show SEM.

From the MTT results obtained it appeared as through some of the isolated FPLC fractions had very slight anti-proliferative effects on the cancer cell lines, with some of the fractions appearing to have exerted proliferative effects on some of the cell lines. Therefore new doses for the FPLC fractions were chosen based on the activity noted in the FPLC fraction MTTs, these doses were 10-fold higher than previous ones and were tested in subsequent assays carried out by the research group. The new doses are shown below in table 3.7. Fraction 14 was not carried forward into these tests due to the low sample volume.

Table 3.7 The maximum doses (mg/ml) of each fraction number (3, 4, 5, 6, 8, 9, 10, 11, 12, 13, run off sample) in the well of an MTT plate.

Fraction number	New maximum dose (mg/ml)
3	10
4	10
5	20
6	20
8	7
9	10
10	25
11	10
12	20
13	20
Run off sample	10

3.4 Discussion

3.4.1 MTT results key findings

- Confirmed the anti-proliferative effects of the crude cockle extract on the MOLT-4 and K562 cell lines as noted by Aldairi, Ogundipe and Pye (2018).
- For the first time this research identified the antiproliferative activity of the crude cockle and whelk GAG extracts on the lymphoblastic lymphoma cell line U698.
- This study provided significant insight into the effects of novel marine sourced GAG compounds isolated from the common cockle and whelk on healthy lymphocytes (both activated and naïve).

3.4.2 Discussion

Previous studies have demonstrated the potential medicinal properties of marine GAGs (DeJesus Raposo, 2015) and the potential anti-cancer activity of GAG like compounds (Afratis et, al., 2012). GAG compounds isolated from the common cockle have also been identified as

having anti-cancer properties in breast cancer cell lines and the leukemic cell lines MOLT-4 and K562 (Aldairi, Ogundipe and Pye, 2018). However there were no current studies identifying the effects of these marine mollusc derived GAG compounds on healthy lymphocytes or on the lymphoblastic lymphoma cell line U698.

This research identified that GAGs extracted from the common cockle and whelk had a significant inhibitory effect on cell viability in the MOLT-4 and U698 cell lines. In the MOLT-4 cell line post 3-day incubation with the cockle and whelk extract the cell viability was reduced by up to 80% and 90% respectively with an IC50 values of 15.56 µg/ml and 10.4 µg/ml respectively as can be seen in figures 3.1 and 3.2 and table 3.1. The U698 cell viability was significantly reduced by both the cockle and whelk extract treatment (p= 0.0117 and p= 0.0001 respectively), with IC50 values ranging 7.51 µg/ml and 102.55 µg/ml (table 3.3). U698 cell line viability was reduced by up to 90% post treatment with both the cockle and whelk extracts (figures 3.8 and 3.9). Some level of activity was also noted in the K562 cell line with growth inhibition of up to 50% and Ic50 values ranging 32.8 µg/ml and 186.06 µg/ml (Figures 3.5 and 3.6 and table 3.2). The whelk extract reduced K562 cell viability significantly post 3 day incubation period with an IC50 value of 71.49 µg/ml (p=0.047). In the K562 cell line the IC50 values of the cockle extract treated cells increased post 5 day incubation in comparison to the 4 day incubation period, which could suggest that the cell line had potentially developed some level of immunity to the treatment. Interestingly neither the cockle or whelk GAG isolates exerted a cytotoxic effect on the healthy lymphocytes (either active or naïve), both extracts failed to reduce cell viability by 50% and thus did not produce an IC50 value (tables 3.4 and 3.6; figures 3.11, 3.12 3.17, 3.18). In this regard the cytotoxic effects noted in the cancer cell lines of the novel GAG compounds appeared to be acting in a selective manner towards the MOLT-4, K562 and U698 leukemic and lymphoma cell lines and non-toxic to the healthy lymphocytes either the naïve or proliferating lymphocytes (stimulated). It would have been interesting to have determined the nature of the seemingly selective nature of the GAG compounds, however that was beyond the scope of this research but should be considered in future work towards the possibility of the use of mollusc derived GAG compounds for use in the clinic. Our data supports that found by Aldairi, Ogundipe and Pye (2018) that the mollusc derived GAGs appear to show specificity towards the leukemic and lymphoma cells as opposed to the healthy lymphocytes and would further support the potential therapeutic

use of these GAG compounds in the clinic. The effects of cisplatin on PBMCs noted in this research was similar to the anti-proliferative effects noted by Sakai et al., (2013), however incubation times were different in this research and so there was some level of difference in the noted activity.

Understanding the structural and specific biological roles of the mollusc derived GAGs may help lead to the development of the novel therapeutic approaches (Afratis et al., 2012). In order to further identify the structural properties of the whelk extract, the crude extract was purified by ion exchange chromatography and the resulting fractions were then tested for anti-proliferative activity on the cancer cell lines through the MTT assay (figures 3.20-3.40). All eluted fractions appeared to be non-toxic to the MOLT-4, K562 or U698 cell lines, with no obtainable IC50 values even at maximum dose. Aldairi, Ogundipe and Pye (2018) identified the cytotoxic effect of 'fraction E' on a breast cancer cell line but also noted a lack of toxicity in the MOLT-4 and K562 cell lines. Their results suggested selectivity against breast cancer cell lines as was noted in the crude extracts, suggesting that fraction E may be responsible for the cytotoxic effects of the crude whelk extract. However in this research no eluted fraction exerted a toxic effect on any of the cancer cell lines. This could be due to low levels of GAGs in the isolated fractions, which could be combated by doing further FPLC runs using a higher initial weight of the crude GAG compounds. It could also be that as demonstrated by Aldairi, Ogundipe and Pye (2018) the isolated GAG compounds are not active in the MOLT-4 or the K562 cell lines and may not be toxic to the U698 cell line at low doses; as the new suggested doses appeared to exert an effect on the MOLT-4 and U698 cell lines in placement student studies. Further understanding into the exact structural features seen in 'fraction E' by Aldairi, Ogundipe and Pye (2018) may open a new therapeutic approach to cancer therapy.

CHAPTER 4- ANNEXIN V/PI APOPTOSIS ASSAY AND CFSE PROLIFERATION ASSAY

4.0 Annexin V/ Propidium Iodide apoptosis assay and CFSE proliferation assay results

4.1 Introduction

4.1.1 Annexin V/ Propidium Iodide apoptosis assay

The work carried out by Aldairi, Ogundipe and Pye (2018) identified that in the MOLT-4 cell line cells accumulated in the G1 and G2/M phase of the cell cycle and a subsequent drop in the S phase of the cell cycle, 24 hours post treatment with extracted cockle polysaccharides. They suggested that this could indicate a complex cell death mechanism potentially mediated by apoptosis. The annexin V/ propidium iodide apoptosis assay is commonly used to assess apoptotic cells (Cornelissen, Phillippe, De sitter and De Ridder, 2002). Significant increases in late apoptotic cells (annexin V^+/PI^+) were identified by Aldairi, Ogundipe and Pye (2018) in the MOLT-4 cell line post cockle polysaccharide treatment. They also identified little changes in necrotic cells (annexin V^-PI^+) post cockle polysaccharide treatment. The results of the research group therefore indicated apoptosis potentially as the cause of cytotoxicity in MOLT-4 cells post treatment with cockle polysaccharides (Aldairi, Ogundipe and Pye, 2018). The results in chapter 3 identified limited decreases in cell viability (MTT) in healthy lymphocytes, however in activated, especially in the PHA activated, cells some level of activity on cell viability was noted. Therefore it is important to establish the mechanism of cell death induced by treatment with the cockle and whelk extract. This research aimed to use the annexin V/ PI assay (BD Bioscience, UK) to identify any apoptotic effects of the GAGs isolated from the common cockle and the common whelk on healthy lymphocytes (naïve and stimulated), in order to establish possible side effects from GAG treatment. Annexin V and propidium iodide are used in conjunction with each other in order to evaluate cell viability and the presence of apoptotic or necrotic cells (Vermes, Haanen, Steffens-Nakken and Reutelingsperger, 1995). Propidium iodide is often used to indicate cell viability as it has the ability to omit living cells (Reiger, Nelson, Konowalehuk and Barreda, 2011). PI can only enter a cell if the membrane is compromised, therefore as early apoptotic and living cells possess intact cell membranes PI does not stain them (Vermes et al., 1995). Whereas in late apoptotic and necrotic cells the integrity of the cell membrane is disrupted, and so PI can cross the membrane and intercalate itself with nucleic acids (Reiger et al., 2011).

4.1.2 CFSE proliferation assay

The CFSE (carboxyfluorescein succinimidyl ester) proliferation assay was designed to allow the monitoring of cell activity occurring over a longer period of time thus increasing sensitivity of detecting cell death (up to 5 days) (Jedema, Van der Werff, Barge, Willemze and Falkenburg, 2004). CFSE is a long lived fluorescent cell label; upon division of that cell, the daughter cells possess half the amount of CFSE tagged molecules (Quah and Parish, 2010: Jedema et al., 2004). The halving of florescence during mitosis is the principle the assay uses to the monitor the number of cell divisions labelled cells have undergone, through the identification of the decrease in the fluorescence of a cell through flow cytometry analysis (Quah and Parish, 2010). The proliferative or anti-proliferative activity of the common cockle and common whelk GAG extracts was unknown in healthy lymphocytes. This research utilised the CFSE proliferation assay in order to build on the information gained in the annexin V/PI apoptosis assays, and to further the identification of potential side effects from the GAG extracts. The CFSE proliferation assay is compatible for use with other fluorescent dyes and therefore allows for the identification of cell replications within individual cell types (Jedema, 2004). In order to identify the actions of cisplatin, the cockle and the whelk extract treatments on the naïve and memory T-helper and cytotoxic T-cell populations, this research used fluorescently stained antibodies to identify individual cell types (naïve (CD45RA) and memory (CD45RO), T-helper (CD4) and cytotoxic T-cells (CD8)), as were used in the apoptosis assay.

The CD45 RA (naïve) and RO (memory) antibodies were used in order to evaluate whether the cockle and whelk derived GAG extracts exerted different potencies on cells which had come into contact with and responded to antigens previously and those which had no prior encounters with antigens.

4.2 Method

4.2.1 Annexin V/ Propidium Iodide apoptosis assay

The annexin V/ propidium iodide apoptosis assay was carried out as set out in method 2.5.1 as per the manufacturer's instructions. Antibody staining was also performed (as per method 2.5) for the annexin V/PI assays, in order to get detailed information as to the type of cell death occurring and the individual cell types within the PBMC samples (both naïve and

stimulated) which may be affected by apoptosis, post treatment with either the cockle or whelk extracts or the cisplatin treatment. The annexin V/PI assays were carried out using all three cancer cell lines (MOLT-4, K562 and U698) and the naïve and PMA/ Ionomycin stimulated PBMCs. In all assays, cells were seeded at 1 x 10^6 cells/ml, and cisplatin was used as a control treatment comparison. The PBMC assays were carried out in line with the cancer cell assays and were dosed using the IC50 values obtained from the MTT assays. Doses used for the annexin V/PI assay were 6 µg/ml for cisplatin, 12 µg/ml for both the cockle extract and whelk extract treatments.

As the K562 cell line has been described as having T-cell properties (Klein et al., 1976), the research stained for $CD3^+$ populations of the K562 cell line, in order to gain insight into the effects of GAG isolates on T-cell specifically. However characterisation of the K562 cell line showed that very few K562 cells were positive for CD3 and so the whole population data only is displayed in the results section 4.3.1.1.2. The results obtained from the $CD3^+$ K562 cells are demonstrated in the appendix section 8.2.

All annexin V/PI assays were carried out in triplicate and repeated three times. Therefore the data displayed in the figures represents average values and the error bars shown represent SEM.

4.2.2 CFSE proliferation assay

The CFSE proliferation assay was carried out as per the manufacturers recommendations and as set out in method 2.5.2, antibody staining for individual cell types was also carried out as per method 2.5. Cells were seeded to 1 x 10^6 cells/ml for the cancer cell assays and for the PBMC assays. Cisplatin was used as a control treatment in all assays and was used at a dose of 6 µg/ml as per the IC50 value obtained from the MTT assays. The cockle and whelk extract treated cells were dosed with 12 µg/ml as per the IC50 values calculated from the MTT results.

All CFSE proliferation assays were carried out in triplicate and repeated 3 times, therefore the data shown in the figures represents the averages of the repeats and error bars shown are representative of SEM.

4.2.3 Annexin V/ Propidium Iodide apoptosis assay gating method

Figure 4.1 and 4.2 show the gating process performed in order to establish the individual cell types present in the cancer cell lines (figure 4.1) or the PBMCs (figure 4.2).

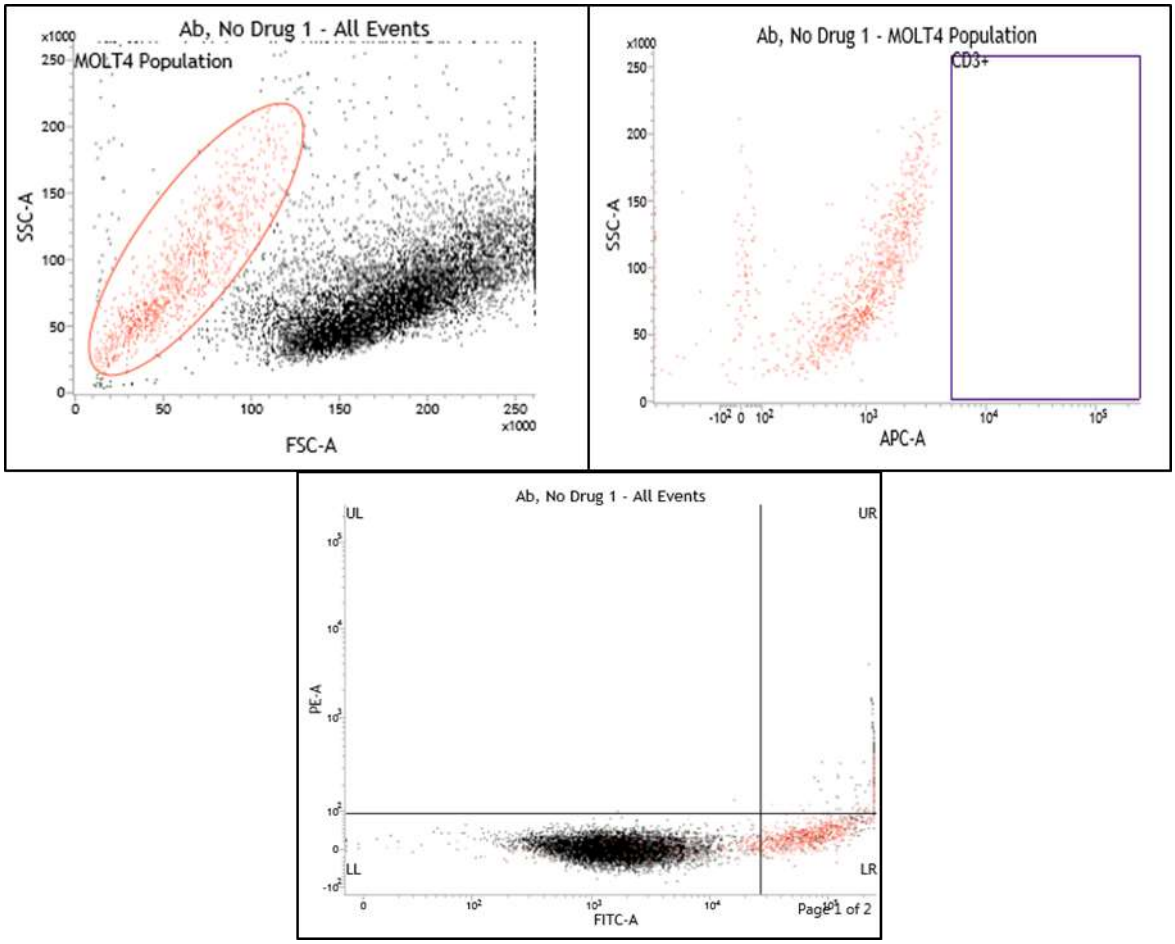

Figure 4.1 Raw data graph obtained from cancer cell line annexin V/PI apoptosis assay and the gating process involved. Identifies the raw data graph and gates drawn in a typical cancer cell line apoptosis assay, identifying the process of gating and how the stages of apoptosis were determined e.g. UL= late stage apoptosis, UR= mid stage apoptosis, LR= early stage apoptosis and LL= no apoptosis. The example shown is untreated and not stained with antibody in order to represent the initial placing of the gates. All apoptosis assays had a 3-day incubation period and N=3.

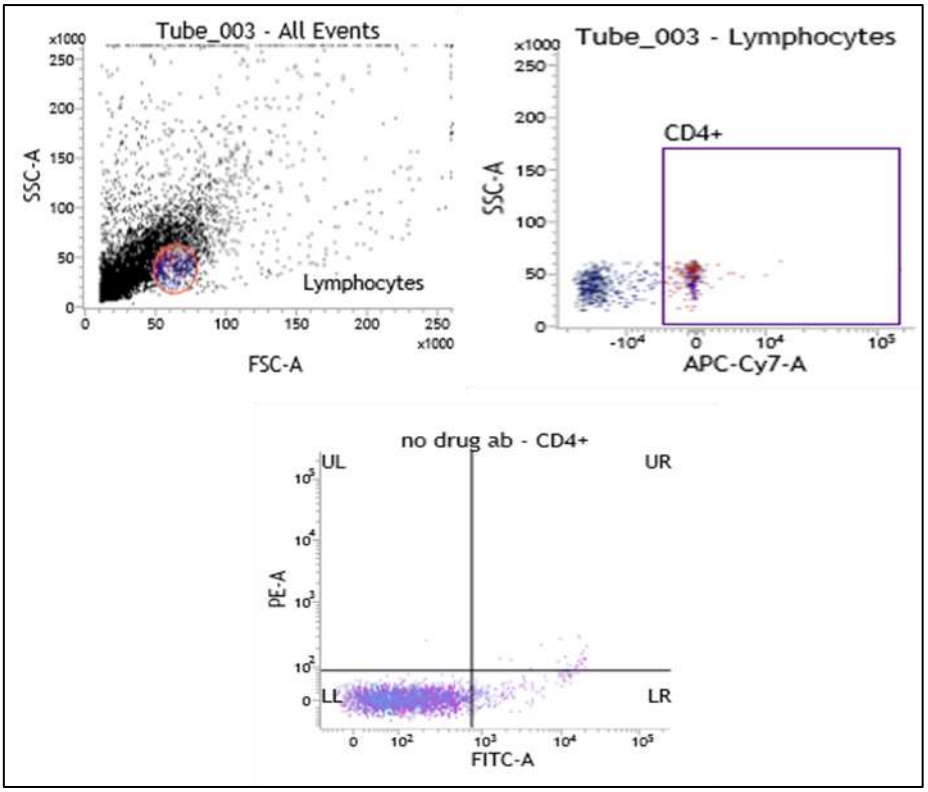

Figure 4.2 Raw data obtained from PBMC annexin V/PI apoptosis assay and the gating process involved. Identifies the raw data and gates drawn in a typical PBMC apoptosis assay in order to determine cell types and quantities and stage of apoptosis; where UL= late stage, UR= mid stage, LR= early stage and LL= no apoptosis. The example shown is untreated and antibody free in order to represent the initial placing of the gates. All apoptosis assays had a 3-day incubation period and N=3.

For the labelling of the graphs Late (UL)= late, Mid (UR)= mid stage apoptosis, early (LR) = early stage apoptosis and no apoptosis (LL)= no cell death occurring.

4.2.4 Method of obtaining peak numbers through the raw data graphs

Figure 4.3 and 4.4 show the typical graphs obtained for the cancer cell lines (figure 4.3) or the PBMCs (figure 4.4). Proliferation results were obtained via the determination of the number of peaks in the control graphs. The peak number was then determined for the three treatments (cisplatin, cockle extract and whelk extract). Percentage proliferation was obtained by assuming the control cells were at 100% proliferation and then obtaining percentage proliferation for the treatment was done by dividing the proliferation peak number by the control peak number and multiplying by 100.

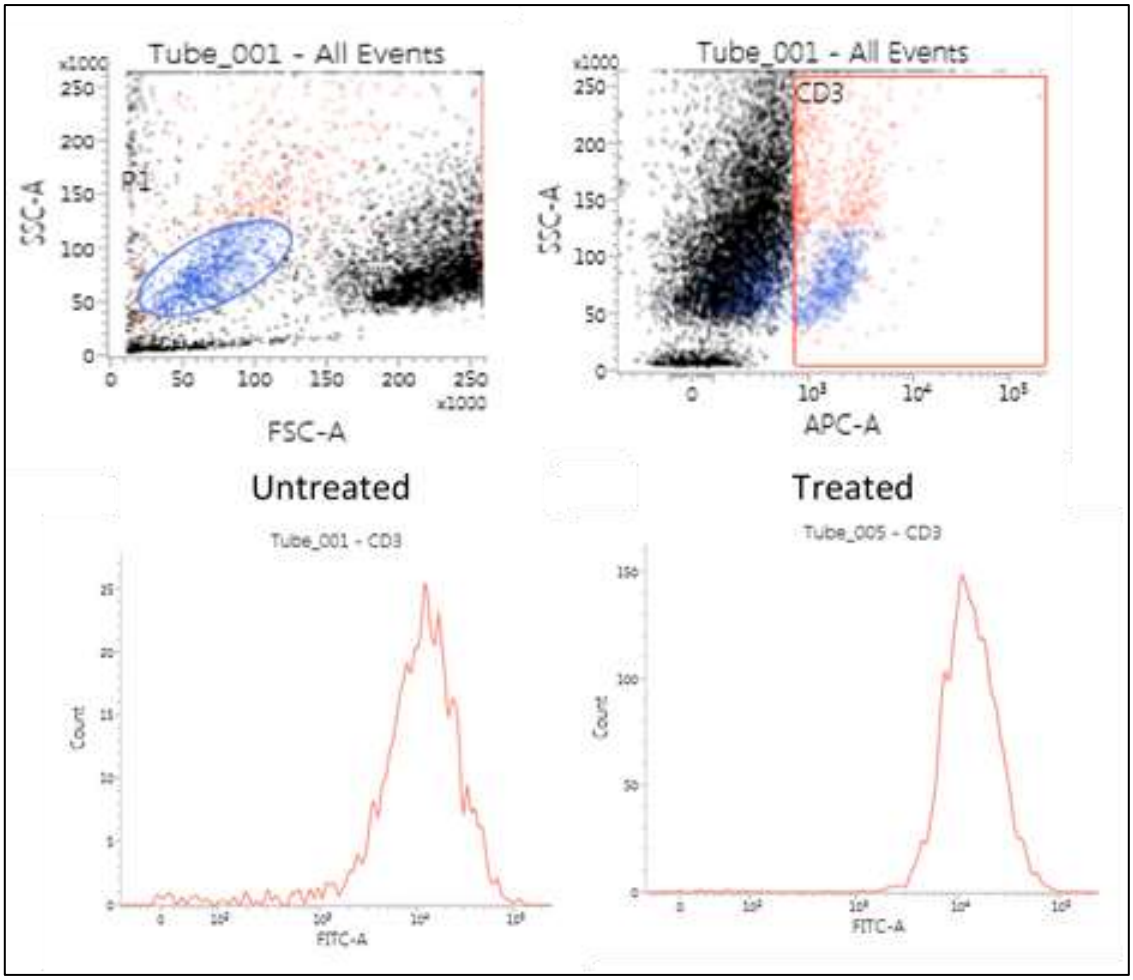

Figure 4.3 Raw data graphs obtained from cancer cell line using CFSE proliferation assay. The raw data graphs obtained in a typical cancer cell line proliferation assay, identifying the quantity of replications (each peak) each cell type has performed i.e. CD3+, in comparison to the untreated control. The example shown is untreated but stained with antibodies in order to represent the control number of replications for the cell line and treated with cisplatin. All cancer cell CFSE proliferation assays had a 3-day incubation period and for cancer cell assays N=2.

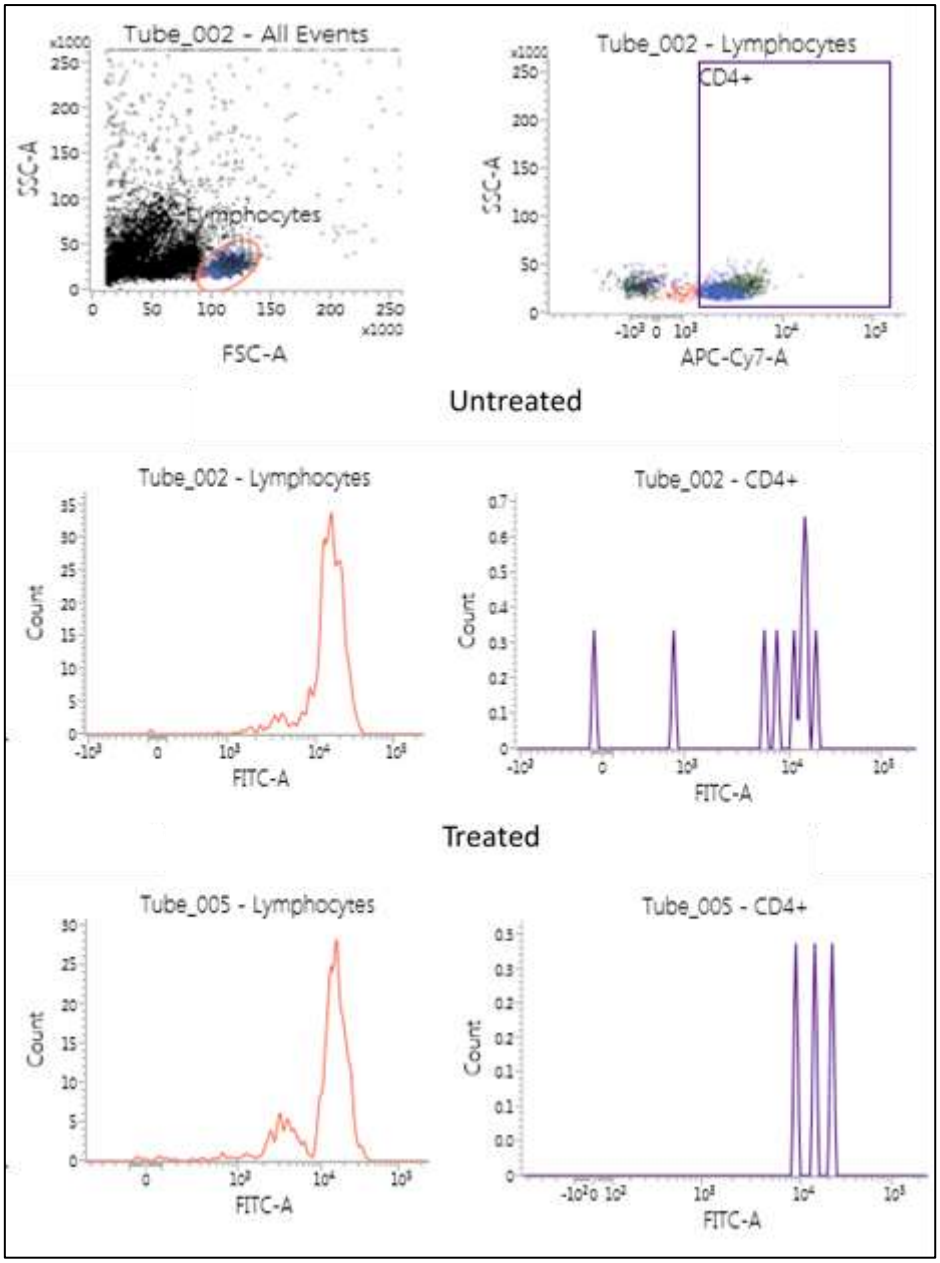

Figure 4.4 Raw data obtained from PBMC CFSE proliferation assay. Identifies the raw proliferation peak data obtained from a typical unstimulated/ naïve PBMC assay in order to determine the proliferation in each cell type. The example shown is untreated and contains the antibodies in order to represent the control number of proliferations and cisplatin treated cells. All PBMC CFSE proliferation assays were incubated for a 3-day period and N=3.

4.3 Results

4.3.1 Annexin V/ Propidium Iodide apoptosis assay results

4.3.1.1 Cancer cell assays

The annexin V/ propidium iodide apoptosis assay was carried out on all three cancer cell lines in order to establish any apoptotic responses to the treatment with novel GAG compounds.

4.3.1.1.1 MOLT-4 cell line

4.3.1.1.1.1 Entire MOLT-4 cell population

Cisplatin (figure 4.5) demonstrated a 7.3% increase in MOLT-4 cell death, with the largest increase being in early stage apoptotic cell death (figure 4.5, p=0.4317). Whelk extract treatment (figure 4.5) caused the largest increase in cell death (13.8%) within the MOLT-4 cell line out of all three treatment methods. The largest increases were in mid stage apoptosis (p=0.0179) and early stage apoptosis (p=0.0310). This can be seen by the decrease in cells not undergoing cell death (figure 4.5, p=0.008). In figure 4.5 it can be noted that the cockle extract treatment brought about a 6% increase in MOLT-4 cells undergoing some stage of apoptosis. It can also be seen in figure 4.5 that the treatment with the cockle extract resulted in a decrease in the percentage of cell in the early apoptotic stages (p=0.0003), and an increase in late apoptotic cells (p=0.0345).

The results of the entire MOLT-4 apoptosis assays correspond to that of the MTT assay, in that the whelk extract brought about the largest effect on the MOLT-4 cells compared with the cisplatin and cockle extract treatment. However, the cockle extract did bring about similar results to that of cisplatin with the largest increase in the percentage of cells undergoing late stage apoptosis compared to cisplatin; therefore, both GAG extracts appear to be effective when compared with cisplatin.

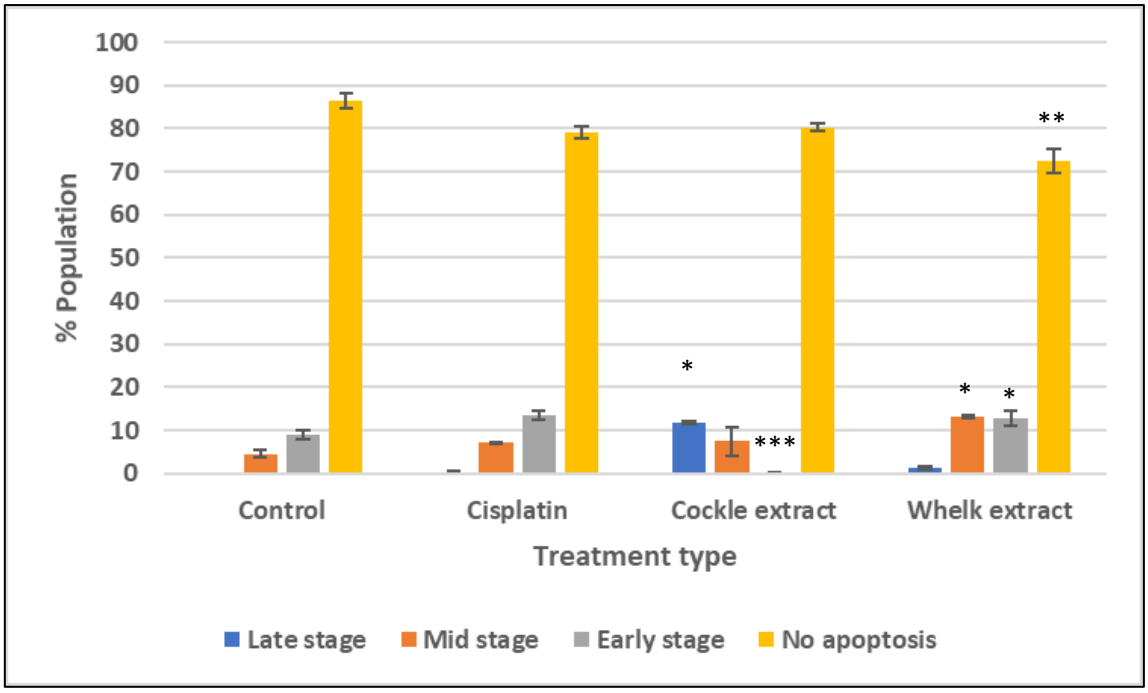

Figure 4.5 Average cell death activity in MOLT-4 cells obtained using the annexin V/PI apoptosis assay. Average percentage population graphs for MOLT-4 cells treated with the IC50 dose of cisplatin, cockle extract and whelk extract (6 µg/ml, 12 µg/ml and 12 µg/ml respectively). Showing the stage of cell death that the cells are in where early= early stages of apoptosis, mid= mid stages of apoptosis, Late= late stage apoptosis and no apoptosis= no cell death. Using an incubation period of 3 days. Where N=3, error bars show SEM, significance is denoted by *, absence of * indicates no significance.

4..3.1.1.1.2 $CD3^+$ MOLT-4 cell population

As MOLT-4 cells are T-cell derived (McCaffrey, Smoler & Baltimore, 1973), the research focused on the CD3+ population of MOLT-4 cells to gain further insight on GAG effects on T-cells specifically. Approximately 86% of untreated/ control MOLT-4 cells tested positive for CD3. Cisplatin (figure 4.6) identified an 81.5% increase in the percentage of MOLT-4 $CD3^+$ cells that were not undergoing any form of cell death (p=0.0109). This was due to a large decrease in the percentage of cells undergoing early stage apoptosis (p=0.0576) and a decrease in mid stage apoptosis (p=0.1097). Figure 4.6 also identifies a large increase in cells not undergoing cell death post treatment with the cockle extract (figure 4.6, p=<0.0001).Figure 4.6 also identifies that the cockle extract resulted in a decrease in early apoptotic cells (p=0.0478) In a similar way the $CD3^+$ MOLT-4 cells experienced a 31% increase in cells which weren't in any stage of cell death post whelk extract treatment (figure 4.6, p=0.4549) and a decrease in the percentage of early apoptotic cells (figure 4.6, p=0.0478).

The results in figure 4.6 identify that all three treatment methods resulted in increases in non-apoptotic CD3$^+$ MOLT-4 cells. Treatment of CD3$^+$ MOLT-4 cells with the cockle extract resulted in the largest increase in non-apoptotic cells in comparison to the cisplatin treatment and treatment with the whelk extract. The whelk extract treated CD3$^+$ MOLT-4 cells however, experienced the least percentage increase in non-apoptotic cells in comparison to the cisplatin and cockle extract treatments (figure 4.6). As from the results shown in figures 4.5 and 4.6 the GAG extracts exerted similar and in the case of whelk treatment better effects on the entire MOLT-4 cell populations and the CD3$^+$ MOLT-4 cell population (in the case of the whelk extract treatment), which was supported by the MTT assay results.

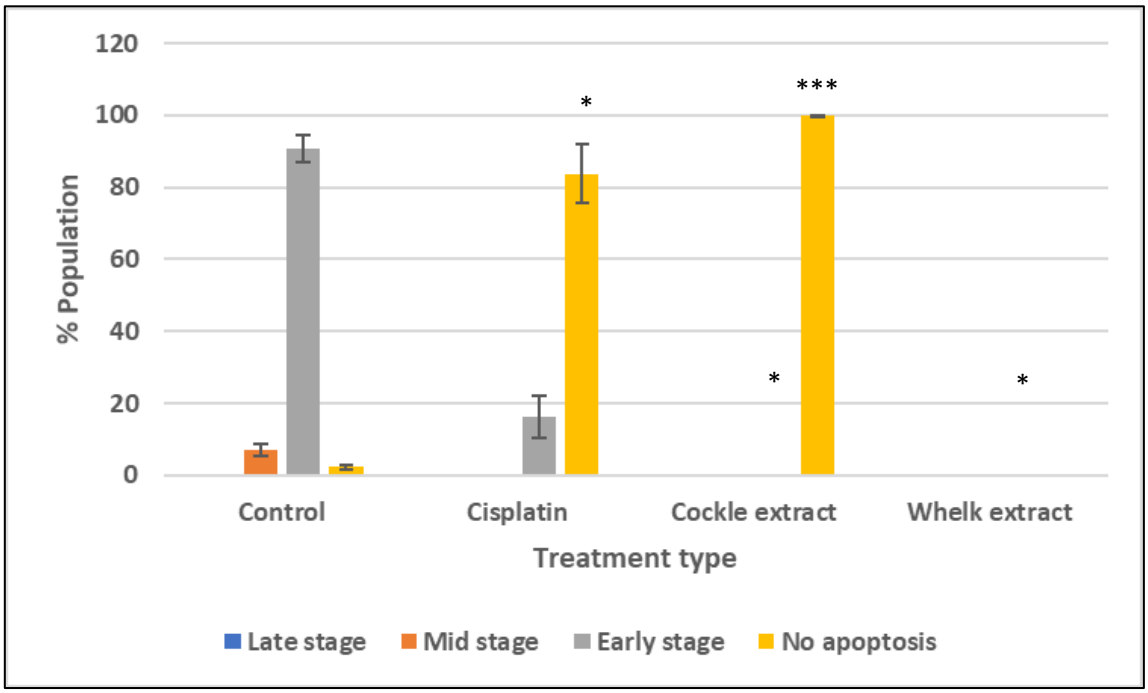

Figure 4.6 Average cell death activity in CD3$^+$ MOLT-4 cells obtained using the annexin V/PI apoptosis assay. Average percentage population graphs for CD3$^+$ MOLT-4 cells treated with the IC50 dose of cisplatin, cockle extract and whelk extract (6 µg/ml, 12 µg/ml and 12 µg/ml respectively). Showing the stage of cell death that the cells are in where early= early stages of apoptosis, mid= mid stages of apoptosis, Late= late stage apoptosis and no apoptosis= no cell death. Using an incubation period of 3 days. Where N=3, error bars show SEM, significance is denoted by *, absence of * indicates no significance.

4.3.1.1.2 K562 cell line

4.3.1.1.2.1 Entire K562 cell line

As K562 cells have a tendency to aggregate they proved to be problematic when performing flow cytometry analysis on them. Therefore firm pipetting and careful gating was employed in order to separate cells and avoid duplicate readings when performing flow cytometric analysis.

Figure 4.7 shows that cisplatin treatment (figure 4.7) brought about the largest increase in cells undergoing some stage of apoptosis (9.5%); this is noted through the corresponding drop in cells which were not undergoing any form of cell death (p=0.0756). There was also a slight drop in cells experiencing late stage apoptosis (p=0.0497). There was also a corresponding rise in the percentage of cells in the early stages of apoptosis (p=0.1540) which saw the largest increase however there was also a slight increase in the percentage of cells in the mid stages of apoptosis (p=0.1464). Treatment with the cockle extract brought about a 3.6% increase in apoptosis (seen in figure 4.7). This increase was seen mainly in the early stage of apoptosis (p=0.0925) but there was also a slight rise in the percentage of cells in the mid stages of apoptosis (p=0.0848). In a similar way to cisplatin treatment the cockle extract brought about a small decrease in the percentage of late apoptotic cells (p=0.0713). Finally figure 4.7 identifies the whelk extract treatment (figure 4.7) resulted in a small increase in the percentage of cells which were not undergoing any stage of apoptosis (p=0.5835). Whelk extract treatment also brought about small decreases in the percentage of cells undergoing late stage apoptosis (figure 4.7, p=0.0497), mid stage apoptosis (figure 4.7, p=0.0292) and early stage apoptosis (figure 4.7, p=0.022) This also corresponds to the MTT assay results as the whelk extract did not elicit much of a response after a 3-day incubation period in the K562 MTT assays either.

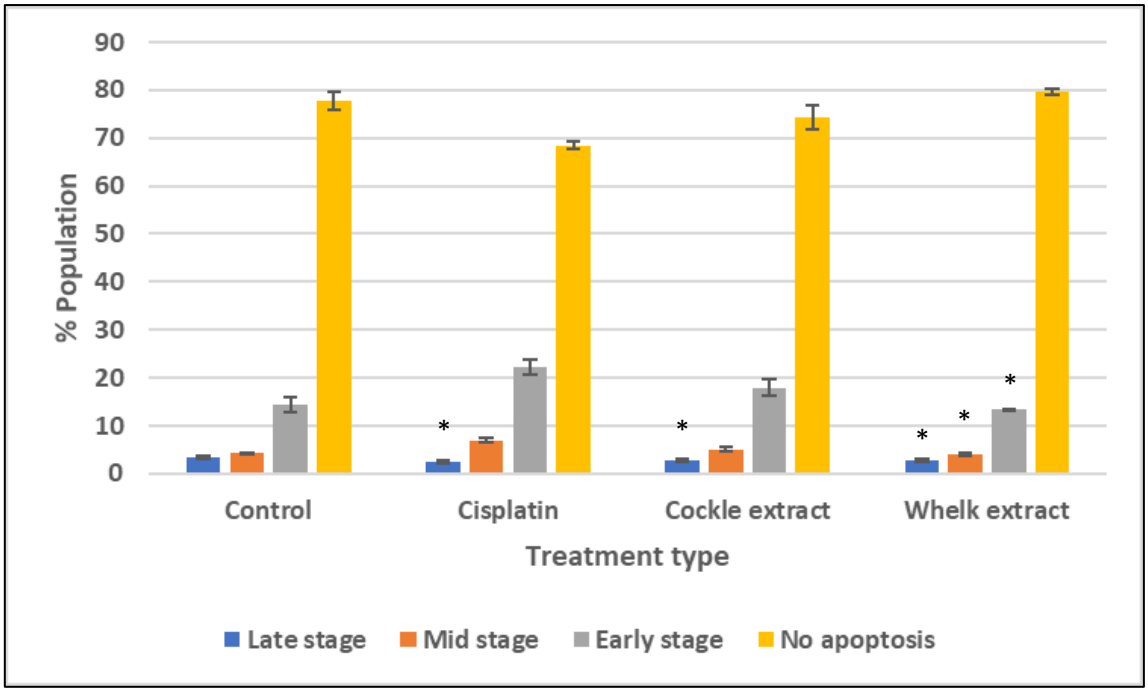

Figure 4.7 Average cell death activity in K562 cells obtained using the annexin V/PI apoptosis assay. Average percentage population graphs for K562 cells treated with the IC50 dose of cisplatin, cockle extract and whelk extract (6 µg/ml, 12 µg/ml and 12 µg/ml respectively). Showing the stage of cell death that the cells are in where early= early stages of apoptosis, mid= mid stages of apoptosis, Late= late stage apoptosis and no apoptosis= no cell death. Using an incubation period of 3 days. Where N=3, error bars show SEM, significance is denoted by *, absence of * indicates no significance.

Although the GAGs did appear to exert some effect on the K562 cell line cisplatin treatment appeared to be the most effective treatment method on the K562 cell line in the apoptosis assay. However the tendency of K562 cells to aggregate may have potentially caused some issues with the flow cytometry assays.

4.3.1.1.3 U698 cell line

4.3.1.1.3.1 Entire U698 cell population

In the U698 cell population cisplatin treatment (figure 4.8) brought about a 1.3% decrease in cells which were not undergoing cell death (p=0.4781). Figure 4.8 also demonstrates slight decreases in the percentage of U698 cells that were undergoing late stage apoptosis (p=0.0544) or mid stage apoptosis (p=0.0046). This decrease constituted to the 5% rise in U698 cells undergoing early stage apoptosis also noted in figure 4.8, (p=0.083).

The cockle extract treatment (figure 4.8) brought about slight increases in the percentage of mid stage apoptotic (p=0.0516) and late stage apoptotic (p=0.0904) U698 cells. There was also a slight decrease in the percentage of U698 cells undergoing the early stages of apoptosis post cockle extract treatment (figure 4.8, p=0.1523). The whelk extract treatment brought about the greatest effect on the U698 cell line with a 15% decrease in cells not undergoing a form of cell death (figure 4.8, p=0.0426). Post treatment with the whelk extract there was a 9.5% increase in U698 cells undergoing early stage apoptosis (figure 4.8, p=0.5557) and a 4.6% rise in the percentage of U698 cells undergoing the mid stages of apoptosis (figure 4.8, p=0.0165). There was also a slight rise in the percentage of U698 cells undergoing late stage apoptosis post whelk extract treatment (figure 4.8, p=0.3688).

These results correspond to what was noted in the MTT assay results; the whelk extract exerted a profound effect on the cell line even when compared to the known drug cisplatin.

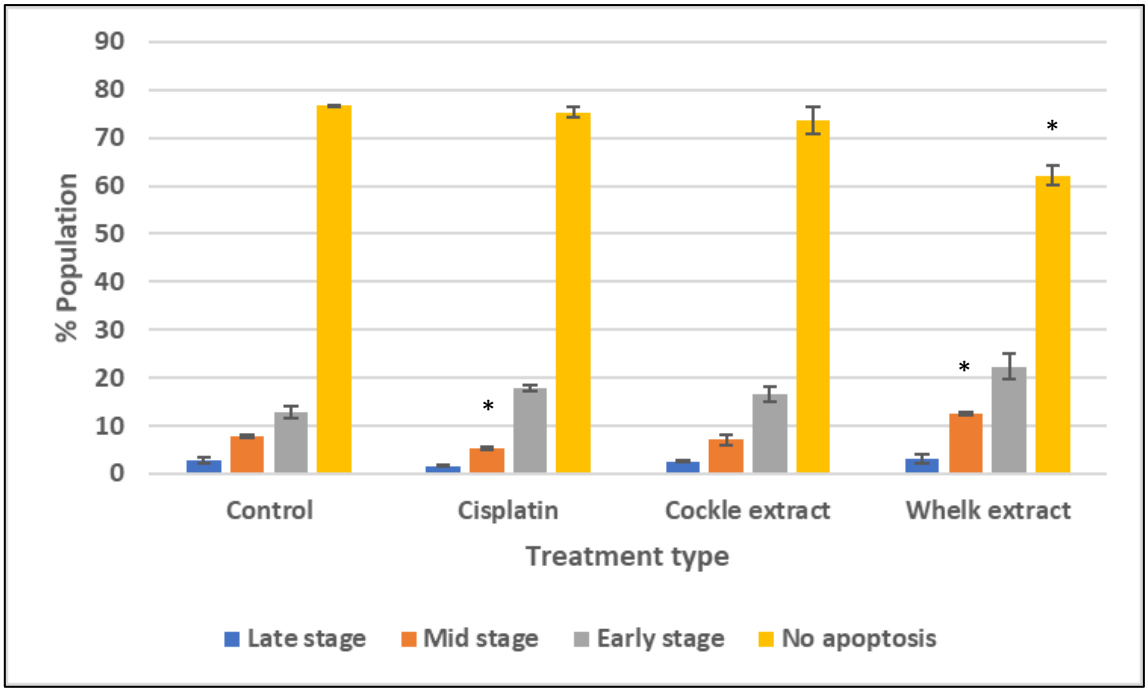

Figure 4.8 Average cell death activity in U698 cells obtained using the annexin V/PI apoptosis assay. Average percentage population graphs for U698 cells treated with the IC50 dose of cisplatin, cockle extract and whelk extract (6 µg/ml, 12 µg/ml and 12 µg/ml respectively). Showing the stage of cell death that the cells are in where early= early stages of apoptosis, mid= mid stages of apoptosis, Late= late stage apoptosis and no apoptosis= no cell death. Using an incubation period of 3 days. Where N=3, error bars show SEM, significance is denoted by *, absence of * indicates no significance.

4.3.1.1.3.2 $CD19^+$ U698 population

The U698 cell line has been described as being of B-cell origin (Godal, 1982), therefore the research focused on the CD19+ populations of the U698 cell line, in order to establish GAG isolate effects on B-cells specifically. Approximately 99% of U698 cells tested positive for CD19. Figure 4.9 demonstrates that cisplatin treatment resulted in around a 1.4% increase in the percentage of $CD19^+$ U698 cells undergoing a form of cell death; this can be seen through the decrease in cells which were not undergoing any form of cell death (figure 4.9, p=0.2184). This resulted in a 1.4% increase in the percentage of $CD19^+$ U698 cells undergoing early stage apoptosis (figure 4.9, p=0.0264), there were also minor increase and a minor decrease in the percentage of cells undergoing mid stage apoptosis (p=0.3612) and late stage apoptosis (p=0.1290) respectively (figure 4.9).

The treatment with cockle extract resulted in a larger increase in the percentage of $CD19^+$ U698 cells which were undergoing a form of cell death, which can be mainly seen in the percentage of $CD19^+$ U698 cells undergoing the early stages of apoptosis (figure 4.9, p=0.4121). The whelk extract treatment elicited the largest increase in cell death in the $CD19^+$ U698 cell population post treatment; this can be seen in the decrease in the percentage of cells which were not undergoing a form of cell death (figure 4.9, p=0.1884). The whelk extract brought about increases of 1.8%, 0.7% and 5% in the percentages of $CD19^+$ U698 cells which were undergoing early (p=0.3143) and mid stage (p=0.5577) apoptosis and late stage apoptosis (p=0.5089) respectively (figure 4.9).

These results support the initial findings of the MTT assay, that the whelk extract exerts the most effect on the U698 cell population.

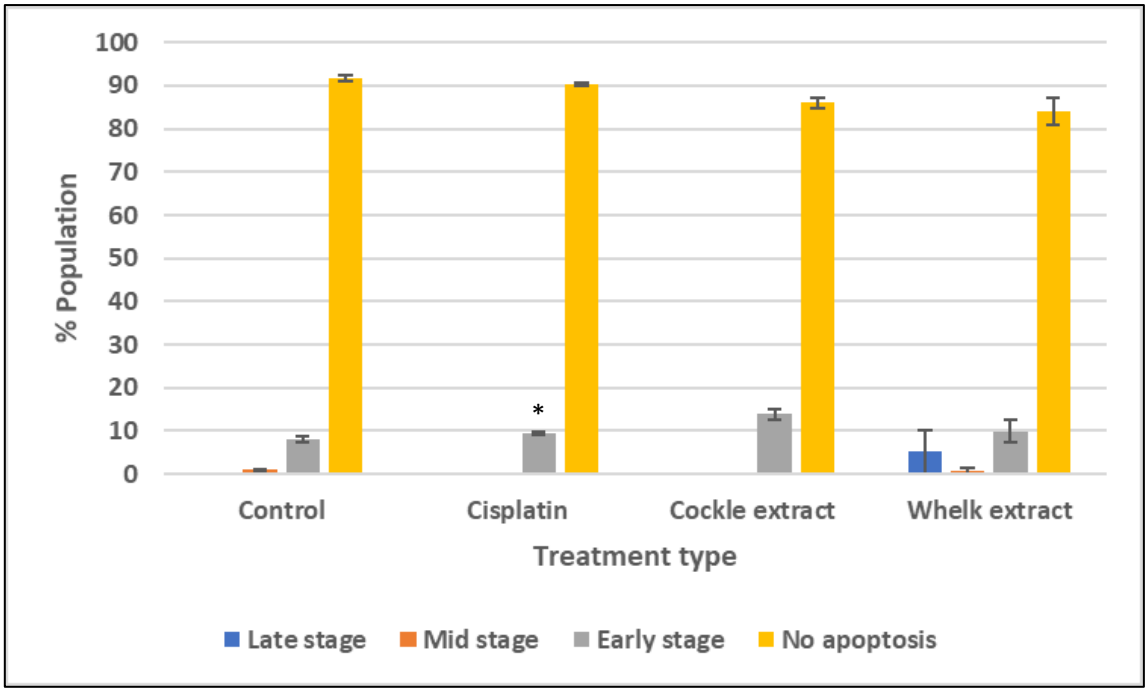

Figure 4.9 Average cell death activity in CD19⁺ U698 cells obtained using the annexin V/PI apoptosis assays. Average percentage population graphs for CD19⁺ U698 cells treated with the IC50 dose of cisplatin, cockle extract and whelk extract (6 µg/ml, 12 µg/ml and 12 µg/ml respectively). Showing the stage of cell death that the cells are in where early= early stages of apoptosis, mid= mid stages of apoptosis, Late= late stage apoptosis and no apoptosis= no cell death. Using an incubation period of 3 days. Where N=3, error bars show SEM, significance is denoted by *, absence of * indicates no significance.

4.3.1.2 Isolated PBMC assays

4.3.1.2.1 Unstimulated/naïve PBMC assays

The use of flow cytometry allowed for the evaluation of 6 colours at once, therefore the research characterised the potency of GAGs to both naïve (CD45RA⁺) and memory (CD45RO⁺) T-cells. Therefore these antibodies were used in a panel with CD8 and CD4 to differentiate cytotoxic and helper T-cells specifically and use remaining fluorescence channels for the annexin V and PI apoptosis detection in all these populations. For logistical reasons this study focussed on T-cells therefore, the B cell marker CD19 was not used during the PBMC assays; however, it is noted that the U698 (B-cell line) did show sensitivity to the GAG isolates, therefore this would be a future line of interest for the lab research team.

Figure 4.10 shows that cisplatin treatment decreased the percentage of lymphocytes not undergoing cell death by around 14% (p=0.3400). This decrease corresponded to increases in the percentage of lymphocytes which were undergoing late stage apoptosis (p=0.4923), mid stage apoptosis (p=0.9309) and early stage apoptosis (p=0.2082) of 7%, 6.5% and 0.57% respectively (figure 4.10).

Cockle extract treatment (figure 4.10) resulted in a rise of around 11.9% in lymphocytes undergoing a form of cell death (p=0.4158). Smaller increases of 1.8% and 0.95% could be seen in the percentage of lymphocytes undergoing early stage apoptosis (figure 4.10, p=0.1804) and late stage apoptosis respectively (figure 4.10, p=0.4248). Finally figure 4.10, identifies that whelk extract treatment results in the smallest decrease in the percentage of cells which were not undergoing cell death with a drop of 10.97% (figure 4.10, p=0.3417). This treatment method also resulted in a small drop of 3% in the percentage of lymphocytes which were undergoing late stage apoptosis (figure 4.10, p=0.4957). In a similar way to the cockle extract treatment, the largest increase in cell death was seen in the mid stages of apoptosis post whelk extract treatment (figure 4.10, p=0.7155); this accounted for 13% of the increase in cell death. Finally, whelk extract treatment brought about a 1% rise in the percentage of lymphocytes which were undergoing the early stages of apoptosis (figure 4.10, p=0.1629).

From these results it can be determined that the whelk extract elicited the least damage to the lymphocyte population of the naïve PBMCs. Although the largest increase in mid stage was post whelk extract treatment it can be seen in figure 4.10 that some of this increase was related to a decrease in the percentage of lymphocytes undergoing late stage apoptosis. The cockle extract treatment also resulted in less damage to the naïve PBMC lymphocytes than the known drug cisplatin; this could suggest that the GAG extracts may provide a beneficial treatment option which results in less damage to healthy cells. Although as cell death levels were similar to those in the MOLT-4 cell population seen in figures 4.6 and 4.5, it is important to identify which cell populations are sensitive to the GAG treatment.

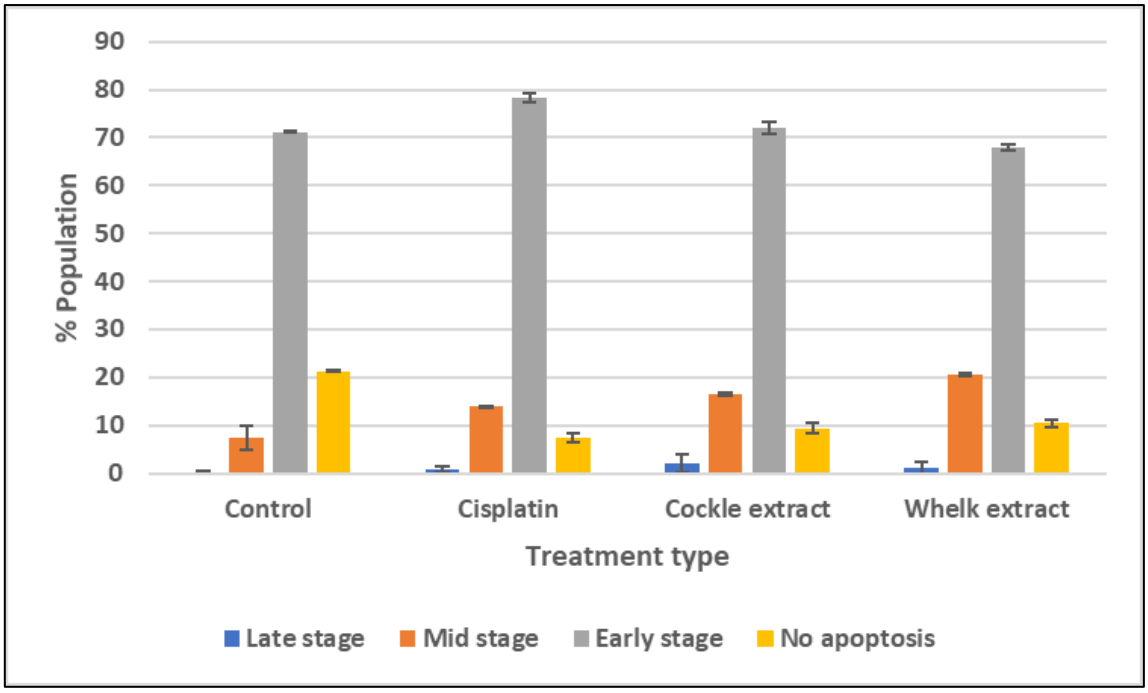

Figure 4.10 Average cell death activity in the lymphocyte population of naïve PBMCs obtained using the annexin V/PI apoptosis assays. Average percentage population graphs for the lymphocyte population of naïve PBMCs treated with the IC50 dose of cisplatin, cockle extract and whelk extract (6 µg/ml, 12 µg/ml and 12 µg/ml respectively). Showing the stage of cell death that the cells are in where early= early stages of apoptosis, mid= mid stages of apoptosis, Late= late stage apoptosis and no apoptosis= no cell death. Using an incubation period of 3 days. Where N=3, error bars show SEM, significance is denoted by *, the absence of * indicates no significance.

Figure 4.11 identifies that post cisplatin treatment there was a 6.59% increase in the percentage of memory T-helper cells ($CD4^+CD45RO^+$) experiencing a form of cell death. Late stage apoptotic cells (figure 4.11, p=0.4226) had the largest increase in memory T-helper cells with a 5.6% increase in the percentage of memory T-helper cells in this stage of apoptosis. There were also minor increases in the percentage of memory T-helper cells experiencing the early (p=0.1986) and mid stages (p=0.8410) of apoptosis (as represented in figure 4.11).

The cockle extract treatment (figure 4.11) resulted in a 4.23% increase in the percentage of memory T-helper cells experiencing cell death. There was also a minor decrease in the percentage of memory T-helper cells experiencing mid stage apoptosis (p=0.0712) and no change in the percentage of late stage apoptotic cells (p=0.4807) (figure 4.11). Treatment with the whelk extract (figure 4.11) resulted in a small 1.73% decrease in the percentage of memory T-helper cells which were not experiencing cell death (p=0.6579). Figure 4.11 also

demonstrates a minor increase in the percentage of memory T-helper cells in the early stages of apoptosis (figure 4.11, p=0.1789). The memory T-helper cell population also resulted in a 0.31% decrease in the percentage of cells in the mid stages of apoptosis (p=0.5631) and a 1.98% increase in the percentage of late stage apoptotic (p=0.4226) memory T-helper cells post whelk extract treatment (figure 4.11).

In terms of memory T-helper cells both the GAG extracts exerted less of an effect on the induction of cell death than the known anti-cancer drug cisplatin. Although all the changes in the memory T-helper cell population were small, the whelk extract treatment resulted in almost six times less cell death induction compared to cisplatin. This again could suggest that GAG treatment could provide a kinder treatment method. Healthy lymphocytes are made up of around 30-50% memory cells and so to capture any difference in sensitivity to GAG action between naïve and memory cells, both antibodies were used.

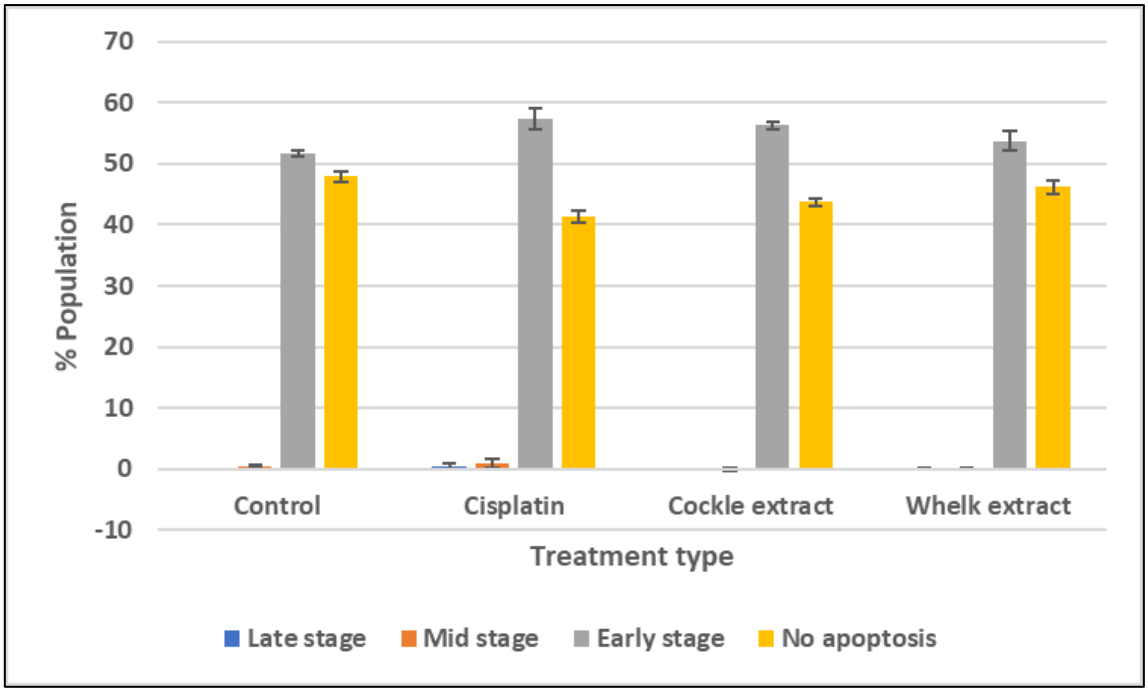

Figure 4.11 Average cell death activity in the memory T-helper cell population ($CD4^+CD45RO^+$) of naïve PBMCs obtained using the annexin V/PI apoptosis assay. Average percentage population graphs for the memory T-helper cell population of naïve PBMCs treated with the IC50 dose of cisplatin, cockle extract and whelk extract (6 µg/ml, 12 µg/ml and 12 µg/ml respectively). Showing the stage of cell death that the cells are in where early= early stages of apoptosis, mid= mid stages of apoptosis, Late= late stage apoptosis and no apoptosis= no cell death. Using an incubation period of 3 days. Where N=3, error bars show SEM, significance is denoted by *, the absence of * indicates no significance.

Cisplatin treatment (figure 4.12) resulted in a 9.5% decrease in the percentage of cells not experiencing cell death (p=0.1641), corresponding to this there was an 8.8% increase in naïve T-helper cells ($CD4^+CD45RA^+$) experiencing late stage apoptosis (p=0.5031) post cisplatin treatment. There were also minor increases in the percentage of naïve T-helper cells undergoing mid stage apoptosis (p=0.6977) and early stage apoptosis (p=0.1788) post cisplatin treatment (figure 4.12).

The cockle extract treatment (figure 4.12) resulted in decreases in the percentage of naïve T-helper cells not experiencing cell death (p=0.5525), experiencing mid stage apoptosis (p=0.2302) and early stage apoptosis (p=0.1788) of 5.24%, 0.31% and 0.02% respectively (seen in figure 4.12). These decreases resulted in a 5.57% increase in the percentage of late apoptotic naïve memory T-cells (figure 4.12, p=0.2302). In a similar pattern to the cockle extract the whelk extract treatment (figure 4.12) resulted in decreases in the percentage of

naïve T-helper cells experiencing early apoptotic stages (p=0.1808), mid apoptotic stages (p=0.2582) and cells which were not experiencing cell death (p=0.4384). These decreases were 0.02%, 0.18% and 5.19% respectively. In correspondence with this the percentage of naïve T-helper cells experiencing late stage apoptosis increased by 5.39% (figure 4.12, p=0.2505) post whelk extract treatment.

From these results again, the GAG extracts appear to cause less damage to the naive T-helper cell population when compared to cisplatin. Suggesting that GAG extract treatment may result in less damage to healthy cells and therefore may provide a kinder treatment option compared to current chemotherapy drugs.

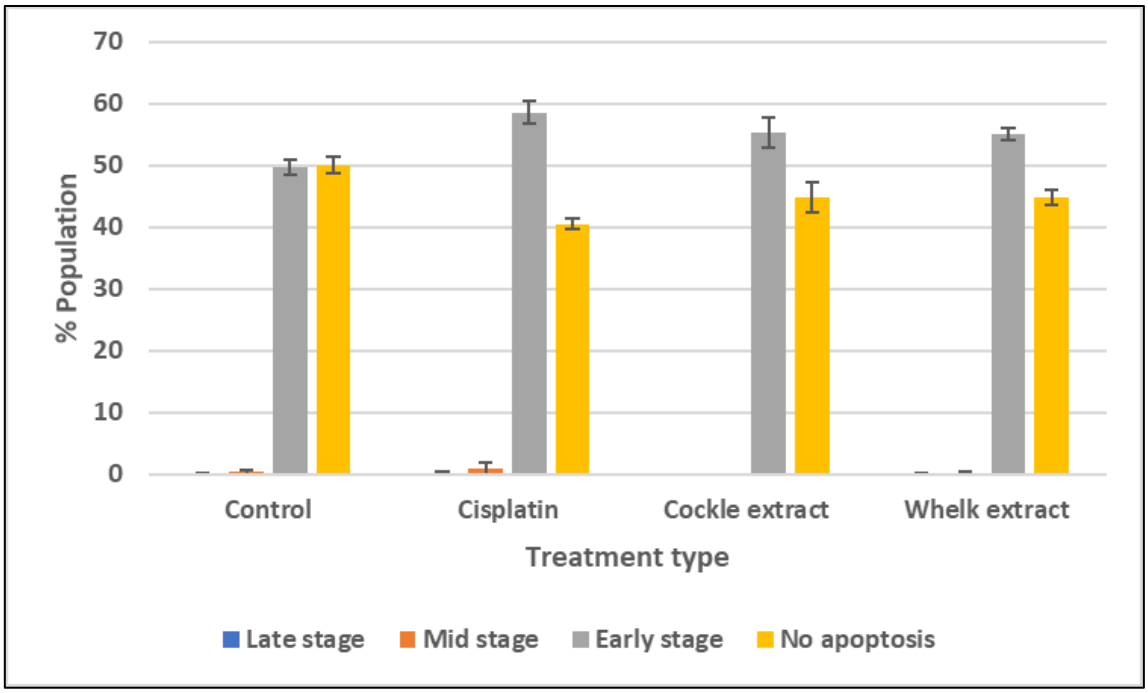

Figure 4.12 Average cell death activity in the naïve T-helper cell population ($CD4^+CD45RO^+$) of naïve PBMCs obtained using the annexin V/PI apoptosis assay. Average percentage population graphs for the naïve T-helper cell population of naïve PBMCs treated with the IC50 dose of cisplatin, cockle extract and whelk extract (6 µg/ml, 12 µg/ml and 12 µg/ml respectively). Showing the stage of cell death that the cells are in where early= early stages of apoptosis, mid= mid stages of apoptosis, Late= late stage apoptosis and no apoptosis= no cell death. Using an incubation period of 3 days. Where N=3, error bars show SEM, significance is denoted by *, the absence of * indicates no significance.

In figure 4.13 it can be seen that cisplatin treatment results in a 26.41% decrease in the percentage of memory cytotoxic T-cells ($CD8^+CD45RO^+$) not undergoing any form of cell death

(p=0.2927). There was also a 7% decrease in the percentage of memory cytotoxic T-cells which were experiencing late stage apoptosis (p=0.3217). These declines resulted in a 26% increase in the percentage of memory cytotoxic T-cells in the mid stages of apoptosis (figure 4.13, p=0.3155) and a 7.4% rise in the percentage of memory cytotoxic T-cells in the early stages of apoptosis (figure 4.13, p=0.0399).

Treatment with the cockle extract (figure 4.13) resulted in the largest decrease in the percentage of memory cytotoxic T-cells not undergoing apoptosis of 30.72% (p=0.3590). The memory cytotoxic T-cell population experienced a 19% increase in the population of cells in the early stages of apoptosis (figure 4.13, p=0.0399) post cockle extract treatment. The memory cytotoxic T-cells in the mid stages of apoptosis also increased by 21.28% (figure 4.13, p=0.3279). Finally, there was a 9.6% decrease in the percentage of memory cytotoxic T-cells in the late stages of apoptosis (figure 4.13, p=0.3487). Whelk extract treatment (figure 4.13) resulted in the least induction of cell death in the memory cytotoxic T-cell population. There was a minor decrease in cells which were not undergoing any form of cell death of 0.29% (figure 4.13, p=0.9538). Late stage apoptosis in memory cytotoxic T-cells was decreased by 12.41% (figure 4.13, p=0.1880). Memory cytotoxic T-cells in mid apoptotic stages increased by 9.25% (figure 4.13, p=0.6272); while cells in the early stages of apoptosis increased by 3.46% (figure 4.13, p=0.0379).

In terms of memory cytotoxic T-cells the cockle extract resulted in the largest decrease in cells which were not undergoing a form of cell death when compared to other treatment methods tested. The whelk extract has consistently been the mildest treatment method again proving to cause the least damage to the PBMC population.

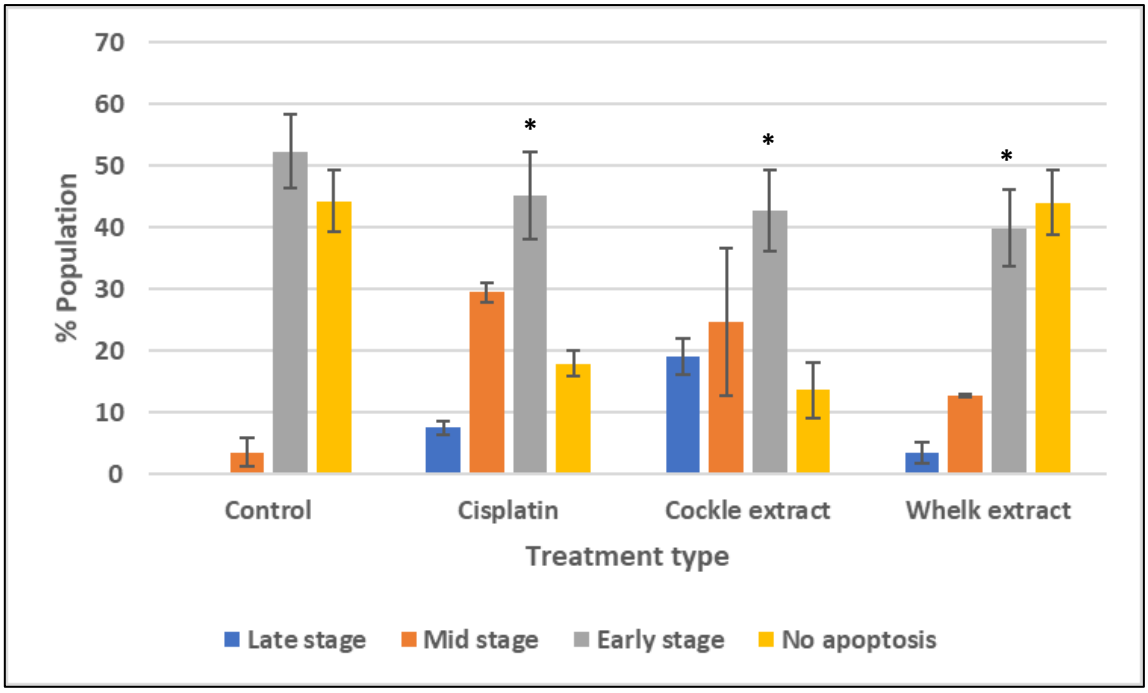

Figure 4.13 Average cell death activity in the memory cytotoxic T-cell population ($CD8^+CD45RO^+$) of naïve PBMCs obtained using the annexin V/PI apoptosis assay. Average percentage population graphs for the memory cytotoxic T-cell population of naïve PBMCs treated with the IC50 dose of cisplatin, cockle extract and whelk extract (6 µg/ml, 12 µg/ml and 12 µg/ml respectively). Showing the stage of cell death that the cells are in where early= early stages of apoptosis, mid= mid stages of apoptosis, Late= late stage apoptosis and no apoptosis= no cell death. Using an incubation period of 3 days. Where N=3, error bars show SEM, significance is denoted by *, absence of * indicates no significance.

In figure 4.14 it can be seen that cisplatin treatment results in a 26% decline in the percentage of naïve cytotoxic T-cells ($CD8^+CD45RA^+$) experiencing no form of cell death (figure 4.14, p=0.2457). This decline brought about a 7% increase in the percentage of naïve cytotoxic T-cells in the early stages of apoptosis (figure 4.14, p=0.1652). Also, cisplatin treatment resulted in a 15.7% increase in the percentage of cells in the mid stages of apoptosis (figure 4.14, p=0.3767). Finally, the treatment with cisplatin resulted in a 3.27% increase in the percentage of late apoptotic naïve cytotoxic T-cells (figure 4.14, p=0.3900).

As was seen in the memory cytotoxic T-cells the cockle extract treatment (figure 4.14) also resulted in the largest decline of naïve cytotoxic T-cells not undergoing any form of cell death (p=0.3590); this decline was of 33.78%. there was also a minor increase in the percentage of naïve cytotoxic T-cells in the early stages of apoptosis (p=0.1471) and in cells experiencing late stage apoptosis (p=0.4226) of 0.6% and 0.5% respectively, post treatment with the cockle

extract (figure 4.14). The cockle extract treatment also brought about a 0.65% decline in the percentage of naïve cytotoxic T-cells in the mid stages of apoptosis (figure 4.14, p=0.4125). Whelk extract treatment again resulted in the least induction of cell death in the naïve cytotoxic T-cell population. The whelk extract treatment reduced the cells which were not undergoing any form of cell death by 2.55% (figure 4.14, 0.6556) and reduced the percentage of cells in mid stage apoptosis by 0.12% (figure 4.14, 0.4472). Also figure 4.14 identifies that the whelk extract treatment increased the population of early apoptotic naïve cytotoxic T-cells by 0.95% (figure 4.14, p=0.1586). Also, there was a 1.73% increase in late apoptotic naïve cytotoxic T-cells post whelk extract treatment (figure 4.14, p=0.1835).

As with what was seen in the memory cytotoxic T-cell population the whelk extract also induced the least amount of cell death when compared to cisplatin and cockle extract treatments. However, when compared to cisplatin the cockle extract did elicit slightly more cell death compared to cisplatin in the naïve cytotoxic T-cell population. The cytotoxic T-cell populations appear to be more susceptible to chemotherapy treatments than T-helper cell populations with the memory population appearing the most susceptible. The whelk extract however induced the fewest changes in the populations and so appears to be the more favourable therapeutic possibility.

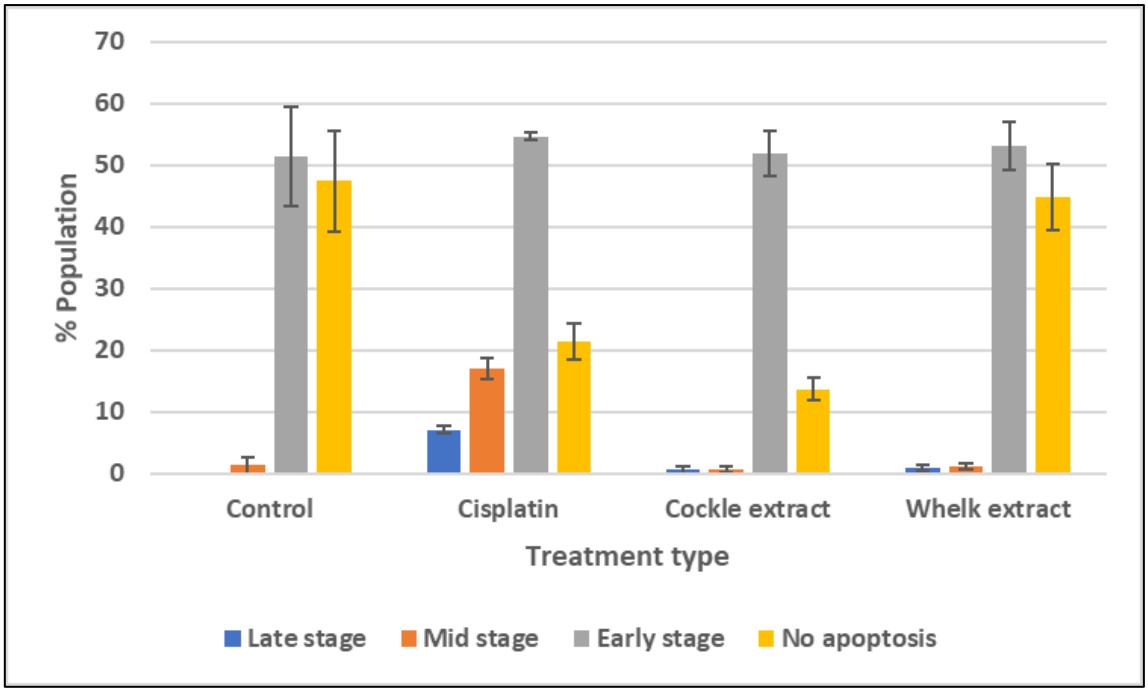

Figure 4.14 Average cell death activity in the naïve cytotoxic T-cell population ($CD8^+CD45RA^+$) of naïve PBMCs obtained using the annexin V/PI apoptosis assay. Average percentage population graphs for the naïve cytotoxic T-cell population of naïve PBMCs treated with the IC50 dose of cisplatin, cockle extract and whelk extract (6 µg/ml, 12 µg/ml and 12 µg/ml respectively). Showing the stage of cell death that the cells are in where early= early stages of apoptosis, mid= mid stages of apoptosis, Late= late stage apoptosis and no apoptosis= no cell death. Using an incubation period of 3 days. Where N=3, error bars show SEM, significance is denoted by * the absence of * indicates no significance.

4.1.3.2.2 PMA/ ionomycin stimulated PBMC assays

All the naïve lymphocyte (unstimulated) assays were repeated using activated T-cells in order to assess if naturally proliferating cells (a model of infection/inflammation) were targeted.

The treatment with cisplatin (figure 4.15) caused a small reduction in the percentage of lymphocytes which were either late stage apoptotic (1.07%, P= 0.2466), in mid stage apoptosis (5.64%, p= 0.3663) or which were not experiencing any form of cell death (1.94%, p=0.4571) as can be seen in figure 4.15. In line with those decreases the percentage of lymphocytes which were experiencing early apoptotic stages (figure 4.15) increased by 8.65% post cisplatin treatment (p=0.027).

The lymphocyte population had minor decreases in late stage apoptotic and mid stage apoptotic cells by 0.92% (p=0.2369) and 0.72% (p=0.3977) respectively post cockle extract

treatment (figure 4.15). The percentage of lymphocytes not experiencing cell death also decreased by 1.73% post cockle treatment (figure 4.15, p=0.4656). In correspondence to these decreases the percentage of lymphocytes experiencing the early stages of apoptosis increased by 3.37% (figure 4.15, p=0.027). Upon treatment with the whelk extract the lymphocyte population experienced a 0.56% decrease in late stage apoptotic lymphocytes (figure 4.15, p=0.6808). There were also decreases of 0.13% and 2.05% in the population of lymphocytes undergoing either mid stage apoptosis (p=0.4162) or which were not undergoing any form of cell death (p=0.0892) respectively, which can be in figure 4.15 respectively. Post whelk extract treatment there was also a 2.75% increase in the percentage of lymphocytes undergoing the early stages of apoptosis (figure 4.15, p=0.0309).

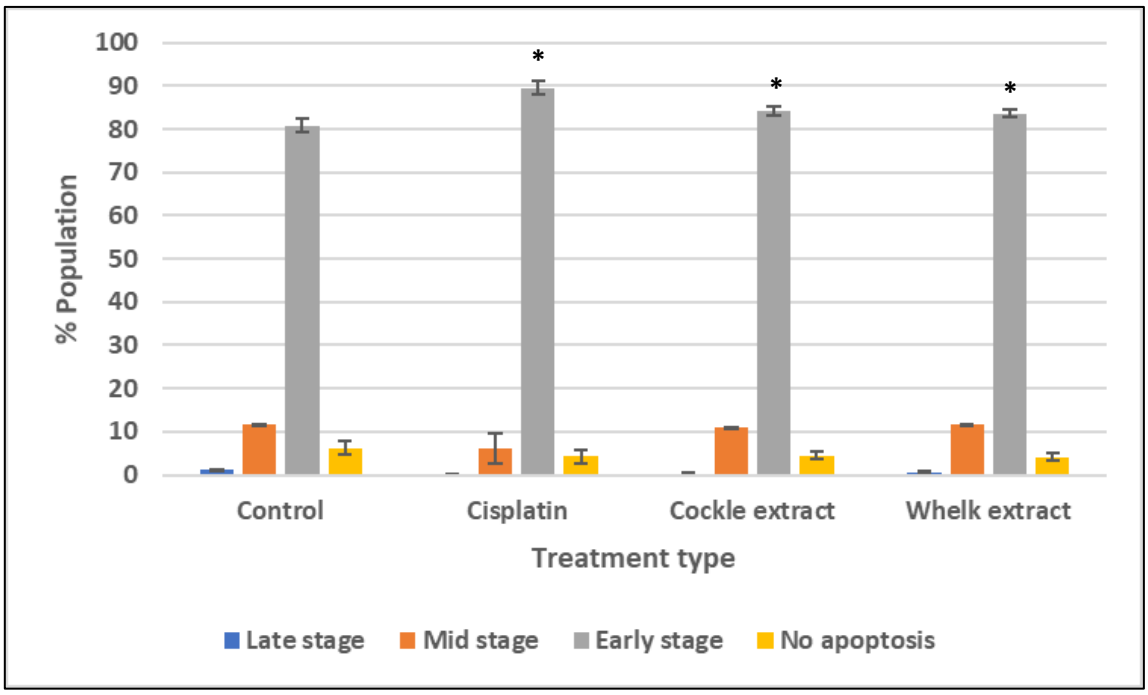

Figure 4.15 Average cell death activity in the lymphocyte population of stimulated PBMCs obtained using the annexin V/ PI apoptosis assay. Average percentage change graphs for the lymphocyte population of stimulated PBMCs treated with the IC50 dose of cisplatin (A), cockle extract (B) and whelk extract (C) (6 µg/ml, 12 µg/ml and 12 µg/ml respectively). Showing the stage of cell death that the cells are in where early= early stages of apoptosis, mid= mid stages of apoptosis, Late= late stages of apoptosis and no apoptosis= no cell death. Using an incubation period of 3 days. Where N=3, error bars show SEM, significance is denoted by *, the absence of * indicates no significance.

Cisplatin treatment (figure 4.16) caused a minor increase (0.03%) late stage apoptotic memory T-helper cells (p=0.4226) as well as a minor decrease in memory T-helper cells which

were undergoing mid stage apoptosis (0.26%, p=0.3188), as can be seen figure 4.16. There was also a decrease of 3.35% in the cells which were not undergoing any form of cell death (p=0.0970); this decrease corresponded with a 3.57% increase in the percentage of memory T-helper cells experiencing early apoptotic stages post cisplatin treatment (noted in figure 4.16, p=0.0502).

Upon treatment with the cockle extract the memory T-helper cell population had no change in the percentage of cells undergoing late stage apoptosis (figure 4.16, p=0.4411). The treatment resulted in minor decreases in the percentage of memory T-helper cells undergoing mid stage apoptosis or the early stages of apoptosis, these decreases were 0.37% (p=0.2302) and 0.32% (p=0.0502) respectively (figure 4.16). After treatment with the cockle extract the percentage of memory T-helper cells which were not undergoing any form of cell death increased by 0.7% (figure 4.16, p=0.1196). There was no change in the percentage of late stage apoptotic memory T-helper cells post treatment with the whelk extract (figure 4.16, P=0.4411). There was a 0.14% decrease in the percentage of memory T-helper cells undergoing mid stage apoptosis post whelk treatment (figure 4.16, P=0.3002). After whelk extract treatment there was a 3.18% increase in the percentage of memory T-helper cells experiencing the early stages of apoptosis, this is represented in figure 4.16, P=0.0502. The treatment with the whelk extract resulted in a 3.04% decrease in the percentage of memory helper T-cells which were not currently undergoing any stage of cell death (figure 4.16, P=0.0603).

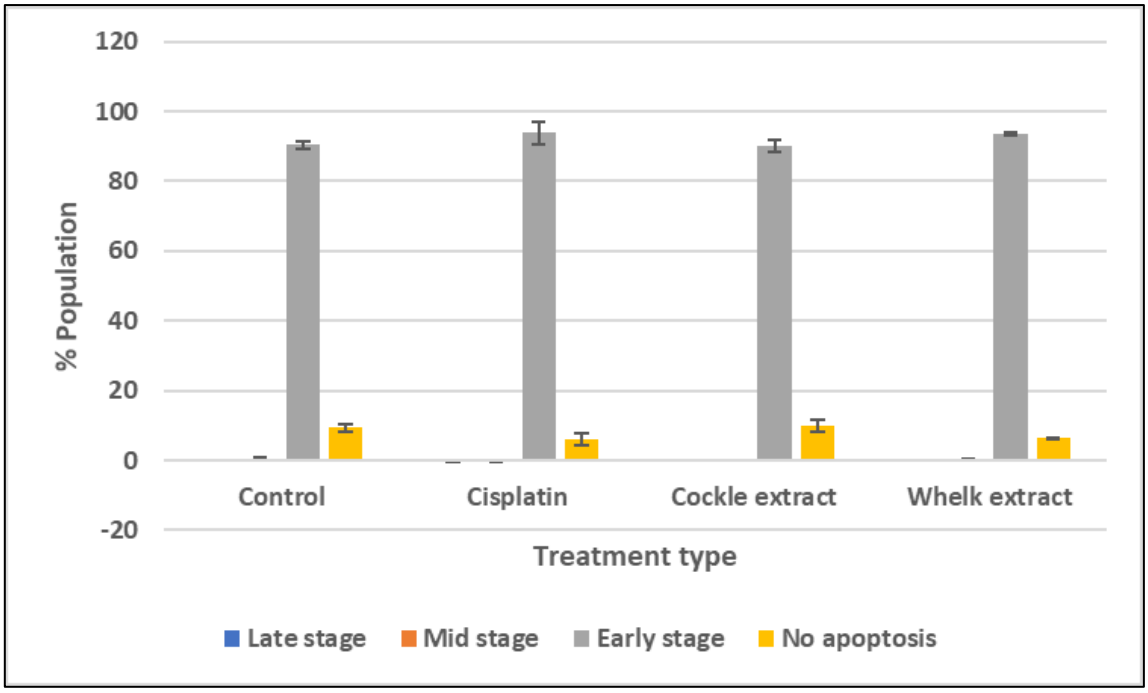

Figure 4.16 Average cell death activity in the memory T-helper cell ($CD4^+CD45RO^+$) population of stimulated PBMCs obtained using the annexin V/ PI apoptosis assay. Average percentage population graphs for the memory T-helper cell population of stimulated PBMCs treated with the IC50 dose of cisplatin, cockle extract and whelk extract (6 µg/ml, 12 µg/ml and 12 µg/ml respectively). Showing the stage of cell death that the cells are in where early= early stages of apoptosis, mid= mid stages of apoptosis, Late= late stages of apoptosis and no apoptosis= no cell death. Using an incubation period of 3 days. Where N=3, error bars show SEM, significance is denoted by *, the absence of * indicates no significance.

The naïve T-helper cell population showed minor increases of 0.04% (p= 0.4226) and 0.06% (p=0.1962) in the populations of cells which were late stage apoptotic or in the mid stages of apoptosis respectively post treatment with cisplatin (figure 4.17). The naïve T-helper cell population which were not undergoing a form of cell death were also decreased by 10.02%, as seen in figure 4.17, p=0.0429. Post cisplatin treatment the population of naïve T-helper cells undergoing early stage apoptosis increased by 9.93% (figure 4.17, p=0.2662).

The cockle extract treatment (figure 4.17) instigated no change to the percentage of naïve T-helper cells undergoing either late stage apoptosis (p= 0.4411) or the mid stages (p=0.1962) of apoptosis. The treatment resulted in an equal 3.48% decrease in naïve T-helper cells which were not undergoing cell death (p=0.0429), to the 3.48% increase in naïve T-helper cells in the early stages of apoptosis (p=0.4732) (figure 4.17). The naïve T-helper cell population

identified no change in the percentage of cells experiencing either late stage apoptosis (p=0.4411) or mid stage apoptosis (p= 0.1962) post whelk extract treatment (figure 4.17). After treatment with the whelk extract there was a 3.78% increase in naïve T-helper cells which were undergoing the early stages of apoptosis (figure 4.17, p=0.1174). Corresponding to this there was a 3.78% drop in the percentage of cells not undergoing cell death (figure 4.17, p=0.0429).

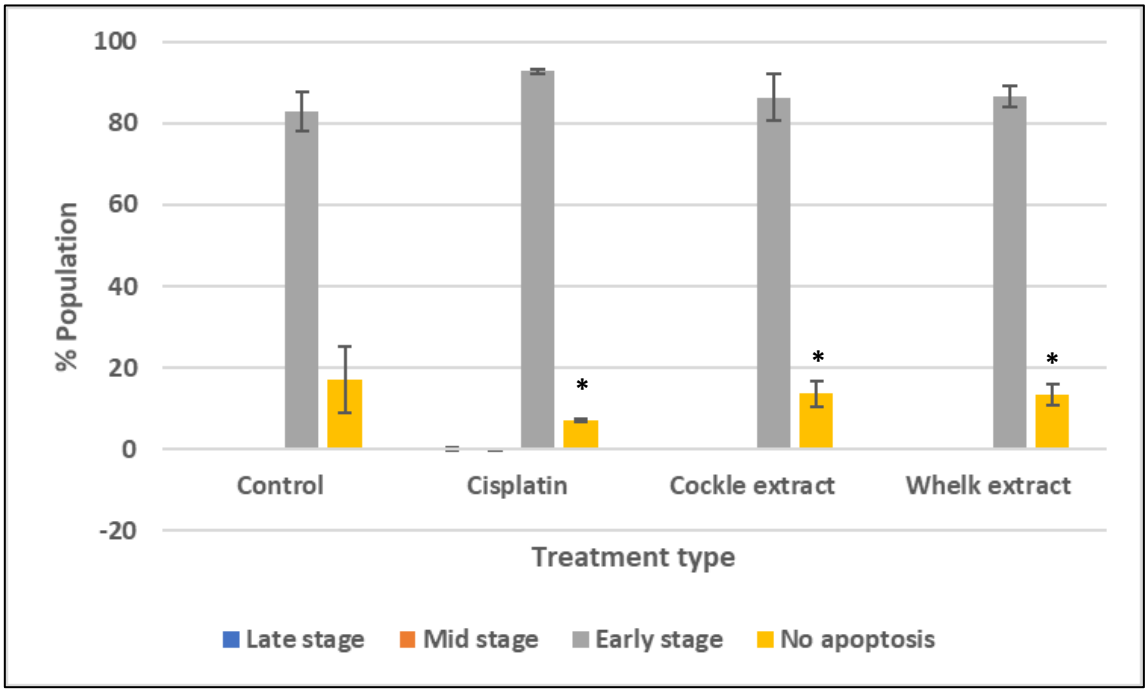

Figure 4.17 Average cell death activity in the naïve T-helper cell ($CD4^{+}CD45RA^{+}$) population of stimulated PBMCs obtained using the annexin V/ PI apoptosis assay. Average percentage population graphs for the naïve T-helper cell population of stimulated PBMCs treated with the IC50 dose of cisplatin, cockle extract and whelk extract (6 µg/ml, 12 µg/ml and 12 µg/ml respectively). Showing the stage of cell death that the cells are in where early= early stages of apoptosis, mid= mid stages of apoptosis, Late= late stage apoptosis and no apoptosis= no cell death. Using an incubation period of 3 days. Where N=3, error bars show SEM, significance is denoted by *, the absence of * indicates no significance.

The memory cytotoxic T-cell population experienced a 2% decline in the number of late stage apoptotic cells (p=0.2432) and a 6.51% decrease in the percentage of cells undergoing mid stage apoptosis (p=0.3835) post cisplatin treatment (figure 4.18). The percentage of memory cytotoxic T-cells which experienced no form of cell death increased by 0.6% (figure 4.18,

p=0.2285) and those in the early stages of apoptosis increased by 7.91% upon treatment with cisplatin (figure 4.18, p=0.0593).

After treatment with the cockle extract (figure 4.18) the memory cytotoxic T-cell population had a 1.74% (p=0.2356) and a 0.57% (p=0.4071) decrease in the percentage of cells undergoing late stage apoptosis and mid stage apoptosis respectively (figure 4.18). Post treatment there was also a 0.9% decrease in the memory cytotoxic T-cells undergoing no form of cell death (p=0.0634). The percentage of memory cytotoxic T-cells in early stage apoptosis increased by 3.21% post cockle extract treatment (figure 4.18, p=0.0445). Upon treatment with the whelk extract (figure 4.18) the memory cytotoxic T-cell population experienced 1.19% (p=0.2649), 0.11% (p=0.4188) and 1.67% (p=0.0171) declines in the percentages of cells undergoing late stage apoptosis, mid stage apoptosis or no cell death respectively (figure 4.18).The memory cytotoxic T-cell population also had a 2.97% increase in cells in the early stages of apoptosis post whelk treatment (p=0.0448).

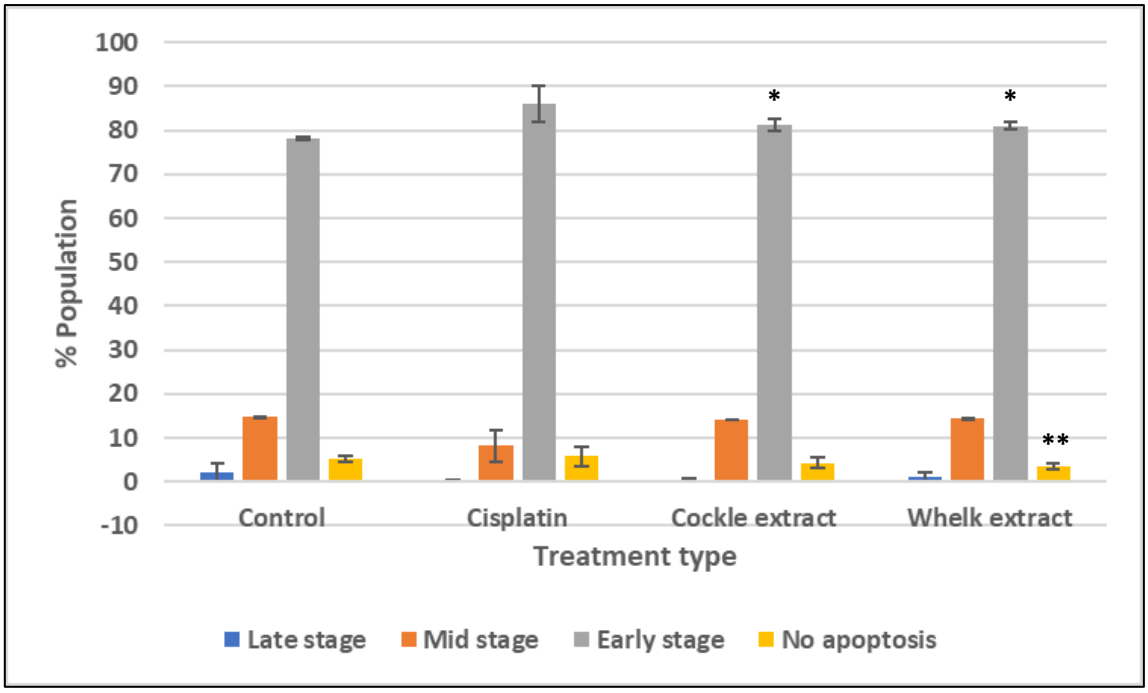

Figure 4.18 Average cell death activity in the memory cytotoxic T-cell ($CD8^{+}CD45RO^{+}$) population of stimulated PBMCs obtained using the annexin V/ PI apoptosis assay. Average percentage population graphs for the memory cytotoxic T-cell population of stimulated PBMCs treated with the IC50 dose of cisplatin, cockle extract and whelk extract (6 µg/ml, 12 µg/ml and 12 µg/ml respectively). Showing the stage of cell death that the cells are in where early= early stages of apoptosis, mid= mid stages of apoptosis, Late= late stages of apoptosis and no apoptosis= no cell death. Using an incubation period of 3 days. Where N=3, error bars show SEM, significance denoted by *, the absence of * indicates no significance.

The naïve cytotoxic T-cell population had a 0.88% (p=0.2619) increase in the percentage of cells not undergoing cell death after cisplatin treatment; this is shown in figure 4.19. The naïve cytotoxic T-cell population also experienced drops in the percentage of cells undergoing both late stage apoptosis (2.2%, p=0.2430) and mid stage apoptosis (5.57%, p=0.3841). The declines were in line with a 6.9% increase in the percentage of naïve cytotoxic T-cells which were experiencing early apoptotic stages which are represented figure 4.19, p=0.0453.

The treatment with the cockle extract (figure 4.19) resulted in 2.05% (p=0.2329) and 0.91% (p=0.3943) decreases in the percentages of naïve cytotoxic T-cells undergoing late stage apoptotic cell death or mid stage apoptosis respectively, this can be seen in figure 4.19. Post treatment with the cockle extract the percentage of cells in early stage apoptosis increased by 3.65% (p=0.0334). Figure 4.19 identifies the naïve cytotoxic T-cell population not

undergoing cell death decreased by 0.7% (p=0.0922) post cockle extract treatment. After treatment with the whelk extract the naïve cytotoxic T-cell population experienced a 1.49% (p=0.2529) and 2.35% (p= 0.0171) decline in the percentage of cells undergoing late stage apoptosis or no cell death respectively (figure 4.19). While the percentages of naïve cytotoxic T-cells undergoing mid stage apoptosis (p= 0.4436) or early stage apoptosis (p=0.0409) increased by 0.68% and 3.16% respectively post whelk extract treatment (figure 4.19).

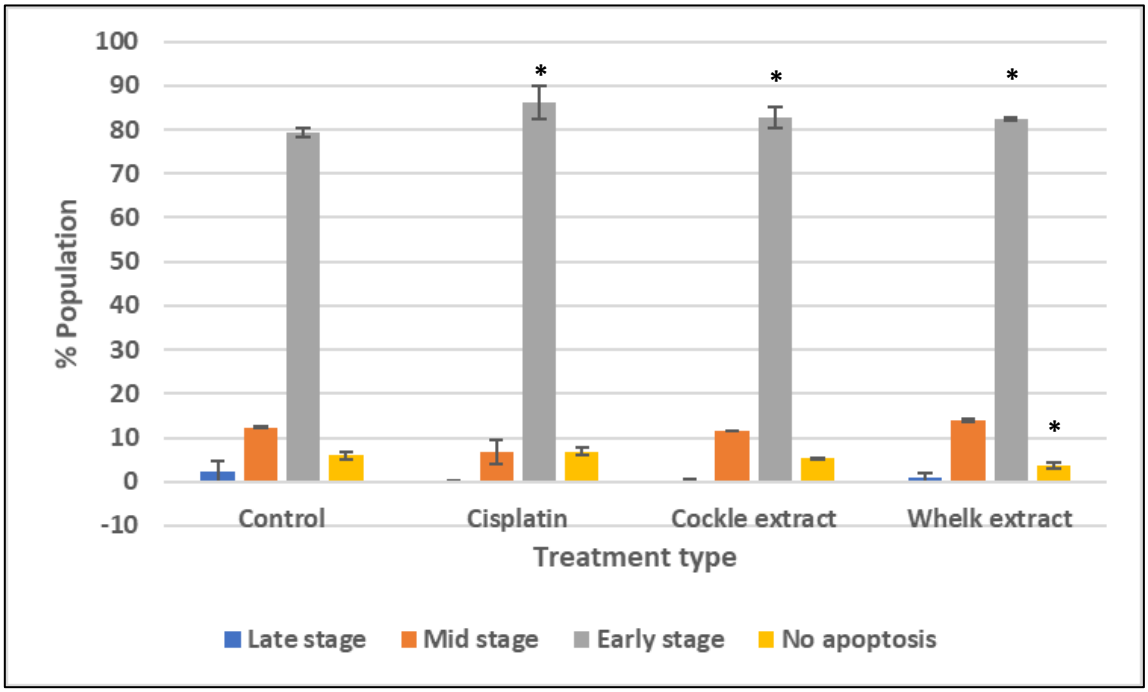

Figure 4.19 Average cell death activity in the naïve cytotoxic T-cell ($CD8^+CD45RA^+$) population of stimulated PBMCs obtained using the annexin V/ PI apoptosis assay. Average percentage population graphs for the naïve cytotoxic T-cell population of stimulated PBMCs treated with the IC50 dose of cisplatin, cockle extract and whelk extract (6 µg/ml, 12 µg/ml and 12 µg/ml respectively). Showing the stage of cell death that the cells are in where early= early stages of apoptosis, mid= mid stages of apoptosis, Late= late stage apoptosis and no apoptosis= no cell death. Using an incubation period of 3 days. Where N=3, error bars show SEM, significance is denoted by *, the absence of * indicates no significance.

Minimal changes in cell death in the lymphocyte population (figure 4.15) occurred which is further reflected in the family populations with small changes in cell death and larger variations in stages indicate that the naturally proliferating cells CD4, CD8, RO and RA populations are not targeted by GAG extract treatments. The whelk extract appeared to exert

the most beneficial effect on the cancer cells while exerting minimal effect on the naïve and activated PBMC populations.

4.3.2 CFSE Proliferation assay results

The CFSE proliferation assays were carried out on the MOLT-4 and U698 cell lines, the K562 cell line was ruled out of subsequent assays at this stage due its nature to aggregate.

4.3.2.1 Cancer cell assays

4.3.2.1.1 MOLT-4 cell line

4.3.2.1.1.1 Entire MOLT-4 population

Figure 4.20 identifies that the whelk extract (yellow bar) treatment reduced proliferation by the largest amount in the entire MOLT-4 population. A reduction of 6.8% in comparison to the control (blue bar), this can also be seen in the blue bar in the control: whelk section of figure 4.21 (p=0.8743). Both the cockle extract (grey bar, figure 4.20) and cisplatin treatment (orange bar, figure 4.20) have increases in proliferation in comparison to the control (blue bar, figure 4.20). This can also be seen in the blue bars in the control: cis (p=0.5) and control: cockle sections (p=0.8743) of figure 4.21. In figure 4.21 it can be seen that the cockle extract treatment increased proliferation in the MOLT-4 cell line by the least amount in comparison to the cisplatin treatment (blue bar, cockle: cis section, p=0.6575).

The results of the CFSE proliferation assay in the entire MOLT-4 cell population further confirm that the whelk extract treatment exerted the most potent effect on the MOLT-4 cell line, as was also seen in both the MTT and annexin V/PI apoptosis assays.

4.3.2.1.1.2 $CD3^+$ MOLT-4 cell population

In figure 4.20 it can be noted that cisplatin had the lowest percentage of proliferation (orange bar, p=0.0704). While the cockle extract had the second lowest proliferation percentage compared to the control (figure 4.20, grey bar, p=0.0424). The whelk extract treatment (yellow bar, figure 4.20, p=0.9576) had the largest percentage proliferation in comparison to the cisplatin (p=0.458) and cockle extract treatment, which can also be seen in the orange bar in figure 4.21.

The results of the $CD3^+$ proliferation assays identify that, although in the annexin V/ PI apoptosis assay the whelk extract exerted the least increase in non-apoptotic cells, the whelk extract results in the largest amount of proliferation in the $CD3^+$ MOLT-4 cells. While the cisplatin treatment in the apoptosis assays resulted in the largest increase in non-apoptotic $CD3^+$MOLT-4 cells, in the CFSE proliferation assay the cisplatin treatment resulted in the least percentage proliferation in the $CD3^+$MOLT-4 cells.

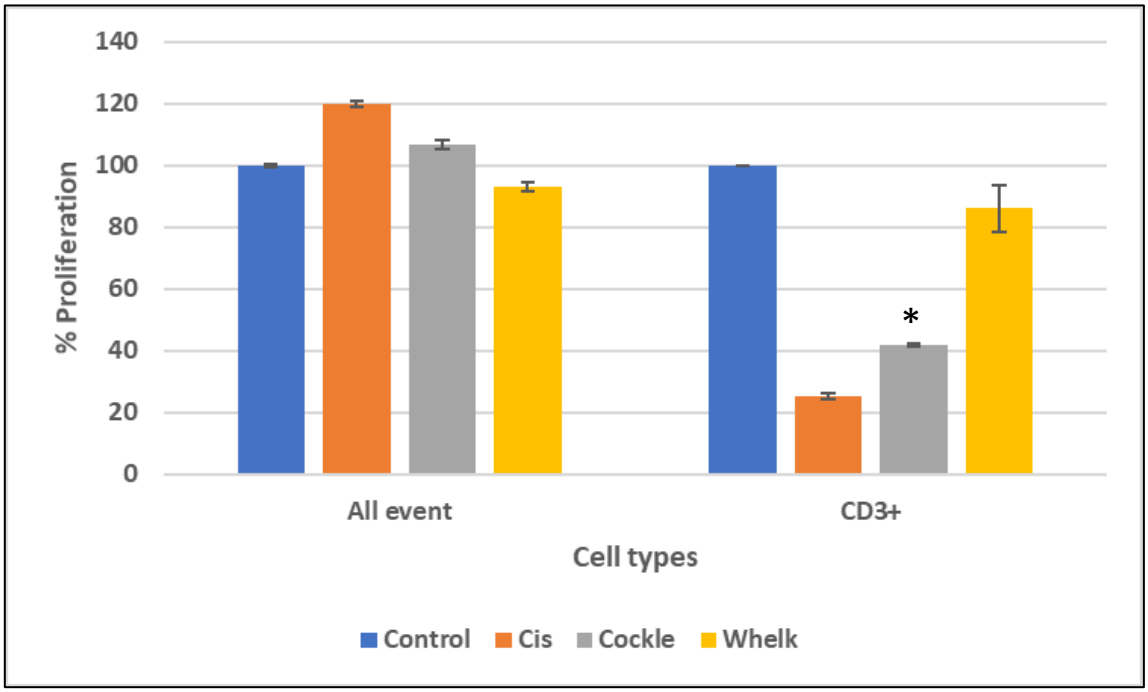

Figure 4.20. Average proliferation in MOLT-4 cells obtained using the CFSE proliferation assay. Average percentage proliferation graph for MOLT-4 cells treated with the IC50 dose of Cisplatin (orange bars), cockle extract (grey bars) and whelk extract (yellow bars) (6 µg/ml, 12 µg/ml and 12 µg/ml respectively). Control/ untreated cells (blue bars) were used as a comparison and were therefore considered to be 100% proliferation. Using an incubation period of 3-days. Where N=2, percentage proliferation was calculated in relation to the untreated cells and error bars show SEM, significance is denoted by *, the absence of * indicates no significance.

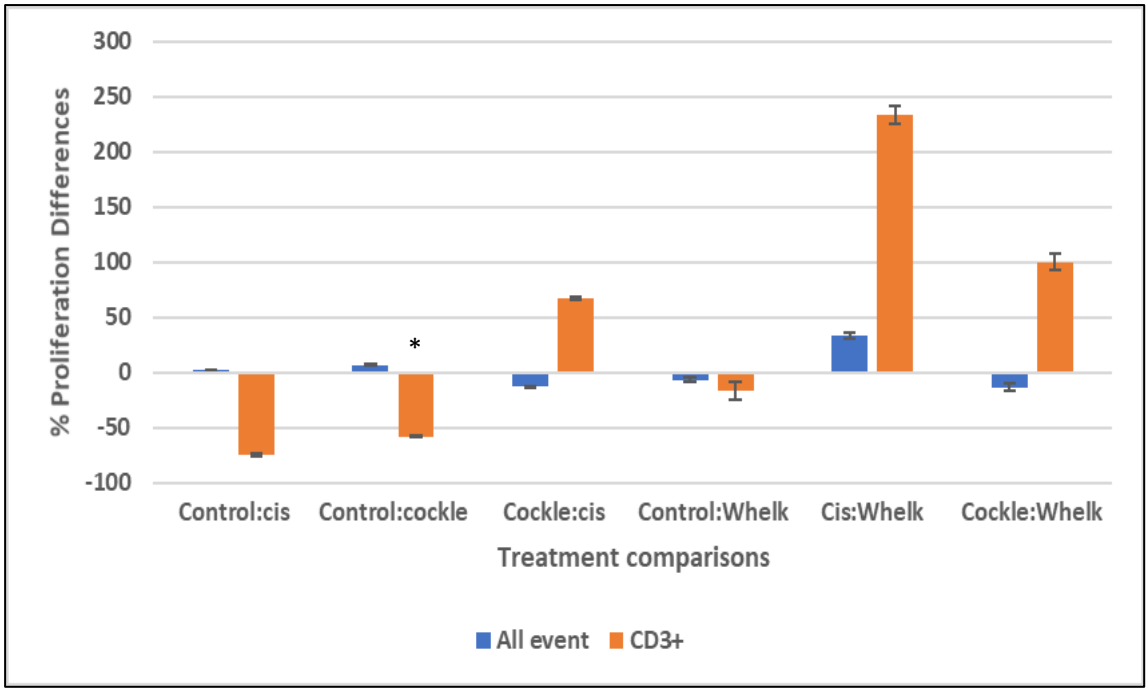

Figure 4.21. Average proliferation differences in MOLT-4 cell line obtained using the CFSE proliferation assay. Average percentage proliferation differences and treatment comparison graph for MOLT-4 cells treated IC50 doses of cisplatin, cockle extract and whelk extract (6 µg/ml, 12 µg/ml and 12 µg/ml respectively). Showing proliferation differences against treatment comparisons between the three treatment types and the untreated control cells. Using an incubation period of 3 days. Where N=2, percentage difference in cells was calculated based on the comparison treatment e.g. where cis: whelk is a comparison of the whelk extract proliferation to the proliferation in cisplatin treated cells, and error bars show SEM, significance is denoted by *, the absence of * indicates no significance.

4.3.2.1.2 U698 cell line

4.3.2.1.2.1 Entire U698 population

Figure 4.22 identifies that cockle extract treated U698 cells had the lowest percentage of proliferation in the entire cell population (grey bar, figure 4.22) in comparison to the control ($p=0.0182$) and the other treatment methods. Figure 4.23 also shows that the cockle extract has the largest percentage difference in proliferation when compared to the other treatment methods and the control (blue bars in control: cockle, cockle: cis, $p=0.3057$, and cockle: whelk sections of figure 4.23). The whelk extract treatment also had a low percentage of proliferation in comparison to the cisplatin treatment ($p=0.3346$) and the control ($p=0.0243$) (figure 4.22, yellow bar) this can also be seen in the control: whelk and cis: whelk sections of figure 4.23 (blue bars). Both the cockle and the whelk extract treatments exhibit less than half the proliferation percentage in the entire U698 population in comparison to cisplatin treatment (orange bar figure 4.22). Cisplatin treatment did however show a decrease in

proliferation in comparison to the untreated cells as can be seen by the orange and blue bars in figure 4.22 respectively and can also be seen in the control: cis section of figure 4.23 (blue bars) (p=0.4455).

4.3.2.1.2.2 $CD19^+$ U698 cell population

As seen in the entire U698 cell population, in the $CD19^+$ population the cockle extract treated cells (grey bar, figure 4.22, p=0.0487) exhibited the lowest level of proliferation. Similar to the entire population the whelk extract treated $CD19^+$ U698 cells (yellow bar, figure 4.22) also had a lower percentage proliferation compared to the control (blue bar figure 4.22, p=0.0487) and cisplatin treated cells (orange bar, figure 4.22, p=0.0706). Cisplatin treated $CD19^+$ U698 cells (orange bar, figure 4.22) did show a very slight reduction in percentage proliferation in comparison to the control (orange bar, control: cis section, figure 4.23, p=0.8986). However, it did have larger levels of proliferation in comparison to both the cockle and whelk extract treated cells as can be seen in figure 4.23 (orange bars, sections cockle: cis and cis: whelk).

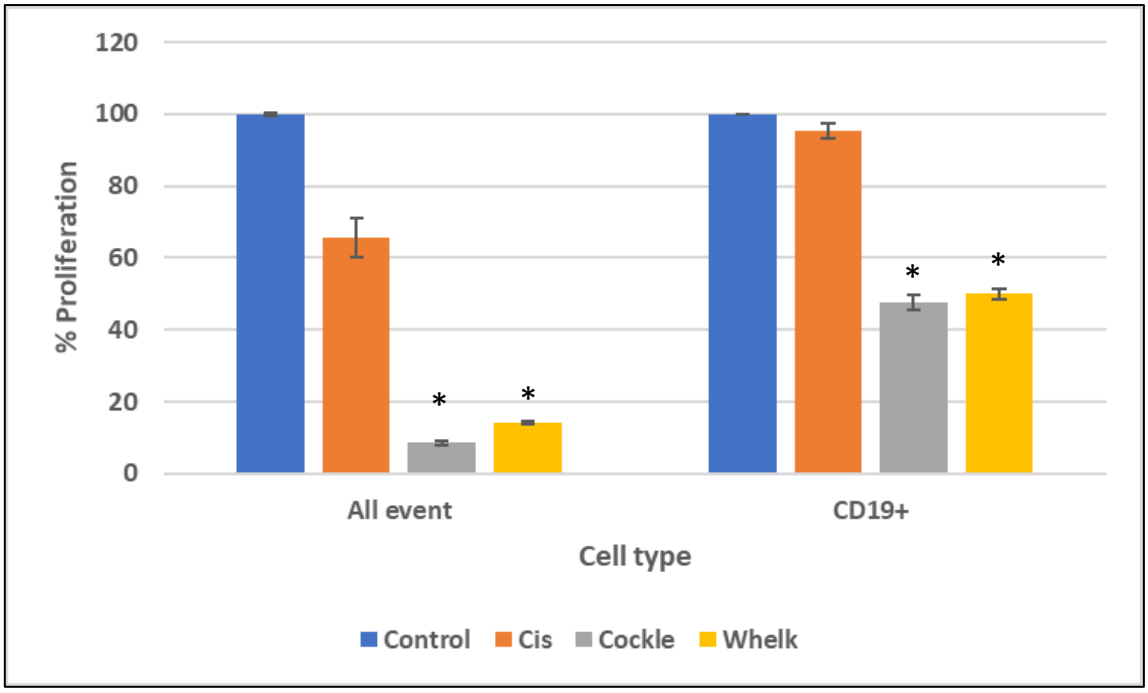

Figure 4.22. Average proliferation in U698 cells obtained using the CFSE proliferation assay. Average percentage proliferation graph for U698 cells treated with the IC50 dose of Cisplatin (orange bars), cockle extract (grey bars) and whelk extract (yellow bars) (6 µg/ml, 12 µg/ml and 12 µg/ml respectively). Control/ untreated cells (blue bars) were used as a comparison and were therefore considered to be 100% proliferation. Using an incubation period of 3-days. Where N=2, percentage proliferation was calculated in relation to the untreated cells and error bars show SEM, significance is denoted by *, the absence of * indicates no significance.

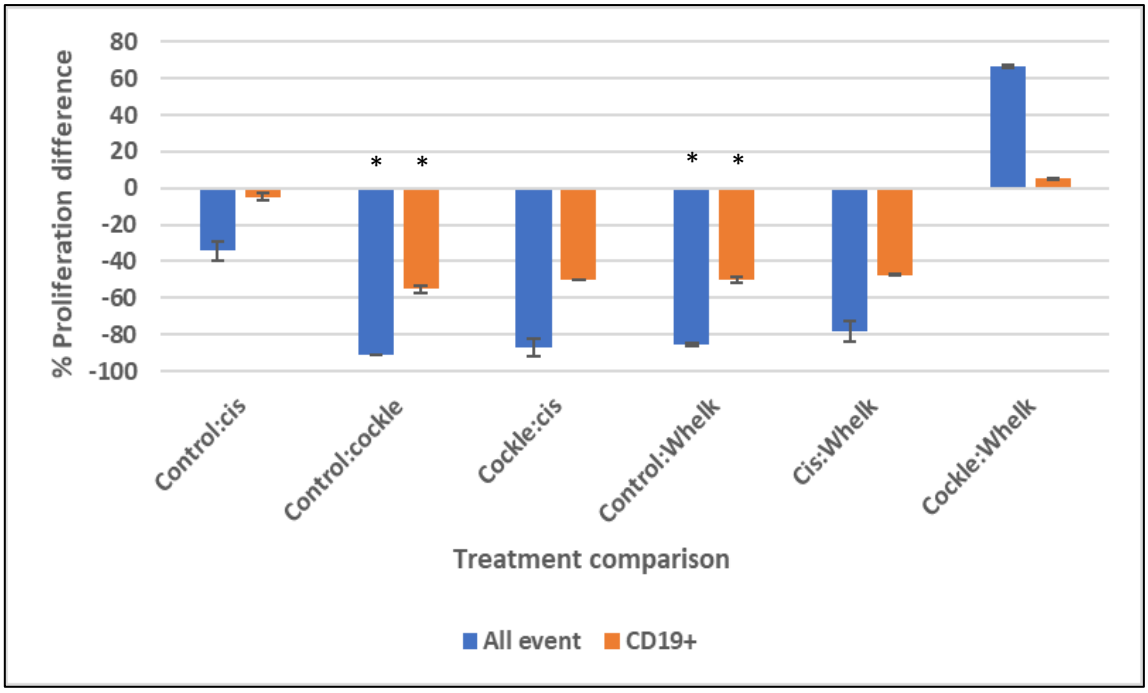

Figure 4.23. Average proliferation differences in U698 cell line obtained using the CFSE proliferation assay. Average percentage proliferation differences and treatment comparison graph for U698 cells treated IC50 doses of cisplatin, cockle extract and whelk extract (6 µg/ml, 12 µg/ml and 12 µg/ml respectively). Showing proliferation differences against treatment comparisons between the three treatment types and the untreated control cells. Using an incubation period of 3 days. Where N=2, percentage difference in cells was calculated based on the comparison treatment e.g. where cis: whelk is a comparison of the whelk extract proliferation to the proliferation in cisplatin treated cells, and error bars show SEM, significance is denoted by *, absence of * indicates no significance.

4.3.2.2 Isolated PBMC assays

4.3.2.2.1 Unstimulated PBMC assays

4.3.2.2.1.1 Entire population

As can be seen in figure 4.24 cisplatin treatment (orange bar) exhibited an increase in proliferation compared to the control/ untreated cells (figure 4.24, blue bar, p=0.3221), this can also be seen in figure 4.25 (mid blue bars, cockle: cis, cis: whelk sections). There are decreases in proliferation percentage in the all event populations when cockle extract treatment (p=0.0626) and whelk extract (p=0.9985) treatment are compared to cisplatin treatment. The whelk extract treatment (yellow bar, figure 4.24) does not have any change in proliferation in comparison to the control (blue bar, figure 4.24). This can also be seen by the lack of mid colour blue bar in the control: whelk section of figure 4.25, p=0.3251. Cockle

extract treatment (grey bar, figure 4.24) had a slight reduction in proliferation percentage in comparison to the control/untreated cells. This can also be seen through the mid blue colour bar in the control: cockle section of figure 4.25, p=0.0626.

4.3.2.2.1.2 Lymphocyte population

Figure 4.24 identifies that the cockle extract treatment (grey bar, p=0.5) and whelk extract treatment (yellow bar, p=0.5) result in slight increases in proliferation percentage of lymphocytes post treatment. This can be seen also in figure 4.25 (orange bars). All comparisons for the cockle extract against the control, cisplatin treatment and whelk extract treatment show increases in proliferation (orange bars, figure 4.25). While the whelk extract has increases in proliferation in comparison to the control or cisplatin (p=0.5) treated cells but slight decrease in proliferation when compared to the cockle extract treatment (orange bars, figure 4.25). The cockle extract exerted the largest percentage of proliferation in the unstimulated lymphocytes as seen in figure 4.24. Figure 4.24 shows cisplatin treatment (orange bar, p=>0.05) had a similar level of proliferation compared to the control (blue bar). This is supported by the lack of orange bar in the control: cis section of figure 4.25.

4.3.2.2.1.3 $CD4^+$/ T-helper cells

In the T-helper cell population the whelk extract, p=0.4226, increased proliferation by around 50% as can be seen by the yellow bar in figure 4.24. This is also seen in figure 4.25, by the grey bar in section control: whelk. Cisplatin treatment (p=0.4226) (orange bar, figure 4.24) and cockle extract treatment (p=0.4226) (grey bar, figure 4.24) increased proliferation in the T-helper cell population by the same amount. This can also be demonstrated by the lack of grey bar in figure 4.25 in the comparison of the cockle extract and the cisplatin treatment (cockle: cis, p=>0.9999).

4.3.2.2.1.3.1 $CD4^+CD45RA^+$/ Naïve T-helper cells

In the naïve T-helper cell populations the cockle extract treatment increased proliferation by 150% in comparison to the control (p=0.0152), this can be seen by the grey bar in figure 4.24. Also, this is identified in figure 4.25 by the yellow bar in the comparison of the cockle extract to the control (control: cockle) section. Whelk extract treatment (yellow bar, figure 4.24) increased proliferation in comparison to the control (blue bar, figure 4.24) by 50%. This is also

noted by the yellow bar in the comparison of the whelk extract to the control section in figure 4.25 (control: whelk) (p=0.2959). Figures 4.25 and 4.26 also identify that cisplatin treatment increased proliferation in the naïve T-helper cell population (orange bar, figure 4.24 and yellow bar, control: cis, figure 4.25, p=0.4226). However, cisplatin treatment increased proliferation by less than the increases of those cells treated with either the cockle extract or the whelk extract (cockle: cis (p=0.0257) and cis: whelk (p=0.3702) sections of figure 4.25, yellow bars).

4.3.2.2.1.3.2 $CD4^+CD45RO^+$/ Memory T-helper cells

In the memory T-helper cell population there were small differences between the treatment types and the control (blue bar, figure 4.24). The cisplatin treatment (orange bar figure 4.24) increased proliferation by the most in the memory T-helper cell population (light blue bars, control: cis, p=0.6209, cockle: cis and cis: whelk sections) as can be seen in figure 4.25. The whelk extract also had a slight increase in proliferation in the memory T-helper cell population in comparison to the control (yellow bar, figure 4.24). This can also be seen in the light blue bar in the control: whelk section of figure 4.25, p=0.9468. Post cockle extract treatment (grey bar, figure 4.24) there was no difference in proliferation percentage in the memory T-helper cell population in comparison to the untreated control cells (blue bar, figure 4.24). This is also seen through the lack of light blue bar in figure 4.25, section: control: cockle, p=>0.05.

4.3.2.2.1.4 $CD8^+$ cytotoxic T-cells

Figure 4.24 identifies that the cockle extract (grey bar) (p=0.0341) had the largest percentage proliferation in cytotoxic T-cells in comparison to the control (blue bar), cisplatin treatment (orange bar) (p=0.6209) and whelk extract treatment (yellow bar), this can also be seen in the green bars in figure 4.25. Whelk extract treatment (yellow bar, figure 4.24) also had approximately 150% more proliferation in comparison to the control (blue bar, figure 4.24), seen also in the green bars (section: control: whelk, p=0.0228) in figure 4.25. Cisplatin treatment (orange bars, figure 4.24) also had an increase in percentage of proliferation in the cytotoxic T-cell population in comparison to the control (blue bars, figure 4.24). This was also seen in figure 4.25 in the section comparing cisplatin treatment to the untreated control cells (control: cis, green bar, p=0.0343).

4.3.2.2.1.4.1 $CD8^+CD45RA^+$/ Naïve cytotoxic T-cells

In the naïve cytotoxic T-cells the cockle extract had the largest percentage proliferation as can be seen by the grey bar in figure 4.24. This was around a 175% increase in proliferation in comparison to the control (dark blue bar, figure 4.25, section: control: cockle, p=0.0194). Whelk extract treatment also brought about around 200% proliferation in the naïve cytotoxic T-cell population (yellow bar, figure 4.24). This is around a 100% increase in naïve cytotoxic T-cells in comparison to the control sample as can be seen by the dark blue bar in figure 4.25 (section control: whelk, p=0.059). Cisplatin treatment brought about the smallest increase in proliferation in the naïve cytotoxic T-cells as can be seen by the dark blue bars in figure 4.25, p=0.0544. Cisplatin treatment did however have a larger percentage proliferation in the naïve cytotoxic T-cell population than the untreated control cells as can be seen by the orange bar in figure 4.24.

4.3.2.2.1.4.2 $CD8^+CD45RO^+$/ Memory cytotoxic T-cells

In the memory cytotoxic T-cell population there were very little changes in proliferation post treatment with either cisplatin (p=0.3800), whelk extract (p=0.4263) or cockle extract (p=0.7482). Whelk extract treatment and cisplatin treatment (yellow bar and orange bar respectively, figure 4.24) both had larger percentages of proliferation in comparison to the control (blue bar, figure 4.24). There was no difference between the percentage of proliferation in the memory cytotoxic T-cell population post whelk extract treatment and post cisplatin treatment, as can be seen in figure 4.25 by the lack of red bar in the comparison of cisplatin treatment to whelk extract treatment (cis: whelk, p=0.9462). Cockle extract treatment brought about no change in proliferation compared to the control which can be seen by the lack of red bar in figure 4.25, section control: cockle, p=0.7482 Therefore, there was still 100% proliferation in the memory cytotoxic T-cells treated with the cockle extract (grey bar, figure 4.24).

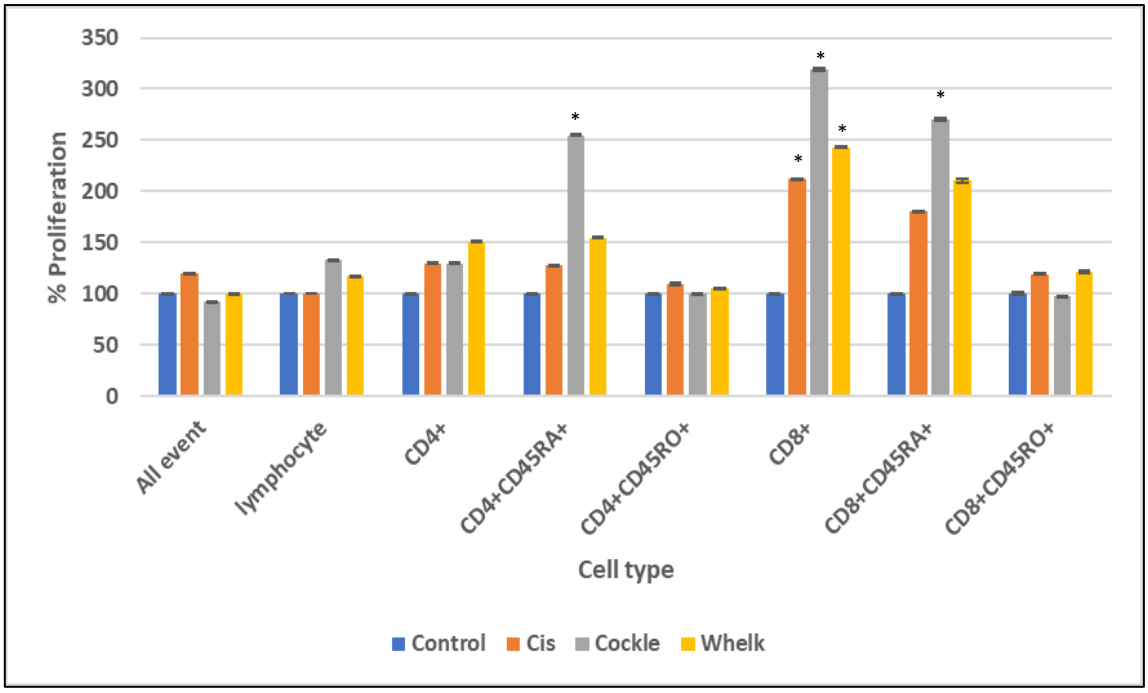

Figure 4.24. Average proliferation in unstimulated PBMCs obtained using the CFSE proliferation assay. Average percentage proliferation graph for unstimulated PBMCs treated with the IC50 dose of Cisplatin (orange bars), cockle extract (grey bars) and whelk extract (yellow bars) (6 µg/ml, 12 µg/ml and 12 µg/ml respectively). Control/ untreated cells (blue bars) were used as a comparison and were therefore considered to be 100% proliferation. Using an incubation period of 3-days. Where N=3, percentage proliferation was calculated in relation to the untreated cells and error bars show SEM, significance is denoted by *, absence of * indicates no significance.

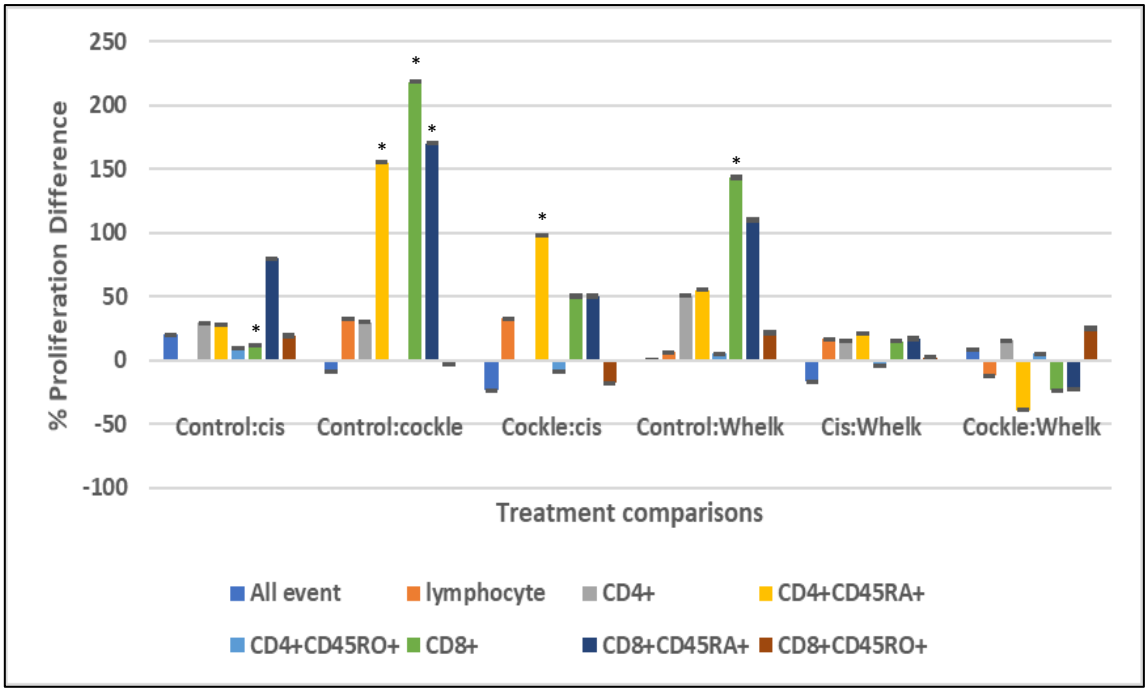

Figure 4.25. Average proliferation differences in unstimulated PBMCs obtained using CFSE proliferation assay. Average percentage proliferation differences and treatment comparison graph for unstimulated PBMCs treated IC50 doses of cisplatin, cockle extract and whelk extract (6 µg/ml, 12 µg/ml and 12 µg/ml respectively). Showing proliferation differences against treatment comparisons between the three treatment types and the untreated control cells. Using an incubation period of 3 days. Where N=3, percentage difference in cells was calculated based on the comparison treatment e.g. where cis: whelk is a comparison of the whelk extract proliferation to the proliferation in cisplatin treated cells, and error bars show SEM, significance is denoted by *, absence of * indicates no significance.

4.3.2.2.2 Stimulated PBMC assays

4.3.2.2.2.1 Entire population

In the entire stimulated PBMC population the whelk extract (yellow bar) treatment had the most percentage proliferation in comparison to cisplatin (orange bar) and cockle extract treatment (grey bar) as can be seen in figure 4.26. In comparison to the control as can be seen in the control: cis (p=0.1057), control: cockle (p=0.1258) and control: whelk (p=0.7155) sections of figure 4.27 (mid blue bars). Whelk extract treatment reduced proliferation the least in comparison to the control. Cockle extract treated (grey bars) cells had the next highest levels of proliferation in comparison to other treatment methods (figure 4.26). this can also be seen in figure 4.27 in the sections control: cockle and cockle: cis (p=0.3345) (mid blue bars). Cisplatin treatment reduced the proliferation in the entire stimulated PBMC population by

the most in comparison to other treatment methods and the control (figure 4.26, orange bar and figure 4.27 sections control: cis, cockle: cis and cis: whelk (p=0.4067), mid blue bars).

4.3.2.2.2.2 Lymphocyte population

In the lymphocyte population cisplatin treated cells had the largest percentage proliferation (orange bar, figure 4.26) in comparison to the other treatments and the control (orange bars, figure 4.27, p=0.0065). The whelk extract treatment also brought about more proliferation (yellow bar, figure 4.26) in comparison to the control and cockle extract treatment (figure 4.27, orange bars, sections: control: whelk, p=0.5718 and cockle: whelk). Cockle extract treatment (grey bar, figure 4.26) also exhibited a larger proliferation percentage than the control (blue bar, figure 4.26). However, cockle extract treatment increased proliferation in the lymphocyte population by the least amount as seen in figure 4.27 sections: control: cockle (p=0.6983), cockle: cis (p=0.2733) and cockle: whelk (orange bars).

4.3.2.2.2.3 $CD4^+$/ T-helper cells

In the T-helper cell population the treatment with the whelk extract (yellow bar, figure 4.26) had the largest percentage proliferation in comparison to the other treatment methods. Whelk extract treatment also had the least reduction in proliferation in comparison to the control (figure 4.27, grey bar, section: control: whelk, p=0.5997). Cisplatin treatment (orange bar, figure 4.26) had a reduced level of proliferation in the T-helper cell population in comparison to the control and whelk extract treatment (figure 4.27, grey bars, sections: control: cis, p=0.0383 and cis: whelk, p=0.957). The cockle extract treatment reduced the percentage proliferation in the T-helper cell population by the most in comparison to the other treatments and the control (figure 4.27, control: cockle, p=0.3095, cockle: cis, p=0.6283 and cockle: whelk sections, grey bars). The cockle extract treated T-helper cells had the lowest percentage proliferation (grey bars, figure 4.26).

4.3.2.2.2.3.1 $CD4^+CD45RA^+$/ Naïve T-helper cells

In the naïve T-helper cells the whelk extract treated cells had the largest percentage proliferation (yellow bar, figure 4.26). Whelk extract treatment increased proliferation in the naïve T-helper cells in comparison to the control and cisplatin and cockle extract treated cells (figure 4.27, sections: control: whelk, p=0.0384, cockle: whelk and cis: whelk, p=0.3957,

yellow bars). Cisplatin treatment had the smallest reduction in proliferation in the naïve T-helper cells (orange bar, figure 4.26) in comparison to the control and cockle extract treated cells (figure 4.27, yellow bars, sections: control: cis, p=0.6738, cockle: cis, p=0.6638). The cockle extract treated cells had the largest decrease in proliferation in the naïve T-helper cells (grey bar, figure 4.26) as can be seen in figure 4.27 (yellow bars, sections: control: cockle, p=0.948, cockle: cis, cockle: whelk).

4.3.2.2.2.3.2 $CD4^+CD45RO^+$/ memory T-helper cells

In the memory T-helper cell population the whelk extract treatment had the most percentage proliferation in comparison to the other treatments (yellow bar, figure 4.26). The whelk extract treatment reduced the proliferation percentage in the memory T-helper cells in comparison to the control cells, cisplatin treated and cockle extract treated cells (figure 4.27, light blue bars, sections: control: whelk, p=0.503, cis: whelk, p=0.7794 and cockle: whelk). Cisplatin treatment (orange bars, figure 4.26) resulted in a decrease in memory T-helper cell population in comparison to the control and whelk extract treatment (figure 4.27, sections: control: cis, p=0.2399 and cis: whelk, p=0.7794). Cockle extract treatment brought about the largest decrease in memory T-helper cells (grey bar, figure 4.26) in comparison to the control and other treatment methods. This can also be seen in figure 4.27 in the light blue bars (sections: control: cockle, p=0.2399, cockle: cis, p=0.4974 and cockle: whelk).

4.3.2.2.2.4 $CD8^+$/ cytotoxic T-cells

In the cytotoxic T-cell population cisplatin treated cells (orange bar, figure 4.26) had the same percentage proliferation as the control (blue bar, figure 4.26). This can be seen through the lack of green bar in the control: cis section in figure 4.27, p=0.8609. The whelk extract treatment resulted in a decrease in proliferation (yellow bar, figure 4.26) in comparison to the control and cisplatin treatment. This can be seen in the green bars in the comparison sections control: whelk, p=0.3248 and cis: whelk, p=0.4738 of figure 4.27. Cockle extract treated cytotoxic T-cells experienced the least percentage proliferation as seen by the grey bar in figure 4.26. The decrease in proliferation post cockle extract treatment in cytotoxic T-cells was the largest in comparison to the control and cisplatin and whelk extract treatments (figure 4.27, green bars, sections: control: cockle, p=0.0068, cockle: cis, p=0.1475 and cockle: whelk).

4.3.2.2.2.4.1 $CD8^+CD45RA^+$/ naïve cytotoxic T-cells

Figure 4.26 demonstrates that in the naïve cytotoxic T-cells both cisplatin treatment (orange bar) and whelk extract treatment (yellow bar) resulted in higher levels of proliferation than the control (blue bar). Cisplatin had the most increase in proliferation in comparison to the control cells and whelk extract treated cells (dark blue bars, sections: control: cis, p=0.0435, cis: whelk, p=0.3101, figure 4.27). In figure 4.27 it can be seen that whelk extract treatment increased proliferation in naïve cytotoxic T-cells in comparison to the control (dark blue bars, control: whelk, p=0.4226). It can also be seen that whelk extract treatment did not increase naïve cytotoxic T-cell proliferation more than cisplatin treatment (dark blue bar, cis: whelk figure 4.27). Cockle extract treatment (grey bar, figure 4.26) had the lowest percentage proliferation in the naïve cytotoxic T-cells. This can also be seen in the dark blue bars in figure 4.26 (sections: control: cockle, p=0.1966, cockle: cis, p=0.0845 and cockle: whelk).

4.3.2.2.2.4.2 $CD8^+CD45RO^+$/ memory cytotoxic T-cells

In the memory cytotoxic T-cells cisplatin treatment brought about the largest percentage proliferation (figure 4.26, orange bar), also an increase in proliferation in comparison to the control, cockle extract and whelk extract treated cells (figure 4.27, red bars, sections: control: cis, p=0.1828, cockle: cis, p=0.5163 and cis: whelk, p=0.9462). Cockle and whelk extract treatments brought about the same level of proliferation (grey and yellow bars respectively, figure 4.26). Figure 4.27 identifies that the cockle (p=0.1563) and whelk extract (p=0.3708) treated memory cytotoxic T-cells experienced a decrease in proliferation in comparison to the control and cisplatin treatments (red bars).

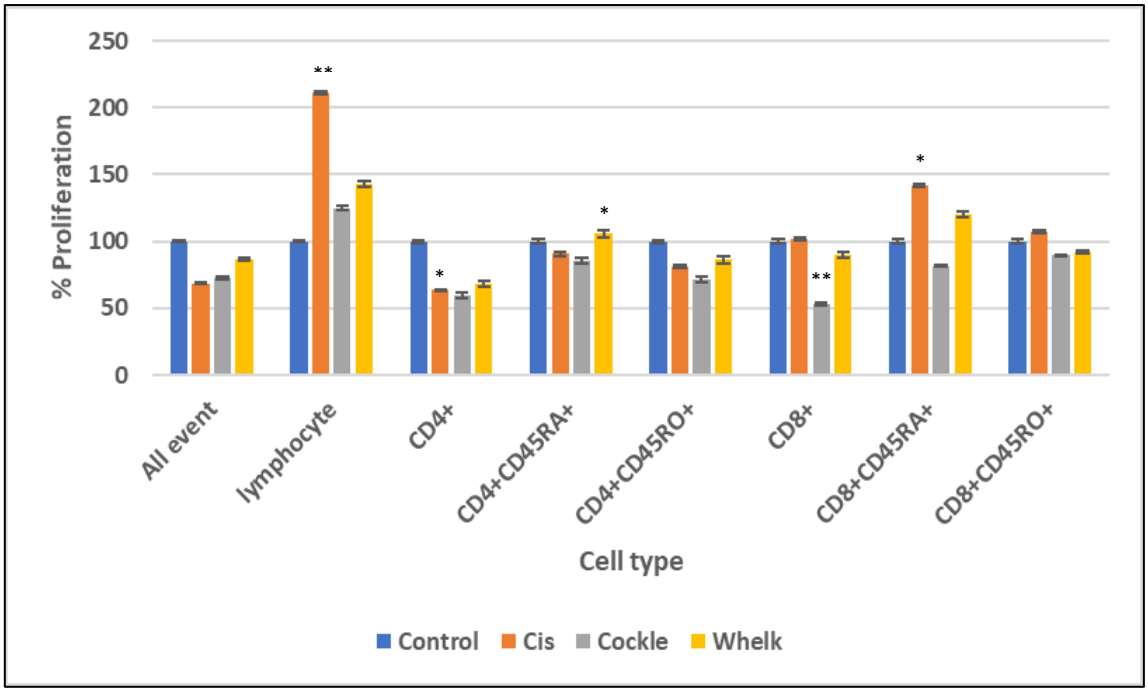

Figure 4.26. Average proliferation in stimulated PBMCs obtained using the CFSE proliferation assay. Average percentage proliferation graph for stimulated PBMCs treated with the IC50 dose of Cisplatin (orange bars), cockle extract (grey bars) and whelk extract (yellow bars) (6 µg/ml, 12 µg/ml and 12 µg/ml respectively). Control/ untreated cells (blue bars) were used as a comparison and were therefore considered to be 100% proliferation. Using an incubation period of 3-days. Where N=3, percentage proliferation was calculated in relation to the untreated cells and error bars show SEM, significance is denoted by *, absence of * indicates no significance.

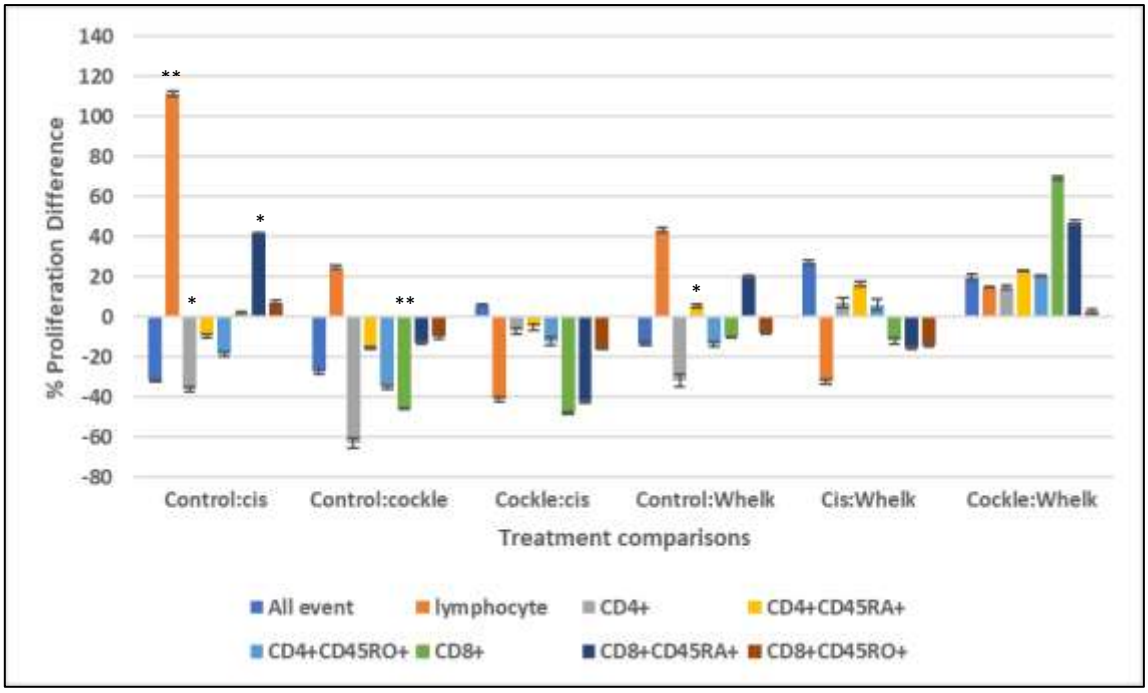

Figure 4.27. Average proliferation differences in stimulated PBMCs obtained using the CFSE proliferation assay. Average percentage proliferation differences and treatment comparison graph for stimulated PBMCs treated IC50 doses of cisplatin, cockle extract and whelk extract (6 µg/ml, 12 µg/ml and 12 µg/ml respectively). Showing proliferation differences against treatment comparisons between the three treatment types and the untreated control cells. Using an incubation period of 3 days. Where N=3, percentage difference in cells was calculated based on the comparison treatment e.g. where cis: whelk is a comparison of the whelk extract proliferation to the proliferation in cisplatin treated cells, and error bars show SEM, significance is denoted by *, absence of * indicates no significance.

4.4 Discussion

4.4.1 Annexin V/ propidium iodide apoptosis assay

4.4.1.1 Annexin V/ propidium iodide apoptosis assay results key findings

- Cockle and whelk extracts exert significant cell death induction in both the MOLT-4 and U698 cell lines.
- Whelk extract treatment effects were consistently milder in naïve PBMC cellular family populations in comparison to treatment with the cockle extract and treatment with cisplatin.
- Stimulated PBMCs treated with the whelk extract exerted little effect on T-helper cell populations but induced more cell death in the cytotoxic T-cell populations in comparison to treatment with cisplatin.
- Treatment with the cockle extract in stimulated PBMCs exerted less of an effect on the cytotoxic T-cell populations compared to treatment with either the whelk extract or cisplatin.

4.4.1.2 Discussion

Apoptosis is a molecular target for new anti-cancer therapies, as during cancer the balance of cellular proliferation and apoptosis shifts towards proliferation (Wesselborg et al., 1999). Therefore the search for the most efficient anti-cancer treatment with the least side effects, which targets apoptosis, is ever pressing (Coppola et al., 2008). Apoptosis has a vital protective mechanism against cancer (Zhou et al., 2009). Apoptosis can be characterised by cell shrinkage, nuclear chromatin condensation and nuclear and apoptotic body fragmentation (Kroemer et al., 1997). Apoptosis can also be characterised by membrane damage which leads to the subsequent leakage of phosphatidylserine into the outer membrane layers of cells. Annexin V is a recombinant phosphatidylserine-binding protein that specifically and strongly binds to phosphatidylserine residues (Cornelissen et al., 2002; Vermes et al., 1995).

This research identified that both the cockle and whelk extracts exerted significant inductions of apoptosis in the MOLT-4 cell line, with the largest increases being in the early stages of apoptosis ($p= 0.0179$ and $p= 0.003$ respectively) (figure 4.5). In the $CD3^+$ MOLT-4 cells the both the whelk and the cockle extract resulted in an increase in non-apoptotic cells, with the

cockle extract increase in early apoptotic $CD3^+$ MOLT-4 cells being significant (p= 0.0478) (figure 4.6). In the K562 cells both the cockle and whelk extracts resulted in non-significant rises in the percentage of non-apoptotic cells (figure 4.7). With the whelk extracts resulting in significant decreases in the percentage of early (p= 0.022), mid (p= 0.0292) and late (p= 0.0497) apoptotic cells. In the U698 cells the whelk extract resulted in significant increases in the induction of apoptosis (p= 0.0426), particularly with the mid stage apoptosis increases (p= 0.0165) (figure 4.8). The cockle extract also resulted in an increase in apoptotic U698 cells, but this was not a significant increase. There were also reductions in the percentage of $CD19^+$ U698 cells which were non-apoptotic post treatment with both the cockle and whelk extracts, these were not significant (figure 4.9).

The results from this research correspond to the results obtained in the MTT assay, with the whelk extract exerting a significant and profound effect on both the MOLT-4 and U698 cell lines, which was more effective than those noted in cisplatin treated cells. Ogundipe (2015) identified marginal induction of early apoptosis in the MOLT-4 cell line post treatment with the whelk extract, which was also demonstrated in this research. Aldairi, Ogundipe and Pye (2018) also noted a significant induction of apoptosis in the MOLT-4 cell line and a small but significant increase in the percentage of late apoptotic cells post treatment with the cockle extract, which was also independently confirmed by this research lab.

In the unstimulated PBMC assays (figures 4.10- 4.14) the whelk extract consistently exerted the mildest effect on the lymphocyte populations and the T-helper and cytotoxic T-cell subpopulations (naïve and memory). Although cytotoxic T-cell populations appeared to be more affected by the treatment with the whelk extract by the most, with a significant increase in the percentage of early stage apoptotic memory cytotoxic T- cells (p= 0.0379). The cockle extract treated unstimulated PBMCs exerted little effect on the lymphocytes and T-helper cell populations. However the cockle extract also induced more cell death in the cytotoxic T-cell populations with a significant decrease in the memory cytotoxic T-cell populations (p= 0.0399). In the stimulated PBMC assays (figures 4.15- 4.19) the T-helper cell subpopulations remained mainly unaffected by treatment with the whelk extract, with a significant increase in the percentage of naïve T-helper cell death (p= 0.0429). In the lymphocyte and cytotoxic T-cell populations the whelk extract resulted in more induction of apoptosis than the treatment with cisplatin, with significant increases in the percentage of early stage apoptotic memory

and naïve cytotoxic T-cells (p= 0.0448 and p= 0.0409 respectively). The cockle extract treatment resulted in the least induction of cell death overall the stimulated PBMC populations. In the cytotoxic T-cell populations the cockle extract resulted in the mildest induction of apoptosis. In the unstimulated PBMC assays the whelk extract proved to be consistently milder than the cockle and cisplatin treatments. This could suggest that the whelk extract may be acting in a selective manner towards the cancer cell lines whilst not targeting healthy lymphocytes, as was also suggested by the MTT assay results, which could suggest that the novel GAG extracts could provide a more favourable therapeutic treatment option. In the stimulated PBMC assays the whelk extract appeared to be targeting the cytotoxic T-cell populations more than the other treatment methods. The increased activity against the $CD8^+$ cells may potentially blunt any immune responses to viral infections during chemotherapy treatment. Despite these observations, relative changes compared to the potency towards cancer cell lines suggests that the novel marine mollusc derived GAG extracts could provide a treatment option that shows some specificity towards tumour cells whilst not targeting healthy lymphocytes. It is encouraging to note that the novel GAG compounds may be acting in a more specific manner and may consequently exert fewer side effects for the patient.

4.4.2 CFSE proliferation assay

4.4.2.1 CFSE proliferation assay results key findings

- Treatment with both the cockle and whelk extracts exerted significant antiproliferative effects in both the MOLT-4 and U698 cell lines.
- In the unstimulated PBMC assays the cockle and whelk extract treatments appeared to exert proliferative effects on some subpopulations of T-helper cells and cytotoxic T-cells.
- In the stimulated PBMC assays there were some antiproliferative effects noted in some of the subpopulations of T-helper cells and cytotoxic T-cells post treatment with the cockle and whelk GAG extracts.

4.4.2.2 Discussion

In recent years the analysis of cell cycle had been used in order to identify a molecular target for new anti-cancer therapies (Ogundipe, 2015; Basappa et al., 2012). As cellular proliferation

is primarily mediated by via the cell cycle, which consists of four stages; G0/G1, S, G2 and M (Yang, 2012). Each stage of the cell cycle is controlled by various cellular signalling mechanisms which have varying levels of expression depending on the stage of the cell cycle (Roos and Kaina, 2006; Schafer, 1998). There are several therapeutic agents which aim to target various points in the cell cycle such as the regulation of checkpoints, this ultimately leads to the arrest of cellular proliferation or the induction of apoptosis in cancer cells (Schafer, 1998). Rapid cellular proliferation is a major factor in describing cancer and there is now evidence to identify that GAGs and proteoglycans play a role in the control of cellular proliferation (Yip, Smollich and Gotte, 2006). Changes in GAG structure such as heparan sulphate on the surface of tumour cells appears to modulate the effects that they exert on the cells, through the regulation of growth factor signalling, metastasis and cellular proliferation (Liu et al., 2002).

The CFSE assay is designed to monitor cellular activity for long periods of times and can detect cell death with increased insensitivity (Jedema et al., 2004). Mitosis is the process of the parent cell splitting into two daughter cells, therefore the fluorescence of CFSE halves during the process of mitosis and allows the monitoring of the number of times the cell goes through proliferation (Quah and Parish, 2010).

In the MOLT-4 cell line assays (figures 4.20 and 4.21) the whelk extract was the only treatment to reduced proliferation in the cell line however the reduction was not significant. Treatment with the cockle extract exerted a non-significant increase in the proliferation of the MOLT-4 cell line. In the $CD3^+$ MOLT-4 population both the cockle and whelk extracts reduced the level of proliferation in the population, with the cockle extract treatment reducing the proliferation level significantly ($p= 0.0424$). Treatment with both the cockle and whelk extracts significantly reduced the proliferation in the U698 cell line ($p= 0.0182$ and $p= 0.0243$ respectively). Both treatment with the cockle and whelk extracts had less than half the proliferation in the U698 cell line than the proliferation in cisplatin treated cells (figure 4.22 and 4.23). In the $CD19^+$ U698 cell population, as with the entire U698 cell population, both the cockle and whelk treatments both reduced the proliferation significantly ($p= 0.0487$ and $p= 0.0487$ respectively).

In the unstimulated PBMC assays (figures 4.24 and 4.25) both the cockle and whelk extracts increased the level of proliferation in the lymphocyte and T-helper cell populations, with the

cockle extract significantly increasing the level of proliferation in the naïve T-helper cell populations (p= 0.0152). In the cytotoxic T-cell populations of the unstimulated PBMCs both the cockle and whelk extract significantly increased the percentage of proliferation in the total cytotoxic T-cell population (p= 0.0341 and p= 0.0228 respectively). In the naïve cytotoxic T-cell population the cockle extract significantly increased the proliferation (p= 0.0194). In the stimulated PBMC assays (figures 4.26 and 4.27) the whelk extract exerted small decreases in the proliferation of the lymphocyte and T-helper cell and cytotoxic T-cell populations. The decrease in proliferation noted in the naïve T-helper cell population was significant (p= 0.0384). In all the cytotoxic T-cell populations the whelk extract resulted small decreases in the proliferation percentage, all of which were non-significant. The cockle extract treated stimulated PBMCs experienced the largest decrease in proliferation in all the T-helper cell populations and in the cytotoxic T-cell populations, all the decreases in proliferation were non-significant.

The results of the proliferation assay demonstrated that the whelk extract exerted a significant effect on both the MOLT-4 and U698 cell lines; whilst also exerting minimal effects on the stimulated PBMC populations and actually exerted a proliferative effect on the unstimulated PBMCs. The cockle extract results demonstrated that there was a proliferative effect also in the unstimulated PBMCs, but an anti-proliferative effect was also noted on the stimulated PBMCs. In the cancer cell assays the cockle extract treatment resulted in a proliferative effect in the MOLT-4 cell line but did exert a significant anti-proliferative effect in the U698 cell line. These results indicate that the cockle extract may exert some level of targeting towards healthy vastly proliferating cells. However the whelk extract treatment results suggest that the whelk extract may exert a selective nature towards cancer cells whilst not targeting healthy lymphocytes (activated or unstimulated), therefore may provide a potential treatment method with minimal side effects. These results confirm the findings of Aldairi, Ogundipe and Pye (2018) and Ogundipe (2015) that GAGs isolated from the common cockle and common whelk exhibit anti-proliferative effects in the MOLT-4 cell line. The results also support the suggest put forward by Basappa et al., (2012) that there are certain GAG chains which may be useful in cancer treatment which could result in fewer side effects for patients.

CHAPTER 5- CYTOKINE AND T-REGULATORY RESPONSE ASSAY

5.0 Cytokine and T-regulatory response results

5.1 Introduction

Cancer cells have the ability to modify the microenvironment of a tumour to become immunosuppressive (Sompayrac, 2015), therefore it is important to understand how a potential anti-cancer therapy interacts with the cells and cytokines responsible for this immunosuppressive nature. Many cancer cells exhibit the expression of immunosuppressive proteins such as CTLA-4, which are responsible for the restraint of cytotoxic T-lymphocytes (CTLs), thus shielding the cancer cell from any potential destruction by tumour specific CTLs (Sompayrac, 2015). Cancer cells also increase the production of T-regulatory (T_{reg}) cells to the tumour microenvironment (Facciabene et al., 2012: Elkord, 2010), which in turn excrete increased levels of TGF-β and IL-10 which create the immunosuppressive environment in which CTLs fail to function (Sompayrac, 2015). Raised T_{reg} cell levels in cancer have been linked to poor prognosis and negative impacts on immunotherapy, thus aiding in tumour progression (Elkord, 2010). This research therefore focussed on the impact of GAG treatment on T_{reg} cell levels in both stimulated and unstimulated PBMCs.

Chapters 3 and 4 indicated that the GAG isolates are both cytotoxic to lymphocytes but also induce proliferation to an extent in unstimulated PBMCs. Given that the mode of action of marine mollusc GAGs has not yet been fully established, the research evaluated any actions of the GAGs on cytokine production and T-regulatory cell numbers and phenotypic properties. In order to gain an insight into the longer term consequences of GAG use in the clinic.

The antibodies for CD4 and CD8 were used to identify T-helper cell and cytotoxic T-cell populations respectively in the lymphocyte population of PBMCs.

T-regulatory cells were identified in $CD4^+$ T-cells through the characterisation of the expression of the transcription factor FOXP3, which is necessary for the development and function of T_{reg} cells (Wang et al., 2009: Probst-Kepper, 2009). FOXP3 is a forkhead/winged-helix transcription factor (Lal and Bromberg, 2009) which is located in the thymus where T_{reg} cells develop. Various intracellular signalling molecules and extracellular stimuli such as IFN-γ, IL-4 and IL-27 aid with the both the function and development of T_{reg} cells (figure 5.1), this

is done through the regulation of FOXP3 (Lal and Bromberg, 2009). FOXP3 can be linked to the potency of T_{reg} cells as mutations in or deficiencies of FOXP3 lead to the development of autoimmune diseases (Lal and Bromberg, 2009). FOXP3 was used to identify the T_{reg} cell populations as its expression in $CD4^+$ T-cells is specific to T_{reg} cells (Probst-Kepper, 2009). In the thymus populations of $FOXP3^+CD4^+$ T-cells develop which are commonly referred to as natural T_{regs} (nT_{reg}), whereas in peripheral lymphoid organs TGF-β can induce the development of $FOXP3^+CD4^+$ T-cells from populations of naïve $CD4^+$ T-cells which are referred to as induced T_{regs} (iT_{reg}) (Zhang and Zhao, 2007). The function of nT_{reg} and iT_{reg} cells are similar with natural T-regulatory cells proving to be more stable (Lal and Bromberg, 2009).

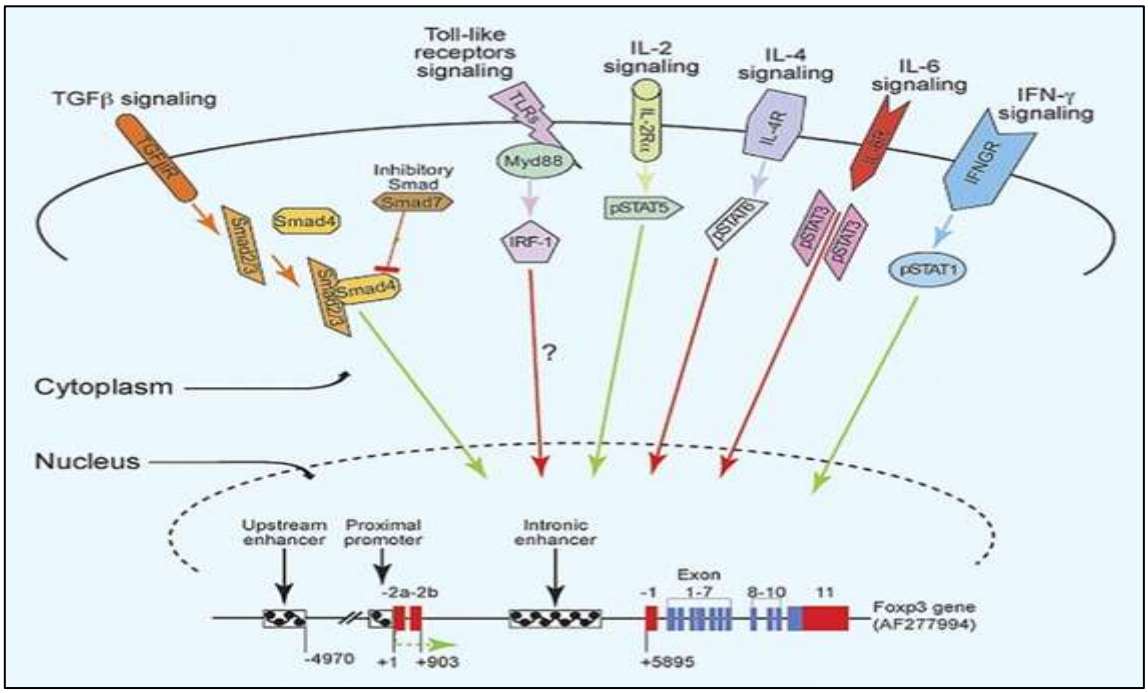

Figure 5.1 The regulation of FOXP3 from extracellular signals. The regulation of FOXP3 from extracellular signals: TGFβ, TLR, IL-2, IL-4, IL-6 and IFN-γ. Red arrows are representative of negative signals and green arrows are representative of positive signals responsible for FOXP3 expression (Lal and Bromberg, 2009).

Wang et al., (2009) and Probst-Kepper et al., (2009) identified that activated T-regulatory cells expressed a transmembrane protein known as glycoprotein A repetitions predominant (GARP). They also noted that the presence of GARP could be correlated with the suppressive activity of T_{reg} cells and that GARP was highly expressed in $FOXP3^+$ T_{reg} cells. Therefore, the

GARP antibody was used to further identify T_{reg} cells in FOXP3 positive cells, due to its specific induction in $CD4^+FOXP3^+$ (T_{reg}) cells (Probst-Kepper et al., 2009).

Interferon-γ (IFN-γ) is a cytokine which is secreted by thymus-derived T-cells such as natural killer (NK) cells, activated T-helper cells and activated cytotoxic T-cells (Boehm, Klamp, Groot and Howard, 1997). IFN-γ plays a role in many cellular functions which include aspects of the immune response as well as cell proliferation and apoptosis (Boehm et al., 1997). IFN-γ also plays a role in the phosphorylation of STAT1 which leads to interactions with the FOXP3 proximal promotor in $CD4^+$ T-cells (figure 5.1) (Lal and Bromberg, 2009). Ultimately leading to the expression of FOXP3 thus promoting T_{reg} cell development.

Interleukin-4 (IL-4) is a cytokine which plays an important role in the immune system (Takeda et al., 1996) and is secreted by activated T-lymphocytes, basophils and mast cells (Hou et al., 1994). IL-4 also has an important role in controlling the balance of T-helper cells (Hou et al., 1994). Figure 5.1 identifies IL-4 as being an opposing cytokine to IFN-γ, in that IL-4 inhibits the expression of FOXP3 through the promotion of the phosphorylation of STAT6 (Lal and Bromberg, 2009).

The common cockle and common whelk extracts effects on cytokine and T_{reg} cell responses were unknown, this research aimed to identify any responses that the extracts may have on cytokines (IL-4 and IFN-γ) and T_{reg} cell responses in healthy PBMCs (+/- stimulation).

5.2 Method

Antibody staining for surface: GARP, CD4 and CD8 and intracellular: IFN-γ, IL-4 and FOXP3, was carried out as per the manufacturer recommendations and as set out in method 2.6. To assess cytokine and T-regulatory cell responses to treatment with the cockle extract and whelk extract in comparison to untreated control cells and cells treated with the control drug cisplatin. In all assays cells were seeded to 1 x 10^5/ml and cisplatin was used as a control drug. PBMCs (stimulated and unstimulated) were incubated with the IC50 doses obtained in the MTT assays: cisplatin, 6 µg/ml, and cockle and whelk extracts both at 12 µg/ml, for a 3-day period. T_{reg} response assays were only carried out using naïve and stimulated PBMCs.

In figure 5.2 the gating process used for the T_{reg} and cytokine response assays in order to establish the individual cell types present in the PBMC populations. Where the CD4 (T-helper

cell) and CD8 (cytotoxic T-cell) populations were obtained in relation to the lymphocyte population. From the CD4 and CD8 gating, quad gates were then set up based on either the CD4 or CD8 populations in order to obtain the percentage of T-regulatory cells. Once the T-regulatory cell population had been identified histogram plots were drawn and gated upon in order to determine the effects of treatment on cytokine production in T_{reg} cells.

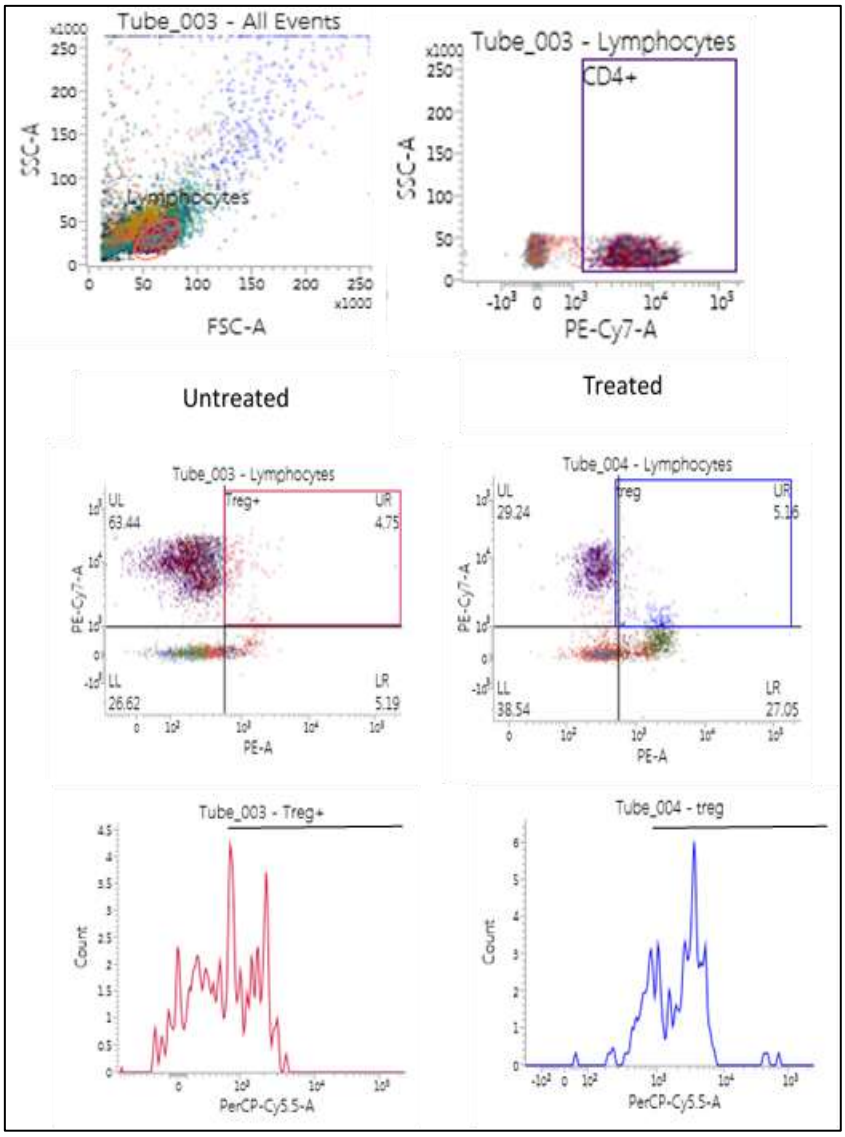

Figure 5.2 Raw data graph and gates drawn in a typical PBMC T_{reg} and cytokine response assays and the gating process involved. Raw data graph and gates drawn in a typical PBMC Treg and cytokine response assays in order to determine cell types and quantities and cytokine production from T_{reg} cells. The example shown is a cisplatin treated stimulated PBMC assay. All T_{reg} and cytokine response assays were performed using a 3-day incubation period and N=3.

5.3 Results: isolated PBMC assays

The results displayed in the T-regulatory cell and cytokine response assay figures demonstrate average data obtained from three repeats each performed in triplicate. The percentage change graphs were obtained by comparing each treatment method with either the control or another treatment method.

5.3.1 Unstimulated PBMCs

The lymphocyte population in unstimulated PBMCs was reduced the most by the cockle extract treatment in comparison to the control, as can be seen by the blue bar (control) and grey bar (cockle extract) in figure 5.3. It can also be seen in the lymphocyte section, cockle: control section of figure 5.4 (dark blue bar, p=0.045). The whelk extract treatment (yellow bar, figure 5.3) also reduced the lymphocyte population by more than the cisplatin treatment (orange bar, figure 5.3) and in comparison to the control, as can also be seen in the lymphocyte section of figure 5.4, p=0.0497. Cisplatin treatment reduced the lymphocyte population by the least out of all the treatment methods, as seen in figure 5.4, p=0.1197.

In the $CD4^+$ populations there was very little difference between the control sample and any of the treatments. This can be seen in the CD4 section of figure 5.3. The whelk extract treatment resulted in the least reduction in the CD4 population in comparison to the control (yellow bar, CD4 section, figure 5.4, p=0.6514). The cockle extract treatment (orange bar, CD4 section, figure 5.4, p=0.3469) resulted in the next smallest reduction in CD4 population. Cisplatin treatment (dark blue bar, section CD4, figure 5.4, p=0.4434) resulted in the largest decrease in CD4 populations in comparison to the control and the other treatment methods, however the reduction is very small.

In the $CD8^+$ population cisplatin treatment resulted in an increase in the CD8 population in comparison to the control, seen in figure 5.3, orange bar, CD8 section (cisplatin, p=0.3156) and dark blue bar (control). There is very little difference in the CD8 population between the cockle extract treatment (grey bar, section CD8, figure 5.3, p=0.9079) and the whelk extract treatment (yellow bar, section CD8, figure 5.3, p=0.7835) and the control (blue bar, section CD8, figure 5.3). This can also be seen by the small bars in the cockle: control and whelk: control bars in figure 5.4, section CD8 (orange and yellow bars respectively).

There were very small populations of GARP$^+$ cells and very little difference in the GARP populations between the control sample, cisplatin treated cells (p=0.4595), cockle extract (p=0.3459) and whelk extract treated (p=0.4778) cells. This can be seen through the small bars in the GARP section of figure 5.3 and the lack of bars in the GARP section of figure 5.4.

In the IL-4 population the cisplatin treatment caused the least reduction in the population (orange bar, IL-4 section, figure 5.3) in comparison to the control cells (blue bar, section IL-4, figure 5.3). This can also be seen in figure 5.4 in the IL-4 section, the cisplatin: control bar (p=0.5645) (dark blue bar) is smaller than that of the cockle: control (p=0.358) (grey bar) and whelk: control bar (p=0.4844) (yellow bar) in figure 5.4. Both the cockle extract treatment and the whelk extract treatment (grey bar and yellow bar respectively, section IL-4, figure 5.3) resulted in the same level of reduction in the IL-4 population of the unstimulated PBMCs. This can be seen due to the lack of green bar in figure 5.4 in the IL-4 section marking the comparison between the cockle extract and the whelk extract treatment. As the bars comparing the cockle extract and the control (orange bar, figure 5.4, IL-4 section) and the whelk extract treatment and the control (grey bar, figure 5.4, IL-4 section) are also at the same level it can be said that the cockle and whelk extract exert the same effect on the IL-4 population as each other in comparison to the control.

The populations of IFN-γ positive cells was quite small which can be seen by the small bars in the IFN-γ section of figure 5.3. There was also little difference between the cisplatin treatment (p=0.3161), the cockle extract treatment (p=0.7125) and whelk extract treatment (p=0.6195) in comparison to the control as can be seen through the lack of bars in the IFN-γ section of figure 5.4. The cisplatin treatment did however result in a small increase in the IFN-γ population which can be seen by the small dark blue bar in figure 5.4.

The FOXP3$^+$ populations of unstimulated PBMCs were also small and had very little difference between the control sample and each of the treatment methods cisplatin (p=0.1983), cockle extract (p=0.0502) and whelk extract (p=0.0592). This can identified by the small bars in figure 5.3, FOXP3 section. It can be noted that the cisplatin treatment resulted in a small increase in FOXP3 positive cells post treatment in comparison to the control (dark blue bar, FOXP3 section, figure 5.4). As there are no other bars in figure 5.4 that are identifiable, there are

minimal differences between the cockle extract treated cells, the whelk extract treated cells and the control cells.

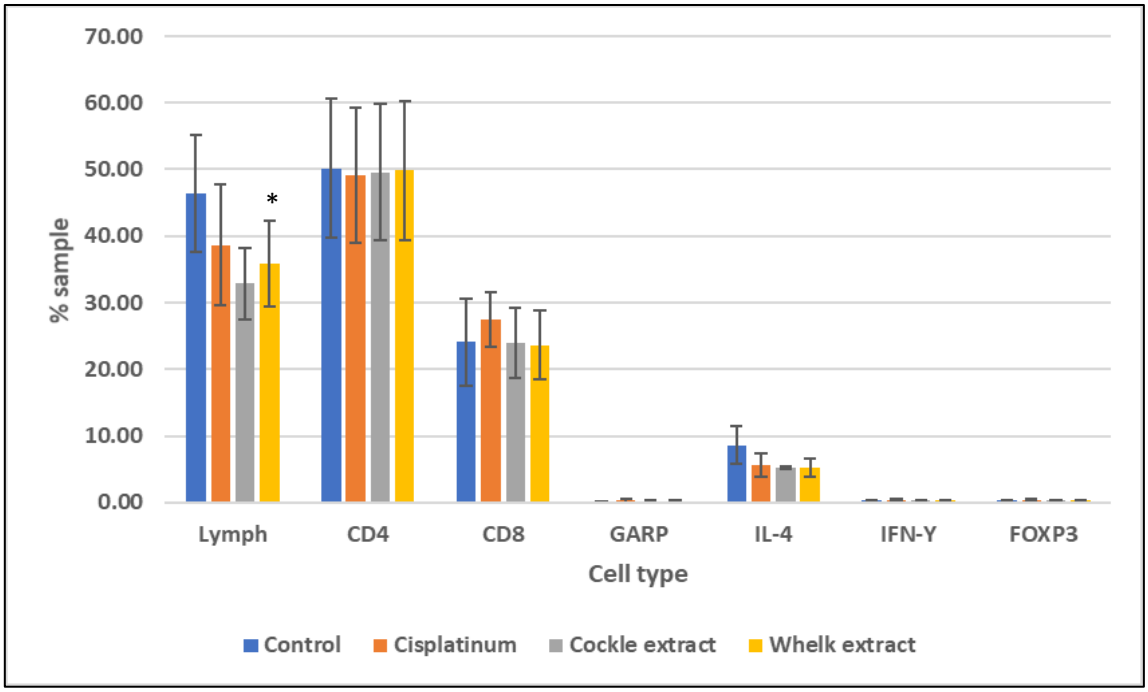

Figure 5.3. Average cell types (CD4, CD8, GARP, IL-4, IFN-γ and FOXP3) in unstimulated PBMCs. Average percentage cell type graph for unstimulated PBMCs treated with the IC50 dose of Cisplatin (orange bars), cockle extract (grey bars) and whelk extract (yellow bars) (6 µg/ml, 12 µg/ml and 12 µg/ml respectively). Control/ untreated cells (blue bars) were used as a comparison. Using an incubation period of 3-days. Where N=3, percentage cell type was in relation to the lymphocyte population and error bars show SEM, significance is denoted by *, absence of * indicates no significance.

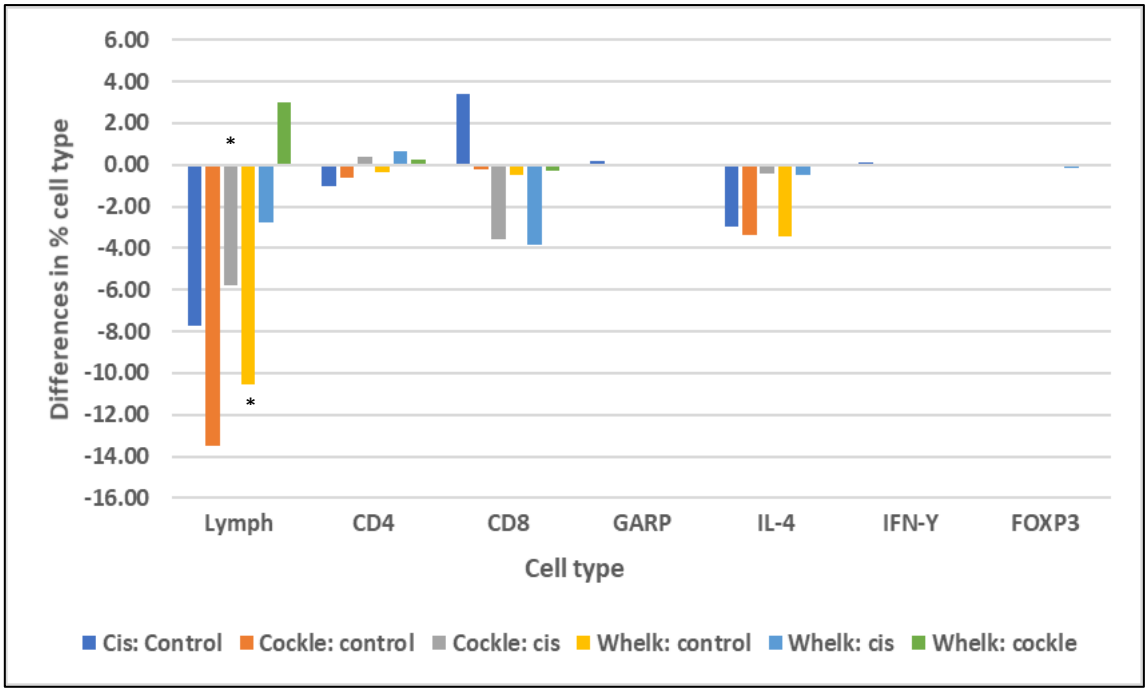

Figure 5.4. Average differences in cell type percentage in unstimulated PBMCs. Average percentage differences in cell type and treatment comparison graph for unstimulated PBMCs treated IC50 doses of cisplatin, cockle extract and whelk extract (6 µg/ml, 12 µg/ml and 12 µg/ml respectively). Showing the differences in cell type percentage in the treatment comparisons between the three treatment types and the untreated control cells. Using an incubation period of 3 days. Where N=3, percentage difference in cells was calculated based on the comparison treatment e.g. where cis: whelk is a comparison of the whelk extract cell population to the cell population in cisplatin treated cells, significance is denoted by *, absence of * indicates no significance.

5.3.1.1 $CD4^+$/T-helper cell populations

There were very small amounts of cells which tested positive for both CD4 and GARP ($CD4^+GARP^+$) as can be seen by the bars in figure 5.5- A, section $CD4^+GARP^+$. There were also no changes in the $CD4^+GARP^+$ population between the control cells and the cisplatin treated cells (p=0.5324). The was a small increase in $CD4^+GARP^+$ cell post treatment with the cockle extract (p=0.3378) and $CD4^+GARP^+$ cells increased by the most post whelk extract treatment (p=0.5326) which can be seen in the $CD4^+GARP^+$ section of figure 5.5- B.

In the $CD4^+$ IFN-γ^+ population the cockle extract treatment resulted in the largest increase in the population percentage (grey bar, figure 5.5- A, section $CD4^+$ IFN-γ^+). This can also be seen in the orange bar in figure 5.5- B (section $CD4^+$ IFN-γ^+) (p=0.6098). The whelk extract treatment also resulted in an increase in the percentage population of $CD4^+$ IFN-γ^+ cells (yellow bars, figures 5.5- A and 5.5- B, section $CD4^+$ IFN-γ^+) (p=0.6648). However the increase

was smaller than that of the cockle extract as seen by the green bar in figure 5.5- B (section $CD4^+$ IFN-γ^+). Cisplatin treatment resulted in the same percentage population as that of the control sample as seen by the orange and blue bars respectively in figure 5.5- A (section $CD4^+$ IFN-γ^+). This is also seen through the lack of dark blue bar in figure 5.5- B (p=0.1029).

In the $CD4^+$IL-4^+ cells the whelk extract treatment resulted in the largest decrease in the percentage population (yellow bars, figures 5.5- A and 5.5- B) (p=0.2872). The cockle extract also resulted in a decrease in the percentage population of $CD4^+$IL-4^+ cells which is identified by the grey bar in figure 5.5- A and the orange bar in figure 5.5- B, p=0.306. The cisplatin treatment resulted in the least reduction in $CD4^+$IL-4^+ cell population in comparison to the control (orange bar, figure 5.5- A and dark blue bar, figure 5.5- B, p=0.516).

5.3.1.1.1 $CD4^+FOXP3^+$/ T-regulatory cells

In the $CD4^+$ T-regulatory cells the whelk extract reduced the population by the largest amount in comparison to the control and the other treatment methods, as seen by the yellow bars in figures 5.5- A and 5.5- B, p=0.0199. The whelk extract resulted in a 50% decline in the percentage of $CD4^+$ T_{reg} cells in comparison to the control. Cisplatin also resulted in a reduction in the percentage of T_{reg} cells in comparison to the control (orange and blue bars respectively, figure 5.5- A, and dark blue bar, figure 5.5- B, p=0.0297) and a slight reduction in comparison to the cockle extract treatment (grey bar, figure 5.5- B). The cockle extract resulted in a similar reduction in the level of T_{reg} cells to that of cisplatin, however the reduction was slight smaller as can be seen by the orange and grey bars in figure 5.5- B, p=0.0362. Cockle extract treatment had a reduced level of T_{reg} cells in comparison to the control cells, seen by the grey bar and blue bar in figure 5.5- A respectively.

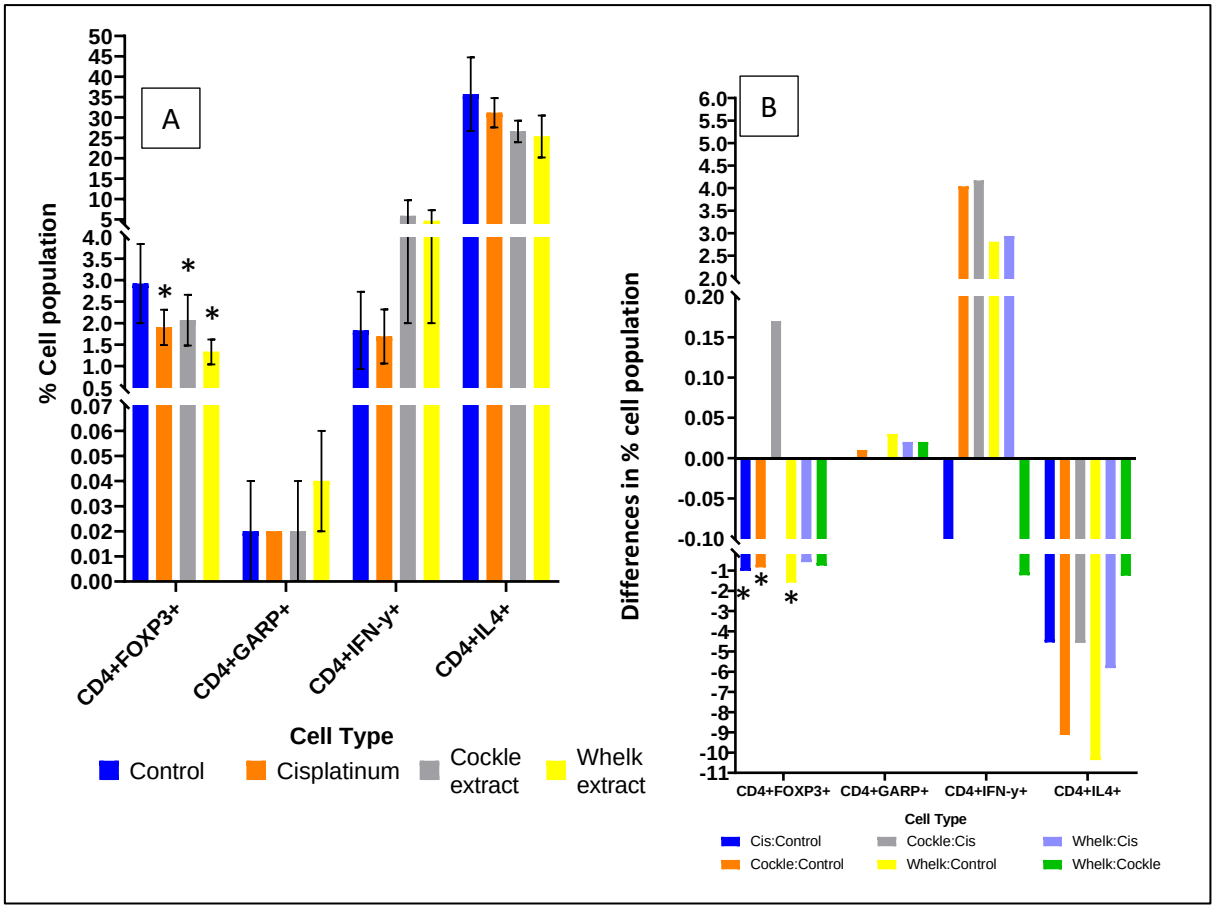

Figure 5.5. A - Average $CD4^+$ cell types (FOXP3, GARP, IFN-γ and IL-4) in unstimulated PBMCs. Average percentage $CD4^+$ cell type graph for unstimulated PBMCs. Figure 5.5. B - Average differences in $CD4^+$ cell type percentage in unstimulated PBMCs. Average percentage differences in $CD4^+$ cell type and treatment comparison graph for unstimulated PBMCs; showing differences cell type percentage against treatment comparisons between the three treatment types and the untreated control cells. Percentage difference in cells was calculated based on the comparison treatment e.g. where cis: whelk is a comparison of the whelk extract cell population to the cell population in cisplatin treated cells. Both figures represent unstimulated PBMCs treated with the IC50 dose of Cisplatin, cockle extract and whelk extract (6 µg/ml, 12 µg/ml and 12 µg/ml respectively). Control/ untreated cells were used as a comparison. Using an incubation period of 3-days. Where N=3, percentage cell type or difference was in relation to the lymphocyte $CD4^+$ population and error bars show SEM. Significance is denoted by *, absence of * indicates no significance.

Figure 5.6 identifies that the GARP population of $CD4^+T_{reg}$ cells was reduced by the cisplatin and whelk extract treatment methods in comparison to the control. Cisplatin treatment had the lowest mean fluorescence value in comparison to the control (p=0.5335) (figure 5.6; orange bar). The whelk extract had a lower median fluorescence value in comparison to the control (p=0.9621) (figure 5.6; yellow bar), however this was not lower than that of the cisplatin treated population. The cockle extract treatment resulted in a higher mean

fluorescence value than the control in the $GARP^{+}CD4^{+}T_{reg}$ cells (p=0.6405) (figure 5.6; grey bar).

In the IFN-$\gamma^{+}CD4^{+}T_{reg}$ cells the cisplatin treatment increased the mean fluorescence in comparison to the control sample by the largest amount (p=0.0599, figure 5.6; orange bar) of all three treatment methods. The cockle extract treatment resulted in an increase in the mean fluorescence in comparison to the control (p=0.0048, figure 5.6; grey bar). Whelk extract treatment resulted in an increase in the mean fluorescence of IFN-$\gamma^{+}CD4^{+}T_{reg}$ cells in comparison to the control (p=0.9621, yellow bar; figure 5.6).

In IL-$4^{+}CD4^{+}T_{reg}$ cells the mean fluorescence was increased by treatment with cisplatin extract (figure 5.6; orange bar, p=0.7057) and by treatment with the whelk extract (yellow bar; figure 5.6, p=0.6432). Treatment with the cockle extract resulted in a decrease in the mean fluorescence of IL-$4^{+}CD4^{+}T_{reg}$ cells (p=0.1707, figure 5.6; grey bar).

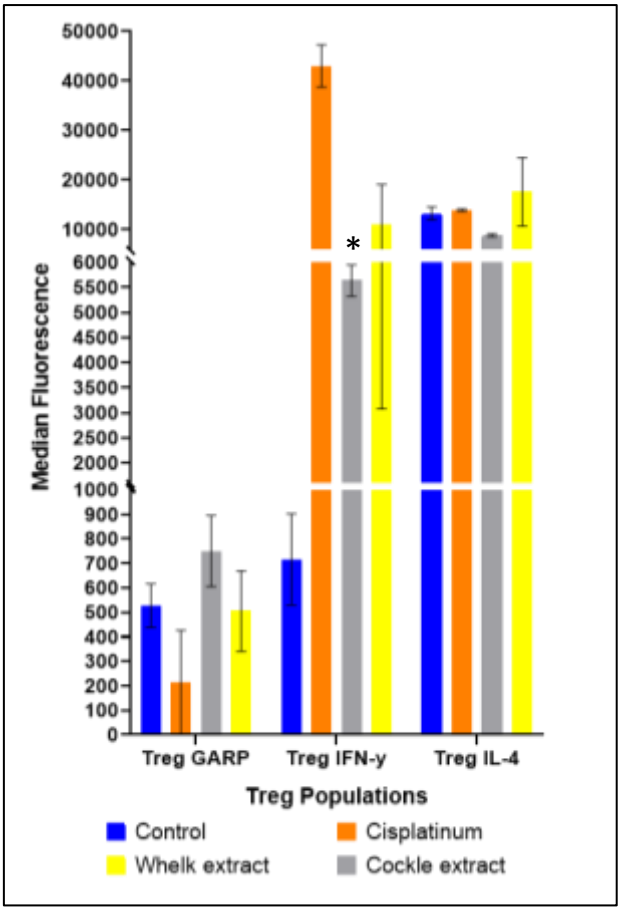

Figure 5.6 The average median fluorescence of biomarker/ cytokine levels in unstimulated $CD4^+T_{reg}$ cells. The average median fluorescence of biomarker/ cytokine levels in unstimulated $CD4^+T_{reg}$ cells obtained from the histogram gating system observed in figure 5.2. Average data obtained from unstimulated PBMCs treated with IC50 values of cisplatin (6 µg/ml), cockle extract (12 µg/ml) and whelk extract (12 µg/ml), with an incubation period of 3-days and N=3. Graph displayed was created using Prism 8.0 software. Error bars represent SEM, significance is denoted by *, absence of * indicates no significance.

5.3.1.2 $CD8^+$/ Cytotoxic T-cell populations

There were very small percentages of $CD8^+GARP^+$ cells in all samples, which can be seen by the small bars in the $CD8^+GARP^+$ section of figure 5.7- A. Treatment with cisplatin (p=0.5712) resulted in the largest increase in $CD8^+GARP^+$ cells (orange bar, figure 5.7- A: blue bar, figure 5.7- B). Cockle extract treatment (p=0.3463) resulted in an increase in the percentage of $CD8^+GARP^+$ cells in comparison to the control, as seen by the grey bar in figure 5.7- A and the orange bar in figure 5.7- B. The whelk extract (p=0.224) treatment resulted in a decrease in the percentage of $CD8^+GARP^+$ cells, as seen by the yellow bars in figure 5.7- A and figure 5.7- B.

In the $CD8^+IFN\text{-}\gamma^+$ cells the treatment with cisplatin resulted in an increase in the percentage population in comparison to the control (orange and blue bars respectively, figure 5.7- A). Which can also be seen in the percentage difference comparison between the control and the cisplatin treatment (dark blue bar, figure 5.7- B, p=0.3548). Cockle extract treatment resulted in a slight increase in the percentage population of $CD8^+IFN\text{-}\gamma^+$ cells in comparison to the control (grey bar, figure 5.7- A and orange bar, figure 5.7- B, p=0.57). The increase in $CD8^+IFN\text{-}\gamma^+$ population was slightly more than that of cisplatin which can be seen by the grey bar in figure 5.7- B, which compared the percentage difference in cell population of the cisplatin treatment and the treatment with the cockle extract. The whelk extract treatment resulted in a decrease in the percentage of $CD8^+IFN\text{-}\gamma^+$ cell population in comparison to the control (yellow bars, figures 5.7- A and 5.7- B, p=0.2773).

In the $CD8^+IL\text{-}4^+$ cell population the treatment with cisplatin resulted in an increase in comparison to the control (orange bar and dark blue bar, figures 5.7- A and 5.7- B respectively, p=0.63). The cockle extract treatment brought about a decrease in the percentage of $CD8^+IL\text{-}4^+$ cells when compared to the control which can be seen by the grey bar in figure 5.7- A and the orange bar in figure 5.7- B (p=0.5018). Treatment with the whelk extract resulted in a decrease in the percentage of the $CD8^+IL\text{-}4^+$ population in comparison to the control which can be seen in the yellow bars in figures 5.7- A and 5.7- B (p=0.2843). The decrease in whelk extract treated populations was slightly more than that of the cockle extract which can be seen by the green bar in figure 5.7- B.

5.3.1.2.1 $CD8^+FOXP3^+$/ $CD8^+T_{reg}$ cells

In the $CD8^+$ T_{reg} cells the whelk extract treatment resulted in the largest decrease in percentage population in comparison to the control and the other treatment methods (yellow bars, figures 5.7- A and 5.7- B, p=0.0361). The decrease was larger than that seen in cisplatin as can be seen by the light blue bar in figure 5.7- B and larger than that of the cockle extract treated cells as can be seen by the green bar in figure 5.7- B. Cisplatin treatment also resulted in a decrease in the percentage of $CD8^+$ T_{reg} cells in comparison to the control as can be seen by the orange bar in figure 5.7- A and the dark blue bar in figure 5.7- B (p=0.0727). The cockle extract also brought about a decrease in the percentage population of $CD8^+$ T_{reg} cells in comparison to the control (grey bar and orange bar, figures 5.7- A and 5.7- B

respectively, p=0.0477). The decrease in the population of $CD8^+$ T_{reg} cells was larger in cockle extract treated cells than in cisplatin treated cells as can be seen by the grey bar in figure 5.7-B.

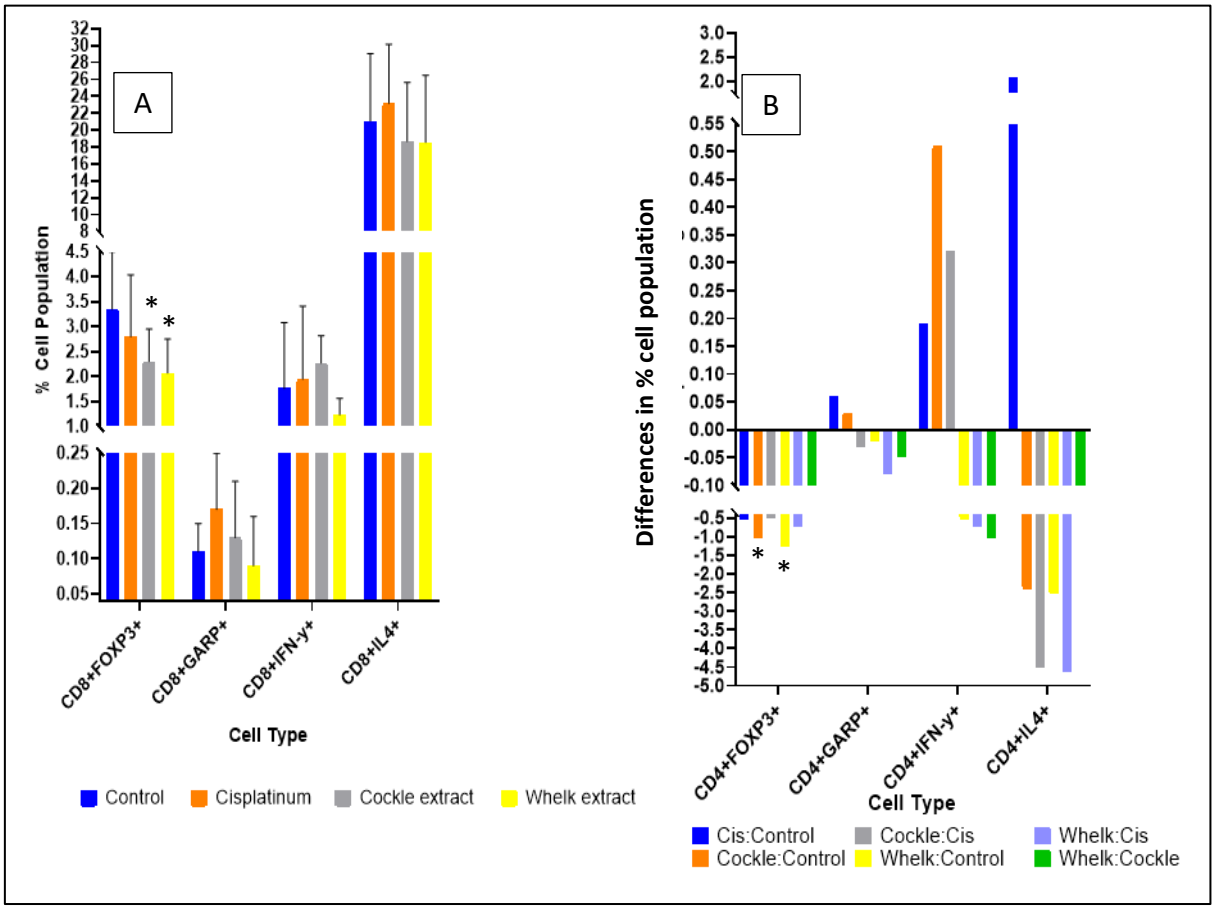

Figure 5.7. A - Average $CD8^+$ cell types (FOXP3, GARP, IFN-γ and IL-4) in unstimulated PBMCs. Average percentage $CD8^+$ cell type graph for unstimulated PBMCs. Figure 5.7. B - Average differences in $CD8^+$ cell type percentage in unstimulated PBMCs. Average percentage differences in $CD8^+$ cell type and treatment comparison graph for unstimulated PBMCs; showing differences in cell type against treatment comparisons between the three treatment types and the untreated control cells. Percentage difference in cells was calculated based on the comparison treatment e.g. where cis: whelk is a comparison of the whelk extract cell population to the cell population in cisplatin treated cells. Both figures represent unstimulated PBMCs treated with the IC50 dose of cisplatin, cockle extract and whelk extract (6 µg/ml, 12 µg/ml and 12 µg/ml respectively). Control/ untreated cells were used as a comparison. Using an incubation period of 3-days. Where N=3, percentage cell type or difference was in relation to the lymphocyte $CD8^+$ population and error bars show SEM. Significance is denoted by *, absence of * indicates no significance.

Figure 5.8 identifies that the mean fluorescence is increased in comparison to the control in the $GARP^+CD8^+T_{reg}$ cells post treatment with all three treatment methods. Cisplatin treatment resulted in the smallest increase in the $GARP^+CD8^+T_{reg}$ cell mean fluorescence (p=0.1465,

figure 5.8; orange bar). While the cockle extract also increased the mean fluorescence of $GARP^{+}CD8^{+}T_{reg}$ cells (p=0.3497, figure 5.8; grey bar). The whelk extract treatment resulted in the largest increase in the mean fluorescence of $GARP^{+}CD8^{+}T_{reg}$ cells in comparison to the control (p=0.5451, figure 5.8; yellow bar).

In the IFN-$\gamma^{+}CD8^{+}T_{reg}$ cells mean fluorescence was decreased by all three treatment methods, with cisplatin treatment reducing the mean fluorescence by the largest amount (p=0.0103, orange bar, figure 5.8). Cockle extract treatment (p=0.0011, figure 5.8; grey bar) and whelk extract (p=0.0027, figure 5.8; yellow bar) treatment also resulted in decreases in the mean fluorescence of IFN-$\gamma^{+}CD8^{+}T_{reg}$ cells.

Mean fluorescence in IL-$4^{+}CD8^{+}T_{reg}$ cell populations was decreased by the most post treatment with the whelk extract (p=0.3421, figure 5.8; yellow bar). Cisplatin treatment also reduced the mean fluorescence of IL-$4^{+}CD8^{+}T_{reg}$ cells post treatment (p=0.3670, orange bar, figure 5.8). The treatment with cockle extract resulted in the smallest decrease in the mean fluorescence of IL-$4^{+}CD8^{+}T_{reg}$ cells post treatment (p=0.3771, figure 5.8; grey bar).

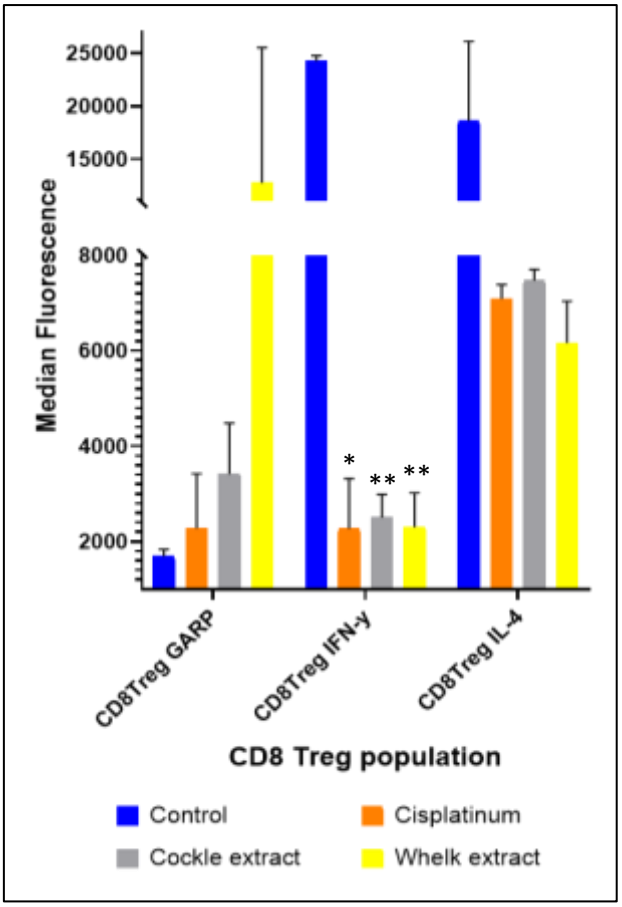

Figure 5.8 The average median fluorescence of biomarker/ cytokine levels in unstimulated $CD8^{+}T_{reg}$ cells. The average median fluorescence of biomarker/ cytokine levels in unstimulated $CD8^{+}T_{reg}$ cells obtained from the histogram gating system observed in figure 5.2. Average data obtained from unstimulated PBMCs treated with IC50 values of cisplatin (6 µg/ml), cockle extract (12 µg/ml) and whelk extract (12 µg/ml), with an incubation period of 3-days and N=3. Graph displayed was created using Prism 8.0 software. Error bars represent SEM, significance is denoted by *, absence of * indicates no significance.

5.3.2 Stimulated PBMCs

PBMCs were stimulated as per method 2.7 and incubated with the IC50 value for each drug type or plain media for the control cells for 3 days. The control sample for figure 5.9, 5.11-A, 5.13- A are represented by the blue bar.

Cisplatin treatment brought about an increase in the percentage of lymphocytes in comparison to the control sample (orange bar, figure 5.9 and the dark blue bar in figure 5.10, p=0.5127). The cockle extract treatment resulted in a decrease in the lymphocyte population in comparison to the control (grey bar, figure 5.9 and orange bar in figure 5.10, p=0.0019) and in comparison to the whelk extract (green bar, figure 5.10). Treatment with the whelk extract

resulted in a decrease in lymphocyte population in comparison to the control sample (yellow bars, figures 5.9 and 5.10, p=0.1234).

The cisplatin treatment resulted in an increase in the percentage of T-helper cells ($CD4^+$) which can be seen by the orange bar in figure 5.9 and the dark blue bar in figure 5.10, p=0.2754. The cockle extract treatment caused an increase in T-helper cells in comparison to the control (grey bar, figure 5.9 and orange bar 5.10, p=0.135), however the increase was not as much as in the cisplatin treated cells as can be seen by the grey bar in figure 5.10. Treatment with the whelk extract demonstrated a decrease in the percentage of T-helper cells (yellow bars, figure 5.9 and 5.10, p=0.7262).

In cytotoxic T-cells ($CD8^+$) the cockle extract resulted in the largest decrease in comparison to the control (grey bar figure 5.9 and orange bar figure 5.10, p=0.4256), also in comparison to cisplatin treatment (grey bar figure 5.10) and whelk extract treated cells (green bar figure 5.10). The whelk extract and cisplatin treatment resulted in a decrease in the percentage of cytotoxic T-cells in comparison to the control (orange bar 5.9 and dark blue bar figure 5.10, p=0.4388, yellow bars figures 5.9 and 5.10, p=0.4573, respectively). This reduction was by the same percentage in both cisplatin and whelk extract treated cells which can be seen by the lack of light blue bar in figure 5.10.

The whelk extract treated cells had a reduction in the percentage of GARP positive cells in comparison to the control (yellow bars figures 5.9 and 5.10, p=0.4366). Cisplatin treatment resulted in an increase in the percentage of GARP positive cells in comparison to the control (orange bar figure 5.9 and dark blue bar figure 5.10, p=0.3581). In cockle extract treated cells the GARP population percentage increased in comparison to the control (grey bar figure 5.9 and orange bar figure 5.10, p=0.2865) and in comparison to the cisplatin treated cells (grey bar figure 5.10).

IL-4 positive cell populations experienced an increase post whelk extract treatment in comparison to the control (yellow bars, figures 5.9 and 5.10, p=0.302), also in comparison to cisplatin treated cells (light blue bar figure 5.10) and in comparison to cockle extract treated cells (green bar figure 5.10). Cockle extract treated cells experienced an increase in the percentage of IL-4 positive cells in comparison to the control (grey bar figure 5.9 and orange bar figure 5.10, p=0.3973) also in comparison to the cisplatin treated cells (grey bar figure

5.10). Cisplatin treatment resulted in an increase in the percentage of IL-4 positive populations in comparison to the control (orange bar figure 5.9 and dark blue bar figure 5.10, p=0.4663).

Treatment with cisplatin resulted in the largest decrease in the percentage of IFN-γ^+ in comparison to the control (orange bar figure 5.9 and dark blue bar figure 5.10, p=0.0718), also in comparison to cockle extract treatment (grey bar, figure 5.10) and whelk extract treatment (light blue bar, figure 5.10). The IFN-γ^+ population experienced a decrease in population percentage post treatment with the cockle extract in comparison to the control (grey bar figure 5.9 and orange bar figure 5.10, p=0.0668) and in comparison to the whelk extract treated cells (green bar, figure 5.10, p=0.1027). The whelk extract treatment resulted in a decrease in the percentage population of IFN-γ^+ cells in comparison to the control (yellow bars, figures 5.9 and 5.10).

FOXP3$^+$ cells experienced a decrease in comparison to the control sample post treatment with cisplatin (orange bar figure 5.9, dark blue bar figure 5.10, p=0.0072) and in comparison to treatment with either the cockle extract or whelk extract (grey bar and light blue bar respectively, figure 5.10). Cockle extract treatment resulted in a decrease in the percentage of FOXP3$^+$ cells post treatment in comparison to the control cells (grey bar figure 5.9 and orange bar figure 5.10, p=0.0145) and in comparison to treatment with the whelk extract (green bar figure 5.10). Treatment with the whelk extract resulted in a decrease in the percentage of FOXP3$^+$ cells post treatment in comparison to the control cells (yellow bars, figures 5.9 and 5.10, p=0.0191).

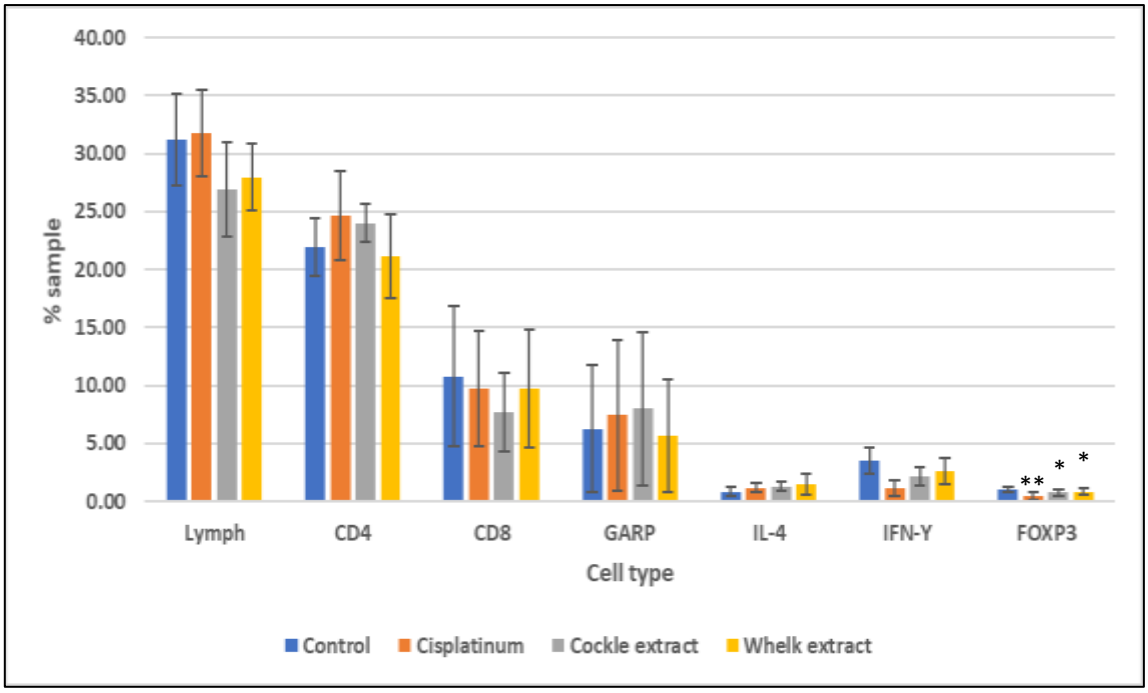

Figure 5.9. Average cell types (CD4, CD8, GARP, IL-4, IFN-γ and FOXP3) in stimulated PBMCs. Average percentage cell type graph for stimulated PBMCs treated with the IC50 dose of Cisplatin (orange bars), cockle extract (grey bars) and whelk extract (yellow bars) (6 µg/ml, 12 µg/ml and 12 µg/ml respectively). Control/ untreated cells (blue bars) were used as a comparison. Using an incubation period of 3-days. Where N=3, percentage cell type was in relation to the lymphocyte population and Error bars show SEM, significance is denoted by *, absence of * indicates no significance.

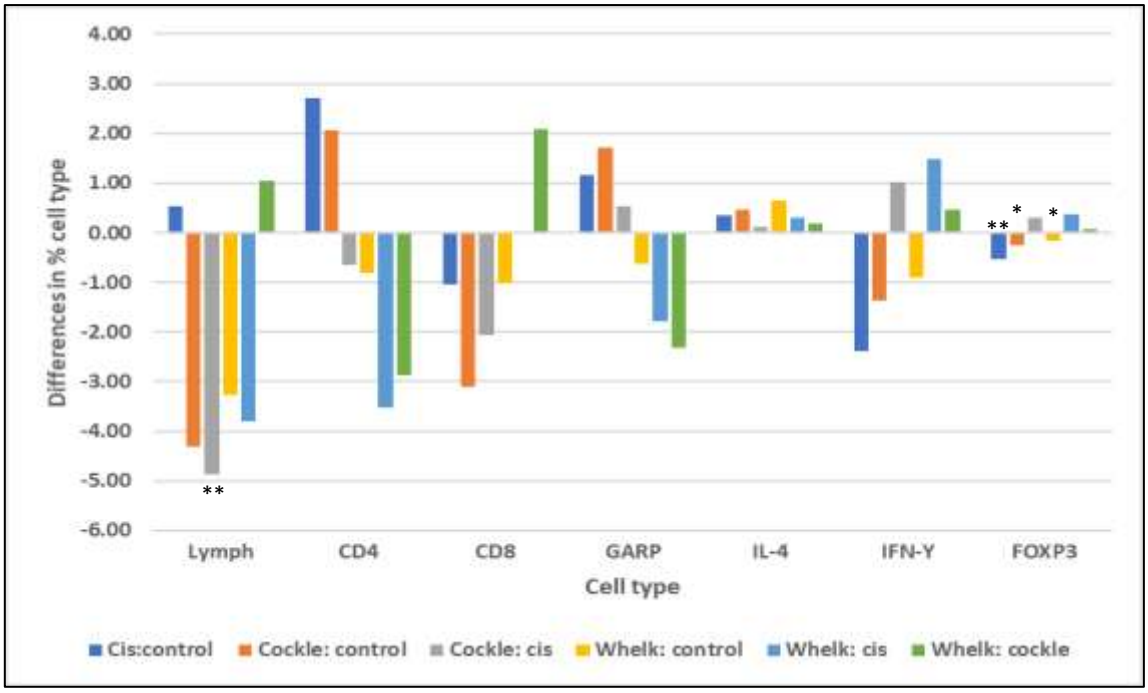

Figure 5.10. Average differences in cell type percentage in stimulated PBMCs. Average percentage difference in cell type and treatment comparison graph for stimulated PBMCs treated IC50 doses of cisplatin, cockle extract and whelk extract (6 µg/ml, 12 µg/ml and 12 µg/ml respectively). Showing differences in cell type against treatment comparisons between the three treatment types and the untreated control cells. Using an incubation period of 3 days. Where N=3, percentage difference in cells was calculated based on the comparison treatment e.g. where cis: whelk is a comparison of the whelk extract cell population to the cell population in cisplatin treated cells, significance is denoted by *, absence of * indicates no significance.

5.3.2.1 $CD4^+$/ T-helper cell populations in stimulated PBMCs

Treatment with the whelk extract resulted in a decrease in the percentage of $CD4^+GARP^+$ population in comparison to the control (yellow bars, figures 5.11- A and 5.11- B, p=0.2074), cisplatin treatment (light blue bar figure 5.11- B) and cockle extract (green bar figure 5.11- B). Cockle extract treatment (p=0.2331) and treatment with cisplatin (p=0.2471) resulted in a decrease in the percentage of $CD4^+GARP^+$ in comparison to the control (orange and grey bars figure 5.11- A and dark blue and orange bars figures 5.11- B, respectively) which can also be seen by the lack of grey bar in figure 5.11- B.

Treatment with the whelk extract resulted in a decrease in the percentage population of $CD4^+IFN\text{-}\gamma^+$ cells in comparison to the control sample (yellow bars, figure 5.11- A and 5.11- B, p=0.0156) and also in comparison to the treatment with cisplatin (light blue bar, figure 5.11- B). Cisplatin treatment resulted in a decrease in the percentage of $CD4^+IFN\text{-}\gamma^+$ population in

comparison to the control (orange bar figure 5.11- A and dark blue bar figure 5.11- B, p=0.8861). The cockle extract treatment resulted in an increase in the percentage population of $CD4^+IFN\text{-}\gamma^+$ cells in comparison to the control (grey bar figure 5.11- A and orange bar in figure 5.11- B, p=0.8766).

In the $CD4^+IL4^+$ percentage population the cisplatin treatment resulted in an increase in the population in comparison to the control sample (orange bar figure 5.11- A and dark blue bar figure 5.11- B, p=0.2141). Also in comparison to the cockle extract treatment (grey bar figure 5.11- B) and whelk extract treatment (light blue bar figure 5.11- B). The cockle extract treated $CD4^+IL4^+$ cells experienced an increase in the percentage population post treatment in comparison to the control (grey bar figure 5.11- A and orange bar figure 5.11- B, p=0.3915) and also in comparison to the whelk extract treatment (green bar figure 5.11- B). Treatment with the whelk extract resulted in an increase in the percentage population of $CD4^+IL4^+$ cells in comparison to the control as can be seen by the yellow bars in figures 5.11- A and 5.11- B, p=0.6377.

5.3.2.1.1 $CD4^+FOXP3^+$/ T-regulatory cells

In the $CD4^+FOXP3^+$/ T-regulatory cell population the cisplatin treatment reduced the percentage population in comparison to the control (orange bar figure 5.11- A, dark blue bar figure 5.11- B, p=0.0499). Treatment with the cockle extract resulted in a decrease in the T_{reg} cell population in comparison to the control sample, as can be seen by the grey bar in figure 5.11- A and the orange bar in figure 5.11- B (p=0.0511), and also in comparison to the cisplatin treatment (grey bar figure 5.11- B). The T_{reg} cell population was reduced by the largest amount post whelk extract treatment in comparison to the control (yellow bars figures 5.11- A and 5.11- B, p=0.0422) and also in comparison to cisplatin treatment (light blue bar figure 5.11- B) and cockle extract treatment (green bar figure 5.11- B).

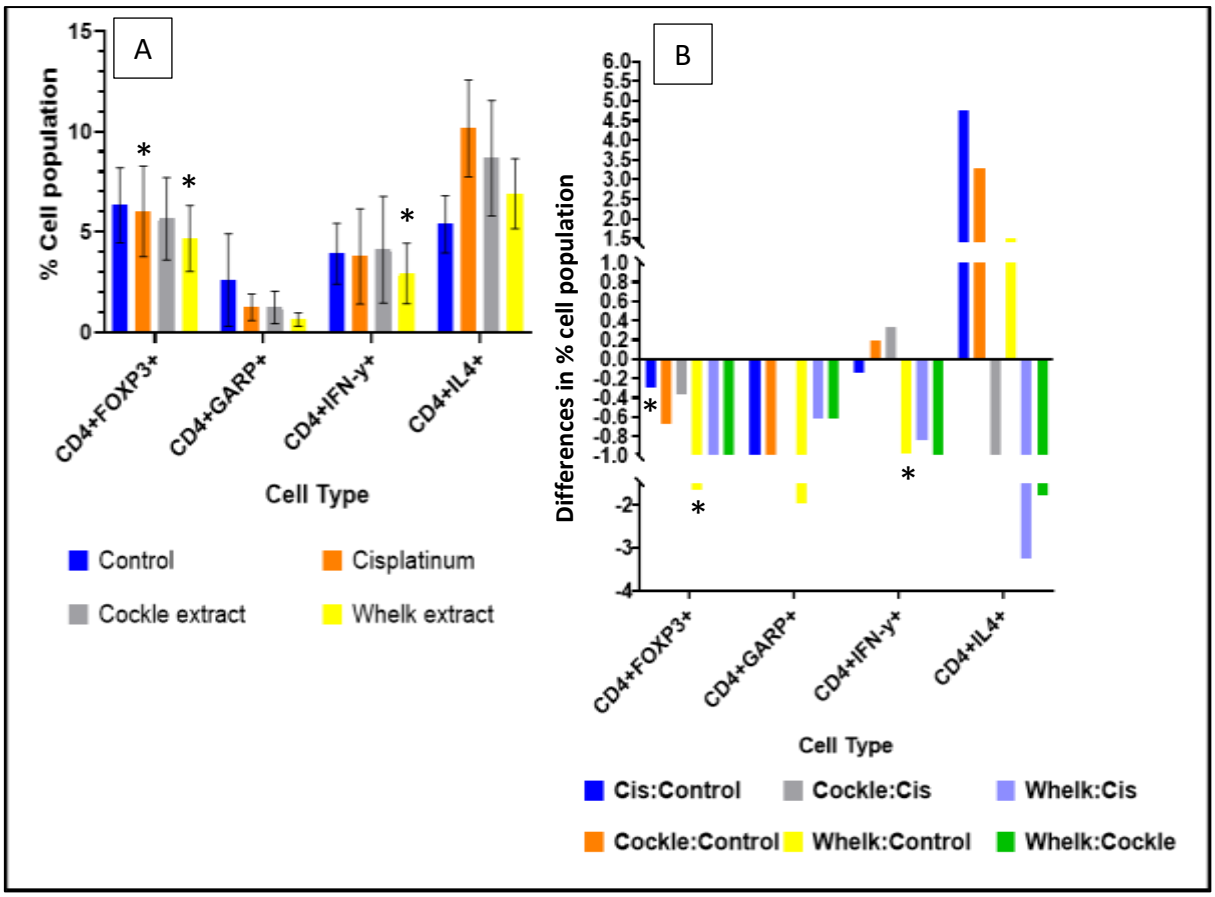

Figure 5.11. A - Average $CD4^+$ cell types (FOXP3, GARP, IFN-γ and IL-4) in stimulated PBMCs. Average percentage $CD4^+$ cell type graph for stimulated PBMCs. Figure 5.11. B - Average differences in $CD4^+$ cell type percentage in stimulated PBMCs. Average percentage differences in $CD4^+$ cell type and treatment comparison graph for stimulated PBMCs; showing differences in cell type against treatment comparisons between the three treatment types and the untreated control cells. Percentage difference in cells was calculated based on the comparison treatment e.g. where cis: whelk is a comparison of the whelk extract cell population to the cell population in cisplatin treated cells. Both figures represent stimulated PBMCs treated with the IC50 dose of cisplatin, cockle extract and whelk extract (6 µg/ml, 12 µg/ml and 12 µg/ml respectively). Control/ untreated cells were used as a comparison. Using an incubation period of 3-days. Where N=3, percentage cell type or difference was in relation to the lymphocyte $CD4^+$ population and error bars show SEM. Significance is denoted by *, absence of * indicates no significance.

Figure 5.12 identifies that the mean fluorescence in stimulated $GARP^+CD4^+T_{reg}$ cells was reduced by both the cisplatin treatment (p=0.0593, orange bar) and by the whelk extract treatment (p=0.0354, yellow bar). The treatment with the whelk extract reduced the mean fluorescence by the most in comparison to the control and the cisplatin treatment. The treatment with the cockle extract resulted in an increase in the mean fluorescence of $GARP^+CD4^+T_{reg}$ cells in comparison to the control (p=0.6095, grey bar, figure 5.12).

Cisplatin treatment resulted in a decrease in the mean fluorescence of IFN-$\gamma^{+}CD4^{+}T_{reg}$ cells (p=0.8794, orange bar, figure 5.12). Both treatment with the cockle extract (p=0.4172) and whelk extract (p=0.5752) resulted in an increase in the mean fluorescence of IFN-$\gamma^{+}CD4^{+}T_{reg}$ cells post treatment, as can be seen by the grey and yellow bars respectively in figure 5.12.

Post treatment with cisplatin the mean fluorescence of IL-$4^{+}CD4^{+}T_{reg}$ cells increased by the largest amount (p=0.1958, orange bar, figure 5.12) in comparison to the control. Treatment with the cockle extract also resulted in an increase in the mean fluorescence of IL-$4^{+}CD4^{+}T_{reg}$ cells (p=0.5817, figure 5.12; grey bar) however this increase was not as much as that of cisplatin treated cells. In IL-$4^{+}CD4^{+}T_{reg}$ cells treated with the whelk extract mean fluorescence decreased in comparison to the control (p=0.2228, figure 5.12; yellow bar).

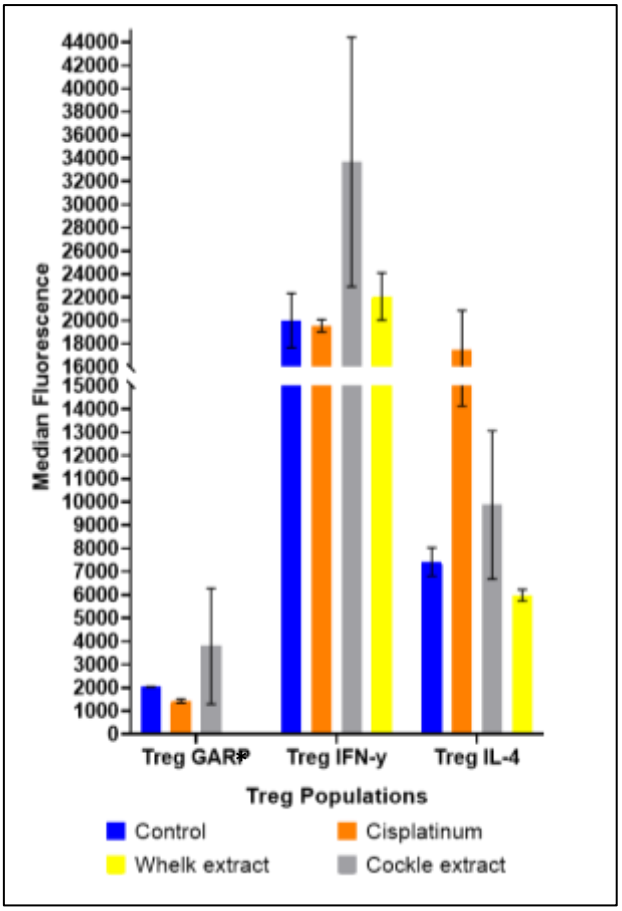

Figure 5.12 The average median fluorescence of biomarker/ cytokine levels in stimulated $CD4^{+}T_{reg}$ cells. The average median fluorescence of biomarker/ cytokine levels in stimulated $CD4^{+}T_{reg}$ cells obtained from the histogram gating system observed in figure 5.2. Average data obtained from stimulated PBMCs treated with IC50 values of cisplatin (6 µg/ml), cockle extract (12 µg/ml) and whelk extract (12 µg/ml), with an incubation period of 3-days and N=3. Graph displayed was created using Prism 8.0 software. Error bars show SEM, significance is denoted by *, absence of * indicates no significance.

5.3.2.2 $CD8^{+}$/ Cytotoxic T-cell populations in stimulated PBMCs

In the $CD8^{+}GARP^{+}$ percentage population there were only small amounts of cell populations which can be seen by the bars in figures 5.13- A. There were also no differences between the control sample and either the cisplatin treatment (p=0.2377) or cockle extract treatment (p=0.1925) which can be seen by the lack of bars in figure 5.13- B. The whelk extract treatment (p=0.1956) resulted in a small increase in the percentage of $CD8^{+}GARP^{+}$ cells as can be seen by the yellow bars in figures 5.13- A and 5.13- B.

The $CD8^{+}IFN\text{-}\gamma^{+}$ cell population experienced a decrease in percentage population post treatment with the cockle extract in comparison to the control (grey bar figure 5.13- A and

orange bar figure 5.13- B, p=0.0829). The decrease in $CD8^+IFN\text{-}\gamma^+$ cell population treated with the cockle extract was also in comparison to the cisplatin treatment (grey bar figure 5.13- B) and the whelk extract treatment (green bar figure 5.13- B). Cisplatin treatment exerted a decrease in the percentage population of $CD8^+IFN\text{-}\gamma^+$ cells post treatment in comparison to the control (orange bar figure 5.13- A and dark blue bar figure 5.13- B, p=0.0154) and in comparison to the whelk extract treatment (light blue bar figure 5.13- B). The whelk extract treatment resulted in a decrease in the percentage population of $CD8^+IFN\text{-}\gamma^+$ cells in comparison to the control (yellow bars figures 5.13- A and 5.13- B, p=0.0612).

The population of $CD8^+IL4^+$ cells experienced a decrease in the percentage population post treatment with the cockle extract in comparison to the control sample as seen by the grey bar in figure 5.13- A and the orange bar in figure 5.13 B, p=0.4754. The population of $CD8^+IL4^+$ cells was also decreased in comparison to the cisplatin treated cells (grey bar figure 5.13- B) and whelk extract treated cells (green bar figure 5.13- B) post treatment with the cockle extract. The whelk extract treatment resulted in a decrease in the percentage population of $CD8^+IL4^+$ cells in comparison to the control sample (yellow bars figures 5.13- A and 5.13- B, p=0.2889) and in comparison to the cisplatin treated cells (light blue bar figure 5.13- B). Cisplatin treatment resulted in a decrease in the percentage population of $CD8^+IL4^+$ cells post treatment in comparison to the control sample (orange bar figure 5.13- A and dark blue bar figure 5.13- B, p=0.7892).

5.3.2.2.1 $CD8^+FOXP3^+$/ $CD8^+$ T_{reg} cells in stimulated PBMCs

In the $CD8^+FOXP3^+$/ $CD8^+$ T_{reg} population the cockle extract treatment brought about a decrease in the population percentage in comparison to the control as can be identified by the grey bar in figure 5.13- A and the orange bar in figure 5.13- B, p=0.1415. The cockle extract treatment reduced the population of $CD8^+$ T_{reg} cells by three times more than the treatment with cisplatin as can be seen by the grey bar in figure 5.13- B. Whelk extract treatment resulted in a decrease in the percentage of $CD8^+$ T_{reg} cells in comparison to the control sample as can be identified by the yellow bars in figures 5.13- A and 5.13- B, p=0.1845. The whelk extract treatment resulted in two times larger a decrease in the population percentage of $CD8^+$ T_{reg} cells in comparison to the cisplatin treatment (light blue bar figure 5.13- B). The cisplatin treatment resulted in a decrease in the percentage population of $CD8^+$ T_{reg} cells in

comparison to the control which can be seen by the orange bar in figure 5.13- A and the dark blue bar in figure 5.13- B, p=0.2302.

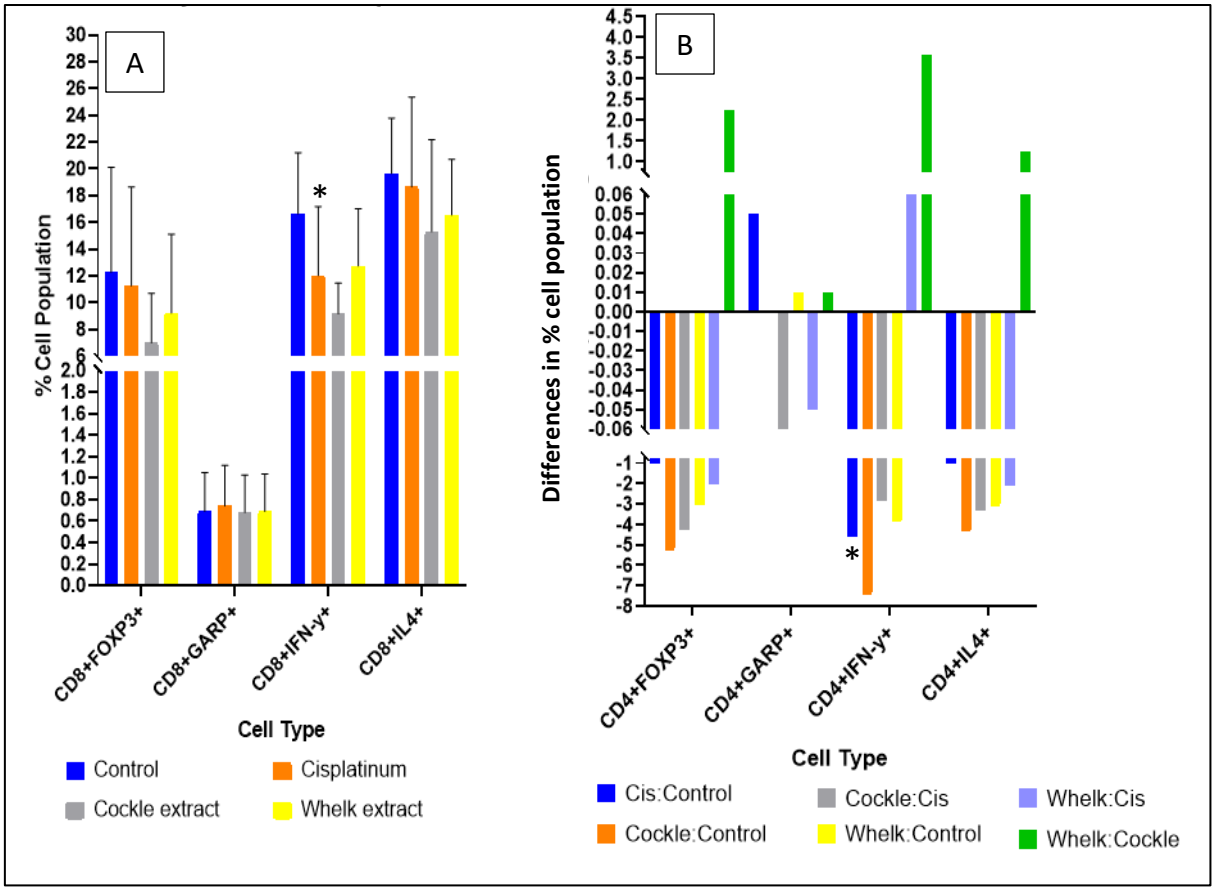

Figure 5.13. A - Average $CD8^+$ cell types (FOXP3, GARP, IFN-γ and IL-4) in stimulated PBMCs. Average percentage $CD8^+$ cell type graph for stimulated PBMCs. Figure 5.13. B - Average differences in $CD8^+$ cell type percentage in stimulated PBMCs. Average percentage differences in $CD8^+$ cell type and treatment comparison graph for stimulated PBMCs; showing differences in cell type against treatment comparisons between the three treatment types and the untreated control cells. Percentage difference in cells was calculated based on the comparison treatment e.g. where cis: whelk is a comparison of the whelk extract cell population to the cell population in cisplatin treated cells. Both figures represent stimulated PBMCs treated with the IC50 dose of cisplatin, cockle extract and whelk extract (6 µg/ml, 12 µg/ml and 12 µg/ml respectively). Control/ untreated cells were used as a comparison. Using an incubation period of 3-days. Where N=3, percentage cell type or difference was in relation to the lymphocyte $CD8^+$ population and error bars show SEM. Significance denoted by *, absence of * indicates no significance.

Whelk extract treatment resulted in a mean fluorescence in $GARP^+CD8^+T_{reg}$ cells equal to that of the control as can be seen by the lack of yellow bar in figure 5.14 (p=0.5416). Both treatment with cisplatin (p=0.3504, orange bar, figure 5.14) and the cockle extract (p=0.5,

grey bar, figure 5.14) resulted in increases in mean fluorescence of $GARP^{+}CD8^{+}T_{reg}$ cells post treatment.

Treatment with cisplatin resulted in a decrease in the mean fluorescence of IFN-$\gamma^{+}CD8^{+}T_{reg}$ cells in comparison to the control cells (p=0.9234, orange bar, figure 5.14). The mean fluorescence of IFN-$\gamma^{+}CD8^{+}T_{reg}$ cells increased post treatment with the cockle extract (p=0.3804, grey bar, figure 5.14) and post treatment with the whelk extract (p=0.8016, yellow bar, figure 5.14).

The mean fluorescence of IL-$4^{+}CD8^{+}T_{reg}$ cells increased post treatment with cisplatin (p=0.9978, orange bar, figure 5.14), the cockle extract (p=0.5544, grey bar, figure 5.14) and the whelk extract (p=0.8219, yellow bar, figure 5.14). With the cockle extract treatment resulting in the highest increase in mean fluorescence of IL-$4^{+}CD8^{+}T_{reg}$ cells.

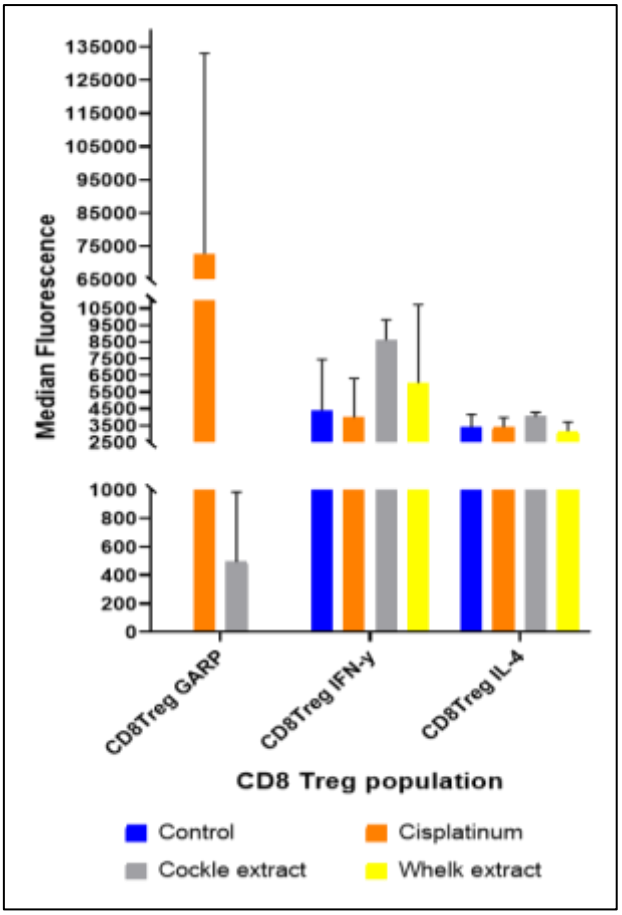

Figure 5.14 The average median fluorescence of biomarker/ cytokine levels in stimulated $CD8^{+}T_{reg}$ cells. The average median fluorescence of biomarker/ cytokine levels in stimulated $CD8^{+}T_{reg}$ cells obtained from the histogram gating system observed in figure 5.2. Average data obtained from stimulated PBMCs treated with IC50 values of cisplatin (6 µg/ml), cockle extract (12 µg/ml) and whelk extract (12 µg/ml), with an incubation period of 3-days and N=3. Graph displayed was created using Prism 8.0 software. Error bars show SEM, significance is denoted by *, absence of * indicates no significance.

5.4 Discussion

5.4.1 Cytokine and T-regulatory cell response results key findings

- Treatment with both the cockle and whelk extracts exerted little effect on the healthy lymphocyte subpopulations (T-helper and cytotoxic T-cells).
- T-regulatory cell populations experienced significant reductions in population percentage post treatment with both the cockle and whelk extracts in both the stimulated and unstimulated PBMC assays.

- The whelk extract treatment significantly reduced the population of IFN-γ^+ T-helper cells in the stimulated PBMCs. While the cockle extract treatment significantly increased the population of IFN-γ^+ T-helper cells in the unstimulated PBMCs.
- Both the cockle and whelk extract treatments significantly reduced mean fluorescence of IFN-γ^+ cytotoxic T_{reg} cells.

5.4.2 Discussion

Cancer cells possess the ability to alter the tumour microenvironment in order to become immunosuppressive (Sompayrac, 2015), therefore understanding how a potential anti-cancer treatment interacts with immune cells and the production of cytokines has become more important in recent years. Cancer cells create the immunosuppressive tumour microenvironment through increased production of T_{reg} cells, which subsequently increase the production of TGF-β and IL-10 (Facciabene et al., 2012; Elkord, 2010). Raised levels of T_{reg} cells have been linked to poor prognosis in cancer patient and can also negatively impact on immunotherapy thus aiding the progression of cancer (Elkord, 2010). T_{reg} cells can be identified through the expression of the winged-helix transcription factor FOXP3 (Lal and Bromberg, 2009), as the transcription factor is essential for the development and function of T_{reg} cells (Wang et al., 2009; Probst-Kepper et al., 2009). Various intracellular signalling molecules and extracellular stimuli can also affect the function and development of T_{reg} cells such as IFN-γ and IL-4; this is achieved through the regulation of FOXP3 and their effects on the cells of the immune system (Lal and Bromberg, 2009). Probst-Kepper et al., (2009) also identified the presence of a transmembrane protein known as glycoprotein A repetitions predominant (GARP) which could be linked to the suppressive nature and identification of T_{reg} cells. The effect of cockle and whelk derived GAGs on Treg cells was unknown therefore an aim of this research was to identify the effects of the marine mollusc derived GAGs on the levels of Treg cells in both unstimulated and stimulated (vastly proliferating) PBMCs.

Interferon-gamma (IFN-γ) is a cytokine which is secreted by T-cells such as NK cells and activated T-helper and cytotoxic T-cells (Mojic, Takeda and Hayakawa, 2018; Boehm et al., 1997). IFN-γ is known to play a role in various cellular functions which include apoptosis and cellular proliferation (Boehm et al., 1997). IFN-γ also has an involvement in the phosphorylation of STAT1 which ultimately leads to interactions with a FOXP3 promotor in T-helper cells (Lal and Bromberg, 2009), this interaction stimulates the expression of FOXP3 and

therefore upregulates T_{reg} cell development. Interleukin-4 (IL-4) is a cytokine which is secreted by activated T-cells, basophils and mast cells (Hou et al., 1994), which play an important role in the immune system (Takeda et al., 1996). IL-4 also plays a vital role in the balance of T-helper cells (Hou et al., 1994). IL-4 also promotes the phosphorylation of STAT6 which exerts an inhibitory effect on the expression of FOXP3 therefore can be deemed as an opposing cytokine to IFN-γ in its effects on T_{reg} cells (Lal and Bromberg, 2009). It is now known that the presence of GAGs on all surfaces allows the interaction of GAGs with cytokines and the interaction of GAGs with cytokines is now thought to play a role in the regulation of cytokine activity and biological action (Fernandez-Botran, Yan and Justus, 1999). Therefore this research also aimed to determine the effects of the novel GAGs isolated from the common cockle and common whelk on IFN-γ and IL-4 cytokine levels.

In the unstimulated PBMC assays both the cockle and whelk extracts exerted small but significant decreases in the percentage population of lymphocytes (figures 5.3 and 5.4) ($p= 0.045$ and $p= 0.0497$ respectively). While in the cytotoxic T-cell, T-helper cell, GARP, IFN-γ, IL-4 and FOXP3 populations experienced very little non-significant effects post treatment with both the cockle and whelk extracts. In the population of GARP positive and IFN-γ T-helper populations cell both the cockle and whelk extract treatments resulted in non-significant increases in the population percentage (figure 5.5). In the IL-4 positive population of T-helper cells both the cockle and whelk extract treatment resulted in non-significant reductions in population percentage. Treatment with both the cockle and whelk extracts resulted in significant decreases in the percentage population of T_{reg} cells ($p= 0.0362$ and $p= 0.0199$ respectively), with the whelk extract treatment resulting in the largest reduction in population percentage. In the mean fluorescence of the T_{reg} cell populations (figure 5.6) both the cockle and whelk extracts resulted in decreases in the fluorescence of GARP. The mean fluorescence of IFN-γ in the T_{reg} cell population increased post treatment with both the cockle and the whelk extracts. Treatment with the whelk extract resulted in an increase in the mean fluorescence of IL-4 in the T_{reg} cell population, while treatment with the cockle extract resulted in a decrease in the mean fluorescence. In the cytotoxic T-cell populations (figure 5.7) positive for IFN-γ and IL-4 treatment with both the cockle and whelk extract resulted in non-significant decreases in the population percentage of the cytotoxic T-cell population. Treatment with the cockle extract resulted in a non-significant increase in the population of

cytotoxic T-cells positive for GARP, while the whelk extract treatment resulted in a non-significant decrease in the population percentage of cytotoxic T-cells positive for GARP. In the $CD8^+$ T_{reg} cells both the cockle and whelk extract treatments resulted in significant decreases in the population percentage ($p= 0.0477$ and $p= 0.0361$ respectively). Both treatment with the cockle and whelk extracts resulted in an increase in the mean fluorescence (figure 5.8) of GARP in the $CD8^+$ T_{reg} cells. The mean fluorescence in the $CD8^+$ T_{reg} cells of IL-4 and IFN-γ decreased post treatment with both the cockle and whelk extracts. The decrease in IFN-γ mean fluorescence was significant post treatment with both the cockle and whelk extracts ($p= 0.0027$ and $p= 0.0011$ respectively).

In the unstimulated PBMCs the reduction noted in IFN- γ post treatment with the whelk extract, could suggest a decrease in T_{reg} cell potency, while the increase in IL-4 populations could indicate potential increases in FOXP3 production. The information obtained from the study suggests that the whelk extract may inhibit the immune evasion of cancer through its reduction in T_{reg} cells also through its reduction in cytokine populations which play a role in immune evasion and prevention of cells death. The cockle extract treatment also results in reductions in those cell types and cytokines however in certain cases the reduction was small in comparison to the whelk extract treatment and the control treatment cisplatin. Both GAG extract treatments appear to reduce the population of cytotoxic T-cells positive for IL-4 and IFN- γ, but this reduction is not significant and would be unlikely to promote a phenotypic change in cytotoxic T-cells. The results obtained from the whelk extract treated unstimulated PBMCs could suggest a potentially beneficial novel GAG treatment which could help with the prevention of immune evasion of cancer, which supports the suggestion of Basappa et al., (2012) that GAG chains may exhibit anti-cancer properties whilst exerting minimal side effects.

In the stimulated PBMC assays both the cockle and whelk extract resulted in decreases in the population percentages of lymphocytes, cytotoxic T-cells and IFN- γ (figures 5.9 and 5.10). Whilst the treatment with both GAG extracts resulted in increases in the population percentages of T-helper cells (figure 5.11) and IL-4. In the GARP positive population of the stimulated PBMCs the cockle extract treatment resulted in an increase in the population percentage and treatment with the whelk extract resulted in a decrease in the percentage population. Treatment with both the cockle and whelk extracts resulted in decreases in the

percentage population of both GARP positive T-helper cells and in T_{reg} cells. With the decreases in the T_{reg} cells treated with both the cockle and whelk extracts being significant (p= 0.0145 and p= 0.0191 respectively). Post treatment with the cockle extract the population percentage of IL-4 positive T-helper cells and IFN- γ positive T-helper cells was increased. The IL-4 positive population of T-helper cells was also increased post treatment with the whelk extract, whilst the population of IFN- γ positive T-helper cells was significantly decreased post treatment with the whelk extract (p= 0.0156). The mean fluorescence of the T_{reg} cells (figure 5.12) of IFN- γ increased post treatment with both the cockle and whelk extracts. Treatment with the cockle extract resulted in increases in the mean fluorescence of both IL-4 and GARP in the T_{reg} cell population. Whelk extract treatment resulted in decreases in the mean fluorescence of both IL-4 and a significant decrease in the mean fluorescence of GARP in the T_{reg} cell population (p= 0.0354). In the population of GARP positive cytotoxic T-cells the cockle extract treatment did not exert an effect on the population percentage, whilst treatment with the whelk extract resulted in a small increase (figure 5.13). Treatment with both the cockle and whelk extracts resulted in decreases in the population percentages of IFN- γ, IL-4 positive cytotoxic T-cells and $CD8^+$ T_{reg} cell populations. Both the cockle and whelk extract treatment resulted in increases in the mean fluorescence of IFN- γ, GARP and IL-4 in the $CD8^+$ T_{reg} cell populations (figure 5.14).

The results from this study suggest that both the cockle and whelk extracts may provide a therapeutic treatment method that results in small effects on vastly proliferating lymphocytes. The GAG extract treatment exerted reductions in T_{reg} cells which may suggest that the treatment with the extracts could prevent the immune evasion of cancer cells. The decrease in the percentage of cytotoxic T-cells may be linked to the decrease in the percentage of IFN- γ cells post treatment with both GAG extracts and may result in less proliferation or apoptosis in treated cells. While the increase in the percentage of IL-4 may be linked to the increase in the percentage of T-helper cells post treatment with the GAG extracts.

The results from the cytokine and T_{reg} response assays show that the novel marine mollusc derived GAG extracts, in particular the whelk extract, resulted in a significant decrease in the percentage of T_{reg} cells (in both stimulated and unstimulated PBMCs). Which could suggest that treatment with the GAG extracts could help to reduce the immune evasion of tumour

cells. Since raised T_{reg} levels have been linked to the progression and immune evasion of cancer (Bayer and Schultze, 2006). The results of this research also support the theory put forward by Aldairi, Ogundipe and Pye (2018) and Ogundipe (2015) that the marine molluscs GAGs derived from the common cockle and whelk appears to target cancer cells but shows some selectivity towards healthy lymphocytes.

CHAPTER 6- DISCUSSION

6.0 Discussion and clinical significance

6.1 Overview of main research findings

This study for the first time has provided a significant insight into the effects of novel GAG compounds isolated from the common cockle and the common whelk on healthy lymphocytes (both activated and naïve). This research has also identified for the first time the activity of the novel cockle and whelk GAG extracts on the lymphoblastic lymphoma cell line (U698). This thesis research has also independently confirmed the cytotoxicity of the cockle and whelk extracts on the acute lymphoblastic leukaemia cell line (MOLT-4) and chronic myeloid leukaemia cell line (K562) previously published by Aldairi, Ogundipe and Pye (2018) and Ogundipe (2015). An overview summary of the main research findings and implications follow:

- Cancer cell line responses: Cockle and whelk extracts exerted a significant and profound inhibitory effect (proliferation) on both the MOLT-4 and U698 cell lines (MTT assay) and further confirmed via the (CFSE proliferation assay). Building on mechanism of action; both the cockle and whelk extracts exerted significant induction of apoptosis in the MOLT-4 and U698 cell lines (annexin V apoptosis assay).
- In contrast, marine GAGs induced relatively minimal proliferation inhibition in both the naïve and stimulated PBMCs (MTT assay). To consider in further detail:
    - Naïve PBMC responses: The whelk extract induced minimal apoptosis for all cell families tested. Both cockle extract and cisplatin treatment did show inhibition of naïve healthy lymphocytes, but the cockle extract was more favourable than the standard cisplatin with less apoptosis induction. In the very sensitive proliferation assay (CFSE/FACS) both cockle and whelk extracts exerted a proliferative effect in some T-helper and cytotoxic T-cell subpopulations indicating the marine GAGs tested are unlikely to negatively impact function of healthy naïve immune cells, and therefore provide an improved therapeutic approach over current standards.
    - Activated PBMC responses (T helper and cytotoxic): Whelk extracts exerted little effect on the T-helper cell populations, but induced apoptosis in the

cytotoxic T-cell populations. Cockle extract induced less apoptosis in the cytotoxic T-cell populations compared to the whelk extract and cisplatin treatment. These findings (for both cockle and whelk extracts) were confirmed via the proliferation assays in some subpopulations of T-helper cells and cytotoxic T-cell populations. These findings indicate the marine GAG actions may have impact on an already activated immune system e.g. during an infection and thus, similarly to standard chemotherapy treatments may compromise immune memory to pathogens and clearance of infections.

- Lymphocyte cytokine responses: Marine GAG extracts exerted little influence on helper T-cell cytokines in naïve or activated healthy lymphocyte population. GAG action on TH1 and/or CD8/CTLs, reduced memory TH1 activity while raising TH1 activity in naïve cells. The likely clinical outcome of this is reduced effective immune responses during a pre-established infection while undergoing therapy, while not influencing naïve T-cell functions.
- T-regulatory cell responses: T_{reg} numbers were significantly reduced post treatment with both the cockle and whelk extracts in both naïve and stimulated PBMCs. This reduced regulation of immunity may prove beneficial and provide protective action to reduce tumour immune evasion seen in various forms of cancer (Elkord et al., 2010)

6.2 The role of glycosaminoglycans in biological processes

Glycosaminoglycans (GAGs) and Proteoglycans (PGs) are located in the ECM of all cells, PGs are made up of a protein core with covalently bonded GAG chains, the specific sulphation pattern present on the GAG chains are thought to be responsible for the regulation of several physiological functions including: development, inflammation and immunity and pathological processes such as: cancer, inflammation, Alzheimer's disease as well as bacterial and viral infections (Morla, 2019; Ghatak et al., 2015). GAGs play a crucial role in the maintenance of the structural integrity of both cells and tissues and have also shown to interact with chemokines, interleukins and pro-inflammatory cytokines such as IFN-γ (Varki et al., 2009: Proudfoot et al., 2001). Interactions with the GAG chains on endothelial cell surface PGs contribute to the localisation of chemokines and in the formation of a concentrated immobilised gradient of chemokine which facilitates the migration of leukocytes towards a site of inflammation or injury (leukocyte chemotaxis) (Proudfoot et al., 2017: Springer, 1995).

Chemokine-GAG interaction also contribute to the physical adhesion-resistant barrier function of the glycocalyx (carbohydrate coating of cells) and mediates the cell-cell interactions required for leukocyte adhesion and transmigration (Nikitovic et al., 2008: Constantinescu, Vink and Spaan, 2003). HS interacts with cytokines through ionic interactions between the basic amino acids present on the cytokines and the GAG sulphated domain (Pye et al., 1998). Longer chain GAGs have shown to exert a higher affinity for chemokines in comparison to short chain GAGs (Ziarek et al., 2013). The sulphation pattern of GAGs is also a crucial factor for GAG binding of chemokines e.g. 2-O-de-sulphation of heparin results in significant loss of chemokine affinity (Ziarek et al., 2013).

The research of Carter, Ali and Kirby (2003) investigated the role of the modulation of HS sulphation in endothelial inflammation. Cater, Ali and Kirby (2003) identified that N-deacetylase/N-sulfotransferase (NDST) upregulation played an important role in the activation of endothelial cells during the process of inflammation and that stimulation with proinflammatory cytokines TNF-α and IFN-γ resulted in significant changes to NDST-1 and NDST-2 expression in the HMEC-1 endothelial cell line. These changes correlated with structural changes in HS on the cell surface (Carter, Ali and Kirby, 2003). Carter, Ali and Kirby (2003) concluded that the biological activity of chemokines can be increased through the appropriation of chemokines to cell surface GAGs, which is essential in chemokine mediated migration of leukocytes across cell monolayers. Post translational modifications (PTMs) of chemokines is also known to affect their interactions with GAGs, therefore PTMs in chemokines could be a potential mechanism for the regulation of chemokine-dependent cell migration (Barker et al., 2017).

Wound healing is a highly regulated process with several overlapping phases resulting in the regaining of tissue integrity (Menke et al., 2007). Failure in the regulation of wound healing can result in pathological conditions such as fibrosis and can lead to organ failure and ultimately death (Misra et al., 2011). In the process of wound healing the ECM not only provides structural support for the tissue but is also a platform for the regulation of inter- and intra- cellular signalling (Bissell, Hall and Parry, 1982). ECM molecules such as Hyaluronan (HA), PGs such as veriscan and aggrecan and receptors, such as the HA receptor CD44, play a role in the regulation of wound healing (Ponta, Sherman and Herrlich, 2003). PGs are involved in multiple processes associated with wound healing, versican-V3 (CS-PG) is associated with

the transformation of fibroblasts into myofibroblasts, perlecan (HS-PG) is associated with the induction of angiogenesis, while the syndecans -1 and -4 (HS-PG) also stimulate angiogenesis and the migration of keratinocytes and endothelial cells to the wound site in murine models (Cattaruzza and Perris, 2005). In wound healing concentration of GAGs are adjusted depending on the stage of the inflammatory response, in the initial stages of inflammation production of HA by fibroblasts is high and is followed by increases in both CS and DS PGs (Clark, 1998). As the rate of proliferation slows in the later stages of inflammation the volume of HS PGs increases at the wound site (Clark, 1998). Proteases also degrade the PGs which releases GAG fragments also aiding with the modulation of wound healing (Peplow, 2005). The presence of HS in the wound site contributes to the release of proangiogenic factors such as IL-1 and IL-6 (Taylor and Gallo, 2006: Ortéga, L'Faqihi and Plouët, 1998). Due to its presence on almost all cell types HA plays a crucial role in many biological processes such as cell signalling, pathobiology and wound repair and regeneration (Ghatak et al., 2015: Chen and Abatangelo, 1999). HA effects on cells can be regulated through interactions with its receptors CD44 and RHAMM, through these interactions activation of intracellular signalling pathways can occur (Misra et al., 2011). The receptors CD44 and RHAMM are also associated with the injury and repair of tissues as well as cancer cell growth and metastasis (Ghatak et al., 2014: Ponta, Sherman and Herrlich, 2003). During the inflammatory phase HA regulates the early inflammatory response through the concentration of HA in the wound bed, regulation occurs through; modulating both inflammatory cell and fibroblast migration to the wound site, the synthesis of proinflammatory cytokines and phagocytosis of microbes (Chen and Abatangelo, 1999). In the reparative/remodelling phase of wound healing granulation tissue, containing endothelial cells, fibroblasts, PGs ad GAGs, fills the wound in order to protect the wound from the environment and to support capillary growth and the formation of collagen and fibronectin, which must occur before epithelial cells can migrate across to the new tissue (Clark, 1998). However excessive accumulation of fibronectin, collagen, PGs and GAGs or failure to remove HA fragments can lead to unremitting inflammation and the development fibrotic scar tissue (Li et al., 2011). Due to its viscoelastic and hydrated domain properties HA can also be used for exogenous application to promote tissue repair and regeneration, such as can be seen in the acceleration of wound healing post exogenous application of HA to corneal epithelial injury (Nakamura, Hikida and Nakano, 1992). It has also been demonstrated that HA is produced by malignant cells in order to promote tumorigenic

properties, CD44-V6 is also overexpressed in many cancers and the interaction between HA and CD44-V6 plays a crucial role in the onset, survival and growth of many cancers (Misra et al., 2011).

Inflammation is a mechanism of defence utilised by the body to protect against harmful stimuli (Parish, 2006). The events which occur during the inflammatory process are regulated by GAGs especially those present on the surface of endothelial cells and leukocytes (Parish, 2006). GAGs play a crucial role in leukocyte rolling, the regulation of chemokine migration and activation and in leukocyte migration (Parish, 2006). At the injury or infection site macrophages release cytokines and stimulate the activation of endothelial cells which results in P-selectin being displayed (Moore et al., 1995). Activated endothelial cells displaying P-selectin bind with the P-selectin glycoprotein ligand (PSGL-1) on endothelial cells enabling the leukocytes to adhere to the endothelial layer (Moore et al., 1995). The first role of GAGs in inflammation is to regulate leukocyte rolling, this is done through HS on the surface of endothelial cells binding L-selectin on leukocytes (Parish, 2006). Cytokines and chemokines such as IL-8 are released at the site of injury/ infection by macrophages and bind with GAGs on the surface of endothelial cells and leads to cytokine transcytosis (Webb et al., 1993). Syndecan, a HSPG, plays a major role in the migration process, while heparin which is produced and stored in mast cells upon inflammation is co-released with histamine and aids with vascular permeability (Theoharides et al., 2012). Inflammatory responses can be regulated through the proteolysis of chemokines, GAGs can provide protection for chemokines from proteolytic degradation thus GAGs play a role in the regulation of inflammatory responses (Ziarek et al., 2013: Sadir et al., 2004). Protection of chemokines by GAGs could be through steric blockade from the protease binding site or stabilisation of chemokine oligomers may also be responsible (Liang et al., 2016: Ziarek et al., 2013). Therefore GAG protection of chemokines from proteolysis could provide a mechanism for the regulation of intensity and duration of an inflammatory response (Ziarek et al., 2013). Cells shed GAGs in many pathological conditions which could inhibit chemokine-receptor interactions and subsequently inflammatory responses (Sarrazin, Lamanna and Esko, 2011). Interactions between GAGs and chemokines also have the potential for use in the delivery of therapeutics, the encapsulation of chemokines in GAG-containing hydrogels has been reported to preserve the activity and controlled release of the chemokine in order to promote

wound healing (Lohmann et al., 2017: Wang et al., 2013). As GAGs play a vital role in the inflammatory process exogenous sulphated GAGs can be used to down regulate inflammation (Morla, 2019). Heparin has been identified as a potent anti-inflammatory product, for the treatment of bronchial asthma, ulcerative colitis and in burns, in animal models, however due to its anticoagulant properties the risk of bleeding is deemed too high for its use as an anti-inflammatory (Tyrrell et al., 1999). A heparin isolated from shrimp has been found to reduce acute inflammation upon injury through the reduction of the migration of inflammatory cells to the site of injury and has also been found to be non-anticoagulant (Brito et al., 2008). While exogenous DS was found to inhibit P-selectin in inflammation in murine models (Kozlowski, Pavao and Borsig, 2011).

Interactions between cytokines, growth factors and growth factor receptors and GAGs have been implicated in the growth progression and metastasis of cancer (Afratis et al., 2012). GAGs, such as HSPGs, also play a crucial role in multiple signalling cascades which are essential for angiogenesis and the invasion and metastasis of cancer, while other GAGs have been identified as potent inhibitors of tumour progression (Theocharis et al., 2010). Levels of HS in certain cancers are reduced as HS has the ability to promote cell-cell and cell-ECM adhesion thus inhibiting the invasion and metastasis of cancer cells (Nikitovic et al., 2010). While in other cancers reduced levels of HS and alterations in sulphation patterns resulted in increased invasive activity of malignant cells and thus the promotion of tumour progression (Nikitovic et al., 2010). Overexpression of heparinase (HSPE), an enzyme which cleaves HS from HSPGs at the β -1 and -4 positions, has been implicated in the promotion of tumour growth and metastasis and tumour angiogenesis (Sistla et al., 2019). CS and DS have also been shown to have essential roles in the regulation of proliferation, apoptosis, cell migration and adhesion and cellular invasion (Mikami and Kitagawa, 2013). Increased levels of versican (CSPG), with altered sulphation patterns in the CS GAG chains, is related to the progression of early stage breast and prostate cancer (Ricciardelli et al., 1998). Growth factors and chemokines present in tumour microenvironments increase the production of HA, increased levels of HA have also been noted in multiple types of human cancers such as breast, ovarian and lung (Tammi et al., 2011: Auvinen et al., 2000). Heparin has demonstrated anti-cancer properties as well as anticoagulant activity (Borsig, 2010). A non-anticoagulant HS isolated from a bivalve mollusc which inhibits P-selectin-mediated activities like metastasis in Lewis lung carcinoma cells

(Gomes et al., 2014). Heparinase inhibitor Roneparstat has been shown to reduce tumour size significantly in preclinical murine models (Ritchie et al., 2011). Necuparanib is a non-anticoagulant HS and exerts its anti-cancer activity through the inhibition of multiple targets: heparinase, VEGF, FGF 2 and P-selectin which are involved in tumour progression and metastasis. Heparinase 1 (hep 1) and heparinase 3 (hep 3) produce different GAG fragments from the tumour cell surface, hep 1 fragments were found to promote tumour growth while hep 3 fragments inhibited tumour cell growth and metastasis (Liu et al., 2002). Fucosylated CS (FucCS) sourced from sea cucumber was found to block P- and L- selectin mediated activities thus inhibiting malignant cell metastasis (Borsig et al., 2007).

Our marine mollusc derived GAGs may work in a similar way through interacting with growth factors such as VEGF and FGF, or through interactions with P- and L-selectin thus inhibiting cellular processes responsible for malignant cell growth and metastasis. It is difficult to completely identify why the marine mollusc (cockle and whelk) derived GAGs are exerting specific activity in cancer cells, with minimal activity in health lymphocytes, as the overall structure of the isolated GAGs remains unknown. However as identified by Zhang (2010) and Ghatak et al., (2015) the level and pattern of sulphation in GAGs can affect the activity and function of GAGs, thus this could be a potential factor resulting in the cockle and whelk derived GAGs being uniquely potent inhibitors of the leukaemia and lymphoma cell lines tested in comparison to the activity noted in the healthy lymphocytes and the lack of activity noted by Aldairi, Ogundipe and Pye, 2018 and Ogundipe 2015 in commercially available mammalian GAGs tested on cancer cell lines.

Due the heterogenicity of GAGs complete characterisation can be problematic and so GAG mimetics are expected to alleviate this problem and are also predicted to act in a more selective manner with potentially fewer side effects (Mohamed and Coombe, 2017). There are two classes of GAG mimetics which are saccharide based, less heterogenous in comparison to GAGs and built on a sugar backbone, and non-saccharide based, homogenous and built on a non-sugar based backbone with negative charge coming from sulphates, sulfonates, carboxylates and/or phosphates (Desai, 2013). Non-saccharide based mimetics are also thought to be advantageous in comparison to saccharide based mimetics. Both saccharide and non-saccharide mimetics have been developed for the treatment of cancer and inflammation with some already being used in the clinic and others going through the

process of clinical trials (Desai, 2013). Non-anticoagulant heparin mimetics have been developed such as 2-O,3-O-desulfated heparin (ODSH) which does not produce anticoagulant effects but has shown to reduce inflammation in the airways though inhibiting neutrophil elastase (Griffin et al., 2014). Phosphomannopentase sulphate (PI-88) is a HS mimetic developed to inhibit heparinase which is an enzyme with a vital role in angiogenesis and cancer cell metastasis (Khachigian and Parish, 2004). PI-88 was found to inhibit proangiogenic factors VEGF, FGF -1 and -2 through the out competing HS. In addition to the anti-cancer activity noted PI-88 also exhibited anticoagulant action, however although well tolerated in pre-clinical trials, failure to reach a primary disease free survival end point ended clinical trials at the phase 3 stage (Lanzi and Cassinelli, 2018). PG-545 is an analogue of PI-88 and is homogenous with a lipid moiety at the reducing end, pharmacokinetic properties of PG-545 were increased in comparison to PI-88 and the anticoagulant activity was also reduced (Dredge et al., 2011). The lipid moiety was found to bind the hydrophobic pocket of heparinase and demonstrated a higher affinity for heparinase and demonstrated potent anti-tumour and anti-metastatic activity in pre-clinical models (Hammond, Handley, Dredge and Blytheway, 2013). Other HS mimetics have been developed which have shown to be potent inhibitors of growth factors such as FGF and VEGF and which can also inhibit P-selectin all of which are implicated in inflammation and metastasis (Freeman et al., 2005).

6.3 MTT/ cell viability assay

Research has identified the medicinal properties of marine GAGs in both *in vitro* and *in vivo* models (de Jesus Raposo, 2015). Studies have also shown the cytotoxic effects of some GAG like compounds such as low molecular weight heparin and HS mimetics (Afratis et al., 2012). GAG like compounds isolated from the common cockle have also demonstrated anti-cancer properties in the leukemic cell lines K562 and MOLT-4 as well as in some breast cancer cell lines (Aldairi, Ogundipe and Pye, 2018). No current study had identified the therapeutic properties of marine mollusc derived GAGs on the lymphoblastic lymphoma cell line U698 or in healthy lymphocytes (activated or naïve).

The standard put forward by the National Cancer Institute dictates that a crude natural product extract can be deemed to be active against the tested cell line if the IC50 value is 20 µg/ml or lower (Swaya, Aduma, Chelimo & Were, 2017; Chen et al., 1988). In this research

GAGs isolated from the common cockle and the common whelk had a significant inhibitory effect on the cell viability in both the MOLT-4 and U698 cell lines. In the MOLT-4 cell line, cell viability was reduced by up to 80% and 90% post 3-day incubation with the cockle and whelk extract the respectively, the recorded IC50 values were 15.56 µg/ml and 10.4 µg/ml respectively as can be seen in figures 3.2 and 3.3 and table 3.1. Cell viability in the U698 cell line was significantly reduced by both the cockle and whelk extract treatment (p= 0.0117 and p= 0.0001 respectively), with IC50 values ranging 7.51 µg/ml and 102.55 µg/ml (table 3.3). U698 cell line viability was reduced by up to 90% post treatment with both the cockle and whelk extracts (figures 3.8 and 3.9). There were some anti-proliferative effects noted in the K562 cell line post treatment with the cockle and whelk extracts. With cell viability inhibitions of up to 50% and Ic50 values ranging 32.8 µg/ml and 186.06 µg/ml (Figures 3.5 and 3.6 and table 3.2). Cell viability in the K562 cell line was reduced significantly post 3 day incubation period with the whelk extract, with an IC50 value of 71.49 µg/ml (p=0.047). The IC50 value obtained for the K562 cell line treated with the cockle extract increased post 5 day incubation in comparison to the 4 day incubation period, suggesting potential immunity towards the cockle extract treatment had developed in the cell line. Remarkably neither the cockle or whelk GAG isolates appeared to exert much of a cytotoxic effect on the healthy lymphocytes (either active or naïve), with both extracts failing to reduce cell viability by 50% and thus no IC50 value was obtained (tables 3.4 and 3.6; figures 3.11, 3.12 3.17, 3.18). This would suggest that the cytotoxic effects identified in the cancer cell lines in response to the novel GAG compounds appeared to be acting in a selective manner towards the MOLT-4, K562 leukemic and U698 lymphoma cell lines and appeared non-toxic to the healthy lymphocytes either the naïve or proliferating lymphocytes (stimulated). The seemingly selective nature of the GAG compounds would have been interesting to have explored further, that however was beyond the scope of this research, but should be considered in future work to further explore the possibility of the therapeutic use of mollusc derived GAG compounds in the clinic.

The results obtained from the MTT assays identified recorded IC50 values of less than 20 µg/ml for both the MOLT-4 and U698 cell lines treated with both the cockle and whelk extracts. Thus according to the guidelines set by the National Cancer Institute both the cockle and whelk extracts can be categorised as an active anti-leukemic and anti-lymphoma cancer drug. Interestingly neither the cockle or whelk extracts exerted enough of a cytotoxic effect

on either the naïve or activated healthy lymphocytes and can therefore be deemed as inactive against healthy lymphocytes.

Our data supports that found by Aldairi, Ogundipe and Pye (2018) that the mollusc derived GAGs appear to show specificity towards the leukemic and lymphoma cells and has also demonstrated a lack of activity towards the healthy lymphocytes. Further supporting the potential therapeutic use of these GAG compounds in the clinic. In this research the effects of cisplatin on PBMCs noted was similar to the anti-proliferative effects noted by Sakai, et al., (2013), however incubation times were different in this research and so there was some level of difference in the noted activity.

Presently there is a pressing interest in finding new anti-cancer drugs which not only improve the patient response to treatment, thus reducing the number of fatal incidences of cancer, but also to find a treatment with reduced side effects. Reports have suggested that certain types of GAG chains have been identified as potentially promising in cancer therapy and are also predicted to have minimal side effects (Basappa et al., 2012; Aldairi, Ogundipe and Pye, 2018). Our data which identified potentially selective activity of the cockle and whelk GAG extracts against leukemic and lymphoma cell lines and healthy lymphocytes, would support this idea. Making the prospect of the therapeutic use of these marine mollusc derived GAGs an even more attractive possibility.

The whelk extract was identified in this research as being the most effective extract in comparison to both the cockle extract treatment and in some cases in comparison to the control treatment cisplatin. The unique activity noted in the whelk extract across a variety of leukemic cell lines and in the U698 lymphoma cell line may prove to be important as a possible intervention in patients with hard to treat cancers. The differences in IC50 values and cell viability reduction between the cockle extract treated cells and the whelk extract treated cells could suggest that the anti-proliferative effect of the whelk extract could be due to unique fine structural features present in the whelk extract. The research carried out by Ogundipe (2015) and Aldairi, Ogundipe and Pye (2018) found that all commercially available GAGs (HS, heparin, CD and DS) had non-toxic activity against cancer cell lines (including K562 and MOLT-4). Suggesting that the cockle and whelk GAG extracts must therefore possess unique structural details which are not present in commercially available GAGs (Ogundipe, 2015).

These unique structures may be a pharmacological feature which could make the cockle and whelk GAG extracts potential candidates as the basis for a new therapeutic anti-cancer treatment. The differences noted in the obtained IC50 values for the MOLT-4, K562 and U698 cell lines and the lack of IC50 values for the naïve or activated heathy lymphocytes treated with the cockle and whelk extracts could suggest that the GAG extracts may be demonstrating some level of selectivity to certain cancer cell types and healthy cells. This potential selectivity could prove important in the use of marine GAGs as a potential anti-cancer therapy.

In cancer cell lines there are changes within the expression of GAGs and proteoglycans in the ECM and on the cell surface which enable the cancer cells to proliferate and metastasize and induce angiogenesis (Koo et al., 2008). Novel exogenous GAG compounds isolated from cockles and whelks, which possess unique structural features in comparison to mammalian GAGs, may therefore modulate the effects of ECM and cell surface GAGs in various ways, which could therefore lead to the reduction in cell viability noted in this research. The novel marine mollusc GAGs could potentially act in various manners; through the activation or inactivation of protein based receptors, through outcompeting endogenous GAGs and/or inhibiting the biosynthesis of GAGs (Gandhi and Mancera, 2010).

Understanding the fine structures and specific biological roles of GAG compounds could potentially lead to the development of novel GAG based therapies (Afratis et al., 2012). In order to further identify the fine structures of the whelk GAG extract, the crude extract was purified via the use of ion exchange chromatography (FPLC) and the resulting fractions were then tested for activity on the cancer cell lines (figures 3.20- 3.40). All eluted fractions appeared to be non-toxic towards the cancer cell lines, with no IC50 values being obtained even at maximum dose. Ogundipe (2015) identified the cytotoxic effects of ‘fraction E’ a breast cancer cell line but also noted a lack of toxicity towards the MOLT-4 and K562 cell lines. The results obtained by Aldairi, Ogundipe and Pye (2018) also suggested ‘fraction E’ of the cockle extract appeared to be the bioactive component responsible for the activity noted in the cockle extract treated cells. However in a similar way to Ogundipe (2015), this research identified no activity in any fraction of the whelk extract against either the MOLT-4, K562 or U698 cell lines. This could be due to low levels of GAGs in the isolated fractions, which could be combatted by doing further FPLC runs using a higher initial weight of the crude whelk extract. It could also be that as demonstrated by Ogundipe (2015) the isolated whelk fractions

are not active in the MOLT-4 or K562 cell lines and may also be inactive against the U698 cell line at low doses. Further understanding into the structural properties of the whelk GAG fractions may potentially open a new therapeutic approach to cancer therapy.

6.4 Annexin V/ propidium iodide apoptosis assay

As cancer is the result of a shift in the balance of cellular proliferation and apoptosis, which is in favour of proliferation, apoptosis has become an interesting target in the development of new anti-cancer therapies (Wesselborg et al., 1999). Apoptosis is a major protective mechanism against cancer, therefore inducing apoptosis has become a target in the search for new therapies which are efficient and exert less side effects in cancer patients (Coppola et al., 2008; Zhou et al., 2009). The process of apoptosis can be characterised through several processes including; cell shrinkage, nuclear chromatin condensation, fragmentation of the nucleus and the formation of apoptotic bodies (Kroemer et al., 1997). During the process of apoptosis the cellular membrane becomes damaged and begins to allow the leakage of phosphatidylserine into the outer membrane layers, which in turn allows the binding of annexin V and eventually propidium iodide can cross the membrane upon the death of the cell (Reiger et al., 2011; Cornelissen et al., 2002; Vermes et al., 1995). This process of leaking and binding allows for the identification of the stage of apoptosis at which the cell is at.

This study demonstrated that in the MOLT-4 cell line both novel GAG extracts (cockle and whelk) exerted significant increases in apoptosis, particularly in the early stages of apoptosis (figure 4.5, $p= 0.0179$ and $p= 0.003$ respectively). Treatment with both the whelk and cockle crude GAG compounds brought about increases in non-apoptotic $CD3^+$ MOLT-4 cells (figure 4.6). The results of this study correspond to the results noted in the MTT assays in chapter 3, with the whelk and cockle extracts exerting significant increases in apoptosis in the MOLT-4 cell line. The results obtained by Ogundipe (2015) identified an increase in early apoptotic MOLT-4 cells post treatment with the whelk extract which corresponds to the results obtained in this research. Aldairi, Ogundipe and Pye (2018) also demonstrated a significant induction of apoptosis in the MOLT-4 cell line with a small but significant increase in late apoptotic MOLT-4 cells post treatment with the cockle extract, this was also independently demonstrated by this research. The increase in $CD3^+$ non-apoptotic MOLT-4 cells could suggest that there may be a level of resistance to the novel GAG compound treatment in a

population of MOLT-4 cells expressing the T-cell biomarker CD3. The results of the MTT assay could also potentially support this as the percentage of viable MOLT-4 cells plateaus at 10-20% post treatment with the whelk and cockle extracts (figures 3.2 and 3.3). It would have therefore been interesting to have delved into potential resistance further and to have tried various doses of the novel GAG compounds in order to identify any potential further action, however this was beyond the scope of this research, but could be an avenue for further future research. In the K562 cell line treatment with both the cockle and whelk extracts resulted in non-significant increases in non-apoptotic cells (figure 4.7). Aldairi, Ogundipe and Pye (2018) suggested that due to the aggregating nature of the K562 cell line, performing flow cytometry assays using the cell line can prove problematic. This could explain the results of the K562 cell line apoptosis assays in this research, however the MTT assays also noted little effect in the K562 cell line assays post a 3 day incubation period with either the cockle or whelk extract treatments. Again had time allowed it could have been enlightening to have tried various doses of the GAG extracts to identify whether either extract could exert an apoptotic effect on the K562 cell line at higher doses. Treatment of the U698 cell line with the whelk GAG compound resulted in a significant increase in apoptotic cells ($p= 0.0426$), with a significant increase in mid stage apoptotic U698 cells ($p= 0.0165$, figure 4.8). The cockle extract treated U698 cells also had a non-significant increase in the percentage of apoptotic cells. The treatment with both novel GAG compounds (cockle and whelk) resulted in non-significant reductions in the percentage of $CD19^+$ U698 cells not undergoing apoptosis. The results of the U698 cell line apoptosis assays correspond to the MTT results with the whelk GAG extract exerting a significant and profound effect on the U698 cells, which was more than those noted in cisplatin treated cells. This was the first time that apoptosis induction had been demonstrated in the lymphoblastic lymphoma cell line (U698) post treatment with the novel GAG compounds.

The results of this research identified the induction of apoptosis in both the MOLT-4 and U698 cell lines post treatment with the novel GAG compounds. This finding is consistent with the research carried out by Erduran et al., (2007) who demonstrated that chemically modified GAG chains and heparin exerted apoptotic effects on lymphoblasts and other carcinoma types. Erduran et al., (2007) also predicted that the apoptotic effects noted on lymphoblasts was exerted via the extrinsic pathway of apoptosis. Levels of caspase 3 and 8 were also

monitored and identified that treatment with heparin induced the apoptosis of lymphoblasts and activated caspase 3 and 8 (Erduran et al., 2007). These researchers concluded that in lymphoblasts low doses of heparin could induce apoptosis significantly and the induction of apoptosis increased with increasing levels of heparin (Erduran et al, 2007). It could be suggested that the viability inhibition noted in the MOLT-4 and U698 cell MTT assays, could be in part due to the induction of apoptosis identified in the subsequent annexin V/ propidium iodide apoptosis assays. The apoptotic effect exerted by both the cockle and whelk extracts noted in the MOLT-4 and U698 cell lines is consistent with the apoptotic effect of low doses of heparin noted by Erduran et al., (2007) on lymphoblasts and may therefore provide an insight into the mechanism of action of the apoptotic effect of these novel GAG compounds.

The unstimulated PBMC assays (figures 4.10- 4.14) identify the whelk extract (in comparison to the cockle extract and cisplatin) as having consistently exerted minimal activity on the overall lymphocyte populations, as well as the subpopulations (naïve and memory) of both the T-helper cells and cytotoxic T-cells. Although in the unstimulated PBMCs the largest effect exerted by the whelk extract was on the memory cytotoxic T-cells, with a significant increase in early stage apoptotic cells ($p= 0.0379$). Cockle extract treated unstimulated PBMCs experienced little apoptotic induction in the lymphocyte and T-helper cell populations. However the cockle extract induced significant levels of apoptosis in the memory cytotoxic T-cells ($p= 0.0399$) and induced more apoptosis than other treatment methods in the naïve cytotoxic T-cells, but this induction was non-significant. In the stimulated PBMC assays (figure 4.15- 4.19) the subpopulations of T-helper cells remained mainly unaffected by treatment with the whelk extract. There was a significant increase in the percentage of apoptotic naïve T-helper cells post treatment with the whelk extract ($p= 0.0429$). In the lymphocytes and subpopulations of cytotoxic T-cells the whelk extract treatment induced more apoptosis than cisplatin, with significant increases in the percentage of early stage apoptotic naïve and memory cytotoxic T-cells ($p= 0.0448$ and $p= 0.0409$ respectively). The treatment with the cockle extract resulted in the least induction of apoptosis across the subpopulations of stimulated PBMCs. In the subpopulations of cytotoxic T-cells the treatment with the cockle extract resulted in the least percentage induction of apoptosis in comparison to the other treatment methods.

In the unstimulated PBMC assays the whelk extract proved to be consistently milder that treatment with either the cockle extract or cisplatin. This could suggest that the whelk extract may be acting in a selective manner towards the cancer cell lines whilst not targeting healthy lymphocytes, as was initially suggested by the MTT assays. This further supports the suggestion that the novel marine mollusc derived GAG extracts could provide a more favourable therapeutic treatment option. Basappa et al., (2012) suggested that certain GAG chains may have the potential to provide a useful therapeutic treatment option in cancer therapy whilst exerting minimal side effects for the patient. The appearance of the selectivity of the whelk extract demonstrated in the unstimulated PBMC and cancer cell line apoptosis assays identify that the whelk GAG extract may further support this suggestion. The stimulated PBMC assays demonstrated that the whelk extract appeared to target the cytotoxic T-cell subpopulations more than the other treatment methods (cisplatin and the cockle extract). The increased activity noted in the cytotoxic T-cells may potentially blunt any immune responses to viral infections during a patient's chemotherapy treatment. Despite these observations, relative changes in the stimulated PBMC assays compared to the potency observed in the cancer cell assays suggests that the novel marine mollusc derived GAG extracts may be able to provide a treatment option that shows specificity towards tumour cells whilst not targeting healthy lymphocytes. It is encouraging to note that the novel GAG compounds may be acting in a more specific manner and may consequently exert fewer side effects for the patient. Manaster et al., (1996) reported that heparin exerted an apoptotic effect on human cells which included neutrophils, lymphoblasts and mononuclear cells. This could also suggest that the increased targeting noted in the stimulated PBMCs, which were vastly proliferating, could be related to the findings Manaster et al., (1996). The results of the apoptosis assays may provide a slight insight into the mechanism of action of the novel GAG compounds, however in future studies it may be worth investigating the levels of caspase 3 and 8 to further the insight into the molecular mechanism associated with the induction of apoptosis in cancer cells and in cytotoxic T-cells post treatment with the novel GAG compounds.

6.5 CFSE proliferation assay

The rapid proliferation of cells is a key characteristic used to describe a malignant transformation (cancer) (Yip, Smollich and Gotte, 2006). Cancer can ensue when the balance

of proliferation and apoptosis is shifted in the direction of proliferation (King and Cidlowski, 1998). There is now ample evidence to suggest that GAGs play an important part controlling the proliferation of normal cells as well as malignant cells (Yip, Smollich and Gotte, 2006). Therefore novel exogenous GAGs, such as the ones isolated from the common cockle and whelk, with unique structural features may be capable of using this activity in various ways resulting in the inhibition of proliferation noted in this study. This inhibition may have occurred through an agonistic or antagonistic mechanism in protein receptors, via outcompeting the endogenous GAGs present on the cell surface and/or inhibiting the biosynthesis of the cell surface GAGs (Gandhi and Mancera, 2010). Cellular proliferation is primarily mediated via the cell cycle (Yang, 2012), there has been interest recently in the development of anti-cancer therapies which aim to target the cell cycle such as anti-metabolites and DNA-damaging drugs (Schafer,1998). Which take advantage of the dysregulation of the normal cell cycle and aim to target cell cycle checkpoints, with the view to inducing cell cycle arrest or apoptosis in malignant cells (Roos and Kaina, 2006). GAG chains, such as HS, on the cell surface of cancer cells have been demonstrated to possess vital roles in many aspects of the phenotype of a tumour, such as development, growth and metastasis (Liu et al., 2002). HS has also been linked to the ability of cancer cells to modulate the process of angiogenesis (Gandhi and Mancera, 2010). Due to the identified activity of HS on tumour cells the avenue of polysaccharide based anti-cancer therapeutics is further being explored by several research groups (Linhardt, 2004).

Whelk extract treatment of the MOLT-4 cell line (figures 4.20 and 4.21) resulted in a non-significant reduction in proliferation but was the only treatment method to exhibit antiproliferative effects in the MOLT-4 cell line. A non-significant proliferative effect on the MOLT-4 cell line was noted post treatment with the cockle extract and cisplatin. Treatment with both the cockle and whelk extracts resulted in a reduction of proliferation in the $CD3^+$ MOLT-4 cell population. Cockle extract treatment exerted a significant antiproliferative effect on the $CD3^+$ MOLT-4 cell line ($p= 0.0424$). In the U698 cell line (figures 4.22 and 4.23) treatment with both the cockle and whelk extracts resulted in significant reductions in the proliferation of the cells ($p= 0.0182$ and $p= 0.0243$ respectively). With proliferation in the U698 cells being less than half that of the cisplatin treated cells post treatment with both the

cockle and whelk extracts. Cockle and whelk extract treatment resulted in significant decreases in the proliferation of the $CD19^+$ U698 cells (p= 0.0487 and p= 0.0487 respectively).

In the unstimulated PBMC populations (figures 4.24 and 4.25) both the cockle and whelk extracts exerted a proliferative effect on lymphocyte, T-helper cell and cytotoxic T-cell populations. The cockle extract treatment resulted in significant increases in the proliferation of naïve T-helper cells (p= 0.0152), the total population of cytotoxic T-cells (p=0.0341) and in the naïve cytotoxic T-cell populations (p=0.0194). Whelk extract treatment resulted in a significant increase in the proliferation of the total cytotoxic T-cell population (p=0.0228). In the stimulated PBMC populations (figures 4.26 and 4.27) the whelk extract treatment resulted in small decreases in the proliferation of the lymphocyte, T-helper and cytotoxic T-cell populations. The decrease in proliferation in the naïve T-helper cell population was significant (p= 0.0384). Treatment with the cockle extract resulted in antiproliferative activity in the T-helper and cytotoxic T-cell sub-populations of the stimulated PBMCs all of which were non-significant.

As was noted with the MTT and apoptosis assays, in the proliferation assays the whelk extract appears to exert the largest effects on the cancer cell lines whilst exerting minimal effects in both the stimulated and unstimulated PBMCs. These results support the findings of Ogundipe (2015) that the whelk extract exerts an antiproliferative effect in cancer cell lines. Basappa et al., (2012) also reported that certain GAG chains could provide a beneficial therapy for cancer patients which were expected to result in fewer side effects, the outcome of this assay would support this theory. The cockle extract treatment also exhibited antiproliferative effects in the U698 cell line and proliferative effects in the unstimulated PBMCs. The cockle extract did however appear to target the vastly proliferating PBMCs more than the whelk extract. GAGs and PGs are present in vertebrates and non-vertebrates and have been attributed to biological and physiological processes in the body (Raman, Ninomiya and Kuberan, 2011; Cross and Claesson-Welsh, 2001), GAGs are also known to play a part in all stages of the progression of cancer (Yip, Smollich and Gotte, 2006). It is therefore thought that exogenous GAGs, such as the novel cockle and whelk GAGs, may interfere with the function of endogenous GAGs and may provide a potential treatment option with fewer side effects (Gandhi and Mancera, 2010). The results of the CFSE proliferation assays along with the MTT and apoptosis assays would support this theory. Many GAG types have been studied as

potential anti-cancer therapies including heparin and heparin analogues as well as HS and CS (Yip, Smollich and Gotte, 2006). The results of this study also suggest that these novel cockle and whelk GAG compounds, which demonstrate unique structural features in comparison to commercially available mammalian GAGs (Khurshid and Pye, 2018), may potentially provide an anti-cancer therapy which could exhibit fewer side effects than current chemotherapy treatments.

6.6 Cytokine and T_{reg} response assay

Cancer cells modify their microenvironment, through the expression of immunosuppressive proteins, including CTLA-4, which provide protection from destruction by cytotoxic T-lymphocytes (Sompayrac, 2015). Cancer cells also stimulate the increased production of T_{reg} cells in the microenvironment (Facciabene et al., 2012; Elkord, 2010), these T_{reg} cells then upregulate the production of TGF-β and IL-10, which further create an immunosuppressive environment in which cytotoxic T-lymphocytes cannot function. The identification of T_{reg} cells can be carried out through the determination of the expression of the fork-headed/ winged-helix transcription factor FOXP3 (Lal and Bromberg, 2009), as the transcription factor is necessary for the development and function of T_{reg} cells (Wang et al., 2009; Probst-Kepper et al., 2009).There are also various extracellular stimuli and intracellular signalling molecules which also aid with the function and development of T_{reg} cells which include; IL-27, IL-4 and IFN-γ, this is done via the regulation of FOXP3 (Lal and Bromberg, 2009). FOXP3 has also been linked to the potency of T_{reg} cells and deficiencies or mutations in FOXP3 can lead to the development of autoimmune diseases (Lal and Bromberg, 2009). Therefore FOXP3 can be used to specifically identify T_{reg} cell populations as its expression on T-helper cells is exclusive to T_{reg} cells (Probst-Kepper et al., 2009). Probst-Kepper et al., (2009) and Wang et al., (2009) identified that glycoprotein A repetitions predominant (GARP), a transmembrane protein, was highly expressed on activated $FOXP3^+$ T_{reg} cells and correlated with the suppressive activity of T_{reg} cells. Poor prognosis and negative responses to immunotherapy have been linked with raised T_{reg} levels in cancer, thus raised levels of T_{reg} cells aids the progression of cancer (Elkord, 2010). Therefore it is important to understand the effects of any potential anti-cancer therapies on cytokine production and T_{reg} cells, this research aimed to determine the effects of the marine mollusc derived cockle and whelk extract on cytokine production and T_{reg} cell levels in unstimulated and stimulated PBMCs.

Interferon- gamma (IFN-γ) is a cytokine which several cell types from both the adaptive and innate immune system produce, but is primarily secreted by thymus derived T-cell including; natural killer cells (NK) and activated T-helper cells and cytotoxic T-cells (Mojic, Takeda and Hayakawa, 2018; Boehm et al., 1997). Thus the cytokine is indispensable to many physiological processes such as; aspects of the immune regulation, cellular proliferation and apoptosis, anti-microbial and anti-viral defence and IFN-γ has also been shown to play roles in pregnancy allergies and cancer (Mojic, Takeda and Hayakawa, 2018; Boehm et al., 1997). The expression of FOXP3, thus the development of T_{reg} cells, also has links to IFN-γ as the cytokine is involved in the phosphorylation of STAT 1 leading to interactions with the FOXP3 proximal promotor in T-helper cells (Lal and Bromberg, 2009). IFN-γ is also a cytokine which is capable of suppressing tumour cell growth via several mechanisms (Mojic, Takeda and Hayakawa, 2018). However IFN-γ can also be linked to the vast proliferation and immune evasion of tumour cells suggesting IFN-γ also has tumour promoting capabilities (Mojic, Takeda and Hayakawa, 2018). In early studies it was thought that IFN-γ was an anti-cancer cytokine, however it was found that IFN-γ not only had the ability to control the progression or initiation of tumours but could create tumour immunosuppressive environments, thus promoting the proliferation and growth of tumour cells (Mojic, Takeda and Hayakawa, 2018). Therefore it can be said that in terms of cancer IFN-γ has a dual role in the outcome of cancer. The anti-cancer activity of IFN-γ is in part due to its ability to downregulate cellular proliferation through the upregulation of P21 and P27 molecules which induce cell cycle arrest, IFN-γ can also mediate apoptotic cell death (Mojic, Takeda and Hayakawa, 2018). Through the targeting of non-malignant cells in the tumour microenvironment IFN-γ can exert a potent anti-tumour effect via the recruitment of immune cells and the modulation of tumour cells in the tumour microenvironment (Spear, Barber, Rynda-Apple and Sentman, 2012). Garbe et al., (1990) demonstrated that in melanoma IFN-γ was able to inhibit cancer cell growth, however they also noted expression of advanced melanoma markers increased, thus IFN-γ may have the potential to promote the development of aggressive phenotypes in cancer cells. Therefore it is now more evident that although IFN-γ does have anti-tumour capabilities it also is able to facilitate cancer cell proliferation and has a key role in the promotion of immunosuppression in the microenvironment of cancer cells (Mojic, Takeda and Hayakawa, 2018).

Interleukin-4 (IL-4) is a cytokine with a vital role in the immune system (Takeda et al., 1996) and is secreted by T-lymphocytes, mast cells and basophils (Hou et al., 1994). The balance of T-helper cells is also partially controlled by IL-4 (Hou et al., 1994). IL-4 plays a vital role in immunoregulation and has also been detected at high levels in the microenvironment of some tumour cells, where concentrations of IL-4 can be directly linked to the grade of malignancy (Nappo et al., 2017). IL-4 could also be described as an opposing cytokine to IFN-γ in terms of FOXP3 as IL-4 inhibits the production of FOXP3 via the phosphorylation of STAT 6 (Lal and Bromberg, 2009). Inflammation can also be linked to cancer development; chronic inflammation has been associated with immune cells producing a variety of cytokines including IL-4 (Nappo et al., 2017). In the same way as IFN-γ, IL-4 can have dual roles in cancer progression. Nagai and Toi (2000) described the anti-tumour properties of IL-4 in breast cancer cells. IL-4 can stimulate the production of antigen specific cytotoxic T-cells and enhance the ability of immune cells to present antigens and induce the anti-cancer activity of macrophages (Nagai and Toi, 2000). Maerten et al., (2005) identified that T_{reg} cells exposed to IL-4 became more potent in suppressing T-helper cells and also inhibited the production of IFN-γ by T-helper cells. Cytokines can exert actions on immune cells and can also modulate the types of cells within the tumour microenvironment and are able to induce both cellular malignancy and apoptosis (Mojic, Takeda and Hayakawa, 2018; Nappo et al., 2017). The activity of cytokines has also been noted to be controlled by GAGs and the binding of cytokines to GAGs (Fernandez-Botran, Yan and Justus, 1999). GAGs therefore play a role in the modulation of cytokine activity (Fernandez-Botran, Yan and Justus, 1999). This study therefore looked to identify the effects of GAG treatment on cytokine (IL-4 and IFN-γ) production in stimulated and unstimulated PBMCs.

Both the cockle and whelk GAG extract treatments resulted in small but significant reductions in the lymphocyte population of unstimulated PBMCs (figures 5.3 and 5.4) ($p= 0.045$ an $p= 0.0497$ respectively). Post treatment with the cockle and whelk extracts small non-significant effects were noted in; cytotoxic T-cells, T-helper cells, IFN-γ, IL-4 and FOXP3 populations. In the T-helper cells positive for GARP and IFN-γ both treatment with the cockle and whelk extracts resulted in non-significant increases in percentage population (figure 5.5). In T-helper cells positive for IL-4 both the cockle and whelk extract treatments resulted in non-significant population percentage reductions. Both the cockle and whelk extract treatments resulted in

significant reductions in the population percentage of T_{reg} cells (p= 0.0362 and p= 0.0199 respectively), treatment with the whelk extract resulted in the largest reduction in the percentage population. The mean fluorescence of T_{reg} cells (figure 5.6) both treatment with the cockle and whelk extract resulted in reductions in the fluorescence of GARP. Mean fluorescence in IFN-γ of T_{reg} cells was increased post treatment with the cockle and whelk extracts. Whelk extract treatment resulted in resulted in an increase an increase in the mean fluorescence of IL-4 T_{reg} cells, while cockle extract resulted in a decrease in mean fluorescence of IL-4 in T_{reg} cells. In cytotoxic T-cells (figure 5.7) positive for IL-4 and IFN-γ both cockle and whelk extract treatments resulted in non-significant declines in population percentage of cytotoxic T-cells. In GARP positive cytotoxic T-cell populations the whelk extract treatment resulted in a non-significant decrease in the population percentage, while cockle extract resulted in a non-significant increase in population percentage. Treatment with both the cockle and whelk extracts resulted in significant decreases in the population percentage of $CD8^+$ T_{reg} cells (p= 0.0477 and p= 0.0367 respectively). Cockle and whelk extract treatments resulted in increases in the mean fluorescence (figure 5.8) of GARP in $CD8^+$ T_{reg} cells. In the $CD8^+$ T_{reg} cells the mean fluorescence of IL-4 and IFN-γ was decreased after treatment with both the cockle and whelk extracts. The decrease noted in IFN-γ mean fluorescence was significant post treatment with both the cockle and whelk extracts (p= 0.0027 and p= 0.0011 respectively).

The unstimulated PBMC assays whelk extract treatment demonstrated a reduction in IFN-γ and could suggest a decrease in T_{reg} cell potency (Lal and Bromberg, 2009). The decrease in IFN-γ could also be linked to the slight changes in T-helper cell and cytotoxic T-cell populations, due to its role in immune cell regulation (Mojic, Takeda and Hayakawa, 2018; Boehm et al., 1997). The reduction of IFN-γ noted in the whelk extract treated cells may also prove to be beneficial as an anti-cancer therapy due to the role of IFN-γ in cancer proliferation and progression (Mojic, Takeda and Hayakawa, 2018). While the increase in IL-4 cytokine population noted post treatment with the whelk extract, could indicate potential increases in FOXP3 production (Lal and Bromberg, 2009). As with IFN-γ the decline in IL-4 could be linked to the observed changes in T-helper cell and cytotoxic T-cells, due to the vital role IL-4 plays in in immunoregulation (Nappo et al., 2017). An increase in IL-4 may play a beneficial role in the use of marine mollusc derived GAGs as an anti-cancer therapy, as IL-4 has the ability to

induce increased antigen presentation and the anti-cancer activity of macrophages (Nagai and Toi, 2000). Maerten et al., (2005) also identified that IL-4 could increase the potency of T_{reg} cells at suppressing T-helper cells and IFN-γ production. Our results would support this due to the noted decrease in IFN-γ population percentage. The results of this study demonstrate the potential of the whelk extract to inhibit the immune evasion of cancer through the significant reduction in T_{reg} cells noted (Facciabene et al., 2012; Elkord, 2010). Also through the reduction in cytokines which play a role in the promotion of immune evasion and prevention of cell death (Mojic, Takeda and Hayakawa, 2018; Nappo et al., 2017) post treatment with the whelk extract. The cockle extract treatment also resulted in similar reductions in T_{reg} cells and cytokine changes, however in some cases the reductions were small in comparison to those noted in the whelk extract and the control treatment cisplatin.

Both GAG extract treatments appear to reduce the population of cytotoxic T-cells positive for IL-4 and IFN-γ. These reductions may be beneficial in the use of GAGs as an anti-cancer therapy as although increased levels of IL-4 has been linked to anti-cancer activity in some cell lines, in other cancer cell lines lower levels of IL-4 have been linked to decreased malignancy (Nappo et al., 2017) and lower levels of IFN-γ have been linked to decreased T_{reg} potency and decreased cellular proliferation (Mojic, Takeda and Hayakawa, 2018; Lal and Bromberg, 2009). The reductions noted in cytotoxic IFN-γ and IL-4 levels were non-significant and would be unlikely to promote a phenotypic change in cytotoxic T-cells. The results obtained from the whelk extract treated unstimulated PBMCs assays could suggest a potentially beneficial novel marine mollusc derived GAG treatment, which could help with the prevention of cancer immune evasion. Supporting the idea that GAG chains may exhibit anti-cancer properties whilst exerting minimal side effects (Basappa et al., 2012).

In the stimulated PBMC assays treatment with both the cockle and whelk extracts resulted in decreases in the population percentages of lymphocytes, cytotoxic T-cells and IFN-γ (figures 5.9 and 5.10). Treatment with both the GAG extracts exerted an increase in the T-helper cell population percentage (figure 5.11) and IL-4. The GARP population of stimulated PBMCs experienced an increase in population percentage post treatment with the cockle extract, while treatment with the whelk extract resulted in a decrease in the population percentage. Both the cockle and whelk extract treatments resulted in reductions in both the GARP T-helper cells and T_{reg} cells. The reductions in the T_{reg} cell populations exerted by the cockle and

whelk extract treatments were significant (p= 0.0145 and p= 0.0191 respectively). The population of IL-4 positive T-helper cells and IFN-γ positive T-helper cells was increased post cockle extract treatment. In whelk extract treated cells the IL-4 positive T-helper cells increased, while the IFN-γ positive T-helper cells significantly decreased post treatment with the whelk extract (p= 0.0156). The mean fluorescence (figure 5.12) of IFN-γ in the T_{reg} cell population increased post treatment with both the cockle and whelk extracts. The cockle extract treatment exerted increases in IL-4 and GARP mean fluorescence in T_{reg} cells. The mean fluorescence of IL-4 decreased and GARP mean fluorescence significantly decreased (p= 0.0354) post treatment with the whelk extract. Treatment with the cockle extract did not exert an effect on the population GARP cytotoxic T-cells, whilst whelk extract treatment exerted a small population increase (figure 5.13). Both cockle and whelk extract treatments demonstrated decreases in the population percentage of IFN-γ, IL-4 cytotoxic T-cells and $CD8^+$ T_{reg} cell populations. The mean fluorescence of IFN-γ, GARP and IL-4 in the $CD8^+$ T_{reg} cells increased post treatment with both the cockle and whelk extracts (figure 5.14).

The results demonstrated in this study suggested that both the cockle and whelk extracts may provide a therapeutic treatment method that results in small effects on vastly proliferating lymphocytes is in support of the theory put forward by Basappa et al., (2012). The treatment with both the GAG extracts demonstrated reductions in the percentage of T_{reg} cells, this could suggest that treatment with the novel marine mollusc derived GAGs may potentially prevent the immune evasion and prevention of cell death in cancer cells (Facciabene et al., 2012; Elkord, 2010). The noted decrease in cytotoxic T-cells could potentially be linked to the decrease in percentage IFN-γ, as IFN-γ is partially responsible for the regulation of immune cells (Mojic, Takeda and Hayakawa, 2018); it may also result in less proliferation and apoptosis in treated healthy lymphocytes (Mojic, Takeda and Hayakawa, 2018). Declines in IFN-γ can also be linked to anti-cancer activity in some cancers (Mojic, Takeda and Hayakawa, 2018) which could further support the use of marine mollusc derived GAGs as an anti-cancer therapy. The increase noted in the percentage of IL-4 may be linked to the increase in the percentage of T-helper post treatment with the GAG extracts. This is down to the ability of IL-4 to regulate that levels of T-helper cells and its role in the recruitment of immune cells (Nappo et al., 2017). The increase in IL-4 in some cancers can also be linked to the production of antigen specific cytotoxic T-cells and enhanced antigen presenting ability as well as an

increase in the anti-cancer activity of macrophages (Nagai and Toi, 2000). However increased levels of IL-4 have also been linked to increased malignancy in some cancers (Nappo et al., 2017). Therefore the effects of GAG extract treatment on vastly proliferating lymphocytes may need to be further explored.

The results from the cytokine and T_{reg} response assays identify the novel marine mollusc derived GAG extracts, in particular the whelk extract, resulted in a significant reduction in the percentage of T_{reg} cells (in both stimulated and unstimulated PBMCs). This could suggest that treatment with the GAG extracts could aid with the reduction of the immune evasion of cancer cells; since raised levels of T_{reg} cells has been attributed to the progression of cancer and the ability of cancer to evade the immune system (Bayer and Schultze, 2006). Further research to identify different dose and time responses of cancer cells and healthy lymphocytes (stimulated and unstimulated) to both the GAG extract treatments in the apoptosis and proliferation assays may further increase the knowledge on the effects of these novel GAG compounds on healthy lymphocytes. Also further research into the effects on IFN-γ and IL-4 and the effects on T_{reg} cells of both the GAG extracts in healthy lymphocytes, could potentially further determine whether the GAG extracts could provide a treatment option for cancer patients that would elicit fewer side effects. Further investigation into the effects of the FPLC fractions on the cancer cell lines and healthy lymphocytes in the apoptosis, proliferation and cytokine and T_{reg} response assays would further aid to determine the potential use of the GAG extracts as an anti-cancer therapy. This however was all beyond the scope of this research study. The results of the cytokine and T_{reg} response assays teamed with the results of the MTT, apoptosis and proliferation assays also supports the idea put forward by Aldairi, Ogundipe and Pye (2018) and Ogundipe (2015) that the marine mollusc GAGs derived from the common cockle and common whelk appear to selectively target cancer cells as opposed to targeting healthy lymphocytes (in both stimulated and unstimulated PBMCs). This study therefore furthers the potential for the future use of the marine mollusc derived GAGs for therapeutic use in the clinic.

6.7 Timeline of previous and current work on GAG isolates

Figure 6.1 identifies previous work carried out on both the cockle and whelk GAG extracts, where the results of this study fit with the research carried out on the cockle and whelk extracts and finally the expected progression of the research.

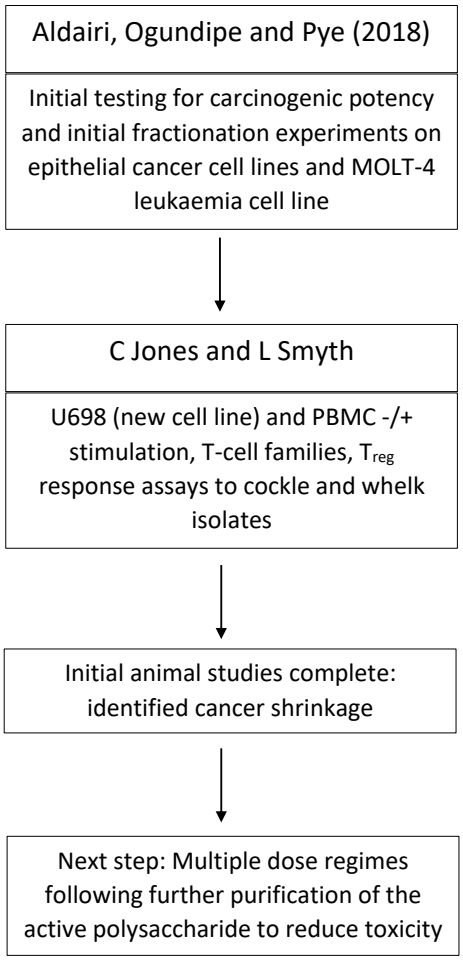

Figure 6.1 The timeline of previous and current work being carried out on GAG isolates.

References

Afratis, N., Gialeli, C., Nikitovic, D., Tsegenidis. T., Karousou, E., Theocharis, A. D., … & Karamanos, N. K. (2012). Glycosaminoglycans: Key players in cancer cell biology and treatment. *Federation of European Biochemical Societies Journal, 279*(7): pp.1177-1197.

Agauayo, A., Kantarjian, H., Manshouri, T., Gidel, C., Estey, E., Thomas, D., … & Albitar, M., (2000). Angiogenesis in acute and chronic leukaemia's and myelodysplastic syndromes. *Blood, 96*(6): pp.2240-2245.

Aldairi, A. F., Ogundipe, O. D., & Pye, D. A., (2018). Antiproliferative activity of glycosaminoglycan-like polysaccharides derived from marine molluscs. *Marine Drugs, 16*(63).

Antony, P.A. Piccirillo, A.C. Akpinarli, A. Finkelstein, S.E. Speiss, P.J. Surman, D.R. Palmer, D.C, Chan, C. Klebanoff, C.A. Overwijk, W.W. Rosenberg, S.A. and Restifo, N.P. (2005). CD8+ T-cell immunity against a tumour/self-antigen is augmented by CD4+ Thelper cells and hindered by naturally occurring T regulatory cells. *Journal of Immunology. 174*: pp.2591-2601.

Appelbaum, F. R., Niederhuber, J. E., Armitage, J. O., Doroshow, J. H., Kastan, M. B., & Tepper, J. E. (2014). Chapter 98: Acute leukaemias in adults. *Abeloff's Clinical Oncology E-Book*. Elsevier Health Sciences. Philadelphia.

Arbor, A. and Garber, K. (2002). Angiogenesis inhibitors suffer new setbacks. *Nature Biotechnology. 20*: pp. 1067-1068.

Auvinen, P., Tammi, R., Parkkinen, J., Tammi, M., Agren, U., Johansson, R., … and Kosma, V. M. (2000). Hyaluronan in peritumoral stroma and malignant cells associates with breast cancer spreading and predicts survival. *The American Journal of Pathology, 156*(2): pp. 529-536.

Avendano, C. Menendez, C.J. (2015). *Medicinal chemistry of anticancer drugs.* (2nd edition). Burlington: Elsevier Science.

Barker, C. E., Thompson, S., O'boyle, G., Lortat-Jacob, H., Sheerin, N. S., Ali, S., & Kirby, J. A. (2017). CCL2 nitration is a negative regulator of chemokine-mediated inflammation. *Scientific reports*, *7*: p. 44384.

Barthel, S. R., Gavino, J. D., Descheny, L., & Dimitroff, C. J., (2007). Targeting selectins and selectin ligands in inflammation and cancer. *Expert Opinion Therapeutic Targets, 11*(11): pp.1473-1491.

Basappa, Sugahara, K., Kuntebommanahalli, N., Thimmaiah, K.N., Bid, H.K., Houghton, P.J., and Rangappa, K.S. (2012). Anti-tumour activity of a novel HS-mimetic vascular endothelial growth factor binding small molecule. *PLoS ONE. 7*(10): 10.137.

Bassan, R., Maino, E., & Cortelazzo, S., (2016). Lymphoblastic lymphoma: an updated review on biology diagnosis and treatment. *European Journal of Haematology, 96*(5): pp.447-460.

Becker, W.M. Kleinsmith, L.J. Hardin, J. and Raasch, J. (2003). *The world of the cell* (vol. 6.). San Francisco: Benjamin Cummings.

Bergsbaken, T. Fink, S.L. and Cookson, B.T. (2009) Pyroptosis: host cell death and inflammation. *Nature Reviews: Microbiology. 7:* pp.99-109.

Berridge, M. V., Herst, P. M., & Tan, A. S., (2005). Tetrazolium dyes as tools in cell biology: new insights into their cellular reduction. *Biotechnology Annual Review, 11*: pp.127-152.

Beyer, M. and Schultze, L. (2006). Regulatory T-cells in cancer. *Blood Journal. 108*(3): pp.804-811.

Birbrair, A. Zhang, T. Wang, Z. M. J. Messi, M. L. Olson, J. D. Mintz, A. and Delbono, O. (2013). Type-2 pericytes participation in normal and tumoral angiogenesis. *APJ: Cell Physiology. 307*(1): p.25 doi:10.1152/AJPCell.00171.2013.

Bissell, M. J., Hall, H. G., & Parry, G. (1982). How does the extracellular matrix direct gene expression?. *Journal of theoretical biology*, *99*(1): pp. 31-68.

Boehm, U., Klamp, T., Groot, M., & Howard, J. C., (1997). Cellular responses to interferon-γ. *Annual Review of Immunology, 15*(1): pp.749-795.

Bogenrieder, T. and Herlyn, M. (2003). Axis of evil: molecular mechanisms of cancer metastasis. *Oncogene. 22*(42): pp.6524-6536.

Borsig, L. (2010). Heparin as an inhibitor of cancer progression. *In Progress in Molecular Biology and Translational Science. (Vol: 93):* pp. 335-349. Academic Press.

Borsig, L., Wang, L., Cavalcante, M. C., Cardilo-Reis, L., Ferreira, P. L., Mourao, P. A., … and Pavao, M. S. (2007). Selectin blocking activity of fucosylated chondroitin sulfate glycosaminoglycan from sea cucumber effect on tumour metastasis and neutrophil recruitment. *Journal of Biological Chemistry, 282*(20): pp. 14984-14991.

Brito, A. S., Arimateia, D. S., Souza, L. R., Lima, M. A., Santos, V. O., Medeiros, V. P., … and Leite, E. L., (2008). Anti-inflammatory properties of a heparin-like glycosaminoglycan with reduced anticoagulant activity isolated from a marine shrimp. *Bioorganic and Medicinal Chemistry, 16*(21): pp. 9588-9595.

Buzzle (2015). Proteoglycan structure [online]. Available at: http://www.buzzle.com/images/diagrams/proteoglycan-basic-structure.jpg [accessed 10/07/2016].

Calabretta, B. and Perrotti, D. (2004). The biology of chronic myeloid leukaemia blast crisis. *Blood. 103:* pp. 4010-4022.

Cancer research UK (2019). Cancer statistics [online]. Available at: https://www.cancerresearchuk.org/health-professional/cancer-statistics/cancer-stats-explained. [accessed on 14/01/2019].

Canadian cancer society (2016). Cell cycle [online]. Available at: www.cancer.ca/en/cancer-information/cancer-101/what-is-cancer/the-cell-cycle/?region=on [accessed on 10/07/2016].

Cao, Y. (2001). Endogenous angiogenesis inhibitors and their therapeutic implications. *International Journal of Biochemistry Cell Biology. 33*(4): pp.357-369.

Carelle, N., Piotto, E., Beuanger, A., Germanaud, T., Thuillier, A., & Khayat, D., (2002). Changing patient perceptions of the side effects of cancer chemotherapy. *Cancer, 95*(1): pp.155-163.

Carter, N. M., Ali, S., and Kirby, J. A. (2003). Endothelial Inflammation: the role of differential expression of N-deacetylase/ N-sulphotransferase enzymes in alteration of the immunological properties of heparan sulphate. *Journal of Cell Science, 116*: pp. 3591-3600.

Cattaruzza, S., & Perris, R. (2005). Proteoglycan control of cell movement during wound healing and cancer spreading. *Matrix Biology*, *24*(6): pp. 400-417.

Cederbom, L. Hall, H. and Ivars, F. (2000). CD4+CD25+ regulatory T cells down-regulate co-stimulatory molecules on antigen presenting cells. *European Journal of Immunology. 30*: pp.1538-1543.

Chanmee, T., Ontong, P., & Itano, N., (2015). Hyaluronan: cancer and cancer metastasis. *Glycoscience: Biology and Medicine:* pp.1411-1417.

Chatzinikolaou, G. Nikitovic, D. Asimakopou, A. Tsatsakis, A. Karamanos, N. K. and Tzanakakis, G. N. (2008). Heparin – a unique stimulator of human colon cancer cells' growth. *IUBMB Life. 601*(5): pp.333-340.

Chautan, M. Chazal, G. Cecconi, F. Gruss, P. and Golstein, P. (1999). Interdigital cell death can occur through necrotic and caspase-independent pathway. *Current Biology. 9:* pp.967-970.

Chen, W. J., & Abatangelo, G. (1999). Functions of hyaluronan in wound repair. *Wound repair and regeneration*, *7*(2): pp. 79-89.

Chen, C. F., Hwang, J. M., Lee, W., Chiang, H. C., Lin, J. C., & Chen, H. Y., (1988). Search for anti-tumour agent for Chinese herbs. *I. Taipei.* 41: pp. 177-184.

Children with cancer UK, Cancer statistics, Available at: www.childrenwithcancer.org.uk/childhood-cancer-info/childhood-cancer-facts-figures. [accessed Jan 2019]

Clark, R. A. (1998). Overview and general considerations of wound repair. In *The molecular and cellular biology of wound repair* (pp. 3-33). Springer, Boston, MA.

Constantinescu, A. A., Vink, H., & Spaan, J. A. (2003). Endothelial cell glycocalyx modulates immobilization of leukocytes at the endothelial surface. *Arteriosclerosis, thrombosis, and vascular biology*, *23*(9): pp. 1541-1547.

Cooper, G. M., (2000). *The cell: a molecular approach* (Vol. 2). Washington, DC: ASM press.

Coppola, J.M., Ross, B.D., and Rehemtulla, A. (2008). Non-invasive imaging of apoptosis and its application in cancer therapeutics. *Clinical Cancer Research*. *14*: pp. 2492-2501.

Cornelissen, M., Philippe, J., De Sitter, S., & De Ridder, L., (2002). Annexin V expression in apoptotic peripheral blood lymphocytes: An electron microscope evaluation. *Apoptosis, 7*: pp.41-47.

Corrie, P. G., (2008). Cytotoxic chemotherapy: clinical aspects. *Medicine, 36*(1): pp.24-28.

Cortelazzo, S. Ponzoni, M. Ferreri, A.J.M. and Hoelzer, D. (2011). Lymphoblastic lymphoma. *Critical Reviews in Oncology and Haematology. 79*: pp.330-343.

Cross, M. J. and Claesson-Welsh, L. (2001). FGF and VEGF function in angiogenesis: Signalling pathways, biological responses and therapeutic inhibition. *Trends in Pharmacological Sciences Cell Press. 22*(4): pp.201-207.

Cyclacel (2016). Cell cycle [online]. Available at: http://www.cyclacel.com/research_science_cell-cycle.shtml [accessed 10/07/2016].

Daiziel. K., Round. A., Stein. K., Garside. R., & Price. A., (2004). Effectiveness and cost-effectiveness of imatinib for first-line treatment of chronic myeloid leukaemia in chronic phase: a systematic review and economic analysis. *Health and Technology Assessment, 8*(28): pp. 1-120.

Danial, N.N. and Korsmeyer, S.J. (2004). Cell death: critical control points. *Cell. 116:* pp.205-219.

De Jesus Raposo, M. F., de Morais, A. M., de Morais, R. M., (2015). Marine polysaccharides from algae with potential biomedical applications. *Marine Drugs, 13:* pp.2967-3028.

De Lavallade, H. (2013). Chronic myeloid leukaemia. *Medicine. 45(5):* pp.275-277.

De Mello, V., Ferreira, D., Kolehmanien, M., Schwah, U., Pulkkinen, L., & Uusitupa, M., (2012). Gene expression of peripheral blood mononuclear cells as a tool in dietary intervention studies: what we know so far?. *Molecular Nutrition and Food Research, 56*(7): pp.1160-1172.

DeAngelis, P. L., (2002). Microbial glycosaminoglycan glycosyltransferases. *Glycobiology, 12*(1): pp.9R-6R.

DeCicco-Skinner, K. L., Henry, G. H., Cataissan, G., Tabib, T., William, J. C. G., Watson, N. J., … & Wiest, J. S., (2014). Endothelial cell tube formation assay for the invitro study of angiogenesis. *Journal of Visualised Experiments, 91*: 51312.

Deed, R. Rooney, P. and Kumar, P. (1997). Early response gene signalling is induced by angiogenic oligosaccharides of Hyaluronan in endothelial cells: Inhibition by non-angiogenic high molecular weight Hyaluronan. *International Journal Cancer. 71*: pp.251-256.

Delves, P. J., Martin, S. J., Burton, D. R., & Roitts, I. M., (2017). *Essential immunology.* John Wiley & Sons.

Deng, C., Zhang, P., Harper, J. W., Elledge, S. J., & Leder, P. (1995). Mice lacking p21CIP1/WAF1 undergo normal development, but are defective in G1 checkpoint control. *Cell*, *82*(4), pp:675-684.

Desai, U. R. (2013). The promise of sulphated synthetic small molecules as modulators of glycosaminoglycan function. *Future Medicinal Chemistry, 5*(12): pp. 1363-1366.

Dicker, K. T., Gurski, L. A., Pradhan-Bhatt, S., Witt, R. L., Farach-Carson, M. C., & Jia, X., (2014). Hyaluronan: a simple polysaccharide with diverse biological functions. *Acta Biomaterialia. 10*(4): pp.1558-1570.

Diehl, J. A., Zindy, F., & Sherr, C. J. (1997). Inhibition of cyclin D1 phosphorylation on threonine-286 prevents its rapid degradation via the ubiquitin-proteasome pathway. *Genes & Development*, *11*(8): pp.957-972.

Divoli, A. Eneida, A. Mendonca, J. Evans, A. Zhetsky, A.R. (2011). Conflicting biomedical assumptions for mathematical modelling: the case of cancer metastasis. *PLoS Computing Biology. 7*(10).

Dredge, K., Hammond, E., Handley, P., Gonda, T. J., Smith, M. T., Vincent, C., … and Bytheway, I. (2011). PG545, a dual heparinase and angiogenesis inhibitor, induces potent anti-tumour and anti-metastatic efficacy in preclinical models. *British Journal of Cancer, 104*(4): p. 635.

Drexler, H. G. Gignac, S. M. von Wasielewski, R. Werner, M. and Dirks, W. G. (2000). Pathobiology of NPM-ALK and variant fusion genes in anaplastic large cell lymphoma and other lymphomas. *Leukemia. 14*(9): pp.15333-2559.

DSMZ (2016). Product information leaflet ACC4.

Duprez, L. Wirawan, E. Vanden Berghe, T. Vandenabeele, P. (2009). Major cell death pathways at a glance. *Microbes and Infection II.* pp. 1050-1062.

Elise, F. and Rodeghiero, F. (2012). Side effects of anti-angiogenic drugs. *Thrombosis Research. 1*: pp.80-83.

Elkord, E. Alcantar-Orozco, E.M. Dovedi, S.J. Tran, D.Q. Hawkins, R.E. and Gilham, D.E. (2010). T regulatory cells in cancer: recent advances and therapeutic potential. *Expert Opinion on Biological Therapy. 11*: pp.1573-1586.

Elmore, S. (2007). Apoptosis: a review of programmed cell death. *Toxicologic Pathology. 35*(4): pp.495-516.

Erduran, E., Deger, O., Albayrak, D., Tekelioglu, Y., and Ozdemir, T. (2007). *In Vitro* investigation of the apoptotic effect of heparin on lymphoblasts by using flow cytometric DNA analysis and fluorometric caspase-3 and -8 activities. *DNA Cellular Biology. 26*: pp. 803-808.

Evans, L. S., and Hancock, B. W., (2003). Non-Hodgkin lymphoma. *The Lancet, 362*(9378): pp.139-146.

Facciabene, A. Motz, G.T. and Coukos, G. (2012). T-regulatory cells: key players in tumour immune escape and angiogenesis. *Cancer Research. 72*(9): pp.2162-2171.

Fadok, V.A. Bratton, D.L. Guthrie, L. and Henson, P.M. (2001). Differential effects of apoptotic versus lysed cells on macrophage production of cytokines: role of proteases. *Journal of Immunology. 166:* pp.6847-6854.

Fernandez-Botran, R., Yan, J., and Justus, D.E. (1999). Binding of interferon-gamma by glycosaminoglycans: a strategy for localisation and/ or inhibition of its activity. *Cytokine. 11*(5): pp. 313-315.

Festjens, N. Vanden Berghe, T. and Vandenabeele, P. (2006). Necrosis a well-orchestrated form of cell demise: signalling cascades, important mediators and concomitant immune response. *Biochimica et Biophysica Acta. 1757:* pp.1371-1387.

Fiedler, W., Graeven, U., Ergün, S., Verago, S., Kilic, N., Stockschläder, M., & Hossfeld, D. K. (1997). Vascular endothelial growth factor, a possible paracrine growth factor in human acute myeloid leukemia. *Blood*, *89*(6): pp.1870-1875.

Folkman, J., Browder, T., & Palmblad, J. (2001). Angiogenesis research: guidelines for translation to clinical application. *Thrombosis and Haemostasis*, *86*(7): pp.23-33.

Folkman, J., (1995). Clinical applications of research on angiogenesis. *New England Journal of Medicine, 333*(26): pp.1757-1763.

Folkman, J. (2004). Endogenous angiogenesis inhibitors. *APMIS. 112*(7-8): pp.496-507.

Folkman, J. (2006). Anti-angiogenesis in cancer therapy endostatin and its mechanism of action. *Experimental Cell Research. 312*(5 part 2): pp.594-607.

Freeman, C., Liu, L., Banwell, M. G., Brown, K. J., Bezos, A., Ferro, V., and Parish, C. R. (2005). Use of sulphated linked cyclitols as heparan sulphate mimetics to probe the heparin/ heparan sulphate binding specificity of proteins. *Journal of Biological Chemistry, 280*(10): pp. 8842-8849.

Fuentes-prior, P. and Salvesen, G.S. (2004). The protein structures that shape caspase activity, specificity, activation and inhibition. *Biochemical Journal. 384:* pp.201-232.

Funderburgh, J.L. (2000). MINI REVIEW Keratan sulfate: structure, biosynthesis and function. *Glycobiology. 10*(10): pp.951-958.

Galluzi, L. Maiuri, M.C. Vitale, I. Zischka, H. Castedo, M. Zitvogel, L. and Kroemer, G. (2007). Cell death modalities: classification and pathophysiological implications. *Cell Death and Differentiation. 14:* pp.1237-1243.

Gambacorti-Passerini, C. B., Gunby, R. H., Piazza, R., Galietta, A., Rostagno, R., & Scapozza, L., (2003). Molecular mechanisms of resistance to imatinib in Philadelphia-chromosome-positive leukaemia's. *Lancet-Oncology, 4*(2): pp.75-85.

Gandhi, N.S. and Mancera, R.L. (2008). The structure of glycosaminoglycans and their interactions with proteins. *Chemical Biology and Drug Design. 72*(6): pp.455-482.

Gao, F. Yang, C. X. Mo, W. Liu, Y. W. and He, Y. Q. Hyaluronan oligosaccharides are potential stimulators to angiogenesis via RHAMM mediated signal pathways in wound healing. *Clinical & Investigative Medicine. 31* (3): pp.106-116.

Garbe, C., Krasagakis, K., Zouboulis, C.C., Schroder, K., Kruger, S., Stadler, R., and Orfanos, C.E. (1990). Anti-tumour activities of interferon alpha, beta and gamma and their combinations on human melanoma cells *in vitro*: changes of proliferation, melanin synthesis and immunophenotype. *Journal of Investigative Dermatology. 95*: pp. 2315- 2375.

Ghatak, S., Maytin, E. V., Mack, J. A., Hascall, V. C., Atanelishvili, I., Rodriguez, R. M., … and Misra, S. (2015). Roles of proteoglycans and glycosaminoglycans in wound healing and fibrosis. *International Journal of Cell Biology, 2015.*

Ghatak, S., Bogatkevich, G. S., Atnelishvili, I., Akter, T., Feghali-Bostwick, C., Hoffman, S., ... & Padhye, S. B. (2014). Overexpression of c-Met and CD44v6 receptors contributes to autocrine TGF-β1 signaling in interstitial lung disease. *Journal of Biological Chemistry*, *289*(11): pp. 7856-7872.

Godal, T. (2012). On the complexity of the B cell system as assessed by studies on human B cell lymphomas. In *B and T Cell Tumors. UCLA Symposia on Molecular and Cellular Biology 24:* pp.69-72.

Goldman, D., & Fyfe, M. J., (1974). The mechanism of action of methotrexate. *Molecular Pharmacology, 10*(2): pp.275-282.

Goldman, J.M. (2008). Chronic myeloid leukaemia. *Medicine. 37(4):* pp.195-197.

Goldstone, A. H., Richards, S. M., Lazarus, H.M., Tallman, M. S., Buck, G., Fielding, A. K., … & Rowe, J. M., (2008). In adults with standard-risk acute lymphoblastic leukaemia, the greatest benefit is achieved from a matched sibling allogenic transplantation in first complete remission and an autologous transplantation is less effective than conventional consolidation/ maintenance chemotherapy in ALL patients: final results of the international ALL trials (MRC UKA11 X11/ECOG E2993). *Blood, 111*: pp.1827-1833.

Gomes, A. M., Kozlowski, E. O., Borsig, L., Teixeira, F. C., Vlodavsky, I., and Pavao, M S., (2014). Anti-tumour properties of a new non-anticoagulant heparin analogue from the mollusc Nondipecten nodosus: Effect on P-selectin, heparinase, metastasis and cellular recruitment. *Glycobiology, 25*(4): pp. 386-393.

Gonzalez, P. Ruben, R. and Rueda, B.O. R. (2013). *Tumour angiogenesis regulators. Boca Raton*; Taylor & Francis (1st ed) p.347.

Greenberg, J.M. Gonzalez-Sarmiento, R. Arthur, D.C. Wilkowski, C.W. Streifel, B.J. and Kersey, J.H. (1988). Immunophenotypic and cytogenetic analysis of MOLT-3 and MOLT-4: Human T-lymphoid cell lines with re-arrangement of chromosome 7. *Blood. 72*: pp.1755-1760.

Griffin, K. L., Fischer, B. M., Kummarapurugu, A. B., Zheng, S., Kennedy, T. P., Rao, N. V., … and Voynow, J. A. (2014). 2-O, 3-O-desulphated heparin inhibits neutrophil elastase-induced HMGB-1 secretion and airway inflammation. *American Journal of Respiratory Cell and Molecular Biology, 50*(4): pp. 684-689.

Griffiths, R. W., Elkord, E., Gilham, D. E., Ramani, V., Clarke, N., Stern, P. L., & Hawkins, R. E., (2007). Frequency of regulatory T cells in renal cell carcinoma patients and investigation of correlation with survival. *Cancer Immunology Immunotherapy, 56:* pp.1743-1753.

Grigoropoulos, N. F., Peter, R., Van't Veer, M. B., Scott, M. A., & Follows, G. A., (2013). Leukaemia update. Part 1: diagnosis and management. *BMJ, 2013*(346).

Haddad, R. O'Neil, A. Rabinowits, G. Tishler, R. Khuri, F. Adkins, D. Clark, J. Sarlis, N. Lorch, J. Beitler, J. Limayes, S. Riley, S. and Posner, M. (2013). Induction chemotherapy followed by concurrent chemoradiotherapy (sequential chemoradiotherapy) versus concurrent chemotherapy alone in locally advanced head and neck cancer (PARADIGM): a randomised phase 3 trial. *The Lancet Oncology. 14*(3): pp.257-264.

Hammond, E., Handley, P., Dredge, K., and Blytheway, I. (2013). Mechanisms of heparinase inhibition by the heparan sulfate mimetic PG545 and three structural analogues. *FEBS Open Bio, 3*: pp. 346-351.

Hannigan, B.M. Moore, C.B.T. and Quinn, D.G. (2009). *Immunology.* Scion Publishing, Bloxham, UK.

Harrison, C. J., (2001), Philadelphia Chromosome. *Encyclopaedia of Genetics.* pp. 1449-1450.

Hayden, E. C. (2009). Cutting of cancer's supply lines. *Nature. 458*(7239): pp.686-687.

Hehimann, R. Hochhaus, A. and Baccarani, M. (2007). Chronic myeloid leukaemia. *Lancet. 370:* pp.342-350.

Hehlmann, R., (2012), How do I treat blast crisis. *Blood, 120*: pp. 737-747.

Helton, E.S. and Chen, X. (2007). P53 modulation of the DNA damage response. *Journal of Cellular Biochemistry. 100:* pp.883-896.

Hickson, G. R., Echard, A., & O'Farrell, P. H. (2006). Rho-kinase controls cell shape changes during cytokinesis. *Current Biology*, *16*(4): pp.359-370.

Hirsova, P. and Gores, G.J. (2015). Death receptor mediated cell death and proinflammatory signalling in non-alcoholic steatohepatitis. *Cellular and Molecular Gastroenterology and Hepatology. 1*(1): pp.17-27.

Hochhaus, A., Larson, R. A., Guilhot, F., Radich, J. P., Branford, S., Hughes, T. P., ... & Ortmann, C. E. (2017). Long-term outcomes of imatinib treatment for chronic myeloid leukemia. *New England Journal of Medicine*, *376*(10): pp.917-927.

Hochhaus, A. O'Brien, S.G. Guilholt, F. Drucker, B.J. Branford, S. Foroni, L. Goldman, J.M. Muller, M.C. Radich, J.P. Rudoltz, M. Mone, M. Gathmann, I. Hughes, T.P. and Larson, R.A. (2009). Chronic myeloproliferative neoplasias: six year follow up of patients receiving Imatinib for the first line treatment of chronic myeloid leukaemia. *Leukaemia. 23*: pp.1054-1061.

Hoelzer, D. and Gokbuget, N. (2003). Treatment of lymphoblastic lymphoma in adults. *Best Practice and Research Clinical Haematology. 15*(4): pp.713-728.

Holland, A. J., & Cleveland, D. W. (2009). Boveri revisited: chromosomal instability, aneuploidy and tumorigenesis. *Nature Reviews: Molecular Cell Biology*, *10*(7): p.478.

Holland, J. C., Anderson, B., Breitbart, W. S., Compas, B., Dudley, M. M., Fleishmann, S., … & Hoofring, L., (2010). NCCN clinical practice guidelines in oncology: Distress management. Version 1. *Journal of The National Comprehensive Cancer Network 8*(4): pp.448-485.

Holler, N. Zaru, R. Micheau, O. Thome, M. Attinger, A. Valitutti, S. Bodmer, J.L. Schneider, P. Seed, B. and Tschopp, J. (2000). FAS triggers an alternative caspase-8-independent cell death pathway using the kinase RIP an effector molecule. *Nature Reviews: Immunology. 1:* pp.489-495.

Holmegren, L. O'Reilly, M. S. and Folkman, J. (1995). Dormancy of micrometastases: Balance proliferation and apoptosis in the presence of angiogenesis suppression. *Natural Medicine*. pp. 49-53.

Honda, A. Iwama, M. Umeda, T. and Mori, Y. (1982). The teratogenic mechanism of 6-aminonicotinamide on limb formation of chick embryos: abnormalities in the biosynthesis of glycosaminoglycans and proteoglycans in micromelia. *Journal of Biochemistry. 91*(6): pp. 1959-1970.

Hori, T. Nakamura, N. Tateishi, R. and Hattori, S. (1981). Glycosaminoglycans in human lung cancer. *Cancer. 48*(9): pp.2016-2021.

Hou, J., Schindler, U., Henzel, W. J., Ho, T. C., Brasseur, M., & McKnight, S. L., (1994). An interleukin 4 induced transcription factor: IL4 STAT. *Science, 265*(5179): pp.1701-1706.

Hu, Q. Sun, W. Wang, C. and Gu, Z. (2016). Recent advances of cocktail chemotherapy by combination drug delivery systems. *Advanced Drug Delivery Reviews. 98:* pp.19-34.

Hunger, S.P. Lu, X. Devidas, M. Camitta, B.M. Gaynon, P.S. Winick, N.J. Reaman, G.H. and Carroll, W.L. (2012). Improved survival for children and adolescents with ALL between 1990 and 2005: a report from the childrens oncology group. *Journal of Clinical Oncology. 30:* pp.1663-1669.

Hussong, J. W., Rodgers, G. M., & Shami, P. J., (2000). Evidence of increased angiogenesis in patients with acute myeloid leukaemia. *Blood, 95*(1): pp.309-313.

Inaba, H. Greaves, M. Mullighan, C.G. (2013). Acute lymphoblastic leukaemia. *Lancet*. *381:* pp.1943-1955.

Itano, N. and Kimata, K. (2002). Mammalian hyaluronan synthases. *IUBMB life. 54*(4): pp.195-199.

Jackson, R.L. Busch, S.J. and Cardin A.D. (1991). Glycosaminoglycans: molecular properties, protein interactions and role in physiological processes. *Physiological Reviews. 71*(2): pp.481-539.

Jedema, I., Van der Werff, N. M., Barge, R. M. Y., Willemze, R., & Falkenburg, J. H. F., (2004). New CFSE-based assay to determine susceptibility to lysis by cytotoxic T cells of leukemic precursor cells within a heterogenous target cell population. *Blood, 103:* pp.2677-2682.

Jia, J., Maccarana, M., Zhang, X., Bespalov, M., Lindahl, U., & Li, J. P., (2009). Lack of I-iduronic acid in heparan sulphate affects interaction with growth factors and cell signalling. *Journal of Biological Chemistry. 284* (23): pp.15942-15950.

Jobbour, E. Cortes, J. and Kantarjian, H. (2009). Nilotinib for the treatment of chronic myeloid leukaemia: an evidence based review. *Core Evidence. 4:* pp.207-213.

Johnstone, J.B. Barrett, J.W. Nazarian, S.H. Goodwin, M. Ricciuto, D. Wang, G. Mcfadden, G. (2005). A poxvirus encoded pyrin domain protein interacts with ASC-1 to inhibit host inflammatory and apoptotic responses to infection. *Immunity. 23:* pp. 587-598.

Jorge, E., Cortes, M. D., Hagop, M., & Kantarjian, M. D., (1995). Acute Lymphoblastic Leukaemia. *Leukaemia and Lymphoma Oncology Journal.*

Journal of Leukaemia, (2018), 6 (3). Available at: Omicsonline.org>leukaemia. [Accessed Jan 2019].

Kabarowski, J. H., and Whitte, O. N., (2000), Consequences of BCR-ABL expression within the hematopoietic stem cell in chronic myeloid leukaemia. *Stem Cells, 18*(2000): pp. 39-408.

Kalidas, M. Kantarjian, H. and Talpaz, M. (2001). Chronic myelogenous leukaemia. *Journal of The American Medical Association. 286*(8): pp.895-898.

Karbownik, M.S. and Nowak, J.Z. (2013). Hyaluronan: towards novel anti-cancer therapeutics. *Pharmacological Reports. 65*(5): pp.1056-1074.

Kato, J. Y., Matsushime, H., Hiebert, S. W., Ewen, M. E., & Sherr, C. J. (1993). Direct binding of cyclin D to the retinoblastoma gene product (pRb) and pRb phosphorylation by the cyclin D-dependent kinase CDK4. *Genes and Development*, *7*: pp.331-331.

Kaur, J. and Reinhardt, D.P. (2015). Extracellular matrix molecules. *Stem Cell Biology and Tissue Engineering in Dental Science.* pp.25-43. Elsevier, New York, NY.

Kawamoto, H., & Minato, N., (2004), Myeloid cells. *The International Journal of Biochemistry and Cell Biology, 36*(8): pp. 1374-1379.

Kelwick, R., Desantis, I., Wheeler, G. N., & Edwards, D. R., (2015). The ADAMTs (A disintergin and metalloproteinase with thrombospondin motifs) family. *Genome Biology, 16*(1).

Kersey, J. H., Weisdorf, D., Nesbit, M. E., LeBien, T. W., Woods, W. G., McGlave, P. B., … & Ramsay, N. K. C., (1987). Comparison of autologous and allogenic bone marrow transplantation for treatment of high-risk refractory acute lymphoblastic leukaemia. *New England Journal of Medicine, 317:* pp.461-467.

Khachigian, L. M., and Parish, C. R., (2004). Phosphomannopentaose sulfate (PI-88): heparan sulfate mimetic with clinical potential in multiple vascular pathologies. *Cardiovascular Drug Reviews, 22*(1): pp. 1-6.

Khurshid, C. and Pye, D.A. (2018). Isolation and compositional analysis of bioactive glycosaminoglycans from whelk. *Marine Drugs. 16*(5): p. 171.

Kim, Y. S. Jo, Y. Y. Chang, I. M. Toida, T. Park, Y. and Linhardt, R. J. (1996). A new glycosaminoglycan from the giant African snail *achatina Fulica*. *The Journal of Biological Chemistry. 271*(20): pp.11750-11755.

King, K.L., and Cidlowski, J.A. (1998). Cell cycle regulation and apoptosis. *Annual Review of Physiology. 60*: pp. 601-617.

Kini, A. R., Peterson, L. C., & Kay, N. E., (1998). Evidence for abnormal angiogenesis in the bone marrow of patients with B-cell chronic lymphocytic leukaemia (CLL) (abstract). *Blood. 92:* 716a.

Klein, E. Ben-Bassat, H. Neumann, H. Ralph, P. Zeuthen, J. Pollack, A. and Vanky, F. (1976). Properties of the K562 cell line, derived from a patient with chronic myeloid leukaemia. *International Journal of Cancer. 18*(4): pp.421-431.

Kleiveland, C. R., (2015). Peripheral blood mononuclear cells. *In the Impact of Food Bioactives on Health,* Springer. Chem: pp.161-167.

Koch, A. E., (1998). Angiogenesis: implications for rheumatoid arthritis. *Arthritis Rheumatism, 41*(6): pp.951-962.

Koike, T. Izumikawa, T. Tamura, J. and Kitagawa, I. F. (2009). FAM20B is a kinase that phosphorylates xylose in the glycosaminoglycan protein linkage region. *Journal of Biochemistry. 421*: pp.157-162.

Koo, H. H., (2011). Philadelphia chromosome-positive acute lymphoblastic leukaemia in childhood. *Korean Journal of Paediatrics, 54*(3): pp. 106-110.

Koo, C.J., Sen, Y., Bay, B., and Yip, G.W. (2008). Targeting HS proteoglycans in breast cancer treatment. *Anticancer Drug Discovery. 3*: pp. 151-158.

Kozlowski, E. O., Pavao, M. S., and Borsig, L. (2011). Ascidian dermatan sulfates attenuate metastasis, inflammation and thrombosis by inhibition of P-selectin. *Journal of Thrombosis and Haemostasis, 9*(9): pp. 1807-1815.

Kroemer, G. Galluzzi, L. and Brenner, C. (2007). Mitochondrial membrane permeabilisation in cell death. *Physiological Reviews. 87:* pp.99-163.

Kroemer, G., Zamzami, N., and Susin, S. A. (1997). Mitochondrial control of apoptosis. *Immunology Today. 18*(1): pp. 44-51.

Krysko, D.V. Brouckaert, G. Kalai, M. Vandenabeele, P. and D'Herde, K. (2003). Mechanisms of internalization of apoptotic and necrotic L929 cells by a macrophage cell line studied by electron microscopy. *Journal of Morphology. 258:* p.336-345.

Krysko, D.V. and Vandenabeele, P. (2008). From regulation of dying cell engulfment to development of anti-cancer therapy. *Cell Death and Differentiation. 15:* pp.29-38.

Kubaski, F. Osago, H. Mason, R.W. Yamaguchi, S. Kobayashi, H. Tsuchiya, M. Orii, T. and Tomatsu, S. (2017). Glycosaminoglycan defection methods: applications of mass spectrometry. *Molecular Genetics and Metabolism. 120:* pp.67-77.

Kuhnl, A., Goekbuget, N., Stroux, A., Burmeister, T., Newmann, M., Heesch, S., … & Baldus, C. D., (2010). High BAALC expression predicts chemoresistance in adults B-precursor acute lymphoblastic leukaemia. *Blood, 115*: pp.3737-3744.

Labbe, K. and Salen, M. (2008). Cell death in the host response to infection. *Cell Death and Differentiation. 15:* pp.1339-1349.

Lal, G., and Bromberg, J. S., (2009). Epigenetic mechanisms of regulation of FOXP3 expression. *Blood,* 114(18): pp.3727-3735.

Lanzi, C., and Cassinelli, G. (2018). Heparan sulfate mimetics in cancer therapy: the challenge to define structural determinants and the relevance of targets for optimal activity. *Molecules, 23*(11): p. 2915.

Lecoeur, H., (2002). Nuclear apoptosis detection by flow cytometry: influence of endogenous endonucleases. *Experimental Cell Research, 277*(1): pp.1-14.

Levine, A.J. (1997). P53 the cellular gate keeper for growth and division. *Cell. 88*: pp.323-331.

Linhardt, R. J. (2004). Heparin-induced cancer cell death. *Chemical Biology. 11*: pp. 420-422.

Li, Y., Jiang, D., Liang, J., Meltzer, E. B., Gray, A., Miura, R., ... & Noble, P. W. (2011). Severe lung fibrosis requires an invasive fibroblast phenotype regulated by hyaluronan and CD44. *Journal of Experimental Medicine*, *208*(7): pp. 1459-1471.

Liang, W. G., Triandafillou, C. G., Huang, T. Y., Zulueta, M. M. L., Banerjee, S., Dinner, A. R., ... & Tang, W. J. (2016). Structural basis for oligomerization and glycosaminoglycan binding of CCL5 and CCL3. *Proceedings of the National Academy of Sciences*, *113*(18): pp. 5000-5005.

Liu, D., Shriver, Z., Venkataraman, G., El Shabrawi, Y., and Sasisekharan, R. (2002). Tumour cell surface HS as cryptic promotors or inhibitors of tumour growth and metastasis. *Proceedings of the National Academy of Sciences. 99*(2): pp. 568-573.

Lohmann, N., Schirmer, L., Atallah, P., Wandel, E., Ferrer, R. A., Werner, C., ... & Freudenberg, U. (2017). Glycosaminoglycan-based hydrogels capture inflammatory chemokines and rescue defective wound healing in mice. *Science translational medicine*, *9*(386): eaai9044.

Lui, Q. Kreider, T. Bowdridge, S. Liu, Z. Song, Y. Gaydo, A.G. Urban, J.F. Jr. and Gause, W.C. (2010). B-cells have distinct roles in host protection against different nematode parasites. *Journal of Immunology. 184:* pp.5213-5223.

Ludwig, R. J., (2009). Therapeutic use of heparin beyond anticoagulation. *Current Drug Discovery Technologies, 6*(4): pp.281-289.

Maccarana, M. Olander, B. Malmstrom, J. et al. (2006). Biosynthesis of Dermatan sulphate CHONDROITIN-GLUCURONATE-EPIMERASE IS IDENTICAL TO SART2. *Journal of Biological Chemistry. 281*(17): pp.11560-11568.

Maerten, P., Shen, C., Bullens, D.M., Van Assche, G., Van Gool, S., Geboes, K., Rutgeerts, P., and Ceuppens, J.L. (2005). Effects of interleukin 4 on CD25 and CD4 and regulatory T-cell function. *Journal of Autoimmunity. 25*(2): pp. 112-120.

Maiuri, M.C. Zalckvar, E. Kimchi, A. and Kroemer, G. (2007). Self-eating and self-killing: crosstalk between autophagy and apoptosis. *Nature Reviews: Molecular Cell Biology. 8*(9): pp.741-752.

Makatsori, E., Karamanos, N. K., Papadogiannakis, N., Hjerpe, A., Anastassiou, E. D., & Tsegenidis, T., (2001). Synthesis and distribution of glycosaminoglycans in human leukemic B- and T- cells and monocytes studied using specific enzymic treatments and high-performance-liquid-chromatography. *Biochemical Chromatography, 15*: pp.413-417.

Malavaki, C. Mizumoto, S. Karamanos, N. and Sugahara, K. (2008). Recent advances in the structural study of functional chondroitin sulphate and dermatan sulphate in health and disease. *Connective Tissue Research. 49*(3-4): pp.133-139.

Manaster, J., Chezar, J., Shurtz-Swirski, R., Shapiro, G., Tendler, Y., Kristal, B., ... and Sela, S. (1996). Heparin induces apoptosis in human peripheral blood neutrophils. *British journal of haematology*. *94*(1): pp. 48-52.

Mandavili, A. (2013). Leukaemia. *Nature. 498(S1):* p.7455.

Mangi, M. H., & Newland, A. C., (2008). Angiogenesis and angiogenic mediators in haematological malignancies. *British Journal of Haematology, 111*(1): pp.43-51.

Marcus, R., Sweetenham, J. W., & Williams, M. E., (2013). *Lymphoma: Pathology, diagnosis and treatment.* Cambridge University Press.

Maton, A., Hopkins, J., McLaughlin, C. W., Johnson, S., Warner, M. Q., Lahart, D., & Wright, J. D., (1993), Human biology and health. Englewood Cliffs New Jersey, USA. Prentice Hall. ISBN 0-13-981176-1.

McCaffrey, R., Smoler, D. F., & Baltimore, D., (1973). Terminal deoxynucleotidyl transferase in a case of childhood acute lymphoblastic leukaemia. *Proceedings of The National Academy of Sciences USA, 70*(2): pp.521-525.

McDougall, S. R. Anderson, A. R. A. and Chaplain, M. A. J. (1971). Mathematical modelling of dynamic adaptive tumour induced angiogenesis: Clinical implications and therapeutic targeting strategies. *Journal of Theoretical Biology*. P. 241.

Meisenberg, G. Simmons, W. H. (2006). Principles of medical biochemistry. *Elsevier Health Sciences*. p. 243.

Mendez-Vidal, M. J. Molina, A. Ancdo, U. Chirivella, I. Etxaniz, O. … & Gallardo, E. (2018). Pazopanib: Evidence review and clinical practice in the management of advanced renal cell carcinoma. *BCM Pharmacology and toxicology.* 19: p.77.

Menke, N. B., Ward, K. R., Witten, T. M., Bonchev, D. G., & Diegelmann, R. F. (2007). Impaired wound healing. *Clinics in dermatology*, *25*(1): pp. 19-25.

Mikami, T. and Kitagawa, H. (2013). Biosynthesis and function of chondroitin sulphate. *Biochimica et Biophysica Acta (BBA)-General Subjects. 1830*(10): pp.4719-4733.

Miller, K.D. Siegel, R.L. Lin, C.C. Mariotto, A.B. Kramer, J.L. Rowland, J.H. Stein, K.D. Alteri, R. and Jemal, A. (2016). Cancer treatment and survivorship statistics in 2016. *CA: A Cancer Journal for Clinicians. 66*(4): pp.271-289.

Minowada, J. Ohnuma, T. and Moore, G. E. (1972). Rossetta forming human lymphoid cell lines. Establishment and evidence for origin of myeloma derived lymphocytes. *Journal of The National Cancer Institute. 49*: pp. 891-895.

Misra, S., Heldin, P., Hascall, V. C., Karamanos, N. K., Skandalis, S. S., Markwald, R. R., & Ghatak, S. (2011). Hyaluronan–CD44 interactions as potential targets for cancer therapy. *The FEBS journal*, *278*(9): pp. 1429-1443.

Mohamed, S., and Coombe, D. (2017). Heparin mimetics: Their therapeutic potential. *Pharmaceuticals, 10*(4): p. 78.

Mojic, M. Takeda, K. and Hayakawa, Y. (2018). The dark side of IFN-γ: its role in promoting cancer immunoevasion. *International Journal of Molecular Science. 19*(1): p. 89.

Moore, G. Knight, G. and Blann, A. (2010). *Haematology.* Oxford University Press.

Moore, K. L., Patel, K. D., Bruehl, R. E., Li, F., Johnson, D. A., Lichenstein, H. S., … and McEver, R. P. (1995). P-Selectin glycoprotein ligand-1 mediates rolling of human neutrophils on P-Selectin. *The Journal of Cell Biology, 128*(4): pp. 661-671.

Morla, S. (2019). Glycosaminoglycans and glycosaminoglycan mimetics in Cancer and Inflammation. *International Journal of Molecular Sciences, 20*(8): 1963.

Mossman, T., (1983). Rapid colorimetric assay for cellular growth and survival: application to proliferation and cytotoxicity assays. *Journal of Immunological Methods, 65*(1-2): pp.55-63.

Motzer, R. J. Escudier, B. Gannon, A. Figlin, R.A., (2017). Sunitinib: Ten years of successful clinical use and study in advanced renal cell carcinoma. *Oncologist. 22*(1): pp. 41-52.

Mummery, C., Van de Stolpe, A., Roelen, B., & Clevers, H. (2014). Chapter 3: What are stem cells? *Stem Cells: Scientific Facts and Fiction*. pp: 53-68. London Academic Press.

Murphy, K. McLay, N. and Pye, D. (2008). Structural studies of heparan sulphate hexasaccharides: insights into iduronate conformational behaviour. *Journal of The American Chemical Society. 130*: pp.12435-12442.

Muthukkaruppan, V. R. Kubai, L. and Auerbach, R. (1982). Tumour-induced neovascularization in the mouse eye. *Journal National Cancer institute. 69*: pp.699-705.

Nadanaka, S. Zhou, S. Kagigawa, S. Shoji, N. Sugahara, K. Sugihara, K. Asano, M. and Kitagawa, H. (2013). EXTL2 a member of the EXT family of tumour suppressors, controls

glucosaminoglycan biosynthesis in a xylose kinase dependant manner. *Journal of Biological Chemistry. 288*(3): pp. 9321-9333.

Nagai, S., and Toi, M. (2000). Interleukin 4 and breast cancer. *Breast Cancer. 7*(3): pp. 181-187.

Nakamura, M., Hikida, M., & Nakano, T. (1992). Concentration and molecular weight dependency of rabbit corneal epithelial wound healing on hyaluronan. *Current eye research*, *11*(10): pp. 981-986.

Nakano, T. Betti, M. and Pietrasik, Z. (2009). Extraction, isolation and analysis of chondroitin sulphate glycosaminoglycans. *Recent Patents on Food, Nutrition & Agriculture. 2*(1): pp.61-74.

Nappo, G., Handle, F., Santer, F.R., McNeil, R.V., Seed, R.I., Collins, A.T., Morrone, G., Culig, Z., Maitland, N.J., Erb, H.H.H. (2017). The immunosuppressive cytokine interleukin 4 increases the clonogenic potential of prostate stem-like cells by activation of STAT 6 signalling. *Oncogenesis. 6*.e342.

National centre for biotechnology information (2019). Pubchem compound database; CID= 3657. Available at: https://pubchem.ncbi.nlm.nih.gov/compound/3657. [accessed 9-2-2019].

Nelson, D. L. and Cox, M. M. (2008). *Lehniger principles of biochemistry* (5th ed) New York: W. H. Freeman and Company.

Neumar, R.W. (2000). Molecular mechanisms of ischemic neuronal injury. *The Annals of Emergency Medicine. 36:* pp.483-506.

Nikitovic, D., Assouti, M., Sifaki, M., Katonis, P., Krasagakis, K., Karamanos, N. K., and Tzanakakis, G. N. (2008). Chondroitin sulfate and heparan sulfate-containing proteoglycans are both partners and targets of basic fibroblast growth factor-mediated proliferation in human metastatic melanoma cell lines. *The International Journal of Biochemistry and Cell Biology, 40*(1): pp. 72-83.

Nikitovic, D. Tsatsakis, A. M. Zafiripoulos, A. Karamanor, N. K. and Tzanakakis, G. N. (2004). TGF-β2 by modulating the biosynthesis of glycosaminoglycan/ proteoglycans may regulate osteosarcpoma cell growth. *Anticancer Research. 24*(51): pp. 3581-3582.

Nilsson, K. and Sundstrom, C. (1974). Establishment and characteristics of two unique cell lines from patients with lymphosarcoma. *International Journal of Cancer. 13*: pp.808-823.

Nishida, N. Yano, H. Nishida, T. Kamura, and Kojiro, M. (2006). Angiogenesis in cancer Review. *Vascular Health and Risk Management. 2*(3): pp.213-219.

Nurgali, K., Jagoe, R. T., & Abalo, R., (2018). Editonal: adverse effects of cancer chemotherapy: anything new to improve tolerance and reduce sequelae? *Frontiers in Pharmacology, 9*: pp.245.

Nyberg, P. Xie, L. and Kalluri, R. (2005). Endogenous inhibitors of angiogenesis. *Cancer Research. 6l5*(10):3967-3979.

O'Donnell, A. Leach, M. Trigo, J. Scurr, M. Raynaud, F. Phillips, S. Aherne, W. Hardcastle, A. Workman, P. Hannah, A. and Judson, I. (2005). A phase I study of the angiogenesis inhibitor SU5416 (semaxanub) in solid tumours, incorporating dynamic contrast MR pharmacology end points. *Biological Journal of Cancer 93*(8): pp. 876-883.

Oeffinger, K. C., Mertens, A. C., Sklar, C. A., Kawashima, T., Hudson, M. M., Meadows, A. T., … & Schwartz, C. L., (2006). Chronic health conditions in adult survivors of childhood cancer. *New England Journal of Medicine, 355*: pp.1572-1582.

Ogundipe, O.D. (2015). Isolation and characterisation of a novel glycosaminoglycan with anticancer activity. (unpublished PhD thesis), University of Salford, Salford.

Ortéga, N., L'Faqihi, F. E., & Plouët, J. (1998). Control of vascular endothelial growth factor angiogenic activity by the extracellular matrix. *Biology of the Cell*, *90*(5): pp. 381-390.

Pallister, C.J. and Watson, M.S. (2011). *Haematology.* Scion Publishing, Banbury, UK.

Pardue, E. L. Ibrahim, S. and Ramathurth, A. (2008). Role of hyaluronan ion angiogenesis and its utility to angiogenic tissue engineering organogenesis. *Landes Bioscience. 4*(4): pp.203-213.

Parish, C. R., (2006). The role of Heparan Sulphate in inflammation. *Nature Reviews: Immunology, 6*: pp.633-643.

Pecorino, L. (2012). *Molecular biology of cancer: mechanisms, targets, and therapeutics*. Oxford university press.

Penn, J. S. (2008). Retinal and choroidal angiogenesis. *Springer*. p.119.

Peplow, P. V. (2005). Glycosaminoglycan: a candidate to stimulate the repair of chronic wounds. *Thrombosis and Haemostasis*, *94*(07): pp. 4-16.

Perez-Atayde, A. R., Sallan, S. E., Tedrow, U., Connors, S., Allred, E., & Folkman, J., (1997). Spectrum of tumor angiogenesis in the bone marrow of children with acute lymphoblastic leukaemia. *American Journal of Pathology, 150*(3): pp.815-821.

Pollack, A. Lampen, N. Clarkson, B.B. Harven, D.E. Bentwich, E.Z. Siegal, F.P. and Kunker, H.G. (1973). Identification of human B and T lymphocytes by scanning electron microscopy. *Journal of Experimental Medicine. 138*: pp.607-623.

Pomin, V. H. (2010). Structural and functional insights into sulfated galactans: a systematic review. *Glycoconjugate Journal*, *27*(1), 1-12.

Pomin, V.H. (2015). Keratan sulphate: An up-to-date review. *International Journal of Biological Macromolecules. 72*: pp.282-289.

Ponta, H., Sherman, L., & Herrlich, P. A. (2003). CD44: from adhesion molecules to signalling regulators. *Nature reviews Molecular cell biology*, *4*(1): p. 33.

Porta, R. Borea, R. Coelho, A. Khan, S. AraÚjo, A. … & Roifo, C. (2017). FGF a promising druggable target in cancer: molecular biology and new drugs. *Critical Reviews in Oncology/ Haematology*. 113: pp. 256-267.

Probst-Kepper, M., Geffers, R., Kroger, A., Veigas, N., Erck, C., Hecht, H. J., … & Ocklenburg, F., (2009). GARP: a key receptor controlling FOXP3 in human regulatory T-cells. *Journal of Cellular and Molecular Medicine, 13*(96): pp.3343-3357.

Proudfoot, A. E., Johnson, Z., Bonvin, P., and Handel, T. (2017). Glycosaminoglycan interactions with chemokines add complexity to a complex system. *Pharmaceuticals, 10*(3): 70.

Proudfoot, A. E., Fritchley, S., Borlat, F., Shaw, J. P., Vilbois, F., … and Wells, T. N., (2001). The BBXB motif of RANTES is the principle site for heparin binding and controls receptor selectivity. *Journal of Biological Chemistry, 276:* pp. 10620-10626.

Pui, C.H., & Evans, W. E., (2006). Treatment of Acute Lymphoblastic Leukaemia. *New England Journal of Medicine, 354:* pp. 116-178.

Pui, C.H. and Robinson, L.L. (2008). Look at lymphoblastic leukaemia. *Lancet. 371:* pp. 1030-1043.

Pule, M. A., Gullmann, C., Dennis, D., McMation, C., Jeffers, M., & Smith, O. P., (2002). Increased angiogenesis in bone marrow of children with acute lymphoblastic leukaemia has no prognosis significance. *British Journal of Haematology, 118*(4): pp.991-998.

Pye, D. A., & Kumar, S., (1998). Endothelial and fibroblast cell-derived heparan sulphate bind with differing affinity to basic fibroblast growth factor. *Biochemical and Biophysical Research Communications, 248*: pp.889-895.

Pye, D. A., Vives, R. R., Turnbull, J. E., Hyde, P., and Gallagher, J. T. (1998). Heparan sulphate oligosaccharides require 6-O-sulphation for promotion of basic fibroblast growth factor mitogenic activity. *Journal of Biological Chemistry, 273:* pp. 22930-22942.

Quah, B. J., & Parish, C. R., (2010). The use of carboxyfluorescein diacetate succinimidyl ester (CFSE) to monitor lymphocyte proliferation. *Journal of Visualised Experiments: JoVE, 44.*

Quast, U., (2006). Whole body radiotherapy: A TBL-guide line. *Journal of Medical Physics, 31*(1): pp.5-12.

Rabbitts, T. H. (1991). Translocations, master genes, and differences between the origins of acute and chronic leukemias. *Cell*, *67*(4), 641-644.

Rah, M.J. (2011). A review of Hyaluronan and its ophthalmic applications. *Optometry-Journal of The American Optometric Association. 82*(1): pp.38-43.

Raman, K. Ninomiya, M. and Kuberan, B. (2011). Novel glycosaminoglycans biosynthetic inhibitiors affect tumour-associated angiogenesis. *Biochemistry Biophysics Res Community. 404*(1): pp.86-89.

Raymond, E. Faiure, S. and Armand, J. (2000). Epidermal growth factor receptor tyrosine kinase as a target for anticancer therapy. *Drugs. 60*(1): pp. 15-23.

Ricci, M. S., & Zong, W. X., (2006). Chemotherapeutic approaches for targeting cell death pathways. *Oncologist, 11*(4): pp.342-357.

Ricciardelli, C., Mayne, K., Sykes, P. J., Raymond, W. A., McCaul, K., Marshall, V. R., and Horsfall, D. J. (1998). Elevated levels of versican but not decorin predict disease progression in early-stage prostate cancer. *Clinical Cancer Research, 4*(4): pp. 963-971.

Rieger, A. M., Nelson, K. L., Konowalehuk, J. D., & Barreda, D. R., (2011). Modified annexin V/Propidium iodide apoptosis assay for accurate assessment of cell death. *Journal of Visualised Experiments: JoVE,* (50).

Rini, B. I. (2007). Vascular endothelial growth factor- targeted therapy in renal cell carcinoma: current status and future directions. *Clinical Cancer Research. 13*(4): pp. 1098-1106.

Ritchie, J. P., Ramani, V. C., Ren, Y., Naggi, A., Tori, G., Casu, B., … and Zunino, F. (2011). SST0001, a chemically modified heparin, inhibits myeloma growth and angiogenesis via disruption of the heparinase/ syndecan-1 axis. *Clinical Cancer Research, 17*(16): pp. 1382-1393.

Roos, W. P., & Kaina, B., (2006). DNA damage-induced cell death by apoptosis. *TRENDS in Molecular Medicine, 12*(9): pp.440-450.

Sadir, R., Imberty, A., Baleux, F., & Lortat-Jacob, H. (2004). Heparan sulfate/heparin oligosaccharides protect stromal cell-derived factor-1 (SDF-1)/CXCL12 against proteolysis induced by CD26/dipeptidyl peptidase IV. *Journal of Biological Chemistry*, *279*(42): pp. 43854-43860.

Sakai, H., Kokura, S., Ishikawa, T., Tsuchiya, R., Okajima, M., Matsuyama, T., … & Handa, O., (2013). Effects of anti-cancer agents on cell viability proliferative activity and cytokine production of peripheral blood mononuclear cells. *Journal of Clinical Biochemistry and Nutrition, 52*(1): pp.64-71.

Salmivirta, M. Lidholt, K. and Lindahl, U. (1996). Heparan sulfate A piece of information. *FASEB. 10*: pp.1270-1279.

Sanderson, R. D., (2001). Heparan sulphate proteoglycans in invasion and metastasis. *Seminars in Cell and Developmental Biology, 12*: pp.89-98.

Sanguine Biosciences (2012). Types of immune cells present in Human PBMCs [online]. Available at: http://technical.sanguinebio.com/types-of-immune-cells-present-in-human-pbmc/ [accessed 03/08/2016].

Sarrazin, S., Lamanna, W. C., & Esko, J. D. (2011). Heparan sulfate proteoglycans. *Cold Spring Harbor perspectives in biology*, *3*(7): a004952.

Sasisekharan, R., Shriver, Z., Venkataraman, G., & Narayanasami, U., (2002). Roles of heparan-sulphate glycosaminoglycans in cancer. *Nature Reviews: Cancer, 2*: pp.521-528.

Schafer, K. A., (1998). The Cell Cycle: A Review. *Veterinary Pathology, 35*(6): pp.461-478.

Schoenfelder, M. and Einspanier, R. (2003). Expression of hyaluronan synthases & corresponding hyaluronan receptors in differentially regulated during oocyte maturation in cattle. *Biology Reproduction. 69*: pp.269-277.

Shah. N. P., Tran. C., Lee, F. Y., Chen. P., Norris. D., & Sawyers. L. L., (2004). Overriding imatinib resistance with a novel ABL kinase inhibitor. *Science, 305*(5682): pp.399-401.

Shephard, E. A., Neal, R. D., Rose, P. W., Walter, F. M., & Hamilton, W. (2016). Symptoms of adult chronic and acute leukaemia before diagnosis: large primary care case-control studies using electronic records. *British Journal of General Practice*, *66*(644), pp:182-188.

Sherr, C. J., & Roberts, J. M. (1995). Inhibitors of mammalian G1 cyclin-dependent kinases. *Genes & Development*, *9*(10): pp.1149-1163.

Shibuya, M. (2011). Vascular Endothelial Growth Factor (VEGF) and its receptor (VEGFR) signalling in angiogenesis. *Genes Cancer. 2*(12): pp. 1097-1105.

Siegel, R., DeSantis, C., Virgo, K., Stein, K., Mariotto, A., Smith, T., ... & Lin, C. (2012). Cancer treatment and survivorship statistics, 2012. *CA: A Cancer Journal for Clinicians*, *62*(4): pp.220-241.

Siegel, R.L. Miller, K.D. and Jemal, A. (2015). Cancer statistics. *CA: A Cancer Journal for Clinicians. 65:* pp. 5-29.

Sistla, J. C., Morla, S., Alabbas, A. H. B., Kalathur, R. C., Sharon, C., Patel, B. B., and Desai, U. R. (2019). Polymeric fluorescent heparin as one-step FRET substrate of human heparinase. *Carbohydrate Polymers, 205:* pp. 385-391.

Sjoblom, T. Jones, S. Wood, L.D. Parsons, D.W. Lin, J. Barber, T.D. et al. (2006). The consensus coding sequences of human breast and colorectal cancers. *Science. 314:* pp.268-274.

Skak, K. Kragh, M. Hausman, D. Smyth, M.J. and Sivakumar, P.V. (2008). Interleukin 21: combination strategies for cancer therapy. *Nature Reviews: Drug and Discovery. 7:* pp.231-240.

Skidmore, M.A. Guimond, S.E. Dumax-Vorzet, A.F. Yates, E.A. and Turnbull, J.E. (2010). Disaccharide compositional analysis of heparan sulphate and heparin polysaccharides using UV or high-sensitivity fluorescence (BODIPY) detection. *Nature Protocols. 5*(12): pp.1983-1992.

Sompayrac, L. M. (2015). *How the immune system works*. Wiley-Blackwell.

Spear, P., Barber, A., Rynda-Apple, A., Sentman, C.T. (2012). Chimeric antigen receptor T cell shape myeloid cell function within the tumour microenvironment through IFN-γ and GM-CSF. *Journal of Immunology. 188*: pp. 6389-6398.

Springer, T. A. (1995). Traffic signals on endothelium for lymphocyte recirculation and leukocyte emigration. *Annual review of physiology*, *57*(1): pp. 827-872.

Stasiak-Barmuta, A. Luczynski, W. Ilendo, E. Krawczuk-Rybak, M. and Szymanski, M. (2009). Regulatory T cells in children with acute lymphoblastic leukaemia. *Medycyna Wieku Rozwojowego. 13*: pp.53-58.

Stegmann, T. J. (1999). New approaches to coronary heart disease: Induction of neovascularisation by growth factors. *Biodrugs & Clinical Immunotherapeutic's & Biopharmaceuticals & Gene Therapy. 11*(5): pp. 301-308.

Stuppia, L., Calabrese, G., Peila, R., Guanciali-Franchi, P., Morizio, E., Spadano, A., & Palka, G., (1997). p53 loss and point mutations are associated with suppression of apoptosis and progression of CML into myeloid blastic crisis. *Cancer Genetics Cytogenetics, 98:* pp. 28-35.

Sugahara, K. and Kitagawa, H. (2000). Recent advances in the study of the biosynthesis and functions of sulphated glycosaminoglycans. *Current Opinion in Structural Biology. 10*: pp. 518-527.

Swaya, T. O., Aduma, P., Chelimo, K., and Were, O., (2017). Assessment of anti-proliferative activities of selected medicinal plant extracts used for management of diseases around Lake Victoria basin. *Journal of Carcinogenesis and Mutagenesis.* 8: p. 286.

Takeda, K., Tanaka, T., Shi, W., Matsumoto, M., Minami, M., Kashiwamura, S. I., … & Akira, S., (1996). Essential role of stat6 in IL4 signalling. *Nature, 380*(6575): p. 627.

Tammi, R. H., Passi, A. G., Rilla, K., Karousou, E., Vigetti, D., Makkonen, K., and Tammi, M. I. (2011). Transcriptional and post-translational regulation of hyaluronan synthesis. *The FEBS Journal, 278*(9): pp. 1419-1428.

Taylor, R.C. Cullen, S.P. and Martin, S.J. (2008). Apoptosis controlled demolition at the cellular level. *Nature Reviews: Molecular Cell Biology. 9:* pp.231-241.

Taylor, K. R., & Gallo, R. L. (2006). Glycosaminoglycans and their proteoglycans: host-associated molecular patterns for initiation and modulation of inflammation. *The FASEB Journal*, *20*(1): pp. 9-22.

Thelin, M. A., Bartolini, B., Axelsson, J., Gustafsson, R., Tykesson, E., Pera, E., … & Malmstrom, A., (2013). Biological functions of iduronic acid in chondroitin/ dermatan sulphate. *Federation of European Biochemical Societies Journal. 280* (10): pp.2431-2446.

Theocharides, T. C., Alysandratos, K. D., Angelidou, A., Delivanis, D. A., Sismanopoulos, N., Zhang, B., … and Kalogeromitros, D. (2012). Mast cells and inflammation. *Biochimica et Biophysica Acta (BBA)-Molecular basis of Disease, 1822*(1): pp. 21-33.

Theocharis, A. D., Skandalis, S. S., Tzanakakis, G. N., and Karamanos, N. K. (2010). Proteoglycans in health and disease: Novel roles for proteoglycans in malignancy and their pharmacological targeting. *The FEBS Journal, 277*(19): pp. 3904-3923.

Thomas, X., Olteanu, N., Charrin, C., Lheritier, V., Magaud, J. P., & Fiere, D., (2001). Acute Lymphoblastic Leukaemia in the elderly: the Edouard herriot hospital experience. *American Journal of Haematology, 67*: pp.73-83.

Tiong, K.H. Mah, K.Y. & Leong, C., (2013). Functional roles of fibroblast growth factor receptors (FGFRs) signalling in human cancer. *Apoptosis. 18*(12): pp. 1447-1468.

Towbridge, J.M. and Gallo, R.L. (2002). Dermatan sulphate: new functions from an old glycosaminoglycan. *Glycobiology. 12*(9): pp.117R-125R.

Trujillo, A., McGee, C., & Cogle, C. R., (2012). Angiogenesis in acute myeloid leukaemia and opportunities for novel therapies. *Journal of Oncology, 2012.*

Twycross, R., (1994). The risks and benefits of corticosteroids in advanced cancer. *Drug Safety, 11*(3): pp.163-178.

Tyrrell, D. J., Horne, A. P., Holme, K. R., Preuss, J. M., and Page, C. P. (1999). Heparin in inflammation: potential therapeutic applications beyond anticoagulation. *Advances in Pharmacology (San Diego, Calif.) 46:* pp. 151-208.

University of Dundee (nd). Cell death and apoptosis [online]. Available at: http://www.lifesci.dundee.ac.uk/technologies/flow-cytometry-cell-sorting/techniques/cell-death-and-apoptosis [accessed 10/07/2016].

Vallen, M. J. E. Massuger, L. F. A. G. Ten Dam, G. B. Bulten, J. and Van Kuppevelt, T. H. (2012). Highly sulphated chondroitin sulfates, a novel class of prognostic biomarkers in ovarian cancer tissue. *Gynecological Oncology. 127*: pp.202-209.

Van Lint, P., & Libert, C., (2007). Chemokine and cytokine processing by matrix metalloproteinases and its effects on leukocyte migration and inflammation. *Journal of Leukocyte Biology, 82*(6): pp.1375-1381.

Van Meerloo, J., Kaspers, G. J., Cloos, J., (2011). Cell sensitivity assays: the MTT assay. *Cancer Cell Culture Humana Press 731:* pp.237-245.

Varki, A., Cummings, R. D., Esko, J. D., Freeze, H. H., Stanley, P., Bertozzi, C. R., … & Etzler, M. E., (2009). *Essentials of glycobiology 2nd edition.* Cold Spring Harbor Laboratory Press, Cold spring harbour, New York.

Vermes, I., Haanen, C., Steffens-Nakken, H., & Reutelingsperger, C., (1995). A novel assay for apoptosis. Flow cytometry detection of phosphatidylserine expression on early apoptotic cells using fluorescein labelled annexin V. *Journal of Immunological Methods, 184:* pp.39-51.

Vigetti, D. Viola, M. Karousou, E. De Luca, G. and Passi, A. (2014). Metabolic control of hyaluronan synthases. *Matrix Biology. 35*: pp.8-13.

Vigneri, P., & Wang, J. Y., (2001). Induction of apoptosis in chronic myelogenous leukaemia cells through nuclear entrapment of BCR-ABL tyrosine kinase. *Nature Medicine, 7*(2): pp.228-234.

Virelizier, E. N., Lagreze, M. J., Waz, D., Rea, D., Coiteux, V., Leguay, T., … & Nicolini (2009). Combined chemotherapy (daunorubicin and cytarabine) and dasatinib as salvage therapy of chronic myeloid leukaemia (CML) in myeloid blast crisis, a pilot study. *Blood, 114*: p. 2195.

Wang, N. X., Sieg, S. F., Lederman, M. M., Offord, R. E., Hartley, O., & von Recum, H. A. (2013). Using glycosaminoglycan/chemokine interactions for the long-term delivery of 5P12-RANTES in HIV prevention. *Molecular pharmaceutics*, *10*(10): pp. 3564-3573.

Wang, R., Kozhaya, L., Frances, M., Khaitan, A., Fuji, H., & Unutmaz, D., (2009). Expression of GARP selectively identifies activated human FOXP3^{+} regulatory T-cells. *Academy of Sciences, 106*(32): pp.13439-13444.

Wang, R.F. (2008). CD8+ regulatory T cell, their suppressive mechanisms and regulation in cancer. *Human Immunology. 69*: pp.811-814.

Ward, E. Desantis, C. Robbins, A. Kohler, B. and Jemal, A. (2014). Childhood and adolescent cancer statistics. *CA: A Cancer Journal for Clinicians. 64*(2): pp.83-103.

Webb, L., Ehrengruber, M. V., Clark-Lewis, I., Baggiolini, M., and Rot, A. (1993). Binding to heparan sulfate or heparin enhances neutrophil responses to interleukin 8. *Proceedings of the National Academy of Sciences, 90*(15): pp. 7158-7162.

Wesselborg, S., Engels, I. H., Rossman, E., Lo, M., and Schulze-Osthoff, K. (1999). Anti-cancer drugs induce caspase-8/ FLICE activation and apoptosis in the absence of CD95 receptor/ ligand interaction. *Blood. 93*: pp. 3053- 3063.

Weyers, A., Yang, B., Yoon, D. S., Park, J. H., Zhang, F., Lee, K. B., & Linhardt, R. J., (2012). A structural analysis of glycosaminoglycans from lethal and nonlethal breast cancer tissues: toward a novel class of theragnostics for personalised medicine in oncology?. *Omics: A Journal of Integrative Biology. 16* (3): pp.79-89.

White Blood Cells, National Cancer institute, (2018). Available at: www.cancer.gov/publications/dictionaries/cancer-terms/def/white-blood-cell. [Accessed on 05-.6-2018].

Witz, I. P., (2006). The involvement of selectins and their ligands in tumor-progression. *Immunology Letters, 104*(1-2): pp.89-93.

Wolf, A.M. Wolf, D. Steurer, M. Gastl, G. Gunsilius, E. and Grubeck-Loebenstein, B. (2003). Increase of regulatory T cells in the peripheral blood of cancer patients. *Clinical Cancer Research. 9*: pp.606-612.

Woo, E.Y. Yen, H. Chu, C.S. Schlienger, K. Carroll, R.G. Riley, J.L. Kaiser, L.R. and June, C.H. (2002). Cutting edge: regulatory T-cells from lung cancer patients directly inhibit autologous T cell proliferation. *Journal of Immunology. 168(9):*4272-6.

Wood, L. D., Parsons, D. W., Jones, S., Lin, J., Sjoblom, T., Leary, R. J., … & Silliman, N., (2007). The genomic landscapes of human breast and colorectal cancers. *Science. 318* (5853)*:* pp.1108-1113.

Wright, D., McKeever, P., & Carter, R., (1997). Childhood non-Hodgkin lymphoma in the United Kingdom: findings from the UK children's cancer study group. *Journal of Clinical Pathology, 50*: pp.128-134.

Xiong, S. Mu, T. Wang, G. and Jiang, X. (2014). Mitochondrial mediated apoptosis in mammals. *Protein Cell. 5*(10): pp.737-749.

Yamada, S. and Sugahara, K. (2008). Potential therapeutic application of chondroitin sulphate/dermatan sulphate. *Current Drug Discovery Technologies. 5*(9): pp.289-301.

Yang, W. (2012). The cell cycle. *Physiology of The Gastrointestinal Tract. 2*(15): pp.451-462.

Yip, G. W. Smollich, M. and Gotte, M. (2006). Therapeutic value of glycosaminoglycans in cancer. *Molecular Cancer Therapeutics. 3*: pp.2139-2148.

Youle, R.J. and Strasser, A. (2008). The BCL-2 protein family: opposing activities that modulate cell death. *Nature Reviews: Molecular Cell Biology. 9:* pp.47-59.

Yue, X. L., Lehri, S., Li, P., Barbier-Chassefiere, V., Petit, E., Huang, Q. F., … & Morin, C., (2009). Insights on a new path of pre-mitochondrial apoptosis regulation by a glycosaminoglycan mimetic. *Cell Death and Differentiation, 16*: pp.770-781.

Zhang, Y. (2014). Screening of kinase inhibitors targeting BRAF for regulating autophagy based on kinase pathways. *Journal of Molecular Medicine Rep*. 9(1): pp. 83-90.

Zhang, L. (2010). Glycosaminoglycan (GAG) biosynthesis and GAG-binding proteins. *In Progress in Molecular Biology and Traditional Science. (Vol: 93)*, PP. 1-17. Academic Press.

Zhang, H. Berezov, A. Wang, Q. Zhang, G. Drebin, J. Murali, R. Greene, M. I., (2007). ERDB receptors: from oncogenes to targeted cancer treatment. *The Journal of Clinical Investigators. 117*(8): pp. 2051-2058.

Zhang, L. and Zhao, Y. (2007). The regulation of FOXP3 expression in regulatory CD4+CD25+ T Cells: Multiple pathways on the road. *Journal of Cellular Physiology. 211*(3): pp.590-597.

Zhivotovsky, B., & Orrenius, S., (2010). Cell cycle and cell death in disease: past, present and future. *Journal of International Medicine, 268*(5): pp.395-409.

Zhou, H., Dussault, N., Cochran, E., Kwan, R., Karlgren, J., Barnes, M., ... and Smith, S. (2009). M-ONC 402-a non-anticoagulant low molecular weight heparin inhibits tumour metastasis. In *Proceedings of the 100th Annual Meeting of American Association for Cancer Research (AACR)*.

Ziarek, J. J., Veldkamp, C. T., Zhang, F., Murray, N. J., Kartz, G. A., Liang, X., ... & Volkman, B. F. (2013). Heparin oligosaccharides inhibit chemokine (CXC motif) ligand 12 (CXCL12) cardioprotection by binding orthogonal to the dimerization interface, promoting oligomerization, and competing with the chemokine (CXC motif) receptor 4 (CXCR4) N terminus. *Journal of Biological Chemistry*, *288*(1): pp. 737-746.

Appendix

FPLC optimisation results

The complex nature of the whelk extract crude mixture limits the ability to identify any particular components responsible for the anti-cancer activity identified. In sight of this ion-exchange chromatography (FPLC) was performed in order to attempt to identify a particular component responsible for the activity. Elution was spectrophotometrically monitored at 232nm in order to detect fragments of the crude extract.

The FPLC technique was carried out using a variety of linear gradient protocols as set out in the methods section, in order to ascertain the highest possible level of separation in the crude extract to allow the identification of the most potent fraction.

An initial FPLC run was carried out using a 3M-3M NaCl gradient in 50mM phosphate buffer pH 7.0, achieved over a 120-minute time frame. The graph presented in figure 8.1 identifies one solid peak (P1) with a small shoulder peak (S1) to the left-hand side. This demonstrated that the entire sample had been eluted at a single time point. This identified the initial gradient as being insufficient to separate out the individual components of the GAG extract.

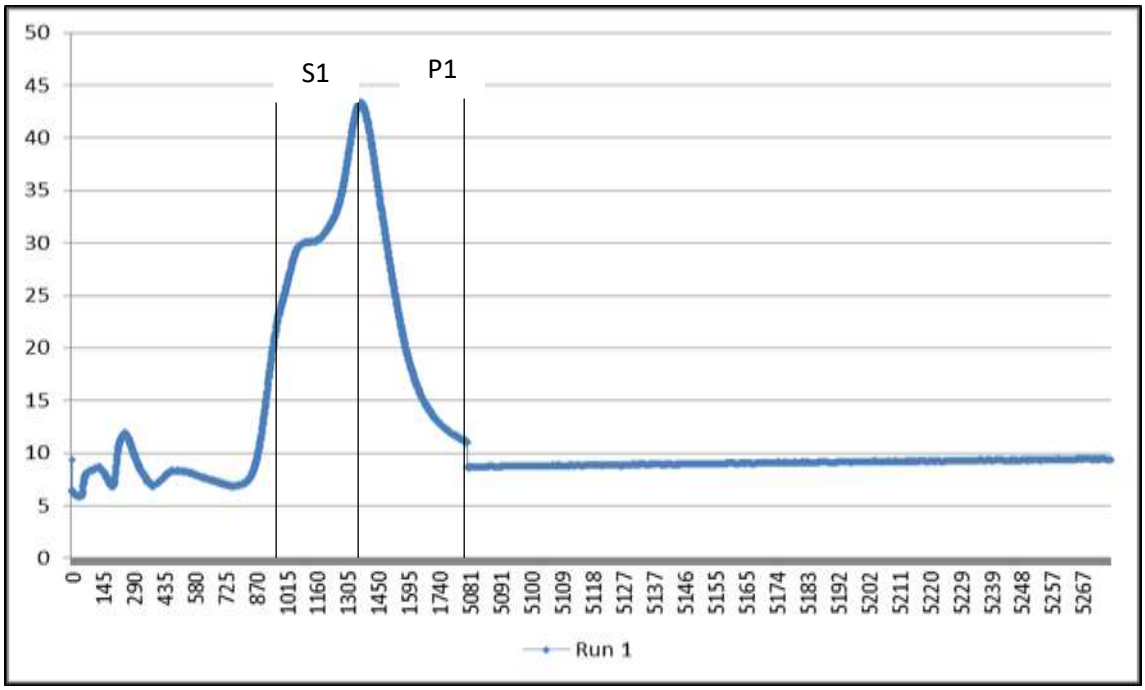

Figure 8.1 FPLC absorbance vs time graph of whelk extract sample method 1. Whelk sample applied to a DEAE-sepharose packed X16-20cm column, eluted using a 0-3M NaCl gradient over a 120-minute time period. Elution was monitored at 232nm.

Due to the lack of separation a further method was created using a 0-0.75M NaCl gradient, which was obtained over a 60-minute period and after a 5-minute hold period was further increased to 2M. This increase occurred over a 30-minute period. It was hoped that through

extending the period of time taken to reach the gradient point where the previous sample peak had been eluted, further separation may occur.

Figure 8.2 identifies still one predominant main peak (P1), however the initial shoulder now appeared broader and further migrated. This suggested the start of some separation not seen in the initial run.

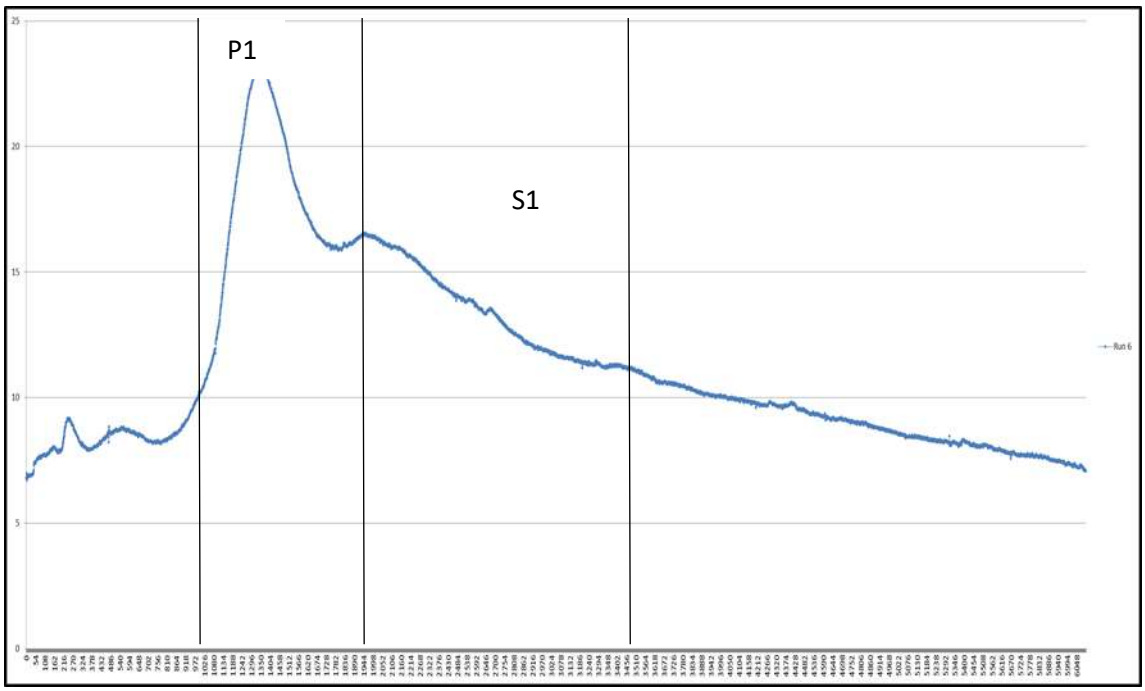

Figure 8.2 FPLC absorbance vs time graph of whelk extract sample method 2. Whelk sample applied to a DEAE-sepharose packed X16-20cm column, eluted using a 0-75M and 0.75M-2M NaCl step gradient over a 100-minute time period. Elution was monitored at 232nm.

The previous gradient appeared sufficient although the final gradient was further reduced for the subsequent run as no sample appeared to be eluted at a higher gradient. This reduction would also prolong the time taken for the gradient to be reached, thus further separation may be noted as the longer time it takes to get to a gradient the more likely it is to pull the individual components of the GAG extracts through the column at different speeds due to their different levels of negativity. Therefore, the subsequent run still used the initial 0-0.5M NaCl gradient achieved over a 60-minute period with a 5-minute hold. Then a further NaCl gradient increase to 1.5M over a 30-minute time point was executed.

In figure 8.3 further separation can be noted with the initial predominant peak starting to split into 2 separate peaks (P1 and P2), the second peak also feature two further signs of separation shoulder peaks S1 and S2. The further level of separation identifies a longer time frame to reach the gradients proved beneficial in promoting a higher level of separation in the whelk extract.

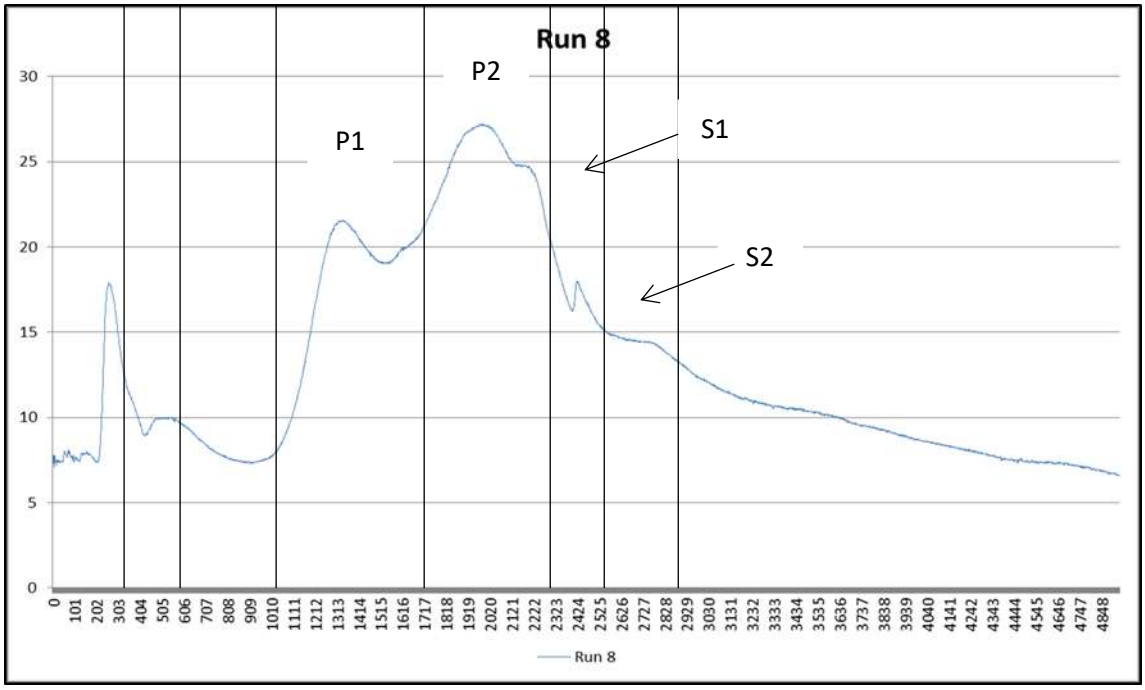

Figure 8.3 FPLC absorbance vs time graph of whelk extract sample method 3. Whelk sample applied to a DEAE-sepharose packed X16-20cm column, eluted using a 0-75M and 0.75M-1.5M NaCl step gradient over a 100-minute time period. Elution was monitored at 232nm.

As the previous run demonstrated a higher level of separation with the increased time taken to obtain the final gradient, further prolongation of the time taken to achieve the initial gradient was decided on after analysis. Therefore, the subsequent run an initial 0-0.25M NaCl was obtained over a 30-minute period and held for 5 minutes. Over a further 30-minute period the NaCl gradient was increased from 0.25M to 0.5M NaCl and again held for 5 minutes. The gradient was then further increased to 1M NaCl over a 60-minute period.

As can be seen in figure 8.4 the new method of achieving a gradual gradient step wise provided a level of separation in the whelk extract that had not previously been achieved. In figure 8.4 14 peaks can be identified (P1-14), with some peaks still identifying small shoulders suggesting there could be further separation still to be achieved. As this was the highest level of separation achieved this method was used to collect and pool the peak fractions. The fractions were de-salted using the PD-10 column gravity method and isolates were freeze dried in order to obtain a powder which was used in subsequent MTT assays. These assays aimed at identifying which peak was responsible for the anti-cancer activity noted in the crude extract assays.

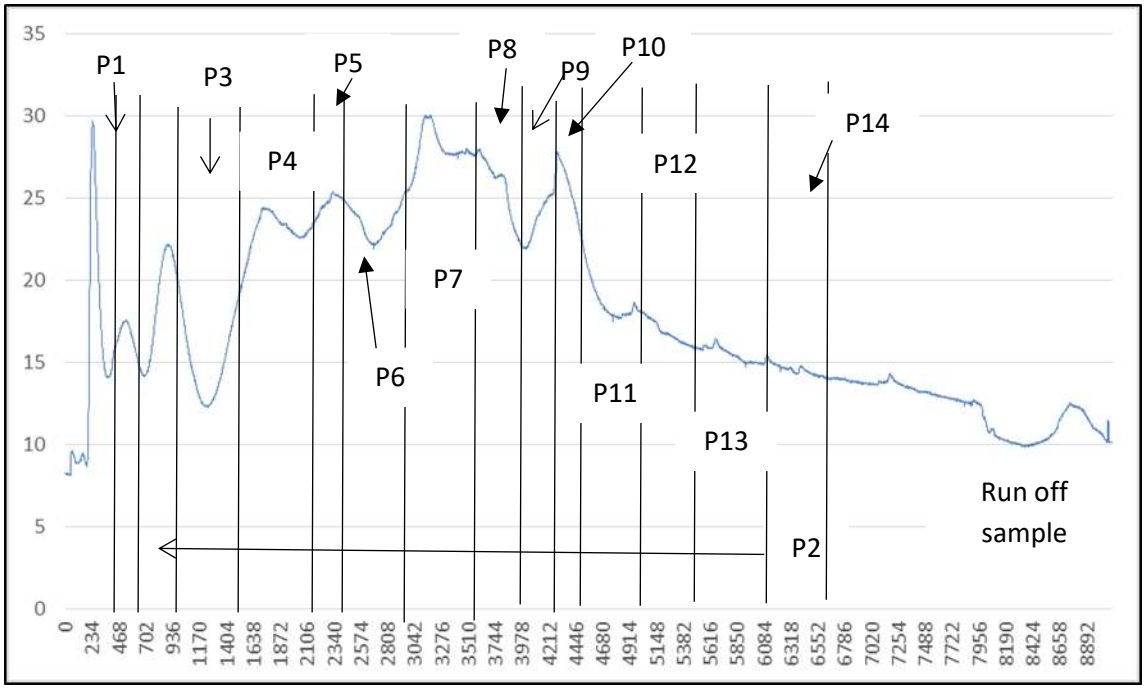

Figure 8.4 FPLC absorbance vs time graph of whelk extract sample method 4. Whelk sample applied to a DEAE-sepharose packed X16-20cm column, eluted using a 0-25M, 0.25M-0.5M and 0.5M-1M NaCl step gradient over a 130-minute time period. Elution was monitored at 232nm.

$CD3^+$ K562 cell line populations obtained from Annexin V/ PI apoptosis assay

As the K562 cell line has been described as having T-cell properties (Klein et al., 1976), the research homed in on the $CD3^+$ populations of the K562 cell line, in order to gain insight into the effects of GAG isolates on T-cell specifically. However only approximately 4% of K562 cells tested positive for CD3. In figure 8.5 section A cisplatin can be identified as having brought about the largest increase in $CD3^+$ K562 apoptotic cells of around 15%; seen through the corresponding drop in cells not undergoing cell death ($p=0.1317$). There was also a decrease in late stage apoptotic cells post cisplatin treatment (green bar, section A of figure 8.5, $p=0.3385$). The largest increase was seen in the early stage apoptotic cells (blue bar, section A figure 8.5, $p=0.6667$). This follows the pattern noted in the entire K562 cell population (figure 8.5 section A).

The cockle extract elicited a small decrease in the percentage of $CD3^+$ K562 cell not undergoing apoptosis ($p= 0.9398$) and a small decrease in late stage apoptotic $CD3^+$ K562 cells ($p=0.2934$) (figure 8.5, section B). Cockle extract treatment also brought about small increases in the percentage of $CD3^+$ K562 cells undergoing mid ($p=0.4542$) and early stage apoptosis ($p=0.4362$) (red and blue bars respectively, section B of figure 8.5). The whelk extract treatment (section C of figure 8.5) resulted in a minor increase of around 1.3% of $CD3^+$ K562 cells which were not undergoing any form of cell death ($p=0.8810$); this increase corresponded with the decrease of cells undergoing late stage apoptosis ($p=0.3961$) seen in figure 8.5 (section C, green bar).

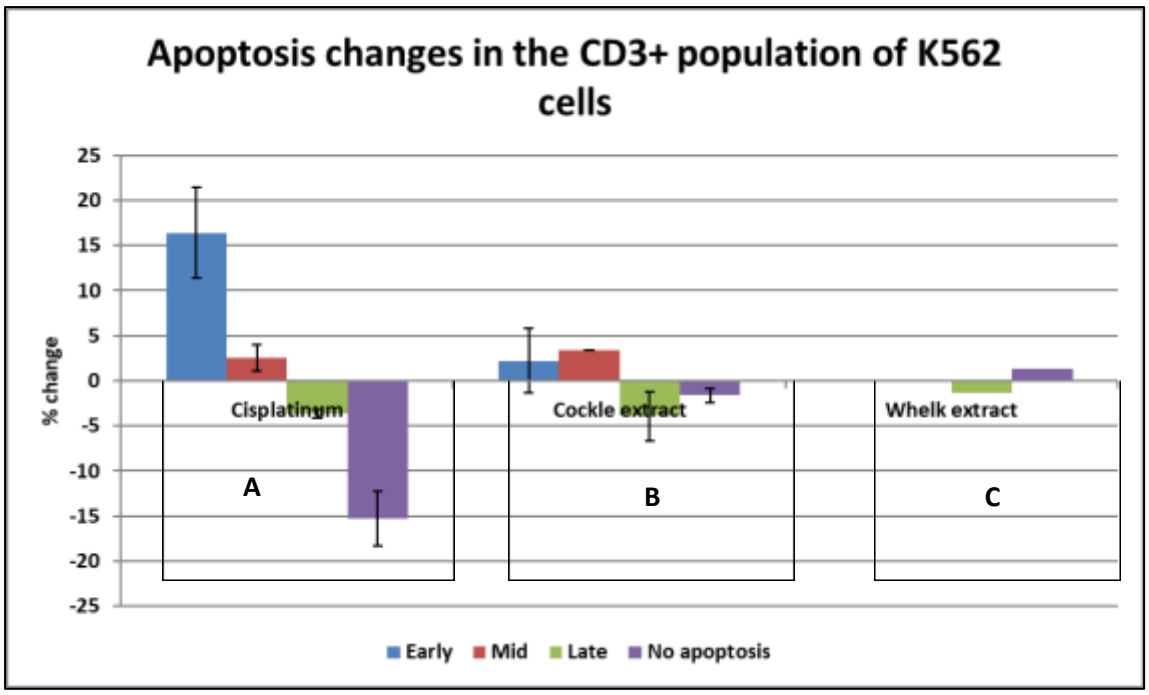

Figure 8.5 Average cell death activity in CD3+ K562 cells obtained using the annexin V/PI apoptosis assay. Average percentage change graphs for CD3+ K562 cells treated with the IC50 dose of cisplatin (A), cockle extract (B) and whelk extract (C) (6 µg/ml, 12 µg/ml and 12 µg/ml respectively). Showing the stage of cell death that the cells are in where early= early stages of apoptosis, mid= mid stages of apoptosis, Late= late stage apoptosis and no apoptosis= no cell death. Using an incubation period of 3 days using the Annexin V/ PI apoptosis assay. Where N=3, percentage change in cells were calculated in relation to untreated cells and Error bars show SEM, significance is denoted by *, absence of * indicates no significance.

Ethical approval for study

University of Salford MANCHESTER

Research, Innovation and Academic Engagement Ethical Approval Panel

Research Centres Support Team
G0.3 Joule House
University of Salford
M5 4WT

T +44(0)161 295 5278

www.salford.ac.uk/

26 January 2016

Dear Chloe,

RE: ETHICS APPLICATION ST16/82 – Validation of Shellfish Isolates (Glycosaminoglycans, GAGs) for development as a novel anti-tumour therapy for children: GAG action on lymphocytes/ Tregulatory cells.

Based on the information you provided, I am pleased to inform you that your application ST 16.82 has been approved.

If there are any changes to the project and/ or its methodology, please inform the Panel as soon as possible by contacting S&T-ResearchEthics@salford.ac.uk

Yours sincerely,

Prof Mohammed Arif
Chair of the Science & Technology Research Ethics Panel
Professor of Sustainability and Process Management,
School of Built Environment
University of Salford
Maxwell Building, The Crescent
Greater Manchester, UK M5 4WT
Phone: + 44 161 295 6829
Email: m.arif@salford.ac.uk

Planned timetable of work

Activity/ 3month intervals	3	6	9	12	15	18	21	24	27	30	33	36
Learning Techniques												
Preparation of GAG isolates and HPLC fractions												
Preparation and storage of PBMC stocks												
MTT assays for the three tumour cell lines and PBMCs												
Apoptosis flow assays												
Proliferation flow assays												
Activation flow assays and ELISPOT assays												
Treg responses assays												
Data analysis												
Report writing												